THE DEVELOPMENT AND CHARACTERIZATION OF THEOPHYLLINE AND BUDESONIDE CO-ENCAPSULATED POLY (LACTIC ACID) (PLA) NANOPARTICLES

MIRA DHIRAJ BUHECHA

A THESIS SUBMITTED IN PARTIAL FULFILMENT FOR THE DEGREE OF DOCTOR OF PHILOSOPHY

APRIL 2016

SCHOOL OF PHARMACY AND BIOMOLECULAR SCIENCES

UNIVERSITY OF BRIGHTON

ABSTRACT

Inhaled drug delivery is ideal for treatment of asthma and chronic obstructive pulmonary disease (COPD) as it allows a local action of the medication at the disease site. Biodegradable polymeric nanoparticles which might allow extended/sustained release of inhaled drugs are synthesized using various methods however; these do not permit high encapsulation efficiency for hydrophilic drugs. The aim of the project was to test the hypothesis that it was possible to develop an efficient method for the co-encapsulation of a hydrophilic and lipophilic drug (theophylline and budesonide respectively) into nanoparticles.

In order to improve the loading efficiency of both hydrophilic and hydrophobic drugs, a modified double emulsification solvent diffusion (DESD) method was developed and both co-encapsulated and mono-encapsulated nanoparticles (containing either drug) were synthesized. Improved loading efficiency, studied using high performance liquid chromatography (HPLC), for both drugs was obtained. Dynamic light scattering (DLS) and scanning electron microscopy (SEM) showed that particles were in the sub-micron range (150-400 nm). Measurement of zeta potential showed that the particles had a negative surface charge and additionally Fourier-transform infra-red (FT-IR) spectroscopy confirmed that this was due to the polymer and no drug was adsorbed on the external surface of the nanoparticles. Resemblance of nanoparticles thermograms, obtained using differential scanning calorimetry (DSC), to those of the polymer alone suggested successful encapsulation of the drugs. Stability studies of the drug encapsulated nanoparticles conducted at different temperatures indicated that storage conditions of 2-8°C over a period of 6 months showed minimal changes in the particle size, zeta potential and morphological characteristics of the nanoparticles. Storage (of the nanoparticles) at 40°C over the course of 6 months resulted in larger variations on the particle size and zeta potential but also loss of morphological features of the nanoparticles, suggestive of changes in the polymer state at this temperature.

Franz diffusion cells were used to study the release of drugs from the nanoparticles over 24 hours at room temperature and at 37^{o}C. The results showed that release of theophylline and budesonide from nanoparticles was biphasic and sustained compared to release of drug from solutions containing an equivalent concentration of drug.

The effect of the nanoparticles on the viability of airway epithelial cells was studied using a human bronchial epithelial cell line (16HBE14o-) using a 3-(4, 5-dimethyl-2-thiazolyl)-2, 5-diphenyl-2H-tetrazolium bromide (MTT) assay. The nanoparticles had no significant effect

on cell viability except at the highest concentration of the suspension studied (5 mg/mL) ($P<0.05$). The permeability of 16HBE14o- cells, cultured at an air-liquid interface, to theophylline and budesonide applied in solution and as mono-encapsulated and co-encapsulated nanoparticles was studied. The nanoparticles and drug solutions did not affect the tight junctions of the cells and similar to the results obtained in the Franz diffusion cells, both drugs crossed the cells more slowly when applied as nanoparticles in comparison to the solutions.

To study deposition of the nanoparticles; nebulized suspensions of the nanoparticles in de-ionized water and dry powder formulations using different grades of lactose were compared. The prepared formulations were studied using a multi-stage liquid impinger (MSLI). The results indicated that drug deposition was greatest in stages 1 and 2 of the MSLI where particle size was greater than 6.8μm from the dry powder formulations in contrast to deposition throughout the five stages of the MSLI from the nebulized suspension. Morphological assessment of the dry powder formulations using SEM showed nanoparticles adhered to the lactose but also included nanoparticles in the absence of lactose and *vice versa*.

In conclusion, theophylline and budesonide nanoparticles were successfully formulated using PLA by application of the DESD method. Nanoparticles possessed desired physicochemical properties including submicron size range and negatively charged surface; however a higher loading efficiency of the hydrophobic drug was obtained despite modifications to the DESD method. Low toxicity of the nanoparticles to human bronchial epithelial cells and sustained release over a period of 24 hours was achieved. Nanoparticles were delivered successfully in the target site at a desired particle size range when formulated as nebulized suspensions.

TABLE OF CONTENTS

LIST OF TABLES

LIST OF FIGURES

ACKNOWLEDGEMENTS

I would like to express my deepest gratitude and appreciation to my supervisors, Dr. Ananth Pannala and Dr. Alison Lansley. Thank you for the guidance, advice, trust, encouragement and helping me develop my knowledge and inspiring me continuously throughout the course of this project. Most importantly thank you for the support, understanding and patience through some of the tough times. The knowledge I gained and experience has been invaluable and this would have not been possible without your guidance.

I would like to thank the University of Brighton for the International Student Research Scholarship. Thank you to all the technical and support staff in PABS (pharmaceutics, chemistry, microbiology, tissue culture and image analysis unit) that I had the wonderful opportunity to work with and always learn from. I would like to especially thank John Stephens, Christine Smith, Petra Kristova and Seija Maata. Additionally, I would like to thank Dr. Guy Standen for all the time and help in dealing with the various HPLC problems! I am grateful to Dr. Satyanarayana Somavarapu and Zahra Merchant (UCL School of Pharmacy) and Dr. Ben Forbes and Joanna Muddle (Kings College London) for their advice and guidance. A Big Thank You especially to Dr. Ken Rutt for helping me confidently evolve from an amoeba to a mammal since the early pharmacy days!

A special thanks to all my friends from IST: Aashna Puri, Fatema Abdallah, Ely Jaffer, Bansi Sagar, Erum Mussa, Ekta Malkan (so much of you is me) and especially Paul Brace (wise words of wisdom, always). Also a big Thank you to Besime Timur (always and the countless coffees from star batch Costa Company), Nafeesa Ullah (for sharing match-day and work stress), Krishna Chauhan, Kushal Sharma (for the advice, education and contribution to the stories), Rob Ingham (you're a great friend- may God always bless you!) and especially to Rahaf Issa, ma meilleure amie and lab neighbor: no amount of thank you (or sorry) I'll say will be enough but I'll try. Thank you^{infinity} for always being there, listening to me, laughing with/at me, believing and having faith in me and convincing me that everything *is* okay. I've had 'funnest' time with you in the last few years and would never be able to justify it in words. So many priceless memories that occurred only at 10.8 or 6.7 in 'Oorooguay' of empresses, pink ninjas, Luigi and co. marriages, wheely chairs endeavors, l'azote liquide, water fountains, definitely *not* walking enough times to the cricket stadium, benya and the successes of FC Guirdo City!

To my family: Santi Ba: for always caring. Amarshi R.B: for *always* looking out for me and staying with me forever (*This one's for you Bapuji!)* and to my Aunty Zadi and Uncle Mobeen. Pratik B: for all the patience in the world. "Mornië utúlië, Mornië alantië." Sorry for being a pain (only sometimes) but I appreciate and love you so much, always!

I would most importantly like to thank my parents, Hina and Dhiraj, for their unconditional love and support forever and financially supporting this research for all the years. Their patience, unwavering belief, energy invested and confidence in me has helped me and will always continue to inspire and be my strength forever. Thank you for setting the best example in everything always. I appreciate everything you do and no words will be enough to say how much I love you. My biggest thank you and love you goes to **God**.

AUTHORS DECLARATION

I declare that the research contained in this thesis, unless otherwise formally indicated within the text, is the original work of the author. The thesis has not been previously submitted to this or any other university for a degree, and does not incorporate any material already submitted for a degree.

Signed

(Mira D. Buhecha)

Dated

LIST OF ABBREVIATIONS

ACh	Acetylcholine
AC	Adenylate cyclase
ANOVA	Analysis of variance
BTS	British Thoracic Society
COPD	Chronic obstructive pulmonary disease
CFD	Computational fluid dynamics
cAMP	Cyclic adenosine monophosphate
CYP	Cytochrome P450
DSC	Differential scanning calorimetry
DPPC	Dipalmitoylphosphatidylcholine
DESD	Double emulsification solvent diffusion
DPIs	Dry powder inhalers
DMEM	Dulbecco's Modified Eagle's Medium
DLS	Dynamic light scattering
ESD	Emulsification solvent diffusion
EPR	Enhanced permeation and retention
FBS	Fetal bovine serum
FPD	Fine particle dose
FPF	Fine particle fraction
FD4	Fluorescein isothiocyanate
FDA	Food and Drug Administration
FEV_1	Forced expiratory volume (1 second)
FVC	Forced vital capacity
FT-IR	Fourier-transform infra-red
GERD	Gastro-esophageal reflux disease
GSD	Geometric standard deviation
Tg	Glass transition temperature
GINA	Global initiative for asthma
GM-CSF	Granulocyte macrophage colony stimulating factor
HPLC	High performance liquid chromatography
HDAC	Histone deacetylase
ICS	Inhaled corticosteroid
ICH	International Conference on Harmonization
LDH	Lactate dehydrogenase
LOD	Limit of detection
LOQ	Limit of quantification
LABA	Long acting beta2-agonist
LAMA	Long acting muscarinic-antagonist
MMI	Marple miller impactor
MMAD	Mass median aerodynamic diameter
MEM	Minimum Essential Medium
MTT	3-(4,5-dimethyl-2-thiazolyl)-2, 5-diphenyl-2H-tetrazolium bromide
MSLI	Multistage liquid impinger
NP	Nanoparticles
NICE	National institute for Health and Care Excellence
NSAID	Non-steroidal anti-inflammatory drug
PBS	Phosphate buffered saline
PDE	Phosphodiesterase
PCS	Photon correlation spectroscopy
PCL	Poly (caprolactone)
PLA	Poly (lactic acid)
PLGA	Poly (lactic –co-glycolic acid)
PVA	Poly (vinyl alcohol)
PBCA	Polybutylcyanocrylate
PEG	Polyethylene glycol
PTFE	Polytetrafluoroethylene
pMDIs	Pressurized metered dose inhalers
RI	Refractive index
RH	Relative humiditiy
RSD	Relative standard deviation
SEM	Scanning electron microscopy
SIGN	Scottish Intercollegiate Guidelines Network
SABA	Short acting beta2-agonist
SLF	Simulated lung fluid
SLN	Solid lipid nanoparticles
SD	Standard deviation
SCF	Supercritical fluid precipitation
TER	Trans-epithelial electrical resistance
TEM	Transmission electron microscopy
TB	Tuberculosis
TSLI	Twin stage liquid impinger
UV	Ultraviolet
VdW	van der Waal's
v/v	Volume per volume
w/v	Weight per volume
XRD	X-ray diffraction

CHAPTER 1 INTRODUCTION

Pulmonary drug delivery can be used for the delivery of drugs for both local and systemic diseases. Airway diseases such as asthma, chronic obstructive pulmonary disease (COPD), cystic fibrosis and local infections are treated using the inhaled route, delivering drugs locally to the site of action. Advantages of local drug delivery include reduced overall dose of drug being administered, reduced risk of systemic side effects and a rapid onset of action. Local drug delivery results in side effects being limited to the delivery site. Systemic drug delivery by the pulmonary route can be achieved as a result of the large surface area, small diffusion barriers and features such as avoidance of first pass metabolism. The delivery of insulin for the treatment of diabetes mellitus has been achieved by the pulmonary route [1, 2].

1.1. ANATOMY OF THE RESPIRATORY SYSTEM

The main function of the airways is the exchange of gases; oxygen for carbon dioxide. This process is known as respiration [3-5]. The other functions of the respiratory system include speech, filtration and metabolic activities. The structure of the airways efficiently prevents the entry, and promotes the removal, of airborne foreign particles [3-6].

There are two main regions of the airways; the 'conducting region' and 'respiratory region' which are the central and peripheral region of the airways, respectively (Figure 1.1). The central region is composed of the trachea, bronchi, bronchioles, terminal and respiratory bronchioles. The respiratory region also consists of the respiratory bronchioles and the alveolar region. The airways can also be described as the upper and lower airways; where the upper airways consists of the nose, throat, pharynx, larynx and trachea and the lower airways consists of the bronchi, bronchioles and alveolar region [3, 4, 6].

The trachea divides into two bronchi which divide further throughout the lungs. Alveoli are present at the terminal part of the bronchi and are the functional unit of the lungs as the site of gas exchange. The trachea is classified as generation 0 and the two main bronchi as generation 1. There is a difference between the right and left bronchi; where the right bronchus is wider and leaves at a smaller angle than the left and, as a result, more material is inhaled. There are five lobar bronchi (three on the right and two on the left). There are 15-20 dichotomous branching's of the bronchi and bronchioles which lead to terminal bronchioles and the alveoli [3, 6]. The different generations of the airways are classified according to Weibel's tracheobronchial classification. In this, the first 16 generations are the conducting airways. Generation 5-11 consist of the small bronchi. Generations 17-23 consist of the

respiratory bronchioles, alveolar ducts and alveolar sacs [3, 6]. The velocity of the inhaled air is reduced as it passes through the airways.

In the alveolar region, there are two main types of cells; Type I and Type II. Type I cells are non-phagocytic and are responsible for gas exchange. Type II cells are larger cells and secrete lung surfactant which plays a role in maintaining the shape and integrity of the alveoli by reducing surface tension [5, 6]. The large surface area of this region (100-140m^2) is efficient for gas exchange [4].

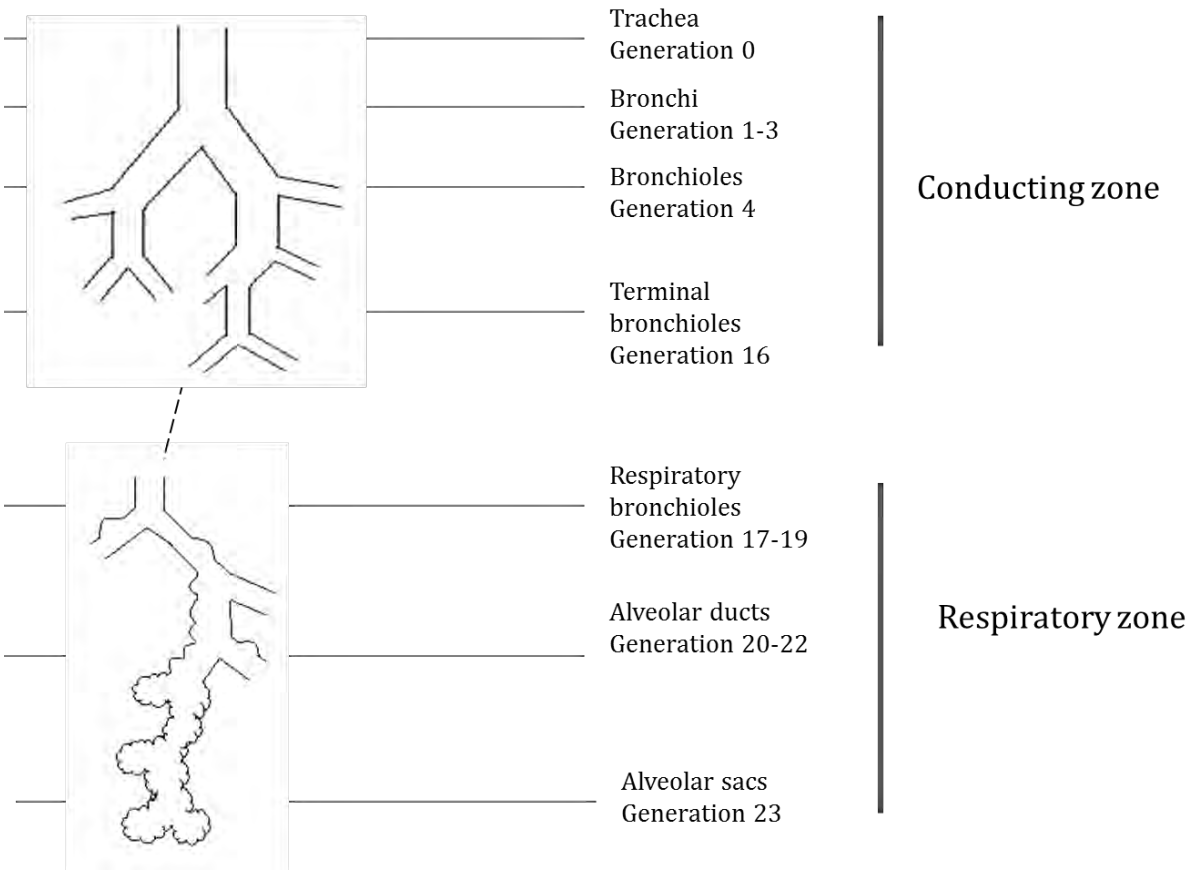

Figure 1.1 Schematic representation of the human airways [4, 7, 8]

1.2. PARTICLE DEPOSITION

The deposition of drugs in the airways depends on four factors[4]:

- The physicochemical properties of the drug (particle shape, density, aerodynamic diameter)
- The formulation
- Delivery device
- Patient factors (breath volume, respiratory rate)

Particle size is very important in determining the deposition of the drug in the airways and is described by the aerodynamic diameter which is defined as the physical diameter of a unit density sphere which settles through the air with a velocity of the particle of interest [3, 4]. Particles deposit in the different regions of the lungs depending on their size and the speed of inhalation. Particles that are less than 1µm in theory can reach the peripheral airways but are likely to be exhaled before depositing [9]. Particles in the size range of 1-5µm deposit in the large and conducting airways where they will exert their clinical effect. Particles that are over 5µm result in mouth and esophageal deposition with no clinical effects, but can result in local side effects [9, 10]. The particles are usually polydispersed, with a variation in their size, which is represented by the geometric standard deviation (GSD). Instead of referring only to the particle size, it is important to quote a MMAD (mass median aerodynamic diameter) too. The MMAD is usually calculated for particles in order to standardize the sizes that are being considered. If kept consistent, the MMAD is the diameter where 50% of the particles are above and 50% are below this diameter [3, 4]. Calculation of the MMAD allows reproducibility of the inhaled dose when controlled. Particles deposit in the airways by three main mechanisms [3-5, 11-13]:

- Impaction: the air stream changes direction at bifurcations and turbulence is caused by the inhaled air which causes particles to leave the air stream and impact on the walls of the airway. Deposition as a result of impaction occurs in the upper respiratory tract and mainly occurs for large particles. Particles over 10µm are deposited in the oropharyngeal region due to their high velocity and turbulence and have minimum therapeutic effect. This method of deposition usually occurs in the first 10 generations of the lung.
- Sedimentation: as the velocity of the airstream decreases further down the airways, most inhaled particles will be deposited by sedimentation as a result of Stokes' Law, by gravity. Deposition depends on the particle size and the density of the particles. Particles that deposit using this mechanism are in the size range of 1-5µm.

- Brownian motion/diffusion: in the deep lung where air velocity is negligible particles still present undergo constant irregular and random motion which causes collision and bombardment with the walls of the respiratory tract. Particles that are smaller than 1µm largely deposit via this mechanism.

Deposition via sedimentation and diffusion is facilitated by patients holding their breath for longer in order to increase the residence time [9, 13].

1.3. DEVICES

Inhaled therapy is usually preferred due to the local action and reduced side effects as described [14, 15]. However, it has been reported that only ~15% of the dose will reach the target site [16, 17].Inhalers are the main vehicles for the effective administration of drugs to the lung [18]. There is a need to develop inhaler devices which are easy to use and deliver a consistent and reproducible dose of the drug to the lungs allowing patient compliance to improve and allowing better control of lung diseases such as asthma overall [19]. Global Initiative for Asthma (GINA) recommended that the inhaler devices should be portable, easy to operate and require minimal coordination and cooperation, with minimal maintenance requirements [19]. Management of chronic disease is 10% medication and 90% education; many patients lack knowledge and skills required to obtain maximum effect from their medication [20, 21]. For conditions like asthma, the severity is often misclassified and therefore insufficient and inappropriate therapy is commonly prescribed [19].

An ideal inhaler device should have an innovative design, which is combined with simplicity and effective performance and low airflow resistance. Along with these, it is important that the inhaler device is convenient, generates a high quality aerosol, reliable, durable, cost-effective and environmentally friendly [14, 19, 22].

Along with selecting the correct and the most appropriate device, it is important to check the compliance and maintenance in order to make sure that the dose being delivered is effectively delivered and an exact dose inhaled. Correct inhalation technique plays a vital role in the effective therapy of asthma along with the appropriate drug being recognized [18, 23]. Dose inhalation errors can be inhalation independent and inhalation dependent errors. For example, not being able to follow instructions of use are inhalation independent factors [24]. Incorrect technique and administration of the drug results in diminished therapeutic effect and results in poor control of symptoms and therefore leads to insufficient disease management [18]. Inhalation dependent factors include factors such as not achieving flow rates required/desired [24].

There are three major categories of devices used for pulmonary drug delivery. These are (pressurized) metered dose inhalers (pMDIs), dry powder inhalers (DPIs) and nebulizers [3, 4, 25-27]. The pros and cons must be considered when selecting an inhaler device for the patient [28].

1.3.1. PRESSURIZED METERED DOSE INHALERS (PMDIS)

Pressurized MDIs usually contain the drug dissolved or suspended in the pressurized propellant liquid. They are very common devices used for the delivery of drugs to the lungs in asthma and COPD. Included in the propellant are other excipients, such as surfactants, and these are put in a pressurized canister with a metering valve to deliver the doses accurately and precisely (Figure 1.2). The main problem that patients face when using pMDIs is the coordination required between patient inhalation and actuation of the dose. Poor coordination can lead to loss of drug and therefore an inconsistent dose being delivered to the correct site in the lung. Inhalation just before actuation of the drug leads to most of the drug being deposited in the throat and then eventually cleared by swallowing. The use of spacer devices and breath-actuated pMDIs can help to overcome this problem. In 2004, the market was dominated by pMDIs but it was observed that these were not user friendly and only delivered 30% of the dose [3, 4, 29].

Advantages of pMDIs [3, 4, 27, 30, 31]

- Low cost
- Disposable
- Multiple and reproducible doses
- Portable and small to carry around
- Canister design prevents contamination and degradation of the drug

Disadvantages of pMDIs [3, 4, 14, 21, 26-32]

- Hand-breath coordination required and a sufficient flow rate (30L/minute) in order to obtain optimal deposition of the inhaled dose
- Need to, for example, shake the canister in order re-disperse drugs that undergo sedimentation over time can result in a variation of the dose delivered
- Needs for patients to hold breath for a sufficient duration to maximize deposition of the drugs, e.g. for approximately 6 seconds.
- Dose counters not present in all devices
- Spacer devices not effective if multiple doses are needed

- The inclusion of a propellant can cause some patients to stop inhaling when the medication hits the back of the throat which is referred to as a cold Freon effect [30, 31]
- Inefficient drug delivery upon actuation due to high velocity when actuated from the canister and results in increased impaction and deposition of the drug in the throat and upper airways.
- Size of the aerosol droplet can be very high and, due to the low volatility of the propellant, it may take a few seconds before the particle size is reduced to the ideal size for drug delivery in the lungs.
- Patient difficulty such as not being able to remove the protective cap can lead to loss of dose, but also patient not receiving the dose.
- When using pMDIs containing corticosteroids, patients need to wash their mouths etc. after use as deposition at the throat causes an oral thrush (Candida infection) in some patients.

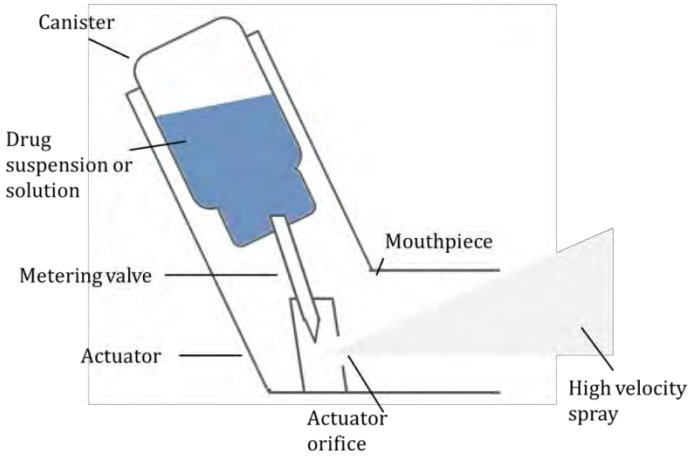

Figure 1.2 Pressurized metered dose inhaler (pMDI). Schematic diagram adapted from 'Pulmonary drug delivery' by Taylor [4]

1.3.2. DRY POWDER INHALERS (DPIS)

The DPI formulation involves particles being inhaled in powder form. DPIs, unlike MDIs, are propellant free and are free of multiple excipients. Their main component is a carrier, which is usually lactose. The purpose of the carrier is to improve flow properties of the active ingredients. The velocity at which the drug is released from the device can cause increased turbulence and may be deposited in the upper airways as a result of impaction. Particles with high porosity are shown to have better delivery in the lungs.

Lactose used in DPIs can consist of several different types/grades depending on the properties of the particles that are going to be inhaled [33]. Whilst pMDIs require coordination between actuation and patient breathing, dry powder inhalers do not require this. The doses delivered by DPIs are generally higher doses when compared to pMDIs. Dry powder inhaler particles that are actuated from the device and their de-aggregation depend on how the patient inhales the medication, i.e. they are passive devices. Patients who have respiratory diseases may have impaired inhaling, and thus limit their dose and de-aggregation of their drug particles, and it is important to consider in the formulation of DPIs that the powder is able to disperse at different flow rate and is independent of flow rates as well.

Dry powder actives can be prepared as carrier-based formulations, i.e. using lactose (as the carrier) or by agglomeration of the drug as particles to be used for the formulation itself. Like pMDIs, DPIs can contain multiple doses. DPIs have the option of packing the doses in blisters which are pierced by the patient before use, or the drug can come in single capsules where patients can insert them into the device and they are pierced just before use (Figure 1.3). There are some important factors to consider when formulating DPIs, which include i) production of the actual drug powder, ii) formulation of the final powder for the device (drug plus carrier) and iii) aerosol generation.

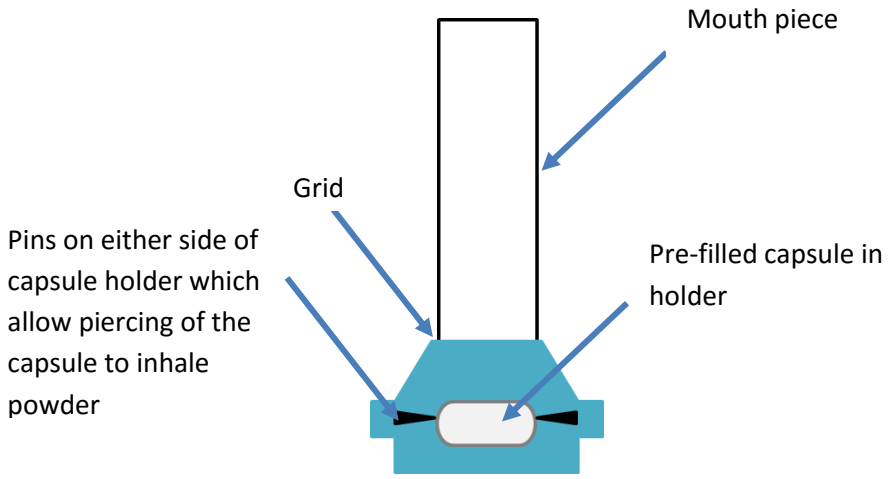

Figure 1.3 Image representing a single dose inhaler device, the Cyclohaler®/Aerolizer® device. Pre-filled capsules containing dry powder are loaded into device and pierced before inhalation. Schematic diagram based on actual device design.

When formulating DPIs, carrier technology is used when drug particles have poor powder flow properties and also when particles are difficult to place in metered doses. Excipients, or carrier powders, such as lactose or mannitol, are used to improve this powder flow for device and capsule filling. Lactose is inert and therefore a good excipient to use [27]. To formulate carrier-based DPI systems, it is important that the mixing of the drug with the

carrier is done sufficiently, i.e. ordered mixing or mixing in a predictable manner. Drug particles will adhere to the carrier particles by adhesive bond formation. When the patient inhales the medication, the energy provided must be great enough to break the adhesive bonds between the drug and carrier particles. The larger lactose particle (>5µm), detaches from the drug and usually deposits in the upper airways (throat) and the smaller drug particles deposit in the lower respiratory region. Drug-carrier particles where the energy provided hasn't been able to break the bonds remain large and deposit in the upper airways by impaction. DPIs are able to provide a consistent dose and flowability by carrier system [4, 34]. Lactose used in DPIs can consist of several different types/grades depending on the properties of the particles that are going to be inhaled. Commercially available lactose includes: Lactohale®100 which is crystalline, fine powdered lactose with a controlled particle size. Lactohale®200 also a controlled particle size and is milled lactose, Lactohale® 201 is similar to Lactohale®200, but is hard-milled and has a controlled particle size of <50µm and Lactohale®300 which is a micronized lactose and, due to the low particle size, it is extremely cohesive. There are other inhalable grade lactose products available such as Respitose® ML001 and Respitose® ML006 [33]. These are further described in Chapter 6.

Agglomerate technologies are systems which contain no excipients and only contain the drug particles made into agglomerates which maintain powder flow and dispersibility. There is a formulation of budesonide, Pulmicort®, that is formulated using this technology [3].

When the drug leaves the DPI, there can be an interaction with the device, and can cause mechanical impaction and an interaction between particle-particle and particle-device that can affect dispersion of the drug. Unlike pMDIs, DPIs do not require hand-breathe coordination as they are breathe-actuated. However, particles that are actuated from the device and their de-aggregation depend on how the patient inhales the medication, i.e. they are passive devices. Patients who have respiratory diseases (or the elderly or young) may have impaired inhaling, and thus limit their dose and de-aggregation of the drug particles. Therefore, it is important to consider in the formulation of DPIs that the powder is able to disperse at different air flow rate and is independent of air flow rates as well.

Advantages of DPIs [3, 4, 18, 27-30, 34-36]

- Breath-actuated and therefore no coordination needed
- Environmental friendly formulation with absence of propellant
- Many different formulations being developed using new technologies
- Portable
- Larger dose can be delivered compared to pMDIs
- Stable if kept in appropriate storage conditions

Disadvantages of DPIs [4, 14, 21, 26-31, 34, 36, 37]

- Passive devices which depend on the patient's inspiratory effort. A flow rate of 30-90L/minute is required, but some patients may not be able to achieve such high flow rates as a result of their disease state. Children may not be able to achieve these flow rates.
- Device could be single dose or multiple doses. Single dose devices require higher flow rates; and multiple dose devices require changes in blisters and have 3 month durability.
- DPI devices require priming of the inhaler, for example, incorrect piercing of capsules or opening blisters incorrectly can result in drug not being delivered to the patient.
- Humidity and moisture in the device can affect the particles' stability. Increased humidity can cause the particles to be aggregated and therefore affect their stability. Moisture affects powder cohesion through capillary force at high relative humidity and at low relative humidity it allows electrostatic interaction. This can be measured using atomic force microscopy. Correct storage is an important factor, especially in patient education, when prescribed DPIs. For example, storage in moisture sensitive areas such as the bathroom cabinet would not be ideal for a DPI. The DPI can be placed as individually sealed doses to provide greater protection but these need to be inhaled straight away once opened.
- Impaction of particles due to high velocity can lead to particles being deposited in the upper airways
- Can initiate cough reflex

A study by Lavorini et al (2008) showed a high number of patients use the inhaler incorrectly [18]. Patients were seen to not comply with the individual steps of the inhalation technique, for example, holding the breath or the position the inhaler should be in. Patients were not able to generate the airflow that was required and therefore drug release from the inhaler was not sufficient affecting overall deposition of the drug [18].

1.3.3. NEBULIZERS

Nebulizers are available in three forms: jet, ultrasonic and vibrating mesh nebulizers. They are usually used when patient is required to take larger doses of drug and when medication cannot be given by the pMDI or DPI formulations. The main advantage of using nebulizers is that patients can just carry out normal (tidal) breathing and inhale the formulation over 10 – 15 minutes [38]. Ultrasonic nebulizers work by using a piezo electric crystal that vibrates at high frequency [24]. This causes the formation of droplets of the liquid and these are inhaled

by the patient. Vibrating mesh nebulizers come in two forms: active and passive. In these nebulizers the liquid passes through multiple apertures in order to generate an aerosol. A piezo electric crystal is used to generate energy in order to obtain suitable droplet size. Due to this, and the requirement of long periods of time over which the medication is being delivered, nebulizers are usually used in settings such as home and hospitals, where patients cannot also move around easily. Nebulizers are also expensive. The nebulizer causes a lot of impaction, within the device mouthpiece as well, and a lot of the drug remains in the device mouthpiece [4].

Nebulizers work by generating fine droplets of liquid which can be inhaled over long periods of time. Jet nebulizers are used more often than ultrasonic nebulizers. Jet nebulizers generally contain a compressor which uses air to convert the liquid into an aerosol, but have also been operated using a squeeze bulb [39]. Pressure, flow rate and type of gas used all affect the performance of the nebulizer. The pressurized gas is forced through a narrow nozzle generating a region of low pressure at the orifice. Aqueous solutions or suspensions can be delivered using a nebulizer [39]. There is a variation in the size of the particles produced, and large particles remain in the nebulizers, or by impaction deposit on the upper airways [3, 4, 39].

Formulation factors such as the viscosity and surface tension of the liquid being used is important as they can affect the formation of aerosols and deposition of the drug. The size of the aerosol droplets is reduced as the viscosity of the liquid is increased in jet nebulizers, but is directly proportional when ultrasonic nebulizers are used when using mesh nebulizers [40]. When an aerosol is produced used the compressed air system a drop in temperature occurs [39]. This low temperature may precipitate bronchoconstriction in patients with asthma or other conditions of the airways. The decrease in temperature may also cause precipitation of the drug from the formulation and this leads to instability of the drug solution.

Advantages of nebulizers [3, 4, 24, 27, 28, 39, 41, 42]:

- No technique or breathing coordination required and can be used for any age group and severity of the disease.
- High drug doses can be administered; for example 300 mg of tobramycin for *Pseudomonas* infections. This high dose cannot be delivered by pMDI but may be possible with improving technology for DPIs.
- Larger volumes can be used over longer duration

Disadvantages of nebulizers [3, 4, 24, 27, 28, 39, 42]:

- Prolonged treatment times

- Variability in size of aerosol produced between models and compressor makes
- Maintenance of equipment is required (e.g. cleaning for infection control)

Many new techniques are being developed to reduce the treatment time by personalizing aerosolization to an individual patient's breathing pattern and thereby maximizing the drug deposition. This is achieved by electronic systems such as Activaevo AKITA® and the Philips Respironics I-Neb®. AKITA® is able to control the flow rate, delivery volume and time and therefore it can optimize the aerosol release as required to target certain regions of the lungs and maximize the delivery. I-Neb® is a hand-held device which has two modes; tidal breathing and a targeted inhalation mode [41].

1.3.4. Other routes of delivery (Oral Route and Parenteral Route):

Some of the medication that is delivered by the pulmonary route can also be delivered by other systemic routes. Examples suggested are for anti-asthmatic and COPD medication, which is discussed in detail in Section 1.5 and 1.6. Medication such as salbutamol and other beta2- agonists are also available in oral formulations. This route is used for patients who cannot manage inhaled therapy. The disadvantage of oral therapy is that it causes a greater risk of systemic side effects. As corticosteroids (anti-inflammatory agents) are preferred to be given by inhaled route, the oral route is mainly used for prednisolone in step 5 of asthma therapy (details on the stepwise treatment of asthma are highlighted in Figure 1.4 in Section 1.5). Other drugs such as theophylline, mast cell stabilizers (e.g., sodium cromoglicate) and leukotriene antagonists (e.g., monteleukast) are available in oral formulation as tablets or granules. The parenteral route is mainly reserved for emergencies; patients that have severe acute asthma, which is life threatening and requires a fast and rapid response. Aminophylline (described in Section 1.9) is given by IV route and salbutamol (IV) is available [43, 44].

1.4. Barriers to drug delivery in the Airways

There are several different factors that need to be considered when formulating products for pulmonary drug delivery. These can be considered as those affecting deposition and those affecting absorption (for systemic delivery). As mentioned, the successful deposition of particles can be affected by patient dependent factors, for example breathing pattern or lung physiology and disease state [3, 4, 6].

Considering lung physiology, the humid conditions of the lungs can affect deposition [6]. The humidity in the lungs is 99.5% and therefore formulated particle size can change when present in the surrounding environment [1, 3]. Formulations synthesized with volatile aerosols

are reduced in size, but hygroscopic materials will increase in particle size or particles can agglomerate and increase in particle size [3]. Disease conditions and exposure to hazards can also affect the deposition. Airway geometry encourages impaction of the particles. Factors such as larger particles, greater velocity, greater bend angle of bifurcations and smaller radius of airways all affect deposition and cause deposition to be by impaction.

The site of deposition can affect clearance of the particles. The principal clearance mechanism in the upper airways is mucociliary clearance and in the lower airways is by phagocytic alveolar macrophages. The conducting airways are lined with ciliated columnar epithelial cells. There are also goblet cells and submucosal glands which secrete mucus that traps inhaled particulates. Foreign material deposited on the ciliated conducting airways is cleared by mucociliary clearance within 24 hours and are ultimately swallowed. Mucociliary transport can transfer particles that are inhaled to the pharynx where they are ingested [1, 4, 6].

Mucus clearance is the primary defense mechanism which has been evolved and protects the airways from inhaled toxins and infections [45]. The current mucus model is a 'gel-on-liquid' mucus clearance model where mucus gel is propelled on top of a 'watery' periciliary layer which surrounds the cilia [45]. In a study by Button et al (2012), a 'gel-on-brush' model was proposed where the periciliary layer is occupied by mucin proteins on the airway surface [45]. There are two components to this system which are i) a non-Newtonian, highly viscous mucus layer which traps the inhaled particles and ii) the periciliary layer to provide a favorable environment for cilia beating and lubrication in the cell surface [45, 46]. The brush prevents mucus penetration into the periciliary space and causes mucus to form a distinct layer [45]. The airway surface liquid is approximately 5-10 μm deep [46]. The mucus layer is composed of water (98%), salt (1%) and glycosylated mucin proteins (1%), secreted by specialized cells [46].

The cilia beat in a synchronized manner and are able to move the mucus gel upwards to the pharynx/ mouth where the particles are removed. This mechanism can be disrupted as a result of disease states that can affect the properties of the mucus, e.g. increase the viscoelasticity of the mucus such as in cystic fibrosis and COPD [45, 46]. The changes in the mucus properties can make it difficult for the movement of the cilia and this can cause defects in the cilia beating activity. The mucus is produced by goblet cells and submucosal glands [4, 6]. Particles in the alveolar region are engulfed by alveolar macrophages by phagocytosis and provide protection [4, 6]. The surfactant that lines the alveoli also can act as a physical barrier (0.1-0.2 μm thickness).

Particles can also be cleared by metabolic/enzymatic activity as a result of enzymes present in the lungs. There is little information on the enzymes and metabolism activity in the lungs.

Enzymes that are present include cytochrome (CYP) P450 enzymes; present at a lower concentration (5-20 times lower) in the lungs than in comparison to the liver [1, 3, 47]. The enzymes are distributed throughout the conducting airways and alveoli. Other enzymes present include flavin containing monooxygenases, mono-amine oxidases, aldehyde dehydrogenase, NADPH- CYP450 reductase enzymes are also present [1]. CYP450 enzymes present in the lungs include: 1A1, 1B1, 2B7, 2E1, 2F1 and 4B1.

For local drug delivery it is undesirable for the drugs to enter the systemic circulation, however, there is often a need for drugs to cross the cell membrane e.g. corticosteroids or the airway epithelium to reach the smooth muscle cells e.g. beta agonists. Small, lipophilic drug molecules can pass readily though the cell membrane and cross the airway epithelium via passive diffusion. Small, hydrophilic molecules most commonly cross the epithelium paracellularly [1, 25].

1.5. ASTHMA

Asthma is a common, inflammatory, chronic, reversible disorder of the lungs thought to be caused by response to allergens or, for some patients, genetic linkage [48]. Asthma can be defined as:

'*Chronic inflammatory disorder of the airways in which many cells and cellular elements play a role. Chronic inflammation causes an associated increase in airway hyper-responsiveness that leads to recurrent episodes of wheezing, breathlessness, chest tightness and coughing; particularly at night or early morning*' [6, 16, 19, 49-51].

Asthma is a chronic disorder affecting up to 300 million people worldwide (over 5% of the population), with an increasing prevalence [50, 52, 53] and results in 250,000 deaths/year [53]; it is predicted to affect an additional 100 million people by 2025 [17, 54]. Asthma and allergic disease prevalence has increased in the past decades in westernized countries [53]. In the UK, approximately 5.2 million people have asthma; in 2005 this resulted in 76,000 hospital admissions of children and adults [53]. Approximately, $56 billion is spent annually in the treatment of asthma worldwide [55].

The major characteristics of asthma are [6, 48, 56-62]:

- Narrowing of the airway, which obstructs the airflow (reversible airway obstruction). In asthma this is reversible by taking medication; however in chronic obstructive pulmonary disease (COPD) it is not reversible.
- Increased sensitivity to stimuli (bronchial hyper-reactivity). This is an abnormal, increased sensitivity to a wide range of stimuli, ranging from chemicals, cold air,

and some drugs which can lead to bronchoconstriction. Allergic asthma sufferers will experience an increased sensitivity to allergens; but once asthma is established in the patient, asthma attacks can be caused by various stimuli such as pollutants, cold air (drying of the airways), viral infections, exercise, etc.

- Increased number of inflammatory cells (inflammation of the airways) (eosinophils, mast cells and neutrophils)
- Increased secretion of mucus (mucus hyperplasia), causing further blocking of the airways and increasing the edema due to inflammation causing vascular leakage, which reduces air flow further.
- In some cases, damage to the epithelial cells occurs (epithelial shedding) in chronic severe asthma, remodeling of the airway wall tissue structure occurs, including increased bronchial smooth muscle content. This causes irreversible narrowing of the airways and limits the effectiveness of the bronchodilators leading to a condition similar to COPD.
- Acute severe asthma, also known as status asthmaticus, is not easily reversed and causes hypoxemia. This is an emergency and requires immediate hospitalization.

The rapid increase in the prevalence of asthma is as a result of increased urbanization and industrialization causing increased air pollution and exposure of an increasing population to the urbanized air [53]. It has been previously demonstrated that the exposure of particulate matter and a decrease in lung function [53]. Pollution sources include fuel combustion from vehicles, construction, industry and power plants. Indoor sources can also affect asthma prognosis, and poor ventilation and over insulation can result in poor air quality. Biological allergens react with specific IgE antibodies to induce an allergic state and originate from animals, mice, plants, insects, fungi and house dust mites. Pollen from trees, grass and weed can result in hyper-responsiveness of the airways [53]. Asthma is more common in the UK, Australia and New Zealand.

Asthma is classified as extrinsic (with an external cause) or intrinsic (genetic) disease [16]. Extrinsic causes are due to response to allergens and a subsequent development of IgE antibodies. This type of asthma tends to develop in childhood. Intrinsic asthma is seen to appear in adults, with no improvement unlike extrinsic asthma (where symptoms become less severe with age).

Asthma affects patients at any age with various severities [63]. Atopy and allergy are associated with early/childhood asthma with varying severities and asthma associated with adult onset is less associated with allergy but more due to eosinophilia, lack of exercise, obesity and other factors. Co-morbidities such as smoking, hormonal changes, infection and

occupation exposures can cause late-onset asthma [63]. Occupational asthma is the most frequent work-related respiratory disease in developed countries, of which 10% of cases are of bronchial asthma and between 15-25% of adult onset asthma is of occupational origin [64-66]. Removal from exposure to the sensitizing agent, which can be chemicals such as isocyanates, dust from grains/flour or insects, has been recommended as the most efficient therapeutic approach; although this may not significantly improve the prognosis of the patients [64].

Asthma can co-exist with rhinitis and studies have shown that a large proportion of patients with asthma (approximately 60-80%) will also have rhinitis [54]. These two conditions share a lot of pathological features as both are closely related to allergic sensitization [67]. In Europe, 25% of the population is affected by IgE associated allergic diseases [53]. In the UK it was seen that a lot of hospitalizations of patients was due to these diseases. Better treatment is being sought for controlling and managing rhinitis which may control asthma better too [68]. Patients may experience gastro-esophageal reflux disease (GERD) which can trigger asthma in certain patients, and subsequently seen in patients that there is an abnormal esophageal acid contact in pH tests carried out over a period of 24 hours. GERD can cause acid to elicit respiratory responses which decrease airflow, oxygen and increase respiratory rate [54]. Obesity can trigger asthma as it causes an increased stress and worsens symptoms [48, 69]. Children show a peak in their asthma-related exacerbations and hospitalizations 2-3 weeks after returning to school from their summer holidays [17]. Flu and colds can also precipitate asthma attacks [6].

Non-steroidal anti-inflammatory drugs (NSAIDs) such as aspirin have been shown to stimulate attacks in 5% of the asthmatic population [70]. Patients with aspirin-sensitive asthma, have an increased production and greater response to cysteinyl leukotriene which leads to the activation of IgE that is similar to that of atopic asthmatic patients [16]. Beta blockers, such as propranolol, (used in cardiac diseases) can cause symptoms of asthma as they act to inhibit adrenaline and thus cause bronchoconstriction by actions opposite to beta2 agonists.

An asthma attack consists of two phases – an immediate and a late/delayed response [16, 59, 61]. An immediate response is obtained when allergens are inhaled, which subsides over 2 hours. The immediate symptomatic response to the allergens is due to antigens and an IgE-induced mast cell degranulation. Patients produce an allergen-specific IgE that binds to the mast cell in the airways [16]. This causes a release of histamine, prostaglandin D2 and leukotrienes C4 and D4 upon degranulation of the mast cell. These chemical substances that are released cause the symptoms associated with asthma (bronchoconstriction and

mucus secretion) [6, 16]. This immediate phase occurs abruptly in patients and is caused mainly due to a spasm of the bronchial smooth muscles. Other chemotaxins and chemokines attract leucocytes such as eosinophils and mononuclear cells, which lead to the delayed/late phase response [6, 16]. In the immediate response, asthmatic patients experience an increased activation of T cells and, as a result, an increased production of cytokines from Th2 helper cells. Examples of these cytokines include interleukin (IL)-4, IL-9, IL-5 and IL-13 and granulocyte macrophage-colony stimulating factor (GM-CSF) [56, 71]. These cytokines cause a co-regulated allergic cascade [56]. Eosinophils are activated via IL-3, IL-5 and GM-CSF which are detected in the sputum [56]. IL-5 and GM-CSF, cause eosinophils to produce leukotrienes which cause damage to the epithelial surface and lead to airway hyper-responsiveness [16]. IL-3 and IL-4 affects responses of Th2 cells, mast cells and IgE receptor expression [56] leading to hyper-responsiveness of the airways to stimuli in some patients [16, 56, 72]. IgE has a large role in the allergen cascade and in disease chronicity and is dependent on the activation of Th2 cells (which secrete more cytokines and chemokines) [56]. IL-10 has inhibitory effects on the symptoms of asthma [56]. IL-9 promotes mast cells proliferation in murine models [56].

Patients experiencing nocturnal asthma may be experiencing the late phase response. Initiation of the late phase response takes place during the immediate attack, but the progression is slower. As this is a delayed inflammatory response, it includes activated eosinophils. A late phase response of the allergens has features of bronchoconstriction and airway inflammation, and occurs 3-12 hours later. Infiltration of neutrophils and eosinophils from mast cells and activated T cells, as a result of mediators occurs in the late phase. The eosinophils release leukotrienes, platelet-activating factor (PAF), proteins and eosinophil cationic protein (ECP). They also release IL-3, IL-5 and IL-8. Major basic protein (MBP) and ECP contribute to epithelial cell damage and cause an increased permeability to allergens, chemo-attractants and cytokines e.g. GM-CSF and exposure of C-fiber afferent nerve endings releasing pro-inflammatory tachykinins. ECP is an eosinophil-derived neurotoxin which plays a major role in the damage and loss of the epithelial surface. The growth factors present act on the smooth muscle itself, and cause hypertrophy and hyperplasia which can also cause release of pro-inflammatory mediators. The loss of the epithelial cells causes more access for irritant receptors and C-fibers to act on the surface and react to irritant stimuli [6, 16]. The release of preformed and generated mediators result in airway modelling with extracellular protein deposition and smooth muscle hypertrophy and increased goblet cell production [61, 66]. This causes the epithelium of the airway to be fragile, causing the sub-basement membrane to become thicker and an increased goblet cell

production resulting in an increased mucus production leading to endothelial leakage and mucosal edema [73].

Complement components can be potential targets for asthma treatment. CD4+ and T cells produce a T helper cell pattern of cytokine release which affects the overall prognosis of the disease. Cytokines such as IL-4, IL-5 and IL-13 contribute to bronchial hyper-reactivity and mucus hyper-secretion leading to activation of mast cells and eosinophils [74].

Airways in chronic asthma exhibit characteristics of a chronic wound with evidence of ongoing epithelial injury and repair, with increased mucus production and airway remodeling [66].

1.5.1. TREATMENT OF ASTHMA

The goal of asthma management is to achieve and maintain control of symptoms and minimize symptoms and exacerbations [29, 75, 76]. GINA guidelines suggest that asthma sufferers need to be managed so that they can live normal lives with few or no symptoms, no exacerbations, minimal need for reliever medication, normal lung function and no side effects [14]. However, inadequate control of asthma continues to be a problem in its treatment and, despite the understanding of the inflammatory basis of asthma and good medication guidelines and strategies, there are still a number of people at high risk of morbidity [54]. Asthma medication depends on the severity of the symptoms of the patient. Asthma can be classified as intermittent, mild, moderate or severe depending on the symptoms patients are experiencing and treatment is usually based on the severity of their asthma [44]. As the severity of asthma increases, the type of medication is changed accordingly to a step-wise treatment regimen (Figure 1.4) [38, 44]. In addition some patients may have co-morbidities with their asthma, which can make it difficult to treat the asthma.

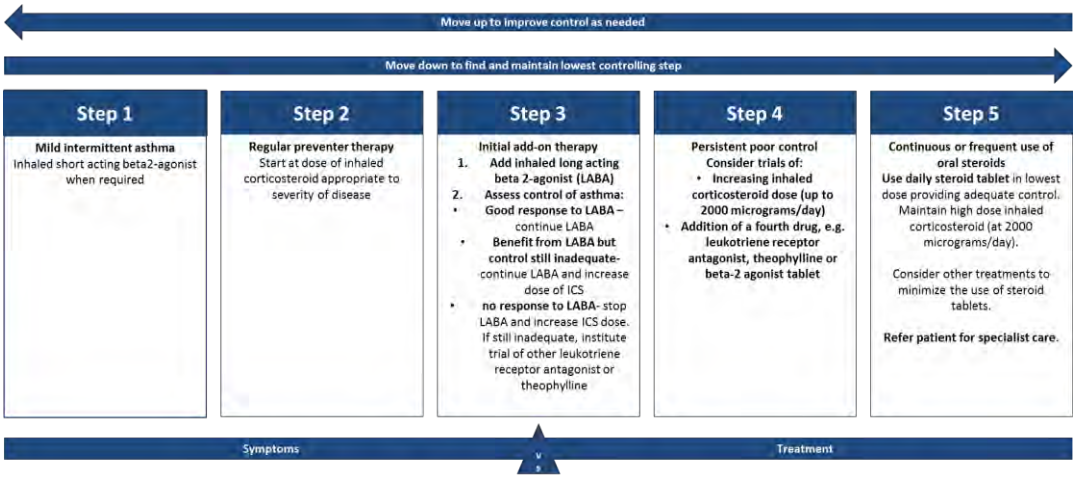

Figure 1.4 Summary of stepwise management of asthma in adults. Stepwise ladder adapted from BTS/SIGN Guidelines (2014) [44].

Non-pharmacological treatment of asthma includes avoidance of allergens (such as pets, house dust mites, food, tobacco and pollutants), relaxation therapy and breathing exercises, while immunization is also recommended [44].

Treatment of asthma can be divided into two major categories. These are relievers and preventers. Relievers are medication that are used for immediate response to asthma symptoms and can be used 'when required'. Preventers are medication that are prescribed for maintenance purposes and are used regularly rather than on a 'when required' basis.

Short-acting beta2-receptor agonists (SABAs), e.g. salbutamol, are the first medication prescribed to patients. They act rapidly at the site of action by activating adenylate cyclase (AC) to increase cAMP and reduce mediator release, e.g. histamine from airway cells. SABAs are usually given to patients when required, i.e., upon onset of symptoms and as they are rapid in action, they are able to offer immediate relief to the patient from their symptoms. The long-acting beta2-receptor agonists (LABAs) act over a longer period of time, and are given regularly, however they are associated with tolerance in patients. Beta2-receptor agonists are also the most effective, reliable and safe medication for asthma. If the treatment with beta2-receptor agonists is more aggressive then the response is also better. Adverse effects, such as tachycardia, tremor, nausea and vomiting are dose related [38, 61]. Medication such as salmeterol is available in inhaled form, given in combination with corticosteroid, fluticasone, or alone (Serevent®). These act for a duration of 10-12 hours and are able to control night time symptoms [38, 77]. Treatment of worsening asthma is by high dose of bronchodilators and with a course of steroid tablets [78]. For severe asthma, several studies have suggested the use of a nebulizer over pMDI with a spacer device [78].

Muscarinic receptor antagonists, such as ipratropium act by blocking the release of acetylcholine (ACh) from parasympathetic nerves and can also reduce mucus secretion. By antagonizing the effects of ACh, the toning of the bronchial smooth muscle is reduced and therefore constriction, and thus results in bronchodilation [77].

Corticosteroids, such as beclometasone and budesonide are anti-inflammatory agents. These are important in reducing the number of eosinophils and activation of macrophages and lymphocytes. Patients are initially started on inhaled corticosteroids (ICS) in Step 2. If ICS cannot control the symptoms of asthma, eventually an oral corticosteroid is given. ICS are associated with side effects such as hoarseness of the voice and oral candidiasis due to lack of rinsing mouth after use of the inhaler. This risk is reduced by rinsing the mouth after use. High doses of the corticosteroids can lead to increased risk of osteoporosis in patients and

growth retardation in children and hence require frequent monitoring [38, 44, 48, 66]. These sorts of side effects are more commonly seen with patients taking oral corticosteroids. Oral corticosteroids are prescribed at a later stage in the asthma treatment when symptoms are not controlled by the inhaled corticosteroids and other prescribed medications and are initiated at the lowest dose possible [44, 66]. Side effects are more severe than ICS and are more generalized. ICS have shown to reduce morbidity, mortality and recommended in guidelines; showing significant improvements in the FEV_1 and peak expiratory flow rate [79, 80].

Several combinations of SABAs and ICS are available. These agents both have different mechanisms of action for treating asthma. ICS are very potent agents and the most effective anti-inflammatory medication for the treatment of asthma. They are able to improve lung function, reduce symptoms and exacerbations [81]. They are able to reduce the hospitalizations and death compared to placebo. The LABA is added when a patient doesn't achieve control over their symptoms when they take only one of these agents (SABA or ICS). Studies carried out showed an increased support for fixed dose combinations as these show an improvement in lung function, and control of exacerbations of asthma symptoms especially when compared to monotherapy with these agents individually [81]. A combination is also cost effective. A twice daily dose is a good frequency and may allow patients to become more compliant with their medication [82, 83]. ICS are cornerstone of asthma therapy and added when asthma is not controlled with the use of only beta2-agonists. Mono-therapy of LABA is contra-indicated, and seen that the combination of two drugs is more efficient [84]. ICS can affect the mechanism of action of beta2-agonist and provide protective effects to avoid tolerance to beta2-agnonist in some patients by also increasing the transcription of beta2-agonist receptors [84, 85].

Mast cell inhibitors such as cromoglicate and nedocromil are also used to treat asthma. These drugs are less effective than corticosteroids and are only used in mild asthma, or asthma that is exercise-induced. The drugs are not effective in acute attacks. They are mainly used for controlling asthma in children.

Xanthine derivatives, such as theophylline and aminophylline are bronchodilators and also possess some anti-inflammatory action. Theophylline is only available as oral dosage formulations including slow release tablets. Aminophylline is available as an intravenous injection as it is more water soluble. They act by inhibiting phosphodiesterase (PDE), which is responsible for breaking down cAMP which causes an increase in the concentration of acetylcholine and therefore increasing asthmatic symptoms such as bronchoconstriction. Theophylline causes a lot of systemic side effects giving it a narrow therapeutic range.

However, it is reported that some patients suffer from side effects in the therapeutic dose range. Therefore, these compounds are used as second line drugs but are particularly useful in controlling symptoms in steroid-resistant asthma.

Anti-leukotriene therapy includes drugs such as monteleukast, an inhibitor for the cysLT receptor (LTC4/D4) and zileuton, a 5-lipoxygenase inhibitor. The effects of these drugs are long lasting, and they are used in severe asthma, along with corticosteroids. Histamine antagonists are not shown to be useful in asthma; however sedating anti-histamines may be able to alleviate some symptoms. Omalizumab, a recombinant anti-IgE antibody has shown to be effective by reducing IgE levels [44, 66, 86].

1.6. CHRONIC OBSTRUCTIVE PULMONARY DISEASE (COPD)

COPD is a major global health problem, with a prevalence of 5-25% among adults worldwide. It is presently among the top ten most common chronic health conditions and is associated with restriction in daily activities leading to a poor quality of life and an increasing social and economic burden [87-91]. By the year 2020, COPD is expected to become the third leading cause of death worldwide [87, 88, 92-97] with approximately $50 billion being spent on COPD treatment per year [55].

The NICE guidelines define COPD as '*airflow obstruction is defined as a reduced forced expiratory volume in 1 second (FEV_1)/FVC ratio, such that it is less than 0.7 and if FEV_1 is equal, or greater than 80% predicted normal, COPD should only be diagnosed if there is a presence of respiratory symptoms such as breathlessness or cough*' [43]. The airflow obstruction that is present is as a result of a combination of airway and parenchymal damage, which is mainly as a result of the chronic inflammation caused due to smoking. Based on the NICE guidelines, COPD is now the preferred term for patients who were previously diagnosed having chronic bronchitis (CB) or emphysema [43].

Previously, COPD was defined as '*a process characterized by the presence of chronic bronchitis or emphysema that may lead to the development of airway obstruction; airways obstruction may not be present at all stages of the process; the airway obstruction may be partially reversible'* [98].

COPD is characterized by an enhanced inflammatory response to inhaled particles and gases [99]. COPD is strongly associated with smoking (at least 20-30% smokers develop COPD) and is usually a progressive disease characterized by airflow limitation that is not fully reversible [88, 91, 92, 100-103].

Symptoms of COPD are chronic and progress over a period of time; these symptoms include dyspnea, cough and sputum production [94]. There are several stages of COPD and these are classified according to the symptoms and signs such reduction in FEV_1 (Table 1.1). Patients experiencing cough and sputum, which are the first symptoms to develop, usually neglect these symptoms. When patients experience dyspnea, they seek medical consultation as this is persistent and progressive and can affect the quality of life. Patients with severe COPD can experience weight loss, anorexia and infection with hemoptysis. This can lead to complications such as cor pulmonale, pulmonary hypertension, depression and/or anxiety [91, 102]. Night time awakening, ankle swelling and occupational hazards are symptoms that should be considered in patients with COPD [43]. CB and/or emphysema are now features and symptoms of COPD which are used in the diagnosis of COPD. CB is associated with airway obstruction caused by chronic mucosal inflammation, mucus gland hypertrophy and mucus hypersecretion coupled with bronchospasm [16, 96, 97]. Emphysema is caused by a progressive destruction and dilatation of the alveolar septa and capillaries, leading to the development of enlarged airways and airspaces, decreased lung elastic recoil and increased airway collapsibility [91, 96, 97, 100-103].

Table 1.1 The classification of COPD and signs patients would express at each stage. [43, 94, 104]

Stage	Classification	Signs
1	*Mild*	$FEV_1 \geq 80\%$ predicted; chronic cough and sputum present, may or may not be aware
2	*Moderate*	$50\% \leq FEV_1 \leq 80\%$; shortness of breath, exertion, cough and sputum production. Patients seek medical advice
3	*Severe*	$30\% \leq FEV_1 \leq 50\%$; greater shortness of breath, decreased exercise capacity, fatigue, repeated exacerbations and great impact on quality of life.
4	*Very severe*	$FEV_1 \leq 30\%$ predicted or ≤50% predicted with chronic respiratory failure. Can lead to effect on the heart (cor pulmonale) and increased jugular venous pressure with pitting ankle edema. Quality of life is very appreciably impaired and exacerbations may be life threatening.

COPD exacerbations are defined as 'a sustained worsening of the patients symptoms from their usual stable state which is beyond normal day-to-day variations, and is acute in onset' [43]. The symptoms that are reported in exacerbations are worsening of the common

symptoms that are reported in patients with COPD, for example worsening of their cough, breathlessness and an increased production and/or color change of the sputum.

Cigarette smoke causes an accelerated decline of lung function and therefore a greater need for rescue medicine [105]. There's an increasing number of smokers in developing countries, and a failure of developed countries to stop smoking [95]. Smoking history in patients can vary a great deal and therefore affect the overall severity of the disease [106]. COPD can also be caused by inhalation exposure to tobacco, occupational hazards (e.g. dust, chemicals; organic or inorganic, fumes, indoor or outdoor air pollution (poor ventilation), severe childhood respiratory infections, socioeconomic status (inversely related but affected by exposure to hazards) [94, 98, 104, 106].

COPD severity is measured by spirometry, which is a reproducible and widely-used technique and should be carried out on patients at risk, for example smokers, ex-smokers and patients who have CB [43, 94]. Other factors that should be measured include the FEV_1, breathlessness based on the scale and specified in the guidelines, health status, exercise capacity, body mass index, and the oxygen and carbon dioxide concentration [43]. Airway inflammation for patients suffering from COPD is slightly different to that of patients suffering from asthma. There is an increase in the T-lymphocytes and macrophages within the airway wall and infiltration of mononuclear cells and macrophages in the peripheral airways. COPD patients show an increase in the neutrophils and IL-8 [105].

COPD is complicated by frequent and recurrent acute exacerbations, respiratory infections are the main risk factor; but exposure to pollutants, allergens, sedatives, congestive heart failure, pulmonary embolism can also cause exacerbations and increase the disease severity [107]. Patients suffering from COPD show a reduced activity of histone deacetylases (HDACs) which can contribute to the abnormal inflammatory response that characterizes the disease [99, 108]. Cigarette smoking also reduces the activity of histone deacetylation which is required by corticosteroids to switch off inflammatory genes [95, 109]. Exacerbations in COPD patients can result in increased NF-κB activation which results in a burst of airway inflammation. This causes oxidative and nitrative stress. The increase in neutrophils, cytokines (for example tumor necrosis factor (TNF)α), IL-8 and IL-6 can also affect and impair the function of HDAC [99].

1.6.1. TREATMENT OF COPD

Inhaled therapy is the cornerstone of the pharmacological treatment of patients with COPD with two major classes of drug: bronchodilators and anti-inflammatory treatment. To

maximize the effects of the medication, patient education is the key. Treatment of COPD, like asthma, needs to be individualized for the patient as discussed previously [23, 110-113].

There are no current therapies preventing disease progression or to reduce mortality [114]. The only success has been found in smoking cessation [88, 95, 105, 115] which results in slowing down disease progression, improving respiratory symptoms and improving the quality of life [93, 116]. Even after smoking cessation, the inflammation process continues [95]. It is important that a smoking history and determination of 'pack years smoked' is determined in order to be able to manage stable COPD. Some patients may get pharmacological or behavioral support to aid smoking cessation [43, 117].

Short acting beta2- agonists and muscarinic antagonists should be the initial treatment to relieve breathlessness and exercise limitations. Inhaled corticosteroids are also prescribed for the treatment of COPD. The combination treatment of LABA and ICS, similar to asthma treatment, is also recommended in the treatment of COPD. This combination is prescribed to patients when the FEV_1 is less than 50% than predicted. If the FEV_1 is greater than 50% than predicted, a long acting muscarinic antagonist (LAMA) or LABA is preferred (Figure 1.5) [43].

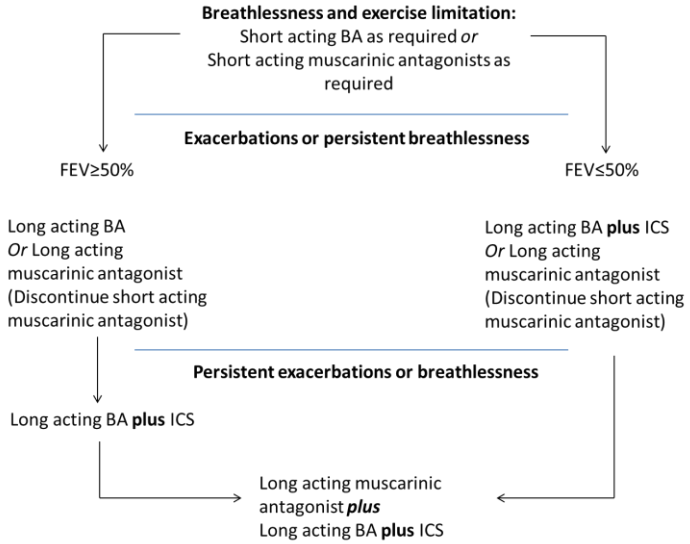

Figure 1.5 Use of inhaled therapy in COPD adapted from BNF [38] based on the NICE guidelines [43]. BA: Beta 2-agonist, ICS: inhaled corticosteroid, FEV: FEV_1

There are known beneficial effects of LABAs in the treatment of COPD where they are able to reduce the frequency and severity of exacerbations. A study carried out by Kim et al (2014), showed benefits of using LABAs which was associated with fewer hospital visits.

The symptoms and the frequency of exacerbations were also reduced. Patients taking a LABA and ICS showed better control of their symptoms and improvement of lung function, with a decreased risk of side effects [87]. The beneficial effects of inhaled beta2-agonists are seen in severe exacerbations of COPD in patients; where an increased FEV_1 is seen [118].

ICS doses are increased in patients with severe disease, frequent exacerbations and an overlap of both asthma and COPD [119]. The use of ICS is well established and reduces the risk of hospital admissions [120]. A study of patients who continued to smoke during treatment of COPD showed that addition of budesonide to the treatment of patients with COPD showed improvement in patients, but also showed greater improvement for patients who smoked less. Anticholinergic drugs are able to improve the exercise capacity, health status and reduce exacerbations. These are commonly prescribed with corticosteroids [88].

As the process of inflammation is different in asthma and COPD, the treatment approach is also different [114]. Unlike in asthma, inflammation in COPD is relatively insensitive to corticosteroids [121]. However, combined inhaler treatment of corticosteroids and bronchodilators results in improved lung function and helps prevent exacerbations [121]. ICS are added to bronchodilator therapy in patients suffering from severe to very severe COPD [116]. The benefit to risk ratio should be assessed when adding an ICS to an optimized maintenance therapy that is obtained with a LABA in patients with stable COPD [116]. This combination shows an improvement in the quality of life, improvement in lung function and a reduction in exacerbations; but not a significant reduction in the disease progression [121, 122]. Budesonide and formoterol is a commonly prescribed and studied combination [123].

Methylxanthines, such as theophylline, are relegated to third line treatment in COPD [120]. Theophylline use is limited but it is useful in patients with stable COPD; where worsening of the condition is seen in patients withdrawn from treatment with COPD and for patients unable to use inhaled therapy [43, 101, 121, 124]. Theophylline is prescribed when patients remain symptomatic on monotherapy with beta2-agonist or an anticholinergic [43].

Other oral therapy includes treatment with mucolytic drugs. This is especially considered in patients who have a production of sputum and chronic cough; however these are not recommended in patients to prevent exacerbations and should only be used if they present symptomatic improvement in the patient. Other oral therapies that can be recommended include antioxidants, anti-tussive therapy [43]. Oral antibiotics as prophylactic therapy are not recommended in patients with stable COPD.

Some patients with more severe disease require rehabilitation programs which are tailored to the individual patient [43, 44]. These programs have been shown to have a lot of success; for

example by Jain et al. (2014) who carried out a Chronic Lung Disease Program (CLDP) modelled for the care of patients with recurrent exacerbations of severe asthma and COPD [55].

1.7. COMPARISON BETWEEN ASTHMA AND COPD

There are many features that can distinguish between asthma and COPD [92]. These are highlighted in NICE Guidelines and shown in Table 1.2 [43].

Table 1.2 Clinical features that differentiate COPD and asthma. This table is adapted from the NICE guidelines, 2010 [43].

Factor	**COPD**	**Asthma**
Smoker/ex-smoker	Nearly all	Possibly
Symptoms under the age of 35	Rare	Often
Chronic productive cough	Common	Uncommon
Breathlessness	Persistent and progressive	Variable
Night time waking with breathlessness and/or wheeze	Uncommon	Common
Significant diurnal or day to day variability of symptoms	Uncommon	Common

Asthma and COPD are both characterized by airway obstruction which is variable and reversible in asthma, but progressive and irreversible in COPD [125]. Both diseases have chronic inflammation of the respiratory tract which is mediated with increased expression of inflammatory proteins especially during acute exacerbations. Despite similarities in the chronic diseases, there are marked differences in the pattern of inflammation with involvement of different inflammatory cells and mediators which as a consequence have different inflammatory processes and differing responses to therapy [125]. Inflammation in the asthma occurs in the large conducting airways with some effect on the smaller airways but no effect on the lung parenchyma. In COPD, the small airways and lung parenchyma are affected with a similar inflammation process. This is presented as small airway obstruction and emphysema which can occur together or alone [16, 94, 96, 97, 125, 126]. This difference in distribution is a result of the distribution of inhaled agents for example allergens in asthma and tobacco smoke in COPD which causes a progressive air flow limitation in the airways [125].

T cells are important for both diseases but there are different subsets involved in the process of inflammation and therefore an effect on the structural changes. B cells are also involved in these processes. There are many cytokines involved in both diseases which are regulated

by NF-κB which is activated by epithelial cells and plays a role in the airway inflammation process.

Histopathological assessment of asthma airways has shown that there is an infiltration of eosinophils, activated mucosal mast cells and activated T cells[125]. The major difference in COPD is that there is no evidence of mast cell activation but there is an infiltration of T-cells and an increase in neutrophils in the airway lumen. In COPD there is also fibrosis around the small airways which is reviewed (by Barnes) to be the main cause for the irreversible airway narrowing in patients with COPD [125]. As a result of cigarette smoke and irritants leading to chronic irritation, but shows pseudostratification. The other major difference is the destruction of alveolar walls due to protease- mediated degradation of connective tissue elements [125].

Mast cells, releasing histamine, in asthma is as a result of allergen triggers (which further release IL-4, IL-5, IL-13) causing bronchoconstriction but in COPD the role of mast cells is minimal. Granulocytes inflammation that is involved in asthma is eosinophilic and in COPD is neutrophilic. Increased neutrophils are also detected in the sputum of patients with COPD and correlate to the disease severity. Macrophages are increased in both diseases- but greater in COPD as a result of monocytes [125].

As mentioned, there are different subsets of T-cells that are involved in the inflammation process [125]. In asthma, an increase in $CD4^{+}$T and Th2 cells which play a major role in the inflammation results in secretion of IL-4 and IL-13 (allowing IgE production by B cells), IL-5 (resulting in eosinophilic differentiation), IL-9 (affecting mast cell differentiation). In COPD, Th1 cells are involved and lead to production of interferon-γ (IFN- γ) and TNF. This is observed in patients with severe asthma [125].

IgE is observed in asthma, but is not observed in COPD as reviewed by Barnes (2008) [125]. An increase in the severity of the disease results in B cells being organized around T-cells. Dendritic cells have an important role in regulation of Th2 cells in response to allergens in asthma; in COPD smoking causes an increase in the dendritic cell population but the role is unclear [125].

Another difference between asthma and COPD is observed in the treatment when corticosteroids are used. As described in the earlier section, (Asthma: Section 1.5), corticosteroids are the mainstay of treatment of asthma and lead to suppression of inflammation. In COPD, there is a poor response to corticosteroids as a result of reduced HDAC (described in Section 1.6) as a result of increased oxidative and nitrative stress. This is only seen when asthma is severe in patients [125].

1.7.1. PATIENT FACTORS IN ASTHMA AND COPD

The main problems with the treatment of asthma and COPD are related to compliance, for example in patients with symptoms controlled, therapy is stopped by the patient thinking their treatment is sufficient and complete, and poor inhaler techniques. The latter can lead to problems with delivery of the drugs to the target area of the lungs [28, 37, 127-129]. Patient education is the key; the most ideal formulation can also lead to insufficient treatment of asthma if it is not administered correctly. Without appropriate training, it can lead to poor control of symptoms and affect the whole prognosis of the disease [130]. It is commonly seen in patients that they use their medication until they become asymptomatic and stop, not understanding the importance of continuing regular therapy [129].

Poor adherence to treatment can be as a result of complicated treatment regimen and poly-pharmacy [26, 75]. Compliance can be improved by simplifying dosing frequency, optimizing drug delivery and relieving symptoms with quick onset of action of the drugs. Along with compliance issues, many patients may have co-morbidities, such as presence of psychiatric illnesses; which can make the treatment more difficult. Asthma, for example, is more difficult to control in older patients, and results in higher morbidity and mortality compared to younger asthmatic patients; this can be due to long-standing asthma, delayed diagnosis and under treatment of asthma [14, 131]. When inappropriately treated or patient receives sub-optimal treatment, the complications associated with asthma can result in increased exacerbations and hospital admission [50, 132].

One problem identified with the medication for asthma is that there is overuse of SABAs but underuse of ICS. As SABAs are the most effective medication because of their rapid bronchodilation, it leads to them to be overused ‘when required’, even when given in a combination product of corticosteroid and SABA. The over use of SABAs masks the underlying inflammation and doesn’t treat it, and therefore patients underestimate the severity of the disease and overestimate the level of control of their asthma symptoms [133]. This overuse of SABAs has made the GINA suggest an increase in the maintenance therapy and a reduction in reliever therapy [54]. In a survey, 70% of patients had not used an ICS in the previous month. These data suggest that patients are unaware of why they are using ICS medication. Not using the ICS increases the inflammation in the airways, leading to more threatening exacerbations. A gap in the self-management education of asthma sufferers may be the reason why patients find taking their reliever medication is more important than taking their maintenance therapy [17, 134]. It has been observed that some patient’s behavior towards their ICS treatment showed that they were concerned about the negative/ adverse effects of the inhaled corticosteroids (ICS) [135]. Patients have also have shown ‘acceptance’

of suboptimal asthma control and the associated symptoms with the thought that they aren't able to further improve their quality of life [17].

Patient factors are extremely important in determining where and how the drug will be deposited in the lungs. Breathing patterns when using a device for inhaling the medication is important in patient education for the control and treatment of asthma and COPD. An increased volume of inhalation will increase the distribution of the particles in the lungs. Faster breaths will also increase the turbulence of air flow in the airways, and this will result in particles depositing by impaction, this can be avoided by the patient inhaling more slowly. In addition, holding the breath after inhaling drug will increase the time available for particles to deposit by sedimentation and diffusion. Thereforea slow, deep breathe which will allow maximum deposition of the drugs in the lungs.

Patient's disease states also affect the deposition of particles in the lungs. Patients who have infections and smokers may experience an increase in mucus production, and this may decrease diffusion of the drugs through the mucus layer even if successful deposition is achieved. In COPD, it is important for patients to understand that in order to obtain maximum effect from treatment, smoking cessation is important; however some patients continue to smoke [91, 102, 136].

Other noted factors in the poor adherence of treatment for asthma include low income, being from an ethnic minority and poor patient-physician understanding [135]. It is important that asthma treatment is individualized for each patient, and important to take into consideration their preference in consent with training and regular monitoring of the inhaler technique [9, 31].

Many COPD patients remain undiagnosed, or not diagnosed according to the specification in the guidelines which leads to an increased risk of mortality in patients [92, 117, 137]. Patient education is extremely important to improve disease knowledge, eliminate risk factors and to provide recommendations for treatment options, improving quality of life and reducing exacerbations [137]. Lower socio-economic status is associated with an increased prevalence of COPD [100]. Middle aged patients usually suffer from COPD as a result of their long term history of smoking and therefore COPD can develop with diseases already present as a result of smoking or aging; careful attention needs to be paid when treating co-morbidities (such as ischemic heart disease or diabetes mellitus) as it can affect the quality of life [94, 114, 117]. Untreated and inadequately treated COPD leads to poor quality of life, permanent deterioration in health status and drives healthcare and social costs up [137]. Poor quality of life in patients suffering from COPD leads to an inability of people to work, social isolation, depression with an effect on the partner of the patient too [88].

1.8. BUDESONIDE

Step 2 of chronic asthma management requires the introduction of inhaled corticosteroids (ICS) such as budesonide, beclomethasone and fluticasone. Corticosteroids work as anti-inflammatory agents in the treatment of asthma.

In asthma, allergic pathways that contribute to airway dysfunction are largely sensitive to corticosteroids [66, 86, 138]. They have several complex molecular mechanisms of action. They act on glucocorticoid steroid receptors to alter the transcription and translation of mRNA and therefore synthesis of new protein (Figure 1.6). Corticosteroids penetrate cells and bond to the specific receptors present in the cytoplasm and expose a glucocorticoid-receptor complex to DNA, are transported to the nucleus, where there is an increased affinity for interaction with DNA. This interaction leads to an alteration in response (increase or decrease) of genes, which thus further affect the encoding of mRNA and proteins. This is a long term action, and takes a longer period of time to work (over a period of days) than it does for beta2-agonists such as salbutamol. Therefore ICS should be taken regularly and not 'as required'.

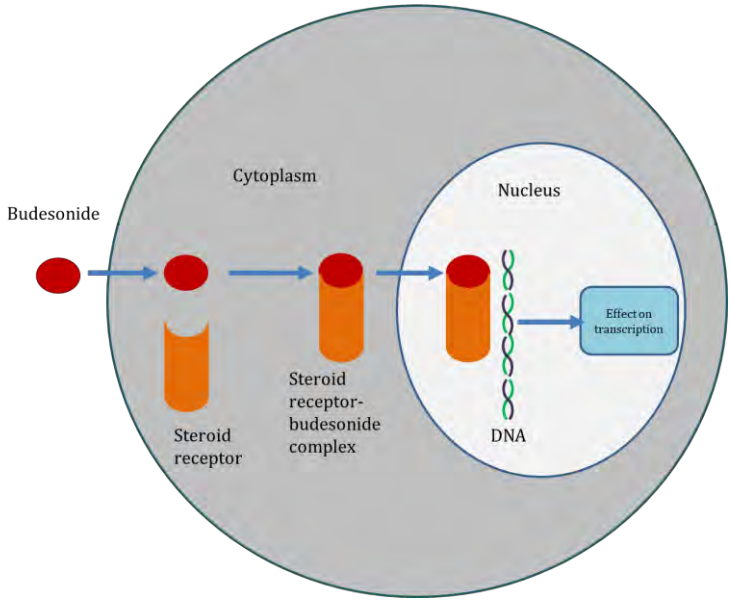

Figure 1.6 Mechanism of action of corticosteroids including budesonide: Corticosteroids act on the steroid receptor to form a steroid-receptor complex which then moves to the nucleus of a cell and acts on DNA to alter gene expression. Schematic diagram adapted from Fahey (1998) [139].

Corticosteroids also inhibit Th2 cytokine production, especially IL-4 and IL-5 and in this way they also reduce the production of IgE and eosinophils, basophils and mast cells [66, 85, 140]. In the lungs, this inhibits the IgE-induced release of histamine and leukotrienes which

therefore also reduces the hypersensitivity episodes. Glucocorticoids are also able to inhibit the production of inflammatory mediators by increasing production of anti-inflammatory mediators due to an increased production of lipocortin, which inhibits phospholipase A2 and thus reduces levels of arachidonic acid, and therefore reduces inflammation [16, 68].

There are ideal pharmacological characteristics that can optimize the effectiveness of ICS: low oral bioavailability, high pulmonary bioavailability, high receptor binding affinity and long pulmonary retention time [84]. Budesonide (Figure 1.7) is a 16, 17 acetal series, non-halogenated potent glucocorticoid exerting local anti-inflammatory effects in the lung [68, 85, 140]. Budesonide has potent glucocorticoid activity and weak mineralocorticoid activity [85, 140] and is a 1:1 racemic mixture of two epimers (22R and 22S) which do not interconvert [140]. Budesonide is the corticosteroid agent with the safest side effect profile as it has high anti-inflammatory effects and low systemic effects due to a high receptor affinity and high selectivity [127]. Budesonide has a low water solubility of 45.7 mg/L and dissolves in the bronchial secretions at the site of deposition. It has and a logP of 2.17, and is moderately lipophilic [85]. This lipophilicity allows rapid uptake in the airway mucosa and reduces the amount of drug cleared by the mucociliary clearance [68, 141]. Budesonide is able to show an improvement in lung function within a time span of 1-4 hours and the response with regards to inflammatory markers within 4-6 hours. Budesonide is extensively metabolized by cytochrome P450-3A which catalyzes its transformation into two other metabolites (16α-hydroxyprednisolone and 6β-hydroxybudesonide) [85, 140, 142].

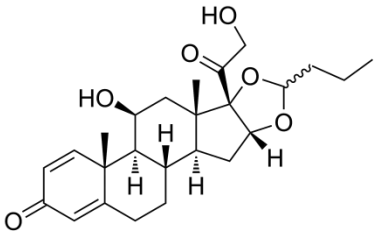

Figure 1.7 Chemical structure of corticosteroid, budesonide [141]

A proportion of inhaled drug will deposit at the back of the throat and be swallowed. The oral bioavailability is 11% for budesonide and this results in lower side-effect risk as little of the swallowed drug will be absorbed. The pulmonary bioavailability is higher, and is approximately 15-30% and the pulmonary retention time is also long for budesonide [84]. Due to a low proportion of the drug reaching the target site in the lungs, corticosteroids are required to be very potent. Budesonide is 50 times more potent than dexamethasone [143] and exhibits 200 times greater affinity to glucocorticoid receptors than cortisol in *in vitro* models

[85]. As there is a high local activity, only a small dose of the corticosteroid is required [85, 140]. Doses of budesonide and other corticosteroids vary between patients and will also depend on the severity of symptoms. If not taken regularly, structural changes to the airway can occur (i.e. remodeling) which can reduce lung function and worsen the symptoms, and therefore increase the need to take rescue medication such as SABA [144].

Budesonide forms lipophilic esters and is retained in the airways for a prolonged period of time and acts as a local depot for drug activity. As the esters are hydrolyzed, active budesonide becomes more available to the receptors [85]. This is discussed in further detail in Chapter 5.

Budesonide is the second most prescribed ICS in a fixed dose combination. The combination of budesonide/formoterol was preferred by approximately 20% of physicians [145]. Budesonide alone was preferred by 52% of physicians; the reasons were familiarity of the drug, effectiveness, flexible dosing with a large clinical trial study evidence [145]. Budesonide is available as a pMDI, DPI and nebulizer. It is available as Symbicort® in combination with the beta2-agonist, formoterol. Pulmicort® is currently the other product of budesonide available in the UK [38]. Monotherapy of the two drugs, if the patient is fully compliant, can ensure that the drugs are being taken, but the LABA, in particular, cannot be used alone or when required as it can cause increased risk of morbidity and mortality. Therefore to ensure that it is taken with the ICS a fixed dose combination is preferred [69]. It has been shown that the combination of the LABA and ICS are able to control asthma better, and trials have been able to highlight that the use of either as monotherapy is not as effective as a co-therapy [146, 147]. The combination shows a protective effect on exacerbations [96, 97, 146, 148]. The STAY study [148], carried out to see the effects of budesonide and formoterol, suggested that the corticosteroids reduce total exacerbations significantly when given for maintenance. They are also able to reduce night time symptoms. If ICS therapy is started early, the risk of inflammation that is attributed to remodeling can be reduced or even reversed which can improve the lung function [149].

Systemic side effects of corticosteroids include adrenal suppression, osteoporosis, growth inhibition, increased glucose leading to diabetes; increased risk of infection, Cushing's syndrome and Addison's crisis when there is a sudden withdrawal of the corticosteroids. These side effects are usually seen with oral corticosteroids. The local side effects associated with ICS include *Candida albicans* infection of the oropharynx. The risk of oropharyngeal thrush is further increased when the patient does not rinse their mouth after use of the inhaled formulation. The risk can be reduced by decreasing the frequency and dose of the inhaler or by using a spacer device. Inhaled corticosteroids can also cause

weakness and hoarseness of the voice. Growth inhibition is seen in children using inhaled corticosteroids [38]. Inhaled budesonide is also currently being explored for the treatment of inflammatory bowel disease [127].

In this study, budesonide is being used because of its hydrophobicity and the safe side effect profile described above. More details on the encapsulation of hydrophobic drugs and the methods used for encapsulation are described in Chapter 2.

1.9. THEOPHYLLINE

Bronchodilators have been used in the treatment of asthma and COPD for over 70 years [150-153]. Theophylline was a popular drug, but over the years, its popularity has declined due to the introduction of more effective bronchodilators (such as salbutamol), with lower risk of side effects. Theophylline was a widely prescribed drug, mainly due to it being inexpensive [151, 154].

The best known methylxanthines are naturally present in food and beverages. These include theophylline, caffeine and theobromine. Theophylline is a 1,3-dimethylxanthine and is present in very low concentrations in tea and coffee.

Theophylline has been relegated to a third line bronchodilator, but is still recognized as a useful treatment in patients with severe COPD. It is given in step 3 of asthma treatment, when there is still the presence of symptoms even after the use of a beta2-agonist, when required, and a regular ICS [6, 16, 143, 155-158]. Theophylline is added rather than doubling the dose of the two drugs. It also shows control in severe asthma patients when not controlled by ICS [151]. In COPD, theophylline is added to inhaler bronchodilator therapy in patients with more severe COPD and gives additional clinical improvement when added to LABA [152, 159].

The relegation of theophylline was reinforced by guidelines [151]. Interestingly, there is evidence that when theophylline was withdrawn from treatment, it led to significant clinical worsening of the disease [152]. Theophylline is effective in exercise and allergen-induced asthma. The slow release formulation of theophylline was seen to be beneficial in controlling nocturnal asthma symptoms and obtaining better control of plasma concentration [160].

Theophylline ($C_7H_8N_4O_2$) has a molecular weight of 180.064 g/mol (Figure 1.8). At 25°C, theophylline has a water solubility of 7.36 mg/mL. The logP of theophylline is very low, -0.02. Theophylline can be present as an anhydrous form or hydrous form [133].

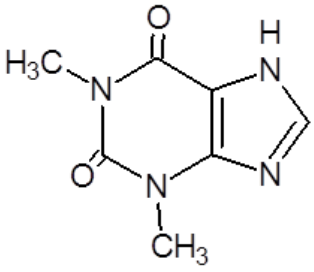

Figure 1.8 Chemical structure of theophylline [133]

Aminophylline, a mixture of theophylline and ethylenediamine is more water soluble than theophylline (1 g/5mL) [161]. Aminophylline is hence suitable for administration as a parenteral formulation and is given in acute severe asthma. A modified release formulation is also used in the treatment of asthma. A hypersensitivity reaction to the ethylenediamine leading to urticaria and pruritus is known, and in some cases more severe hypersensitivity reaction thrombocytopenia [38].

Theophylline is able to relax human airway (bronchial) smooth muscle *in vitro* by non-selective inhibition of PDE enzymes that break down cyclic nucleotides and therefore increase the concentration of cAMP (Figure 1.9). The enzyme phosphodiesterase is responsible for the breakdown of cAMP. Phosphodiesterase-4 (PDE4) is expressed in neutrophils, T-cells and macrophages and when this is inhibited (non-selectively) by theophylline, this controls lung inflammation [114]. This effect however requires a high plasma concentration of theophylline which can cause toxic effects. At 10-20 mg/L theophylline causes relaxation of the airway smooth muscle as a result of phosphodiesterase inhibition (by an increase in cAMP which reduces PDE3 and PDE4 (and cGMP and PDE5) [151, 162]. For this reason, theophylline is not tolerated well in many patients [150-152]. The concentration required for this effect is 20 mg/L. PDE inhibition by theophylline is non-selective and results in the incidence of side effects [89, 98, 101, 126, 151, 154, 163-166].

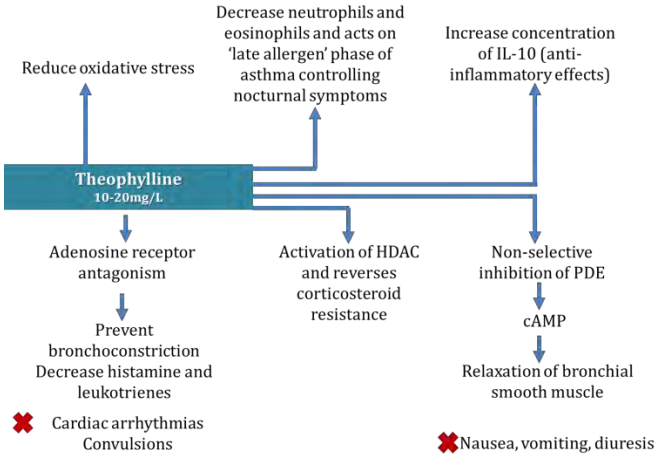

Figure 1.9 Mechanism of action of theophylline and the adverse effects caused by theophylline due to antagonism of PDE or adenosine receptors (adapted from mechanism of actions described in Section 1.9)

Theophylline has inhibitory effects on the airway inflammation at concentration less than 10 mg/L. These anti-inflammatory effects are different to those of high dose corticosteroids [152, 167]. These effects of theophylline occur at concentrations lower than those causing bronchodilator effects and may account for the worsening of the condition after theophylline is withdrawn from treatment [152, 168].

Theophylline has a greater effect on the late response in asthma where it is able to control nocturnal symptoms of asthma and also inhibit the influx of neutrophils and eosinophils in the early morning [150-153, 169, 170]. Patients on theophylline present low concentration of eosinophils in bronchoalveolar lavage and sputum of patients. Upon withdrawal, these concentrations are increased [151]. Adenosine receptor antagonism by theophylline prevents constriction of the airways and release of histamine and leukotrienes [151]. Theophylline also enhances release of IL-10 which has anti-inflammatory effects causing a reduction in serotonin, but this effect occurs at high concentrations [151]. Theophylline has an effect on preventing the translocation of pro-inflammatory transcription factors (NF-κB) and reducing the expression of anti-inflammatory genes and therefore has a protective effect [151]. Theophylline is able to promote apoptosis of eosinophils and neutrophils and reduce the effects of oxidative and nitrate stress associated with COPD [151, 152, 171]. The mechanism of action of theophylline against allergen-induced asthma is by reducing methacholine and histamine reactivity by inhibiting mast cell degranulation and therefore preventing the release of the mediators that cause bronchospasm and airway inflammation [143].

The reduced HDAC function in COPD patients decreases the effect of ICS. However, theophylline is able to enhance HDAC activity and when co-administered with steroids; the function of HDAC is reverted and increased [95, 99, 108, 124, 151, 152, 172]. Thus theophylline improves the effectiveness of the ICS and improves lung function when added to a

glucocorticoid regimen and is how the anti-inflammatory action of theophylline is carried out [153]. Theophylline has additional mechanism of action by PDE inhibition. Theophylline affects HDAC at low concentrations (5 mg/L) and this action is independent of its effect on PDE and adenosine inhibition [150-152]. The combination of low dose budesonide and theophylline showed similar effects when compared to high dose budesonide alone; however the lung function, FEV_1 and FVC showed significant improvement when given theophylline, with a sustained effect [153, 173]. Further studies have supported the use of theophylline and ICS as they both reduce inflammation, but by independent mechanisms of action. The combination of drugs is able to reduce the total sputum eosinophils and ultimately improve the quality of life [121].

At a plasma theophylline concentration of 67 μg/mL, there is a weak bronchodilator effect of the drug. Until this concentration has been achieved, theophylline may have an effect on the other cells and organs other than the airways. Theophylline has been suggested to have poor airway retention as reviewed by Barnes [151].

Low oral doses of theophylline are safer and easier to use with rare occurrence of side effects and due to a mechanism of action that is different to ICS, these two drugs can be used together. The low cost of theophylline in combination with generic ICS is the most cost effective way to manage persistent asthma in developing countries, especially for patients with severe effects [151].

The main disadvantage of treatment with orally administered theophylline is its narrow therapeutic range. Theophylline has a therapeutic range between 10-20 mg/L. It has been observed that there is a relationship between toxic effects in patients and the serum concentration of theophylline. Patients with plasma levels of theophylline exceeding 20 mg/L show signs of severe toxicity. Serious toxicity has not been reported in patients who have had a plasma concentration of less than 20 mg/L [143]; although some patients do show signs of toxicity in the therapeutic range. Patients suffer may suffer from nausea, vomiting (including bloody) diarrhea, arrhythmias, dizziness, CNS stimulation, palpitations, convulsions and tachycardia for example. Patients already suffering from epilepsy will experience a lowered threshold and therefore have an increased risk of seizures [143]. Other CNS effects that theophylline toxicity can cause include insomnia, headache, and irritability. This can occur in patients who are not able to clear theophylline due to various reasons such as age, renal function, liver function and interaction of theophylline with other medication. Patient factors such as smoking can also significantly affect the clearance and toxicity of theophylline. Adverse effects such as nausea, vomiting, headache and diuresis are caused as

a result of PDE inhibition. The effects such as cardiac arrhythmias and seizures are caused due to adenosine receptor antagonism [151, 152, 164, 174, 175].

Theophylline is metabolized by CYP1A2 in the liver; therefore interactions with drugs such as macrolides, quinolone, cimetidine, fluvoxamine can increase the plasma concentrations of theophylline and increase the risk of adverse effects [151, 164, 166]. Theophylline also affects potassium levels by its release of catecholamines, which cause a positive inotropic and dose-dependent response. The anti-diuretic effect of methylxanthines also affects the sodium concentration, and thus effects on the other electrolytes in the body are also seen. The action on cAMP also causes an increased number of monoamines in the brain which causes an inhibition of prostaglandins and adenosine receptors [16].

Due to the theophylline's toxicity being related to the concentration of the drug in the plasma, the pharmacokinetics of theophylline will affect its safe and effective use. Theophylline is completely absorbed, and reaches plasma peak concentrations in 6 hours and has a volume of distribution is 0.045 L/kg. It has been shown that 40% of theophylline is bound to albumin protein. It is metabolized in the liver by demethylation reaction to form an inactive product and is eliminated via the kidneys. Elimination of theophylline from the body depends on the age of patients, where it is shown to be 6/7 hours in adults, but increased to 13 hours in children up to the age of 13 and due to these reasons the half-life of varies between 2-10 hours. In infants, due to hepatic enzyme inactivity elimination of theophylline is slow. If a peak-trough difference ratio is 2:1, this means that there is a 100% fluctuation in dose resulting in not being able to maintain a concentration within the normal plasma range for theophylline [133].

Prescribing theophylline is brand specific due to its variation of pharmacokinetic profile between the brands. Variation causes fluctuations in the plasma concentration and can lead to increased toxicity of theophylline. Due to the large inter-patient variability, it is preferred to keep the same dose of theophylline; as some patients may have a slow elimination of theophylline, causing an increased plasma concentration or in some patients it may have a rapid elimination, requiring a more frequent dosing. This means that it is important that the dose is individualized for each patient.

Theophylline brands such as Slo-phyllin®, Nuelin SA® and Uniphyllin Continus® are available. The medications are available as oral dosage forms only, and in modified release tablets. The oral doses range between 200-500 mg and can be given twice a day. The signs of toxicity are carefully monitored in patients taking theophylline. Typical counselling for modified release tablets is required to be given when patients take theophylline, i.e. to not crush tablet and to swallow whole [38].

Due to the greater efficacy of the other bronchodilator agents, such as salbutamol, and the decreased risk of side effects and toxicity, theophylline use has declined. However, more recently, theophylline has been shown to have a substantial synergistic effect when given with inhaled corticosteroids.

Theophylline is chosen in this study due to its hydrophilic properties and the difficulty to encapsulate hydrophilic drugs in nanoparticles. This is further discussed in Chapter 2.

1.10. NANOTECHNOLOGY AND PULMONARY DELIVERY

Nanoparticles are particles in the size range of 1-1000 nm [176, 177]. They have been defined as solid, sub-micron sized drug carriers that may or may not be biodegradable [176]. Nanoparticles have also been defined as those particles where at least one of the dimensions is between 1-100 nm [178]. They can exist as nanospheres and nanocapsules, in which the drug is dispersed throughout the matrix or at the surface or drug is confined to a cavity surrounded by a polymer membrane, respectively [176, 177, 179, 180]. Nanoparticles have a higher intracellular uptake than microparticles as a result of their submicron size [176, 178, 181-183]. The term 'nanoparticle' can refer to polymeric nanoparticles, nanocrystals, nanotubes, liposomes and solid-lipid nanoparticles [178, 184, 185].

Polymeric nanoparticles can be synthesized using biodegradable polymers such as poly (lactic acid) (PLA) and poly (lactic-co-glycolic acid) (PLGA); these are the most common polymers applied in the synthesis of polymeric nanoparticles [177, 185-188]. Biodegradable polymers are biocompatible and degrade into monomers (for example PLA and PLGA to lactic acid) which are products of the Krebs cycle (and Cori cycle), produced in the body as a process of natural metabolism [177, 185, 189, 190].

Biodegradable polymers can be used for sustained release of the drug and targeted drug delivery [182, 191, 192]. Polymeric nanoparticles have attracted considerable attention, as they are stable and they can encapsulate drugs in high loading capacities, particularly hydrophobic drugs [193-195]. Biodegradable polymers should be non-toxic and biocompatible [190, 196-201]. Other polymers that have been used include synthetic polymers such as polyacrylate and polycaprolactones and naturally-occurring polymers such as chitosan, gelatin and alginate [202]. PLA and PLGA are approved by the FDA for human use and applications in surgery and implants and due to their natural degradation in the body; they do not require surgical removal after completion of drug release [182, 185, 189, 203-209]. These biodegradable polymers are favored due to the lower toxicity risk and inflammatory reactions they cause in comparison to non-biodegradable polymers, such as polystyrene [210, 211]. These polymers are shown to not cause damage in the lungs over a short term when

studied using lung epithelial cells, macrophages or tissues [192, 202, 210]. However, the slow degradation rates (which can last for a duration of months) can result in an unwanted accumulation of the polymer in the lungs and therefore dosing intervals would need to be considered carefully [211]. The safety of the biodegradable polymers in pulmonary applications is of high interest [211]. Polyesters, PLA and PLGA are negatively-charged and shown to have little effect on the cell toxicity due to lower interactions between cells and other negatively-charged particles; but cationic polymers such as chitosan (forming positively-charged nanoparticles) have shown interactions with the cell membrane and affect integrity of the tight junctions in cells [211, 212].

Controlled release of drugs is one of the leading research fields in the pharmaceutical industry [203, 204]. Drugs can be dissolved, entrapped, encapsulated or attached to the nanoparticle matrix, depending on the method of formulation [176, 179, 213, 214] and there are many methods that have been applied for the encapsulation of drugs in polymeric nanoparticles, such as nanoprecipitation, solvent displacement and solvent emulsion diffusion methods discussed in detail in Chapter 2 [176, 177, 185, 215]. Formulation of nanoparticles by encapsulation of drugs using biodegradable polymers allows several advantages including increased bioavailability, biocompatibility and biodegradability, reduced administration frequency and potentially improvement of patient compliance [216-224].

Use of biodegradable polymers in the formulation of nanoparticles and microparticles has allowed for sustained delivery of therapeutic agents. By use of nanoparticles formulated using biodegradable polymers, specific drug targeting can be achieved. Biodegradable polymers such as PLGA and PLA are applied in the preparation of nanoparticles and microparticles for targeted and sustained drug delivery [205]. Biodegradable polymers can be composed of polyesters. The monomer undergoes several chain reactions (polymerization) to form the polymer. An advantage that these polymers possess is their biocompatibility and restorability through natural metabolic pathways. The biodegradable polymers break down to their monomers (lactic acid and glycolic acid), and are eventually further metabolized to carbon dioxide and water as described [176, 185, 203, 204].

PLA and PLGA break down into their monomers by hydrolysis of their ester linkages in the presence of water and the time required to degrade depends on the ratio of the monomers, and on the acidic conditions of the environment. When there is more acid present as a result of the monomers, PLA is able to undergo autocatalytic hydrolysis [179, 189, 214]. The disadvantage of an increased acidic environment as a result of breakdown of the polymers

may affect the physicochemical properties of the drugs being used, and thus affect their overall activity.

There are several methods available to encapsulate drugs in nanoparticles (discussed in Chapter 2). Briefly, common methods that are used include the solvent evaporation method and the emulsification solvent diffusion method. These methods were originally developed for the encapsulation of hydrophobic drugs in order to overcome the difficulty in the delivery of these drugs. With successful encapsulation of hydrophobic drugs, some studies developed co-encapsulated drug systems. Although successful application for hydrophobic drugs was obtained, there was difficulty in obtaining high encapsulation efficiencies when the same method was applied for hydrophilic drugs. This was due to large partitioning of the hydrophilic drugs during the process of encapsulation in preference for the aqueous environment. This is explained in detail in Chapter 2.

Lungs are one of the first major organs to be used as a port of entry for nanoparticles into the body [181]. The main challenge in the delivery of nanoparticles to the lungs is in the formulation development; due to their small size, nanoparticles would be exhaled straight away instead of successfully depositing in the lungs [210, 225]. In order to deliver drugs successfully for local drug delivery to the lungs, suitable formulations need to be developed which allow deposition to the correct site in the airways [211, 226]. Nanoparticles can be developed into micron-sized formulations using carriers such as lactose, mannitol and trehalose, resulting in successful detachment of the nanoparticles from the carrier particles upon inhalation [128, 181, 182, 225, 227, 228].

DPI formulations may be preferred for delivery of drug-containing nanoparticles due to their increased stability as a result of their dry powder state, if ensuring environmental factors such as humidity are avoided [182]. If biodegradable polymers were used and suspended in an aqueous liquid medium such as when using a nebulizer; over a period of time, hydrolysis of the polymer would occur leading to release of the drug [182]. However, it has been commonly seen that nanoparticles are delivered using nebulizer formulation. This allows larger respirable percentage available to the deep lungs due to appropriate particle size being achieved and liberation of the nanoparticles from the deposited droplets [181, 202, 210].

As a result of their size, nanoparticles will deposit in the lungs by diffusion and not by gravitational forces and impaction. They are able to diffuse and deposit throughout the respiratory tract and it has been noted that approximately 20% are deposited in the alveolar region and 5% in the tracheobronchial region. Holding the breath enhances deposition in the deep lung if required for systemic administration of the drugs [181, 182].

Delivery of nanoparticles by the pulmonary route is an attractive concept as both local delivery and sustained release can be achieved [211]. This decreases the dosing frequency, protects the drug, improves bioavailability, decreases overall concentration required for delivery thereby reducing systemic side effects [128, 181, 184, 229]. The reduced frequency in dosing can potentially increase patient compliance and acceptability [181].

Additionally, nanoparticles are able to offer advantages such as an increased surface area in comparison to microparticles and the small size of the polymeric nanoparticles results in a longer retention time of the nanoparticles in the lungs [211, 219]. Applications of nanoparticles being used for local pulmonary delivery include the treatment of respiratory infections and inflammatory diseases of the airways [228, 230-232].

Currently, there are no controlled release products that are delivered by the inhalation route and this is considered to be an unmet need that could be realized using nanoparticles [211, 233, 234]. Release of drugs from polymeric nanoparticles is by a combination of diffusion through the polymer matrix and by erosion/degradation of the polymer matrix [211].

Dry powder formulations of nanoparticles have been successfully made using spray-drying techniques where micron-sized or 'micro-encapsulated' nanoparticles have been developed. This has been used for the delivery of tobramycin-PLGA nanoparticles (for respiratory infections) [210] and chitosan nanoparticles (for protein drug delivery for systemic action) [235]. Porous nanoparticle aggregates can be made for pulmonary drug delivery as these particles have a low density and small aerodynamic diameters, and therefore their deposition is found to be in the deeper lungs rather than the upper airways [230]. Porosity of particles can be increased by use of ammonium bicarbonate [127, 128, 210]. Sildenafil nanoparticles loaded in PLGA have been synthesized for the treatment of pulmonary hypertension [236, 237]. Various types of nanoparticles, for example liposomes, micelles, dendrimers and polymeric nanoparticles have been explored for the delivery of drugs to the lungs [202].

Betamethasone, a corticosteroid used for the treatment of asthma, has been encapsulated using PEG-PLA nanoparticles and studied on a murine asthma model to improve the delivery of the corticosteroid [232]. Budesonide-PLGA manoparticles were also studied in a murine asthma model; the effect of increasing nanoparticle porosity on delivery was studied and found to improve pulmonary drug delivery [127]. Budesonide microparticles also showed advantages of allowing reduced dosage frequency and control of nocturnal symptoms in asthma [238]. Budesonide was formulated as a nanosuspension and showed stability over 1 year and was administered as by a nebulizer formulation [181, 230, 239]. Nanoparticle agglomerates of fluticasone propionate and salbutamol were formulated as dry powder

aerosols. A combination of drugs was used as this showed synergy compared to the use of monotherapy [231].

Another example of the use of inhaled nanoparticles for local delivery was for the treatment of lung cancer using doxorubicin (with polycaprolactone (PCL) as the polymer) [240]. Nanoparticles were concentrated in the tumor site and it was postulated that this was due to the enhanced permeability and retention (EPR) effect (described below). The nanoparticles were developed as dry powder formulations using lactose [240]. PLGA has been used to load siRNA in nanoparticles in the treatment of lung cancer as a dry powder formulation form [208].

Polymeric nanoparticles (of natural or synthetic polymers) have received a lot of attention due to their stability and ease of surface modification [184]. Many studies have delivered nanoparticles via injection where drug targeting is achieved by an effect known as the enhanced permeability and retention (EPR) effect. Tumors have a leakier blood supply allowing nanoparticles to become concentrated preferentially in the tumor areas and inflammation sites [197, 232]. By preferentially entering inflamed and tumor sites, this allows an increase in positive effects at the site of action and subsequently reduces systemic side effects. At these diseased sites, the biodegradable polymers can act as local depots and can provide a source of continuous supply of the encapsulated drug targeted for the disease [184]. Factors such as the nanoparticle size and charge can affect properties such as uptake and distribution which can affect the overall therapeutic efficacy of the drugs [225].

1.11. Aims and Objectives of the Thesis

Nanotechnology can be used to improve the delivery of drugs. Limitations have been seen from previous studies in the successful encapsulation of hydrophilic drugs; and there are limited studies on co-encapsulation of both hydrophilic and hydrophobic drugs. Budesonide is a commonly prescribed inhaled corticosteroid which is shown to have a good safety profile. Theophylline, a bronchodilator which has been relegated to third line therapy in treatment of COPD and asthma, has been shown to be effective and of great importance when prescribed in combination with corticosteroids. However, theophylline has a narrow therapeutic index when given systemically and by delivering it locally, in a nanoparticle formulation, the systemic side effects can be reduced and release of the drug extended.

The principal aim of the study was to develop a method to successfully co-encapsulate theophylline and budesonide in nanoparticles using the polymer, poly (lactic acid) (PLA). This combination of drugs, with widely different values of log P, has not previously been successfully encapsulated in PLA nanoparticles for pulmonary drug delivery.

After successfully formulating nanoparticles containing theophylline and budesonide, the aim was to:

- Characterize the nanoparticles. Initial characterization will include an assessment of particle size, zeta potential, morphological features, thermal and surface properties and, most importantly, the loading efficiency of both the drugs. From these characterization tests a favorable formulation will be selected and used for further characterization (Chapter 2).
- Achieve sustained release of the drugs. Therefore, the release profiles of the drugs from the nanoparticles will be characterized. The aim is to understand the release profiles of theophylline and budesonide from the nanoparticles. Drug release from the nanoparticles depends on the diffusion of the drugs from the nanoparticles, the degradation/erosion of the polymer (extended periods) and the solubility of the drugs in the release medium (Chapter 3).
- Assess whether the nanoparticles are likely to be toxic if delivered to the lung. This will be studied using an *in vitro* model of the airway epithelium. A further aim will be to study the transport of the drugs across an *in vitro* model of the airway epithelium and the effect of the nanoparticles on the tight junctions of the cells (Chapter 4 and Chapter 5).
- Formulate the nanoparticles as a nebulized suspension and dry powder formulations and to study the *in vitro* deposition of the formulation (Chapter 6).
- Study the effect of different storage conditions on the nanoparticles stability. Changes in the physicochemical properties of the nanoparticles stored at under different conditions over a period of time (Chapter 7).

1.12. SIGNIFICANCE OF WORK

Asthma and COPD are chronic, inflammatory conditions of the airways in which controlling symptoms and maintenance of control is extremely important to maintaining a good quality of life. Polypharmacy in asthma and COPD can lead to poor compliance and poor control of asthma and COPD. For good control, regular therapy using bronchodilators and anti-inflammatory agents is recommended and ideally, the duration of drug action should be long in order to control nocturnal symptoms and reduce the frequency of administration of the drugs. There are several advantages of sustained release products, but currently, there are none available for pulmonary drug delivery; although a significant amount of research in sustained release of drugs has been carried out. Advantages include reduced administration frequency (potentially increasing patient compliance) and reduced overall concentration of drug in plasma (in addition to delivery of the drugs locally). In conditions like asthma and

COPD, sustained release allows improved symptom control over a longer period of time, especially for late night or early morning symptoms.

Budesonide is chosen as the drug of choice due to the low risk of side effects in comparison to other corticosteroids as well as high potency and high local bioavailability in the lungs. Budesonide is a commonly prescribed inhaled corticosteroid which supports the use of this drug in the current study. Theophylline is chosen as the second drug due to several reasons. Theophylline is currently available only as an oral dosage formulation, and it is suggested that there is poor retention of theophylline in the airways.

Synthesis of nanoparticles using a method developed to incorporate both hydrophilic and hydrophobic drugs can be applied to encapsulate drugs with a wide range of logP values and different applications. Characterization of the nanoparticles allows modifications to the formulation method in order to develop desired properties in the synthesized nanoparticles. The use of co-encapsulated nanoparticles allows reduction of polypharmacy, for example in the treatment of infections (example tuberculosis (TB)), cancer or inflammation where combinations of drugs may be potentially required. Although mono-encapsulated nanoparticles are commonly formulated and can be used, the advantage of co-encapsulation in nanoparticles involves reduction in the overall quantity of nanoparticles that is required for administration, i.e. using only one type of nanoparticle formulation rather than combining two mono-encapsulated formulations, which would be more ideal if the loading efficiency can be standardized for both drugs (for example theophylline and budesonide). Dosing of the drugs also becomes easier when co-encapsulated nanoparticles are administered, as handling of only one type of nanoparticle sample is carried out.

Along with the therapeutic advantages of using the combination of theophylline and budesonide, this combination was also selected due to the difference in the lipophilicity of the two drugs. Theophylline is a hydrophilic drug which is difficult to encapsulate in polymeric nanoparticles at a high loading efficiency. The encapsulation of theophylline and budesonide allows encapsulation of a hydrophilic and lipophilic drug. This combination of drugs has not been encapsulated in polymeric nanoparticles previously. This study and formulation of the nanoparticles containing a hydrophilic and lipophilic drug can be used as a model for other drugs that can be used as a combination. Although the application is for pulmonary drug delivery in this study; polymeric nanoparticles have been used for delivery via other routes allowing this technology to be extended for different applications.

By delivering the drugs via nanoparticles and achieving sustained release, retention of theophylline could potentially be increased and revitalize the use of theophylline. Theophylline's major disadvantage is the narrow therapeutic range, which has relegated

theophylline to a third line therapy for the treatment of these chronic conditions. By encapsulation of theophylline in nanoparticles and achieving sustained release, the side effects can be limited to a local effect only. Encapsulation of theophylline in nanoparticles also reduces the overall concentration of the drug required and by delivering the drug locally further reduces the need to use high concentration, avoiding the toxic effects of theophylline. Theophylline is also chosen as the second drug due to its importance in the effect of up-regulation of corticosteroids, and due to the synergy when prescribed with steroids, described in detail in Section 1.9.

Overall, by delivering theophylline and budesonide as co-encapsulated nanoparticles directly to the target site (airways) allows local delivery of the drugs to the affected area. Local delivery allows reduced concentration of drug required and reduces the risk of systemic side effects. By delivering the drugs as nanoparticles a depot can be formed where the drugs are released over an extended period of time maintaining control of symptoms. By achieving sustained release, the frequency of administration can be reduced and by encapsulating both drugs in PLA nanoparticles the patient only has to inhale a single product; all factors that can improve patient compliance and control of asthma and COPD symptoms.

CHAPTER 2 SYNTHESIS AND CHARACTERIZATION OF THEOPHYLLINE AND BUDESONIDE NANOPARTICLES

2.1 INTRODUCTION

Nanoparticles were introduced in the 1970s and have been synthesized using biodegradable polymers. Nanoparticles synthesized using biodegradable polymers are easily manufactured and reproducible and were developed as a potential to modify and improve drug delivery, shelf life, increased efficacy and stability [241, 242] and a wide range of applications in pharmaceutics [242-244]. Nanoparticles are defined as solid, colloidal particles in the range of 10-1000 nm [245-250].

Nanoparticles synthesized from biodegradable and biocompatible polymers have been intensively investigated for drug delivery and their effects *in vitro* [188, 205, 251]. Polymeric nanoparticles can be synthesized with natural or synthetic polymers [243, 247]. Nanoparticle and microparticle drug delivery systems developed initially were made with poly (alkylcyanoacrylate) [243]. Nanoparticles have advantages over using free drug mixtures for example protection of the drug, increased stability, reduced toxicity and sustained release, so potentially reducing the frequency of administration [182, 191, 251, 252]. When synthesizing nanoparticles, it is important to consider the size, shape and surface chemistry which can play an important role in interactions with biological systems to achieve therapeutic success [252]. Commonly used biodegradable polymers include poly (lactic-co-glycolic acid) (PLGA) and poly (lactic acid) (PLA) [181, 185, 190, 198-200, 214, 253]. Polymeric nanoparticles (natural or synthetic) have received a lot of attention due to their stability and ease of surface modification [184, 197, 232, 251, 252, 254]. Biodegradable nanoparticle systems are preferred to liposomes due to the increased stability and ability to provide sustained and controlled release [243].

The drug in the nanoparticle can be dissolved, entrapped, encapsulated or attached to the nanoparticle matrix, depending on the method of the preparation. Nanocapsules are particles where the drug is confined to a cavity surrounded by a unique polymer membrane (reservoir system), while nanospheres are particles which are composed of a dense polymeric matrix in which the drug is uniformly and physically dispersed [176, 177, 180, 251].

There are several methods available to formulate nanoparticles such as emulsion polymerization, solvent evaporation methods, emulsion solvent evaporation/diffusion, salting out and nanoprecipitation [185, 188, 215, 243, 245, 251, 255-258]. Most of these methods have been developed for the synthesis of microspheres [245].

Nanoparticles can also be prepared by incorporating drugs with monomers of the polymer, and then reaction between the monomer and the drug together, as reviewed by Pinto-Reis et al (2006) [176]. Most methods have been developed to incorporate hydrophobic drugs. Incorporation of hydrophilic drugs using conventional methods has resulted in low loading efficiencies and a burst release of the hydrophilic drug [194, 199, 259, 260]. Hydrophilic drugs are difficult to encapsulate due to their high partitioning into the aqueous phase.

Nanoprecipitation and solvent displacement:

The solvent displacement method commonly referred to as the nanoprecipitation method was developed by Fessi et al (1989) for the encapsulation of savoxepine [241, 257, 261, 262]. This method is based on interfacial deposition of the polymer after the organic solvent is displaced to form droplets. The system is composed of polymer (and drug), solvent and non-solvent. The most common solvent used is acetone, as reviewed by Rao et al (2011) [262].

This method has been used effectively to formulate nanoparticles containing hydrophobic drugs and relies on the spontaneous formation of an emulsion, as reviewed by Pinto-Reis et al (2006) [176]. The drug and polymer are dissolved in an organic solution, e.g. acetone, and added drop wise to an aqueous environment with constant stirring. The large unfavorable aqueous environment forces the encapsulation and formation of lipophilic drug nanoparticles. The polymer deposition on the interface between water and organic solvent, caused by fast diffusion leads to instant formation of the colloidal suspension [176, 177]. The organic solvent is then removed by evaporation. Surfactants may or may not be used in the production of these nanoparticles.

Salting out

The salting out method was developed by Bindschaedler et al. [257, 262] in which a salting out agent, such as magnesium tetrahydrate or magnesium carbonate dissolved in the aqueous phase is used. The organic solvent (such as acetone) is used to dissolve the drug and polymer. An oil in water emulsion is formed with the aqueous phase in which the organic solvent diffuses to precipitate drug and polymer allowing formation of the nanoparticles. It is a simple and single step method to formulate nanoparticles without a need for high shearing forces [261, 262]. The salting agent is chosen carefully, as this can affect physicochemical characteristics of the particles and affect the encapsulation efficiency of

the drugs. This method is commonly used for hydrophobic drugs and is particularly good for heat sensitive compounds, as there is no heat involved, as reviewed by Pinto-Reis et al (2006) [176].

Nanoparticles prepared from hydrophilic polymers (for example: chitosan, gelatin and alginate):

Chitosan is derived from natural carbohydrate polymer. It is formulated by partial N-deacetylation of crustacean derived natural biopolymer chitin. There are several methods that can be used to formulate nanoparticles using chitosan, which include emulsification solvent diffusion (ESD). Chitosan is dissolved in acetic acid and the ESD method is followed, with or without addition of a surfactant to the chitosan solution. Gelatin, being a non-toxic polymer, is used extensively in food and medicinal products and has also been used in formulation of nanoparticles due to its ability to act as a controlled release polymer. Sodium alginate has also been used to formulate nanoparticles by methods such as emulsification solvent diffusion. It is also naturally occurring and non-toxic [176, 191, 210, 235, 263-269].

Solvent evaporation method

The solvent evaporation method was developed originally for the formulation of microspheres by Vrancken et al (1970) to encapsulate a compound with the use of immiscible solvents and polymers. The immiscible solvent is then removed from the emulsion system to form polymerized particles [270]. The method was further developed by Tice and Gilley (1985) [271].

The solvent evaporation method involves two major steps in which the polymer (and drug) are dissolved in an organic solvent such as dichloromethane followed by high speed homogenization with the aqueous phase and evaporation of the organic solvent leading to the precipitation of the polymer as nanoparticles with the entrapped in the polymer matrix. The drug and the biodegradable polymer are dissolved in an organic phase, which is immiscible with water, such as dichloromethane, and this is then homogenized with an aqueous phase, which may or may not contain a surfactant for example, poly (vinyl alcohol) (PVA). This method is mainly used for lipophilic drugs with polymers such as PLA and PLGA [176].

Emulsification solvent diffusion (ESD) and double emulsification solvent diffusion (DESD) method:

The emulsification solvent diffusion (ESD) method is a very popular, easy and convenient method used to formulate nanoparticles. The emulsion evaporation method was used for

formulation of various polymeric microparticles and developed by Vanderhoff et al (1979) [272] which was then developed further by Gurny et al (1981) [273]. In the method developed by Vanderhoff et al (1979), the process involved polymer being dissolved in a water immiscible organic solvent and this was dispersed in the aqueous phase containing a stabilizer to form an oil in water emulsion [250, 257, 262, 274]. This method was further developed by introducing an additional step which was to obtain mutual saturation between the organic and aqueous phase [241, 257]. The solvent was miscible with water containing the polymer and the emulsion was added to a large amount of water which causes diffusion of the organic solvent and allows formation of nanoparticles [176, 257, 274, 275]. Early references to this method were for the preparation of controlled release microcapsules by Tice and Giley in 1985 [245, 276] which were based on encapsulation of drugs in microparticles [277-279]. This method was used by Ogawa et al (1988) to develop microcapsules using PLA or PLGA [255, 280-282]. This method is similar in principle to the solvent evaporation method.

The ESD method involves formation of a primary emulsion by mixing organic and aqueous phases and removal of the organic solvent. The DESD method involves formation of a primary emulsion, and then addition of an excess aqueous phase which results in destabilization of the thermodynamically stable primary emulsion. The primary emulsion is formed as described in the solvent evaporation method (with or without a surfactant) and this stable emulsion is then added to an excess aqueous phase (with or without surfactant). This causes diffusion/displacement of the solvent allowing instantaneous formation of the nanoparticles as the polymer and drug precipitates into the aqueous medium. The method allows for the use of either water-miscible or immiscible organic solvents. The importance of components such as the stabilizer for formulation of the nanoparticles has been reviewed by Hans and Lowman (2002) [243].

In a study on haloperidol PLGA nanoparticles, the emulsification process was described in detail post the diffusion of the organic solvent stage and how the process of encapsulation occurred. As the organic solvent diffuses to the external phase, this would result in shrinkage of the emulsion droplets and this process can affect the final size of the nanoparticles. This process depends on the use of high shear as a source of external energy. When the droplets solidify, the drug molecules become entrapped in the nanoparticles. Once the polymer solidifies, there is no loss of the drug; the main diffusion of the (hydrophilic) drug occurs from the formation of the nanodroplets to the nanoparticles [244].

The use of toxic organic solvents is one of the main disadvantages of this method. The ESD method is a quick, reliable and efficient method to produce nanoparticles. Nanoparticles produced by this method results in high encapsulation efficiencies of hydrophobic drugs up

to 70% [176, 194, 205, 283] and this method can be developed to scale up to larger quantities. Homogenizers are used to formulate nanoparticles using high shear rates and energy. Alternatively, probe sonicators are also used to formulate nanoparticles [176, 200, 203, 204, 281, 283, 284]. This method has been applied for the synthesis of particles containing both hydrophobic and hydrophilic drugs in recent years [285].

Double emulsification method and the encapsulation of hydrophilic drugs:
Most methods available to formulate drug containing nanoparticles are developed for hydrophobic drugs. The challenge in encapsulating a hydrophilic drug is due to the rapid diffusion and loss of the drug in the aqueous phase resulting in reduced encapsulation efficiency, as described previously [177].

The double emulsion diffusion method has been reviewed by Lai et al (2014) suggesting the suitability of this method for the encapsulation of hydrophilic drugs [247]. The ESD method has been further developed into the double emulsification solvent diffusion (DESD) method: so called because of the formation of a primary and secondary emulsion resulting in the formation of nanoparticles, as described previously. This was to increase the encapsulation efficiency of hydrophilic drugs.

In the DESD method, the hydrophilic drug is dissolved in the inner aqueous phase and the polymer is precipitated when the organic solvent is removed from the emulsion system resulting in the incorporation of the hydrophilic drug. The method to incorporate the lipophilic drug would involve dissolving the drug in the organic solvent. The encapsulation of the hydrophilic drug remains a challenge due to its rapid partitioning into the external aqueous phase [188, 259].

As an attempt to increase the encapsulation efficiency of the hydrophilic drugs, the organic phase can consist of two organic solvents, one of which is miscible with the aqueous phase. This combination is to allow increased encapsulation of the hydrophilic drug by reduced partitioning of the hydrophilic drug to the external phase [188, 205].

Encapsulation of hydrophilic drugs is difficult with conventional methods, such as those described above. Chemical modifications, e.g. esterification can make changes such as making the drug more lipophilic; but this can compromise the activity of the drug. Zinc has also been used to form an insoluble complex which is easier to encapsulate, than the hydrophilic drug [199]. Other techniques to encapsulate hydrophilic drugs also include modifying pH, which affects drug ionization, which can then affect the lipophilicity and increase encapsulation efficiency but also at the cost of affecting the activity of the active [177, 259]. Vrignaud et al (2011), reviewed examples of enhancing the encapsulation efficiency

of hydrophilic drugs in polymeric nanoparticles using various methods such as increased 5-flurouracil loading by increasing the monomer polymerization rate and the use of reversed micelles to encapsulate hydrophilic dyes using an emulsion solvent evaporation method and PLA [251].

High solubility of a hydrophilic drug in both the aqueous and organic phase facilitates the diffusion of the drug to the external phase (resulting in low encapsulation efficiency), and therefore the use of a solvent in which the hydrophilic drug has low solubility in is required [198]. The main solvent used for the primary emulsion is usually dichloromethane. Other solvents tested in the double emulsion method are ethyl acetate and acetone due to their various degrees of miscibility with the aqueous phase [198]. Modification the organic phase (by changing the water-miscibility) can affect the rate at which the polymer precipitates and this can affect the encapsulation efficiency of the drugs. The DESD also causes a lot of drug loss in the formulation process due to diffusion of the drug to the external phase, also resulting in low encapsulation of the drugs [127, 197-199, 251, 255, 286].

Characterization of nanoparticles:

Synthesized nanoparticles are characterized using different techniques such as particle size analysis, loading efficiency [203, 204], morphological assessment, surface charge and surface properties, drug release , stability and effect on cell systems [177, 178, 197, 207, 225, 231, 243, 247, 285-290].

The most common and rapid method to determine particle size is by dynamic light scattering (DLS) or photon correlation spectroscopy (PCS). The size and size distribution is verified by morphological assessment using scanning electron microscopy (SEM) and/or transmission electron microscopy (TEM). Determining the particle size is important as the size and distribution will have a large influence on the fate of the particles *in vivo*. The particle size may also potentially affect the drug release profile and the drug loading efficiency [184]. Smaller particles have a larger surface area resulting in a faster drug release, due to the drug particles being closer to the surface. Larger particles have a larger core allowing increased encapsulation efficiency [184]. The relationship between particle size and encapsulation efficiency has been reviewed by Hans and Lowman (2002) [243]. The size of the particles can also affect stability, which can cause increased aggregation and affect dispersibility [184].

Surface properties such as zeta potential, size and morphology of the nanoparticles are important to determine because they can affect interactions with cells, immune system and stability [184, 189].

Nanoparticles with an increased drug loading can improve the presence of the drug in the pulmonary region [228]. A high loading capacity can potentially reduce the overall quantity of the nanoparticles/carrier required for treatment [177, 184, 189]. High loading efficiencies are usually obtained for hydrophobic drugs, while it is a challenge with hydrophilic drugs [197].

Other common characterization techniques such as differential scanning calorimetry (DSC) or x-ray diffraction (XRD) show if drugs and polymer are present in a crystalline or amorphous state of the nanoparticles [178]. Fourier Transform Infra-red (FT-IR) spectroscopy is also used to determine stability of the nanoparticles and components [178].

2.1.1 AIM OF STUDY:

The purpose of the study was to synthesize nanoparticles of the hydrophilic theophylline and lipophilic budesonide using PLA as the encapsulating polymer. In order to achieve this, an appropriate method was required to be developed in order to allow encapsulation of both drugs with a suitable loading efficiency. From the information available, the double emulsification solvent diffusion (DESD) method was chosen incorporating different variables such as: quantities of drug and polymer used the method of evaporation of the organic solvent, duration of homogenization process and investigating of various organic solvents for the successful preparation of nanoparticles. Budesonide/theophylline co-encapsulated and mono-encapsulated nanoparticles were prepared. The synthesized PLA nanoparticles were characterized for particle size, zeta potential, surface characteristics, morphology and loading efficiency of theophylline and budesonide.

2.2 MATERIALS AND METHODS

2.2.1 MATERIALS

Formulation of nanoparticles

Theophylline (anhydrous >99%) powder, Sigma Aldrich, UK: Lot 120MO211V

Budesonide powder, LKT Laboratories, USA: Lot 2593502

Purasorb® PDL-02 Poly (DL-lactide) (PLA), 17,000 Da, Purac Biomaterials- the Netherlands: Lot 0812000098

Poly (vinyl alcohol) (PVA), 15, 000 Da, Sigma Aldrich, UK: Lot MKBF0587V

18.2MOhm Deionized water

Dichloromethane, Fisher Scientific, UK (D/1856/17)

Acetone, Fisher Scientific, UK (A/0606/17)

Ethyl acetate, Fisher Scientific, UK (E/0906/17)

Acetonitrile (HPLC grade), Fisher Scientific, UK (A/0626/17)

Hexane, Fisher Scientific, UK (H/0406/17)

Toluene, Fisher Scientific, UK (T/2300/17)

Dimethyl sulfoxide (DMSO), Fisher Scientific, UK (D/4120/PB08)

Methanol (analytical grade), Fisher Scientific, UK (M/3950/17)

Ethanol (absolute), Fisher Scientific, UK (E/0650DF/17)

Morphological assessment:

SEM Specimen Stubs (aluminum), 12.5mm diameter, 3.2 x 6mm pin, AGAR Scientific, United Kingdom (AGG301F)

Carbon adhesive double sided disc/tape (Leit Adhesive Carbon Tabs) for SEM stubs, AGAR Scientific, United Kingdom (AGG3347N)

Copper grids, formvar reinforced carbon, 400 mesh, AGAR scientific (AGS-162-4)

Particle size and zeta potential analysis:

Disposable plastic UV cuvettes, Plastibrand (2.5-4.5mL), Fisher Scientific, UK (Product code: 10046731)

Folded capillary Malvern Zetasizer 'Zeta cell', Malvern Instruments, UK (DTS 1061)

Differential scanning calorimetry (DSC):

Aluminum crucibles (without pin) (40µL) (case containing pan and lids), Mettler Toledo, UK (ME-26763)

High performance liquid chromatography (HPLC):

2mL crimp top clear Chromacol Vials- Autosampler Vials crimped (2CV-P220)(Lot: 70734807114), Thermoscientific, Germany

Chromacol 11mm crimp cap- Rubber/ PTFE Type 7 Rubber Lot 9132010752

Acetonitrile (HPLC grade), Fisher Scientific, UK: Lot 1346198

Formic acid (90%), BDH Laboratory supplies, England: Lot 2442640729

Methanol (HPLC grade), Fisher Scientific, UK: Lot: 1493729 (Code: M/4056/17)

2.2.2 METHODS

2.2.2.1 SYNTHESIS OF NANOPARTICLES

The method that was used to formulate nanoparticles of theophylline and budesonide was a double emulsion solvent diffusion (DESD) method. Several different modifications were carried out to formulate PLA nanoparticles of theophylline and budesonide. Modifications included altering the organic solvent used, polymer-drug ratio and the volume of the excess aqueous phase. Details of all the methods used are given in Table 2.1. The theory of the method of formulation was based on producing a stable emulsion with an organic and aqueous phase by aid of the surfactant. The stable emulsion was then disrupted by addition of an excess aqueous phase, which causes the organic solvents to diffuse to the external phase. By removal of the organic solvents from the emulsion system, it causes precipitation of the polymer and drugs in the aqueous medium allowing encapsulation of the drugs and formation of nanoparticles.

Unless specified otherwise, theophylline (50 mg) was dissolved in 2% w/v PVA (10 mL) to form the aqueous phase. Budesonide (5 mg) and the polymer, poly (lactic acid) (PLA) (200 mg) were dissolved in dichloromethane (10 mL). This was mixed with a second organic solvent (10 mL) (unless specified otherwise in Table 2.1) to form the organic phase. The excess aqueous phase was 18.2MOhms deionized water (100 mL), unless specified otherwise. The aqueous phase and the organic phase were homogenized to form a stable emulsion for 5 minutes (unless specified otherwise in Table 2.1). This stable emulsion was added dropwise to an excess aqueous phase and homogenized for a period of 15 minutes (unless specified otherwise in Table 2.1). The organic solvents were evaporated using the methods specified in Table 2.1.The resultant suspension was centrifuged at 15,000rpm, 4°C for 15 min (unless otherwise specified) as a means of removing the surfactant (2% w/v PVA solution). The supernatant was carefully removed using a Pasteur pipette. Care was taken not to disturb the nanoparticle pellet. The nanoparticles (sediment) were re-suspended in 18.2MOhms de-ionized water (1 mL) and the sample was then freeze dried to obtain solid nanoparticles which were characterized as described in Section 2.2.2.2.

Equipment used to prepare nanoparticles:

Homogenizer: IKA®-25 Digital Ultra Turrax, SAP 23059653

Rotary evaporator: IKA®RV-10 control with IKA®HB 10 Control water bath and vacuubrand chemistry diaphragm pumps model MDIC+MDIC+AK+EK (water bath operated at 40°C, pressure used specified in Table 2.1

Centrifuge: Sorvall RC-6 Plus Ultracentrifuge (samples centrifuged at 15,000 RPM for 20 minutes at 4°C)

Freeze dryer: Christ Alpha 2-4 Freeze dryer with a Chemistry hybrid pump RC-6 vacuubrand S/N: 33679408 (operated at 0.250mbar at -80°C for 24 hours).

Table 2.1 Methods used to formulate PLA nanoparticles encapsulating theophylline and budesonide. Unless specified otherwise, the aqueous phase consisted of theophylline (50 mg) dissolved in 2% w/v PVA (10 mL). The organic phase consisted of budesonide (5 mg) and PLA (200 mg) dissolved in dichloromethane (10 mL) with the addition of a second organic solvent (10 mL). ** Method 14 and * Method 15 did not involve centrifugation steps. DCM: dichloromethane, vacuum means rotary evaporator.**

Method number	PLA (mg)	Organic solvent 2 (mL)	Excess aqueous phase (mL)	Method to evaporate organic solvent(s)	Centrifugation specifications	Comments
1	200	-	100	Vacuum (100mbar)	15,000 RPM, 4°C for 15 minutes	Method 1 does not involve a second organic solvent.
2	200	10 (acetone)	100	Overnight stirring (100RPM)	15,000 RPM, 4°C for 15 minutes	
3	200	10 (acetone)	50	Overnight stirring (100RPM)	15,000 RPM, 4°C for 15 minutes	
4	50	10 (acetone)	50	Overnight stirring (100RPM)	15,000 RPM, 4°C for 15 minutes	
5	200	10 (acetone)	100	Pressure (254mbar)	15,000 RPM, 4°C for 15 minutes	
6	200	10 (acetone)	100	Vacuum (44mbar)	15,000 RPM, 4°C for 15 minutes	Method 6 is a mixed emulsion method which involved formation of primary emulsion of the aqueous phase (2%v/v PVA (10 mL) containing theophylline) and dichloromethane (10mL). This primary emulsion was homogenized with the second organic solvent, acetone (10mL) to form a double emulsion. To this the excess aqueous phase was added and homogenized for 15 minutes.
7	200	10 (ethyl acetate)	100	Vacuum (100mbar)	15,000 RPM, 4°C for 15 minutes	
8	200	10 (acetone)	100	Vacuum (70mbar)	15,000 RPM, 4°C for 15 minutes	Mono-encapsulated nanoparticles of theophylline and budesonide as listed for Method 8 were also prepared and characterized.
9	200	10 (acetonitrile)	100	Vacuum (80mbar)	15,000 RPM, 4°C for 15 minutes	
10	200	10 (hexane)	100	Vacuum (335mbar)	15,000 RPM, 4°C for 15 minutes	
11	200	10 (toluene)	100	Vacuum (77mbar)	15,000 RPM, 4°C for 15 minutes	
12	200	10 (Dimethylsulfoxide)	100	Vacuum (250mbar)	15,000 RPM, 4°C for 15 minutes	
13	200	10 (methanol)	100	Vacuum (337mbar)	15,000 RPM, 4°C for 15 minutes	
14	200	10 (acetone)	100	Vacuum (70mbar)	X**	Method 14 involved filtering samples through a syringe filter (0.45µm)
15	200	10 (acetone)	100	Vacuum (70mbar)	X***	Method 15 involved neither centrifugation step nor filtration step.

2.2.2.2 CHARACTERIZATION OF NANOPARTICLES

2.2.2.2.1 Particle size and Zeta Potential analysis

Particle size and zeta potential analysis of the freeze dried nanoparticles was carried out using a Malvern Zetasizer Nanoseries, Nano-ZS690 (Malvern Instruments, UK). Analysis was carried out at 25°C. For particle size analysis detector angle of 90.00° and Refractive Index (RI) was of 1.331 for de ionized water was used. Particle size analysis was carried out using Malvern plastic disposable cuvettes. Samples were analyzed in triplicate (n=3), each run consisting of n=30 repeats. For zeta potential analysis Malvern zeta potential disposable folded capillary cells (0.75µL) were used. Each sample was analyzed n=3 times, with each run set to a minimum of n=10 and maximum of n=100 runs.

Freeze dried nanoparticles (1 mg) were weighed (using a 5 place analytical balance) into a 10 mL volumetric flask and made up to volume with deionized water. The samples were dispersed in water by initially vortex mixing the sample thoroughly for 1 minute followed by sonication for 1 minute.

2.2.2.2.2 Morphological assessment

Scanning electron microscopy (SEM)

A Zeiss-Sigma FEG-SEM was used for SEM imaging. The samples were coated with platinum (Pt) with a thickness of 4-5nm using a Quorum technologies Q150T Turbo-pumped sputter coater. Approximately 5-10 images for each sample were taken using a range of magnification and varying the area on the stub from which they were taken. The working distance was 5-15mm. The carbon adhesive tape was placed on the specimen stub and test nanoparticles samples were placed directly on the carbon adhesive. A small amount is required for SEM examination and this was therefore only measured using a spatula and placed directly on the stub. Sample preparation was carried out under a fume cupboard to avoid other particles adhering on the adhesive tape.

Transmission electron microscopy (TEM)

TEM was used to assess the morphology of co-encapsulated nanoparticle samples. Samples were prepared at a concentration of 1 mg/mL in de-ionized water and pipetted onto carbon-coated TEM support grids. These samples were examined on a Hitachi 7100 TEM at 100kV. The images were acquired with a Gatan Ultrascan 1000 (2Kx 2K pixel) CCD camera.

2.2.2.2.3 Surface characterization study using Fourier-Transform Infra-red (FT-IR) spectroscopy

The FT-IR spectra of the freeze dried nanoparticle samples were obtained using a Perkin Elmer Spectrum 65 spectrophotometer with Universal ATR sampling assessor (Serial number: 87181). A small amount of each sample was used for the analysis. Drug and PLA standards were analyzed separately. A representative mixture of the free drug and polymer mixture containing theophylline (50 mg), budesonide (5 mg) and PLA (200 mg) was prepared and analyzed. The scanning range was from 400cm^{-1} to 4000cm^{-1} and a resolution of 4cm^{-1} was used. Before each scan was obtained, a background scan was carried out.

2.2.2.2.4 Thermal analysis of nanoparticles using differential scanning calorimetry (DSC)

Thermal analysis of the nanoparticles was studied using a Mettler Toledo StarE differential scanning calorimeter. An accurately weighed amount (2 mg) of the test sample was weighed directly into a DSC aluminum pan. The test samples were freeze dried nanoparticles, drug and polymer standards and a physical mixture containing theophylline (50 mg), budesonide (5 mg) and PLA (200 mg) were also analyzed. The pan was then crimped and sealed and lid was pierced and placed in the DSC. An empty aluminum pan (40μL) with lid pierced was used as a reference. Each sample was analyzed from 25°C to 400°C temperature range at a heating rate of 10°C min^{-1} to determine the melting temperatures

2.2.2.2.5 Development of analytical method for determining theophylline and budesonide concentration

HPLC was used to determine the loading efficiency of theophylline and budesonide in the mono- and co-encapsulated nanoparticles. Loading efficiency of the drugs in the nanoparticles can be used to calculate the amount of nanoparticles required for formulation development or for dosing for the treatment of asthma and COPD. A suitable method would allow determining concentration of both the two drugs when studying the release of the drugs and determining the concentration of the drugs transported across a cell monolayer.

There were two principle methods were used to determine the loading efficiency of theophylline and budesonide and the details of the methods and the instrumentation are given in Table 2.2.

Table 2.2 Details on the HPLC system and method used to determine the loading efficiency of theophylline and budesonide in PLA nanoparticles

HPLC system	System 1: System Gold® 126 solvent module, System Gold® 166 UV detection system, System Gold® 508 Autosampler
	System 2: HP1050 Pump system ,HP1050 UV-Vis detector
	System 3: Perkin Elmer Series 2000 pump, Perkin Elmer Series 2000 UV Detector system
Column	Column 1: Zorbax-Agilent Rapid Resolution SB-C8 3.5µm 4.6x75mm (made in the USA; P.N. 866953-906, S.N. USEB011824)
	Column 2: Fortis C18 (4.6x150mm, 5µm particle size, Fortis Technologies Ltd, UK)
Mobile phase	Mobile phase 1: 65:35 (% v/v) acetonitrile: formic acid (0.1% v/v)
	Mobile phase 2: 70:30 (%v/v) methanol: water
Detection wavelength (nm)	260 nm
Flow rate	1 mL/min
Injection volume	20 µL
Sample temperature	Room temperature
Column temperature	Room temperature

Analytical method validation

System suitability testing is an integral part of implementing an analytical method for a test compound and the tests are based on the concept that the equipment, electronics, analytical operations and samples to be analyzed constitute an integral system that can be evaluated as such. A system suitability of the assay was performed by injecting a known concentration of the test compound (theophylline or budesonide) at concentration of 10 µg/mL a total of 6 times and then calculating the parameters that are listed below. The parameters adopted for the test compound are based on ICH guidelines for the validation of analytical procedures, Q2 (R1). These are further discussed in Appendix 1: Synthesis and characterization of theophylline and budesonide nanoparticles, Section 10.1.1.

The parameters that are tested included:

- Capacity factor
- Tailing factor
- Theoretical plate number
- Precision/ injection repeatability
- Accuracy
- Linearity and range
- Sensitivity – *limit of detection, limit of quantification*

2.2.2.2.6 Drug extraction from the nanoparticles and calculation of loading efficiency

An accurately weighed amount of freeze dried nanoparticle sample was weighed and 3mL of methanol was added to it. This mixture was ultra-sonicated for a period of an hour; after which the samples were kept (in methanol) for 24 hours. After 24 hours, the samples were centrifuged (micro centrifuge) at 14, 000rpm for 20 minutes. Supernatant was transferred into a HPLC vial and analyzed. The samples were analyzed in triplicate.

Theoretical loading concentration of theophylline and budesonide were calculated based on the weight of nanoparticles sample that was used for analysis. The concentration of theophylline and budesonide in the nanoparticles was calculated from the calibration plot and a loading dose was determined for both drugs, based on the initial formulation.

Loading efficiency was calculated using Equations 2.1 and 2.2 (below):

$$Theoretical\ Drug\ Concentration\ (DC_T) = \frac{NP_w \times D_w}{TE_w} \qquad \text{Equation 2.1}$$

Where,

DC_T = Theoretical drug concentration (mg)

NP_w = Amount of nanoparticles weighed for HPLC analysis (mg)

D_w = Amount of drug weighed to prepare nanoparticles (mg)

TE_w = Combined weight of drugs and PLA to prepare nanoparticles (mg)

$$\%\ Loading\ Efficiency = \left(\frac{DC_M}{DC_T}\right) \times 100 \qquad \text{Equation 2.2}$$

Where,

DC_M = Drug concentration measured by HPLC analysis (mg)

DC_T = Theoretical drug concentration (mg)

2.2.2.3 STATISTICAL ANALYSIS

A one way ANOVA statistical test was carried out in order to understand if the differences between particle size, zeta potential and loading efficiency of the different samples synthesized using different methods were statistically significant. If $P<0.05$, the difference was considered significant. A Bonferroni post-hoc test was carried out.

2.3 RESULTS

2.3.1 DETERMINATION OF THE PARTICLE SIZE USING DYNAMIC LIGHT SCATTERING (DLS) AND ZETA POTENTIAL OF THEOPHYLLINE AND BUDESONIDE SYNTHESIZED PLA NANOPARTICLES

Overall, sub-micron particle size range was obtained when applying a double emulsion method to synthesize nanoparticles of theophylline and budesonide (Table 2.3). An improvement in the particle size distribution was observed when pressure was applied to remove the organic solvents. The average particle size for Method 1 was calculated to be 278.89±35.67nm (12.79% RSD). A higher average particle size was obtained for Method 2 and 4 which was 483.48±184.46nm (38.15% RSD) and 473.47±153.74nm (32.47% RSD), respectively. A similar variation, but smaller average particle size was obtained for samples synthesized using Method 3. The average particle size was calculated to be 139.13±5.62nm (32.79% RSD). These methods used overnight stirring in order to remove the organic solvent used in the formulation. Lower variation was obtained for nanoparticles synthesized using Method 5, which applied the use of pressure. The average particle size for the samples was 243.80±26.28nm (10.78% RSD). Improvement in the particle size and variation was seen for Methods 6-9 where a greater pressure was also applied in order to aid more rapid removal of the organic solvents. The average particle size range was less than 250nm and percentage RSD ranged from 6.88-11.48% for the samples synthesized using these methods. The average particle size obtained for nanoparticles synthesized using Method 2 and 4 were significantly higher than the average samples obtained using the remaining methods ($P<0.05$).A varied particle size was obtained for the blank nanoparticles and mono-encapsulated nanoparticles formulated using Method 8 (Table 2.4). The particle size variation was greater than 15% for all three samples and the largest mean particle size was obtained for the theophylline mono-encapsulated nanoparticles.

The nanoparticles synthesized using the double emulsion method using PLA resulted in negatively charged nanoparticles (Table 2.3). Similar to the particle size, an improvement in the variation was obtained when the organic solvents were removed using pressure. Samples synthesized using Method 1 had an average zeta potential of -16.90±5.77. A slightly lower, but with a greater variation, zeta potential was measured for nanoparticles synthesized using Method 2 and Method 5. The percentage variation was over 50% for these samples. A very low zeta potential was measured for nanoparticles synthesized using Method 3 (-0.88±3.35). A large improvement in the zeta potential and the variation was obtained when altering the quantity of the polymer and aqueous phase in Method 4. Nanoparticles synthesized using

Method 6-8 showed average zeta potentials that were approximately -20mV. Similar variation was obtained for the nanoparticles synthesized using Method 7 and 8; but greater for the nanoparticles synthesized using Method 6. The average zeta potential for nanoparticles synthesized using Method 9 was lower and was calculated to be -13.55±5.63. The differences in the zeta potential of co-encapsulated nanoparticles synthesized using the different methods were not significantly different ($P>0.05$, except for Method 3 and 5). Similar zeta potentials were obtained for blank and mono-encapsulated nanoparticles as the co-encapsulated samples using Method 8 (Table 2.4). The variation and average zeta potential in these samples, however, was lower than the co-encapsulated counterpart.

Table 2.3 The average particle size and zeta potential for co-encapsulated theophylline and budesonide nanoparticles synthesized using methods 1-9 using 50 mg theophylline, 5 mg budesonide and 200 mg PLA (*P<0.05)

Method number	Average particle size ±SD (nm)	% RSD	Average zeta potential ±SD (mV)	% RSD
1 (n=9)	278.89±35.67	12.79	-16.90±5.77	37.25
2 (n=3)	483.48±184.46*	38.15	-12.35±6.30	50.97
3 (n=3)	139.13±45.62	32.79	-0.88±3.35*	379.91
4 (n=3)	473.47±153.74*	32.47	-20.58±4.02	19.55
5 (n=3)	243.80±26.28	10.78	-8.01±4.16*	51.96
6 (n=9)	230.18±25.57	11.11	-20.92±19.73	94.34
7 (n=9)	186.09±17.27	9.28	-20.33±7.10	34.94
8 (n=9)	216.71±14.90	6.88	-19.26±6.50	33.75
9 (n=9)	191.56±21.99	11.48	-13.55±5.63	41.52

Table 2.4 The average particle size and zeta potential for mono-encapsulated theophylline/ budesonide nanoparticles and blank PLA synthesized using Method 8 (n=3, mean±SD)

Sample	Average particle size ±SD (nm)	%RSD	Average zeta potential ±SD (mV)	%RSD
Blank PLA	337.23 ± 71.63	21.24%	-16.61 ± 1.00	6.02
Theophylline mono-encapsulated	418.78 ± 81.70	19.50%	-16.22 ± 0.56	3.45
Budesonide mono-encapsulated	192.30 ± 63.19	32.86%	-13.17 ± 1.11	8.43

2.3.2 ASSESSMENT OF SURFACE CHARACTERISTICS OF THEOPHYLLINE AND BUDESONIDE NANOPARTICLES USING FT-IR SPECTROSCOPY

FT-IR spectra for PLA, budesonide and theophylline were obtained as standards to which spectra for the nanoparticles were compared. This helps to identify and assign peaks on the spectra to functional groups present in the structure of the drugs and polymer.

PLA (Figure 2.1A) is a poly-ester and a C=O ester bond is seen at 1746.34cm^{-1}. A strong C-O stretch is also seen in the region of 1100-1400cm^{-1}. C-H bond stretches are observed on the spectra at 2960cm^{-1} as well. The OH bond stretch is seen in the region of 3500cm^{-1}. Budesonide (Figure 2.1B) peaks characteristics to the bonds present were shown on the FT-IR spectrum obtained. CH present in the aromatic region of budesonide was seen at 3000-2900cm^{-1}. CH aliphatic peaks were shown on the spectrum at 2940.77cm^{-1}. C=O ketone bond stretches is observed at 1714.77cm^{-1}. C=C double bond stretches are seen at 1665.12cm^{-1}. C=O ring stretches are also seen in the region of 1600cm-1. In the region of 1400-1100cm^{-1}, the C-O bond stretches peaks are shown. The C-C ring stretches are also seen in the region of 1400cm^{-1}.

The spectrum of theophylline (Figure 2.1C) presents peaks in the spectra typical to the chemical bonds present in the structure. An NH stretch is usually observed at 3300cm^{-1} region, and there is a peak present at 3121.19cm^{-1} which represents this bond. Theophylline contains both secondary and tertiary amines, which correspond to this peak. CH peaks are seen at 2960cm^{-1} region, and there is presence of peaks at 2941.11cm^{-1}. A broad peak in this region suggests the CO_2 and H_2O from background spectra, but also due to the CH stretch from theophylline. C=O (stretching) peaks are observed at 1709cm^{-1}. A C=N stretch is observed 1564cm^{-1}. C=N stretches are also seen at 1615-1700cm^{-1} regions. C=C stretches are seen at 1664.54cm^{-1}. These are observed in the region of 1640cm^{-1} and 1680cm^{-1}. Peaks in this region are as a result of the ring stretch. The free drug and polymer mixture consisted of theophylline and budesonide mixed in their powder form with the PLA polymer crystals (Figure 2.1D). The mixture was further crushed and then placed on the FT-IR instrumentation in order to analyze the spectrum. A mixture of peaks from the two drugs and polymer is expected. The peaks shown on the spectrum are a mixture of both the drugs and the polymer. The peak at 3120cm^{-1} shows the presence of theophylline and the amine groups in the structure. The CH bonds present in all three components are shown by a broad peak at 2993cm^{-1}. At 2604cm^{-1} an extremely broad peak is observed; this is also seen in the theophylline spectrum. 1745cm^{-1} has a peak which is observed in the PLA spectrum which represents the C=O of the ester group. The C=O peak at 1714cm^{-1} which is seen in

budesonide is not seen on the spectrum. This may be due to the lower quantity of budesonide compared to theophylline and PLA. As a result this peak must also be masked by the peak representing the ester bond in PLA at the same wavenumber. A peak at 1709cm^{-1} is seen in theophylline as well, and also represents the C=O bonds present and could as a result; mask the ketone peak for budesonide. C=C double bond peak is seen at 1663.42cm^{-1} which is similar to the peaks obtained for theophylline and budesonide. C=N present in theophylline is shown on the free drug and polymer mixture spectrum at 1563.12cm^{-1}. In the region of 1400-1100cm^{-1} is the presence of C-O bonds. This region also shows peaks that are representative of the C-C and C-O ring stretches.

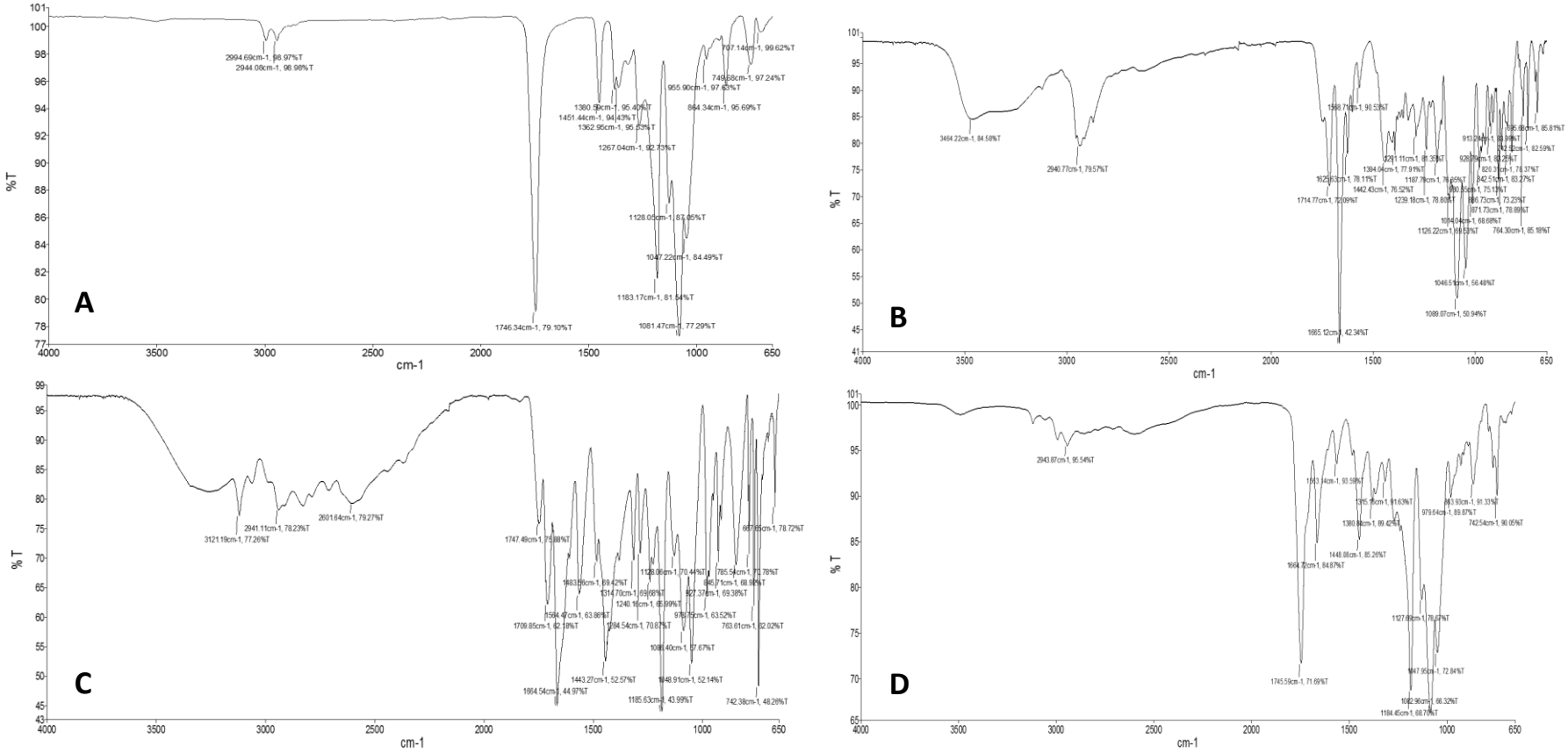

Figure 2.1 FT-IR standard spectrum of (A) PLA , (B) budesonide, (C) theophylline and a (D) free drug and polymer mixture which consisted of theophylline (50 mg) and budesonide (5 mg) mixed in their powder form with the PLA polymer crystals (200 mg) obtained using a Perkin Elmer Spectrometer 65.

FT-IR spectra were obtained for all the nanoparticle samples synthesized using the various methods but only the FT-IR spectra for a co-encapsulated sample using Method 8 is shown in Figure 2.2. This sample contains 50 mg theophylline, 5 mg budesonide and 200 mg PLA. The spectrum and peaks present showed similarity to the PLA spectrum. The spectra obtained show peaks at regions of 1750.04cm^{-1}, which represents the C=O ester bond of the PLA. C-O stretches are seen in the region of 1100-1400cm^{-1} for the samples. C-H bond stretches are present in the region of 2960cm^{-1} as seen for the samples. OH peaks from the background appear in the region of 3500cm^{-1}.

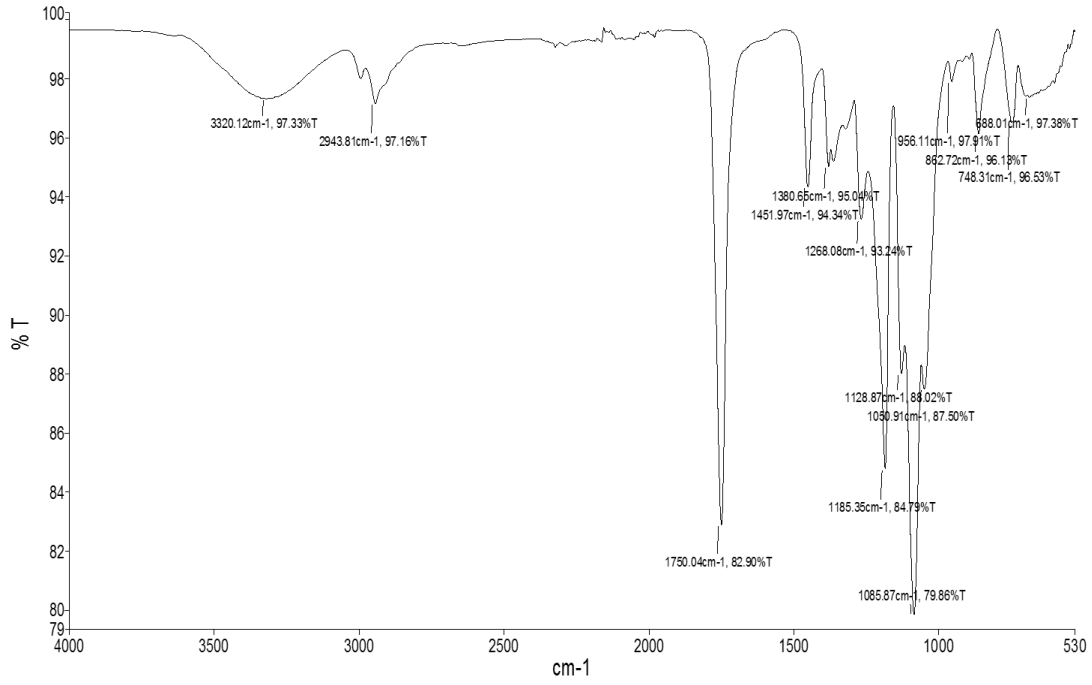

Figure 2.2 The FT-IR spectrum of a theophylline and budesonide co-encapsulated PLA nanoparticles synthesized using Method 8 which used acetone as a second organic solvent in the organic phase

2.3.3 ASSESSMENT OF THERMAL RESPONSE OF CO-ENCAPSULATED NANOPARTICLES USING DIFFERENTIAL SCANNING CALORIMETRY (DSC)

The thermal response of the nanoparticle samples was compared to drug and polymer standards in order to determine any similarities or differences as a result of interactions between the components. The thermograms for samples synthesized using only Method 8 was used for this part of the analysis. The thermogram that is shown in this part represents a co-encapsulated nanoparticle sample which was formulated using 50 mg, 5 mg and 200 mg of theophylline, budesonide and PLA, respectively.

A sharp, single endothermic peak was seen for theophylline which indicates theophylline melting point at 271°C (Figure 2.3A). Budesonide also presented a single, endothermic peak representing the melting point at 260°C (Figure 2.3B). The thermogram for PLA shows a glass transition (T_g) peak at a region of 40-45°C, characteristic of the polymer's physical property. A definite melting point was not visible as the polymer is an amorphous compound. A large, broad peak in the region of 270-400°C suggests degradation of the polymer at extremely high temperatures (Figure 2.3C).

The thermogram for the co-encapsulated nanoparticles synthesized using Method 8 showed the peak at 45°C which represents the glass transition (T_g) of the polymer akin to the thermogram for the PLA standard (Figure 2.3D). There is an absence of the sharp theophylline and budesonide peaks at their respective melting points in the thermogram for the nanoparticles. A large broad peak at the region of 250-400°C was consistent with the polymer thermogram.

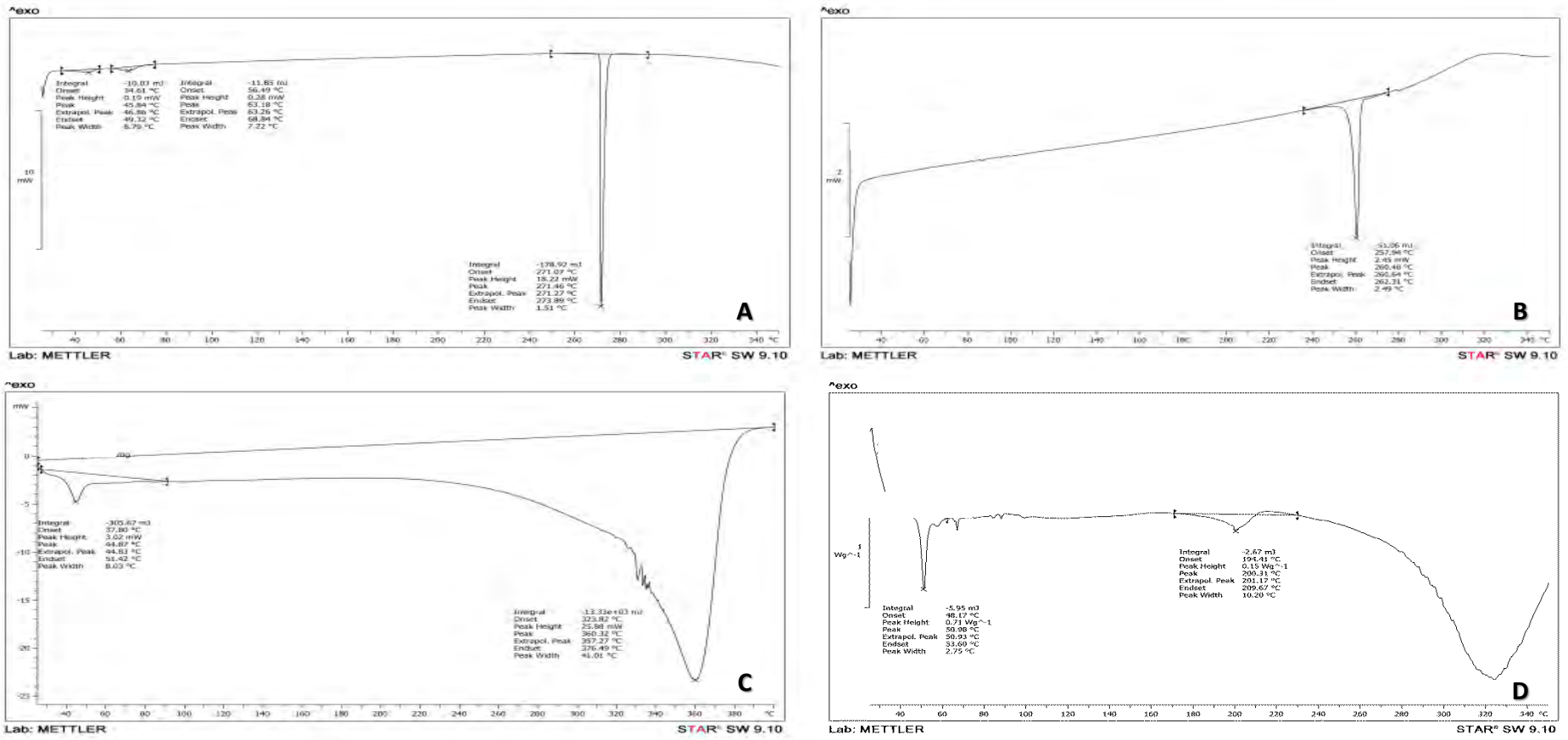

Figure 2.3 DSC thermograms for (A) theophylline standard, (B) budesonide standard, (C) PLA standard and a (D) theophylline and budesonide co-encapsulated PLA nanoparticle synthesized using Method 8 which used acetone as a second organic solvent

2.3.4 MORPHOLOGICAL ASSESSMENT OF THEOPHYLLINE AND BUDESONIDE NANOPARTICLES

Morphological assessment of the nanoparticles was carried out using scanning electron microscopy (SEM) and transmission electron microscopy (TEM). The main aim of this part of the assessment is to determine the surface morphology of the particles. The principle observation was that the particles were spherical in shape with a smooth surface and a wide particle size distribution for the samples formulated using the various methods.

SEM images of samples formulated using all the methods were taken, but only SEM images of co-encapsulated nanoparticles synthesized using Method 8 are shown in this part of the study (Figure 2.4A and B). Method 8 showed spherical particles with a good size distribution where the nanoparticles were present in the nanometer range; but with a few particles having 2 μm size.

Transmission electron microscopy (TEM) was carried out for co-encapsulated nanoparticles formulated using acetone as a second solvent and for samples formulated using the method where the washing step was omitted (Method 14). SEM samples did not reveal nanoparticles due to the presence of the surfactant in the samples (image not shown). Nanoparticles were shown when samples were studied using the TEM (Figure 2.4C).

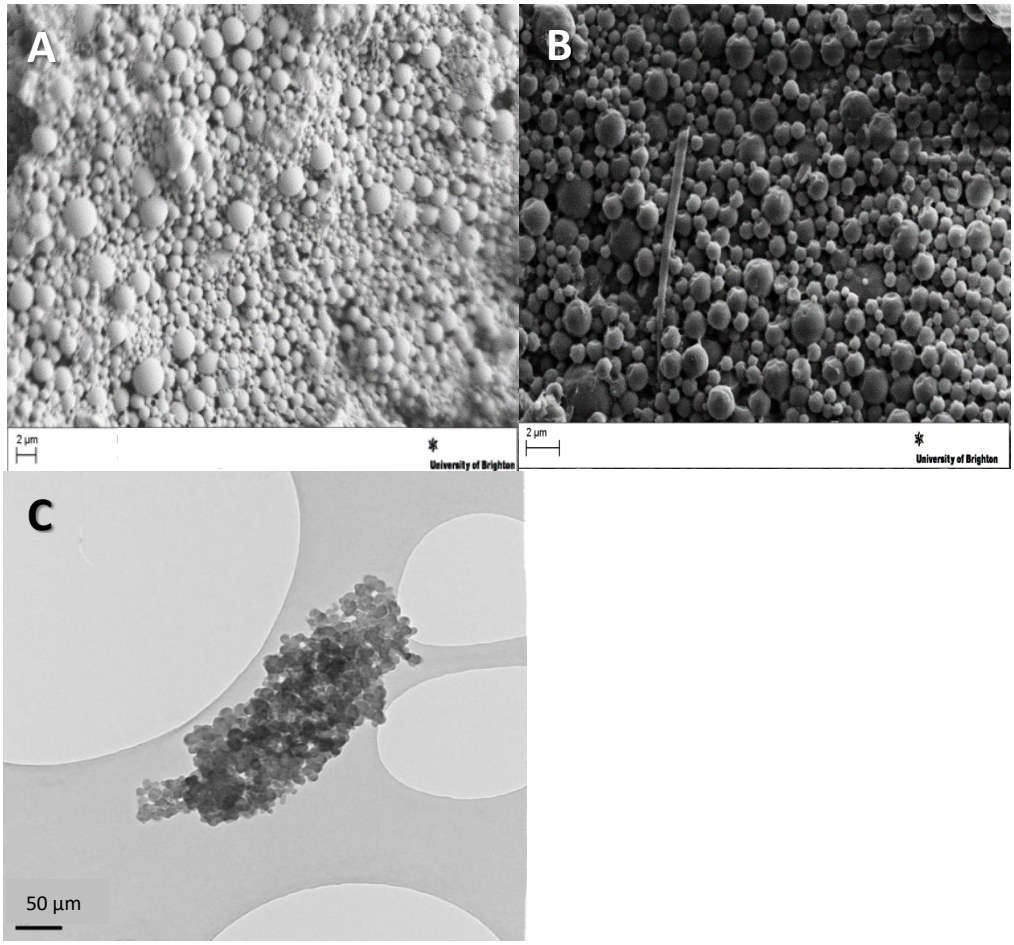

Figure 2.4 SEM images of theophylline and budesonide co-encapsulated nanoparticles synthesized using Method 8 (A & B) showing spherical particles with a smooth surface and a wide distribution of size and TEM images of theophylline and budesonide co-encapsulated nanoparticles synthesized using Method 14 (C).

2.3.5 *Analytical Method Development using High performance liquid chromatography (HPLC) to determine loading efficiency of theophylline and budesonide*

The results of system suitability for both, theophylline and budesonide, are presented in Table 2.5. Using a standard 10 µg/mL concentration of theophylline prepared in methanol, the precision (0.57%), linearity between 1-10 µg/mL (R^2= 0.9986) (Figure 2.5) and tailing factor (0.03±0.00) meet specifications. Theoretical plate number (107±23) and capacity factor (0.22±0.00) do not meet specifications suggesting poor column efficiency and solvent front retention close to the theophylline peak, respectively. The most linear range for theophylline was obtained between 1-10µg/mL. The linearity was assessed at different concentration ranges: 10-100 µg/mL (R^2= 0.996), 0.1-1 µg/mL (R^2= 0.985). The LOD was calculated to be 3.53 ng/mL. The LOQ was calculated to be 10.70 ng/mL.

System suitability calculations were also obtained for budesonide (10 µg/mL) prepared in methanol. Similar to the data obtained for theophylline, the precision (0.21%), linearity between 1-10 µg/mL (R^2= 0.9977) (Figure 2.6), tailing factor (0.10 ± 0.00) and capacity factor (5.01±0.062) meet specifications. The theoretical plate number (396 ± 56) does not meet specifications. The most linear range for budesonide standards was also obtained in the concentration range between 1-10 µg/mL. The same concentration ranges were studied as for theophylline: 10-100 µg/mL (R^2= 0.996), 0.1-1 µg/mL (R^2= 0.986). The LOD was calculated to be 3.98 ng/mL. The LOQ was calculated to be 12.06 ng/mL.

Table 2.5 System suitability assessment for analysis of theophylline and budesonide encapsulated in PLA nanoparticles

System suitability factors	Specification	Theophylline (mean ± SD, n=6)	Budesonide (mean ± SD, n=6)
Capacity Factor (*k'*)	*k'* > 2	0.22±0.00	5.01±0.062
Precision/Injection Repeatability (%RSD)	RSD < 2%	0.57%	0.21%
Tailing Factor (T)	T ≤ 2	0.03 ± 0.00	0.10 ± 0.00
Theoretical Plate Number (N)	N > 2000	107 ± 23	396 ± 56
Accuracy/Repeatability	95-105%	105.02±0.60	100.37±0.21
Linearity	$r^2 \geq 0.995$	0.9986	0.9977
LOD	-	3.53 ng/mL	3.98 ng/mL
LOQ	-	10.70 ng/mL	12.06 ng/mL

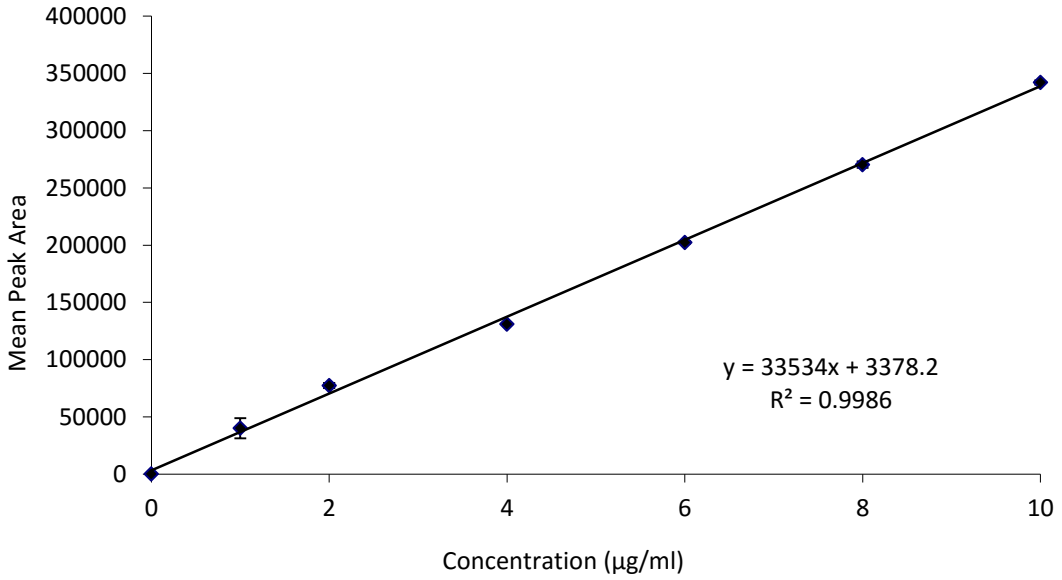

Figure 2.5 Calibration plot for theophylline standards prepared in methanol at a range from 1-10 µg/mL for analytical system suitability (n=3, mean±SD)

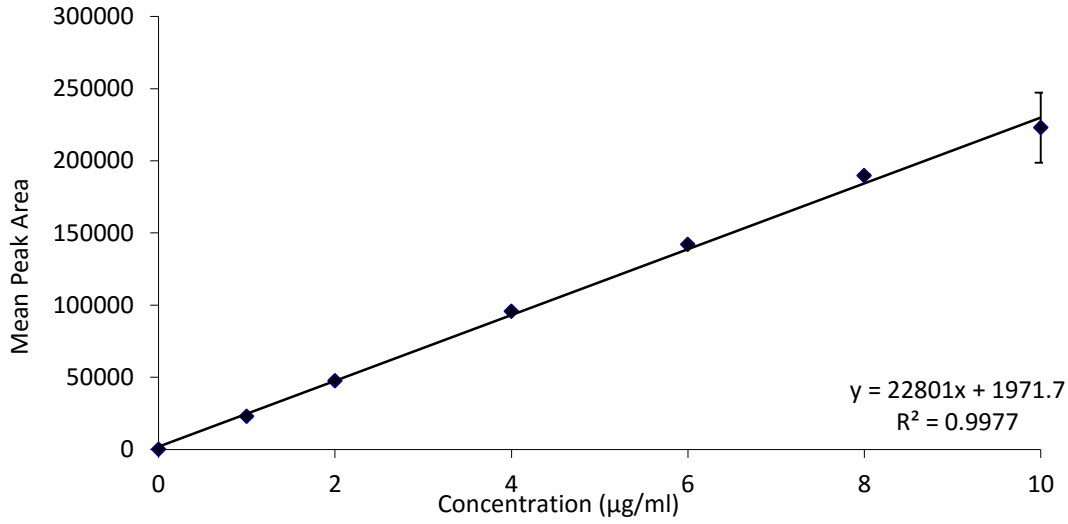

Figure 2.6 Calibration plot for budesonide standards prepared in methanol at 1-10 µg/mL for analytical system suitability (n=3, mean±SD)

2.3.6 DETERMINATION OF THE LOADING EFFICIENCY OF THEOPHYLLINE AND BUDESONIDE IN PLA NANOPARTICLES SYNTHESIZED USING THE DESD METHOD WITH CHANGES IN FORMULATION VARIABLES

To determine the concentration of theophylline and budesonide in the nanoparticles, a suitable analytical method was developed (Section 2.2.2.2.5). For theophylline and budesonide nanoparticles synthesized using the double emulsion solvent diffusion method in the current study; overall a greater loading efficiency was obtained for the hydrophobic drug (budesonide) than hydrophilic drug (theophylline). The loading efficiency of the two drugs is presented in Table 2.6.

Nanoparticles synthesized using Method 1 had an overall loading efficiency of theophylline calculated to be 9.62±5.37% (55.82% RSD) and for budesonide 48.20±27.57% (57.20% RSD). Similar loading efficiency for both drugs was obtained for nanoparticles synthesized using Method 3. Low loading efficiency was calculated for both theophylline (1.16±1.12%) and budesonide (9.88±1.76%) for nanoparticles synthesized using Method 2. Similar loading efficiencies to Method 2 were calculated for nanoparticles synthesized using Method 4 (which involved reduction of both polymer and excess aqueous phase quantity) and Method 5. Extremely low loading efficiencies, suggesting unsuccessful method application, were obtained for both theophylline (0.03±0.01%) and budesonide (0.11±0.06%) for the nanoparticles synthesized using Method 6. A large improvement in the loading efficiency of both theophylline and budesonide was observed for the nanoparticles synthesized using Methods 7-9. The greatest loading efficiency of theophylline and budesonide was obtained for Method 9 which was 29.43±4.90% and 35.09±3.65%. Similar results were obtained for the two drugs encapsulated in the PLA nanoparticles synthesized using Method 7 and 8. Mono-encapsulated nanoparticles of theophylline and budesonide were synthesized and compared to the co-encapsulated nanoparticles synthesized using Method 8 (Table 2.7). Similar loading efficiency was obtained for theophylline in the mono- and co-encapsulated nanoparticles (approximately 18%) but a higher loading efficiency was obtained for budesonide (39%) in the mono-encapsulated nanoparticles compared to the co-encapsulated nanoparticles (31%). The theophylline loading efficiency calculated for co-encapsulated nanoparticles synthesized using Method 2, 4, 5 and 6 was significantly lower than the remaining samples ($P<0.05$). The loading efficiency of budesonide was significantly lower for the nanoparticles synthesized using Method 4 and 6 ($P<0.05$). The loading efficiency of budesonide calculated for Method 1, 3 and 9 was significantly higher than the loading efficiency of budesonide calculated using Method 4-6 ($P<0.05$).

Table 2.6 The average loading efficiency of theophylline and budesonide in co-encapsulated nanoparticles synthesized using methods 1-9 using 50 mg theophylline, 5 mg budesonide and 200 mg PLA (*P<0.05)

Method number	Average theophylline loading ±SD (%)	Average budesonide loading ±SD (%)
1 (n=9)	9.62±5.37	48.20±27.57
2 (n=3)	1.16±1.12*	9.88±1.76
3 (n=3)	13.45±3.03	39.92±4.59
4 (n=3)	1.27±0.07*	3.75±0.27*
5 (n=3)	2.55±0.09*	8.23±2.97
6 (n=3)	0.03±0.01*	0.11±0.06*
7 (n=9)	20.70±5.67	28.39±8.28
8 (n=9)	17.79±5.59	29.84±1.47
9 (n=9)	29.43±4.90	35.09±3.65

Table 2.7 Loading efficiency of theophylline and budesonide in mono- and co-encapsulated nanoparticles synthesized using Method 8 determined using HPLC (n=3, mean ± SD).

Nanoparticles Samples	Average theophylline loading ±SD (%)	Average budesonide loading ±SD (%)
Theophylline mono-encapsulated	18.86 ± 5.28	-
Budesonide mono-encapsulated	-	39.17±18.39

2.4 DISCUSSION

2.4.1 DEVELOPMENT OF THE DESD METHOD TO SYNTHESIZE THEOPHYLLINE AND BUDESONIDE CO-ENCAPSULATED PLA NANOPARTICLES

Drugs can be added to preformed nanoparticles such that they can be adsorbed on the surface, or incorporated during the formulation process. This can occur during monomer polymerization reactions in which covalent bonds between the drug and polymer can form if functional groups are available or by encapsulating the drug in the polymer nanoparticles using various methods [245, 251]. Commonly used methods include solvent evaporation and diffusion methods which were applied in this current study [251]. Encapsulation of the drug has several advantages which include protecting the drug against *in vivo* degradation, decreasing side effects, reducing frequency of administration and therefore potentially increasing patient compliance or can potentially obtain favourable pharmacokinetics [251].

The double emulsion method has been modified and applied for the formulation of hydrophilic drug encapsulated nanoparticles and microparticles synthesized using biodegradable polymers. It has been reviewed by Vrignaud et al (2011), that the lack of chemical interactions between the hydrophilic drug and polymer promotes drug diffusion into the external aqueous medium [251]. In this review, it was also stated that double emulsion method is preferable due to the use of two immiscible phases which can reduce the drug diffusion [251]. Microspheres prepared by the double emulsion diffusion method depend on the stability of the internal water phase and this can influence the loading efficiency of the water soluble drugs [255]. The suitability of the double emulsion method has been reviewed by Lai et al (2014), suggesting formulation of submicron sized nanoparticles by use of high shear to break down emulsion droplets [247]. Theophylline and budesonide nanoparticles were synthesized using a double emulsion solvent diffusion (DESD) method. The nanoparticles were synthesized using a homogenizer as this is able to produce a high shear force and cause collisions of particles with each other [191].

The DESD method that was applied in this current study was modified in several different ways. Several changes in the nanoformulation methods are reviewed in order to increase the encapsulation of the drugs for example increasing the polymer concentration, stabilizing the primary emulsion, ratio between water and oil phase and reducing the concentration gradient between the inner and outer phase [251]. Changes to the polymer quantity, solvents, volume of organic and aqueous phase have been studied in order to develop a suitable method for the encapsulation of theophylline and budesonide.

The polymer quantity used in different studies varied with the drug concentration in consideration. Polymer quantities have ranged between 200-600 mg and up to 20 mg of drug was used in a study by Kraus et al (1985) [291]. In the current study for the synthesis of theophylline and budesonide nanoparticles, 200 mg and 50 mg of PLA were studied. This quantity (200 mg) was previously reported in a study to encapsulate 3 mg of estrogen [205]. A slightly higher quantity of polymer (250 mg) was investigated to encapsulate a hydrophilic drug, voriconazole [228]. Despite the higher quantity of polymer, this did not change the properties of the nanoparticles, the particle size or zeta potential [228].

The nanoprecipitation method has been used with less success to formulate hydrophilic drug nanoparticles. In a study by Barichello et al (1999) an attempt to develop a method to encapsulate hydrophilic and hydrophobic drugs in PLGA nanoparticles using acetone as the organic solvent was not successful despite using 75 mg of the polymer and 2.5 mg of the drug [292]. Similar results were obtained in the current study when 50 mg of PLA was used. A larger quantity of the drug (50 mg) was also used in a study to encapsulate doxorubicin similar to the quantity of theophylline used in the current study [240]. Greater concentrations of theophylline were attempted to be used but this was limited by its solubility in the PVA solution. Nanoprecipitation was also used by Govender et al (1999) to formulate procaine hydrochloride in PLGA nanoparticles [177]. The solvent system used was acetonitrile with various changes in the method parameters were carried out. The polymer quantity used was 50 mg but the overall volumes were lower too. In the study of procaine hydrochloride nanoparticles, it was suggested that an increased drug quantity incorporated in the formulation results in an increased loss of the drug and wastage. For the study of theophylline and budesonide nanoparticles the maximum quantity used was 50 mg and 5 mg in order to allow increased encapsulation of both the drugs.

The ratio between the drug and polymer were also thought to be important and affected some of the characteristics of the nanoparticles. An increase in the ratio of drug and polymer was thought to be more favourable as suggested in a study by Miladi et al (2015) [288]. Method 4 which involved a reduction in the polymer quantity to 50 mg resulted in a 1:1 ratio with theophylline. This reduction in polymer was overall not suitable as a result of low loading efficiency and high variation in the other characterization tests carried out. Various different ratios of the drugs and polymer were studied which included 1 and 5 mg budesonide, 5, 10 and 50 mg theophylline and as described, 50 and 200 mg PLA. All these samples were characterized in the same manner (Appendix 1: Synthesis and characterization of theophylline and budesonide nanoparticles, Table 10.4 and Table 10.5).

When the volume of the excess aqueous phase was reduced to 50 mL, it resulted in the formation of large aggregates in the suspension and was thought to be due to the increased concentration of the polymer resulting in an increased viscosity. This was reported in a study carried out by Bilati et al (2005), where the increase in viscosity may affect the diffusion of the solvent towards the non-solvent and can result in formation of large aggregates, which was not overcome by addition of a stabilizer [261].

The concentration of PVA or other surfactants that was used in the study ranged in the studies. In this study, 2% w/v PVA was chosen as higher concentrations of PVA (5%w/v) and subsequent higher quantities of theophylline resulted in limited dissolution. Higher quantities of theophylline which were still within the prescribed range of theophylline (75 mg, 100 mg and 200 mg) were not soluble in 2% w/v PVA (data not shown). The solubility of theophylline (50 mg) in 5% w/v PVA was also limited (data not shown). PVA concentrations ranging from 1-4% have been previously reported [198, 204, 228, 231, 244]. To encapsulate two hydrophilic drugs, Song et al (2008) optimized the method using 80 mg of polymer and 2% w/v PVA with acetone and dichloromethane as the organic solvents of choice [193, 194]. This concentration of PVA was also used in the formulation of oligonucleotide nanoparticles of PLA using a double emulsion method [281]. Reviewed by Hans and Lowman (2002), 2-4% PVA was ideal for the formulation of nanoparticles[243].

Other studies use lower quantity of PVA such as 0.3%w/v as part of the excess aqueous phase [293]. To encapsulate cyclosporine, PVA (2% w/v) was used in the excess aqueous phase and instead of centrifugation, the sample was filtered through a sintered glass filter [286]. Similarly, 5% w/v PVA was used to formulate PLA nanoparticles using multiple emulsions [294]. In this study, water has been used as the excess aqueous phase which was also commonly used in the other studies to encapsulate hydrophobic drugs [205]. The inclusion of the surfactant in the inner phase can increase the stability of the primary emulsion [198]. However, it has also been stated that the effect of the stabilizer was discussed to be minimal in a study by Kwon et al (2001), where it was stated that the PVA adsorbs at the interface and is washed off in the centrifugation step [205]. One study reported up to 10% w/v PVA in the primary emulsion, which was further added dropwise to a second aqueous phase consisting of 0.75%w/v PVA. This would not be suitable in the study of theophylline and budesonide nanoparticles, as the high concentration of theophylline would not be soluble in the PVA.

Other surfactants that have been used include Tween 80 [197, 199, 207, 295] and Pluronic acid [188]. But PVA is reviewed by Lai et al (2014) to be the most suitable compound as a stabilizer [247] and the most common surfactant [294].

The dissolution of the drug in the correct phase of the emulsion is also important. For the encapsulation of hydrophobic dugs, it was suggested that the drugs should be dissolved with the polymer in the organic phase. For hydrophilic drugs, it should be dissolved in an aqueous phase and then dispersed into the polymer and organic solvent [204, 288]. This method was used here to encapsulate both theophylline and budesonide in PLA nanoparticles. This was reviewed to be the most suitable method to encapsulate hydrophilic drugs using the emulsification method [243].

Various solvents have been used to formulate nanoparticles. Dichloromethane was reported to be the primary solvent in the synthesis of nanoparticles using a solvent evaporation method [198] due to its immiscibility with water. Other commonly used solvents included acetone and ethyl acetate [198, 199, 253, 296, 297]. Acetone and dichloromethane in various ratios were studied by Song et al (2008) and Cheow et al (2010) for the encapsulation of hydrophilic drugs as it affects the overall miscibility and diffusion of the drugs from the aqueous to the organic phase [193, 198]. The choice of organic solvents is important because high solubility of the hydrophilic drug in both aqueous and organic phase can result in difficulty with encapsulation. A high solubility with either one of the phases otherwise would result in the drug leaking out of the nanoparticles when the polymer precipitates [198]. In the formulation of theophylline and budesonide nanoparticles, initially dichloromethane had been used as a lone solvent. This was further modified to include two solvents in the organic phase at 50:50 ratios. The solvents studied were acetone, ethyl acetate and acetonitrile. It was noted that the use of dichloromethane was not completely suitable due to the low solubility of theophylline in this solvent. Using a mixed organic phase was ideal and it considers the effect on both drugs due to the low solubility of budesonide in the aqueous phase. It was important that the changes in the method did not affect the loading efficiency of budesonide.

From the solvents used, acetone produced nanoparticles with greater consistency in the different characterization tests carried out. In a study carried out by Cheow et al (2008), it was suggested that as ethyl acetate is less miscible in water than acetone, it can allow the partitioning of the hydrophilic drug through the phases of the emulsion [198]. Theophylline is readily soluble in acetone but not in ethyl acetate.

In a study conducted by Niwa et al (1993), acetone and dichloromethane were used as a mixed organic phase (evaporated over a period of 3-4 hours). In this study, it was discussed that the addition of acetone to the dichloromethane at increasing ratios decreased the interfacial tension between the dichloromethane and aqueous phase. Acetone in the mixture also helps with the encapsulation of the hydrophilic drug as it allows the polymer to deposit

at the interface between the aqueous and organic phase preventing the leakage of the hydrophilic drug [298]. The time that was taken to evaporate the organic solvent in Methods 7-9 was similar; and this showed improvement in the overall characteristics of the nanoparticles. Co-encapsulated PLGA nanoparticles containing vincristine & quercetin and of vincristine & verapamil synthesized by Song et al (2008) using an emulsion solvent evaporation process used a mixed organic phase of dichloromethane and acetone [193, 194]. These studies also supported the advantage of acetone being able to reduce the interfacial tension between the aqueous and organic phase and affect the overall partitioning of the drugs and therefore the encapsulation efficiency [193, 194]. The study focused on investigation of the ratio of acetone and dichloromethane, PLGA ratio, molecular weight of the polymer, and ratio of aqueous and organic phase [194]. It was seen in this study that a change in the variables do not change the particle size and all are present in the submicron range.

Methods of evaporation altered between continuous stirring and using pressure to evaporate solvents. Some studies showed evaporation of the solvent using continuous stirring [299] for two hours [287] or overnight [197]. PLGA nanoparticles encapsulating voriconazole formulated using a multiple emulsion method was evaporated using pressure resulting in spherical nanoparticles in the submicron range [228]. Overnight stirring resulted in large variations in particle size and zeta potential in the current study, which are discussed in detail in Section 2.4.3 and 2.4.4. Overnight stirring also resulted in lower loading efficiencies of both drugs, especially theophylline (Section 2.4.8) in the current study. It is predicted that due to the presence of the nanoparticles in the aqueous medium for a longer duration, it may result in an increased partitioning of the hydrophilic drug and result in low drug loading. The application of pressure to remove the organic solvents and reduce the formulation time resulted in improved characteristics of the nanoparticles in terms of particle size, zeta potential and loading efficiency, discussed in detail in the following sections.

The washing step is important for the removal of un-encapsulated drug and excess surfactant and is a process carried out by several studies [225]. Methods 14 and 15 represented what the sample would be present as if the surfactant and un-encapsulated drug was not removed. The drug loading calculated for these was also higher; which was thought to be principally due to the presence of free drug present in the suspension (data not shown).

Apart from using a double emulsion method, there are alternative methods used in studies to encapsulate hydrophilic drugs, which include changing physicochemical properties of the drug such as forming complexes or esterification. Ishihara et al (2009) formed a zinc complex of betamethasone in PLGA/PLA nanoparticles which resulted in increased encapsulation efficiency as a result of a hydrophobic interaction between the zinc-

betamethasone complex and polymer [199]. While methods such as the one applied in the current study involve centrifugation as a washing step, it would be easier to remove any un-encapsulated drug with zinc complexes. Other options include addition of salt forms or changes in pH [198, 288]. A change in pH was adopted by Govender et al (1999) to increase the loading efficiency of procaine and as a result of the altered ionization states, the loading efficiency was increased. The disadvantage to this method was suggested that there are an increased number of electrolytes and salts present in the medium and can lead to increased instability [177]. For theophylline and budesonide, changing pH to increase loading would need to be considered as an effect for both drugs and therefore would not be suitable. Alternatively, Govender et al (1999) also replaced procaine hydrochloride with procaine dihydrate [177]. A study conducted by Ito et al (2011) was by freezing the aqueous phase containing hydrophilic drug (blue dextran) where after an emulsion system was made the aqueous phase was frozen and the second organic phase was added manually [259].

An attempt to synthesize theophylline particles using ethyl cellulose and PCL (dissolved in methylene chloride) was carried out by Jelvehgari et al (2012). The method also used PVA in the formulation. This study suggested that theophylline was present at the interface (which can be internal or external). This study also recommended the rapid evaporation of organic solvents in order to obtain rapid precipitation of the polymer to increase the encapsulation efficiency [260].

From the results obtained for the various characterization techniques carried out, the final combination of the drugs and polymers was chosen as: 50 mg theophylline, 5 mg budesonide and 200 mg of PLA. Mono-encapsulated nanoparticles were also synthesized using the same quantity of either drug in the initial formulation.

2.4.2 Analytical Method Development using High performance liquid chromatography (HPLC) to determine loading efficiency of theophylline and budesonide

In order to determine the loading efficiency of theophylline and budesonide encapsulated in the nanoparticles, a suitable analytical method was required to be developed using HPLC. To accurately determine the loading efficiency, careful consideration of the mobile phase, column, detector wavelength and also extraction method were required.

There are several reported reverse phase-HPLC methods that were used for the analysis of theophylline and budesonide, individually; however no method has been reported for the analysis of theophylline and budesonide together. These reported methods included the use of acetonitrile, methanol, various buffers and water as the mobile phases. By considering all these methods, the methods described below were used in order to analyze both theophylline and budesonide. The table below describes some mobile phases that have been used previously for theophylline and budesonide (Table 2.8).

Table 2.8 HPLC methods developed to study theophylline (or other xanthine's) and budesonide

Drug	Mobile phase/ column details
Theophylline (and other xanthine's)	• Acetonitrile: formic acid (7.5: 92.5), C18 Novopak column (particle size 5µm) [300, 301] • Methanol: water: formic acid (19.5:80.2:0.3), C18 [302] • Acetonitrile: 0.1%v/v orthophosphoric acid (gradient) (C18, 250x4.0mm, 5µm) [303] • Methanol: water: acetic acid (gradient method to achieve 67% v/v methanol) (C18, 4.5x250mm, 5µm) [304] • Methanol/ethanol: water: acetic acid (20:75:5)(C18, 150x4.0mm, 5µm) [305] • 0.01M phosphoric acid: methanol: acetonitrile: isopropyl alcohol (420:20:30:30) (C8 column) at 273nm [306] • Methanol: water: orthophosphoric acid (20:79.9:0.1)(C18, 150x4.6mm, 5µm) at 210nm [307]
Budesonide	• Methanol: aqueous buffer mix at pH 3 (69:31), C18 (25cm) column [308] • Methanol: water (80:20), C18 (4.6mmx25cm) (detected at 244nm and a flow rate of 1.5mL/min) [309] • Methanol: water (65:35) (C18 3.9mmx15cm) (at 280nm) [238] • Acetonitrile: potassium dihydrogen orthophosphate buffer at pH 3.2 (60:40) (C8, 4.6mmx15cm, 3.5µm) (at 244nm) [230]

Suitable separation of theophylline and budesonide was required to be achieved when carrying out the analysis. It is ideal to use the same mobile phase for the two drugs as it allows simultaneous analysis of both drugs. Other advantages include limited use of solvents for HPLC method, shorter assessment times (by application of gradient methods) and development of an extraction method that can be used for both drugs.

HPLC methods of xanthine derivatives were considered as they are structurally similar to theophylline and would require small modifications in the method in order to be suitable for both, theophylline and budesonide.

Preliminary analysis of the loading efficiency of drugs in the nanoparticles was carried out using acetonitrile and formic acid as the mobile phase and a Zorbax-Agilent Rapid Resolution SB-C8 (3.5µm, 4.6mmx7.5cm) as the stationary phase (Appendix 1: Synthesis and characterization of theophylline and budesonide nanoparticles, Table 10.2).

The final HPLC method that was used consisted of methanol and water as the mobile phase. This was due to the limitations present in the preliminary method using acetonitrile and formic acid (0.1%v/v). The limitations included theophylline eluting too close to the solvent front which was represented by a negative capacity factor. The second reason was that the use of formic acid in the mobile phase causes ionization of theophylline. The column was also changed to a C18 column. The details of the system used and the column used are provided in Table 2.2 in Section 2.2.2.2.5.

Isocratic mobile phases were explored and these were 50:50 and 60:40 methanol: water. Although there was an improvement in the elution of theophylline, with retention time of over 3 minutes, budesonide elution was not achieved in the mobile phases even at a run time of 20 minutes. Further modification of the mobile phase to 80:20 methanol: water showed improvement in elution of budesonide, however, this mobile phase resulted in very rapid elution of theophylline which also overlapped the solvent front peak. Budesonide peak appeared at 5-6 minutes. Reducing the concentration of methanol in the mobile phase to 70:30 methanol: water showed good separation between both drugs peaks (theophylline and budesonide). Theophylline peak eluted at 2.15 minutes and budesonide at 10.5 minutes.

This HPLC method that is described was used for determining loading efficiency of theophylline and budesonide in the nanoparticles. This method was also used to determine the concentration of theophylline and budesonide when studying the release of the drugs or the transport across a cell layer and the concentration of the drugs in the nanoparticles deposited at different stages of the airways. Further details on the previous HPLC methods developed and validated are presented in the Appendix 1: Synthesis and characterization of theophylline and budesonide nanoparticles, Section 10.1.1.

2.4.3 Determination of the particle size of theophylline and budesonide synthesized PLA nanoparticles using dynamic light scattering (DLS)

Studies carried out on the formulation of polymeric nanoparticles synthesized using emulsion methods resulted in nanoparticles in the submicron size range. For this reason, by applying the DESD method for the formulation of theophylline and budesonide nanoparticles in the current study, it was expected that the nanoparticles would have an average particle size in the sub-micron range, i.e. between 200-500nm. Alendronate nanoparticles synthesized using PCL also showed a similar range in particle size (211-445nm) using this method [288]. A submicron range was obtained for PLGA nanoparticles of voriconazole (between 300-400nm) formulated using a multiple emulsion method [228],

levofloxacin [198] and an oligonucleotide [281]. Several changes in the formulation variables were carried out, which would potentially affect the mean particle size or distribution. Various studies, discussed below, have also presented with changes in the particle size distribution when formulation variables are modified.

Major changes were observed in the particle size distribution when the method to evaporate organic solvents was modified in the current study. Overnight stirring, on average, resulted in larger distribution in the particle size in comparison to when the organic solvents were evaporated under pressure (Methods 2-4). This is thought to be due to the slower formation of nanoparticles as a result of a longer time required for the organic solvents to evaporate and therefore allow polymer and drug to precipitate and form nanoparticles. The use of pressure to remove organic solvents more rapidly showed an improvement in the distribution of the particle size. Nicotine encapsulated PLGA nanoparticles were reported in the literature at approximately 300nm, which were synthesized using an emulsion method which involved overnight stirring to remove the organic solvents which, on average, is similar to the particles synthesized using Method 2 where overnight stirring was applied [310]. Theophylline particles synthesized using ethyl cellulose and PCL resulted in extremely large particles with an average size of approximately 850nm. The solvents were removed rapidly as an attempt to increase the encapsulation efficiency [260].

The relationship between polymer quantity and particle size has been studied extensively. In the current study the initial polymer concentration in the organic phase was reduced from 20 mg/mL to 5 mg/mL. Along with a reduction in the volume to 50 mL the ratio changes from 2:1 to 1:1 in Method 4 which resulted in larger particles but similar effect on the distribution.

This conflicts other work carried out in order to determine the relationship between polymer concentration and particle size. A study on PLGA nanoparticles that involved changing formulation variables and their effect on the particle size showed that an increase in the concentration of PLGA resulted in an increased particle size [285]. However, this was related to the viscosity of the emulsion system formed resulting in a reduced ability to disperse. Sizes over 500nm were obtained when the polymer PLA was used at different quantities ranging from 200 mg to 600 mg of the drug with an ESD method [291]. Quercetrin PLGA nanoparticles synthesized using PLGA by an emulsion solvent evaporation method were in a range of 175-300nm [311].This difference in results obtained in the current study could have been caused as a result of the high concentration of the drugs in comparison to the polymer, i.e., a reduction in the drug: polymer ratio potentially affecting formulation of the nanoparticles, combined with the ratio of the external phase. The reduction in the polymer

quantity in some samples results in a 1:1 ratio with the drug and polymer, e.g. when theophylline and PLA quantity is 50 mg for each compound.

PCL and PLGA nanoparticles of lapazine synthesized using solvent evaporation method were between 180-190nm. Other methods used such as nanoprecipitation [287, 297], solvent deposition method [207] and an anti-solvent method [231] resulted in nanoparticles in a submicron size range. It was shown that regardless of changes in the method, the nanoparticles were present in the submicron range. However, an increase in concentration of the polymer resulted in an increase in particle size [193, 194, 205]. Reduction in the volume of the excess aqueous phase showed similar particle sizes for samples using 200 mg of polymer and a greater particle size for samples formulated using 50 mg of polymer in the current study.

Blank nanoparticles synthesized using Method 8 in comparison to mono-encapsulated nanoparticles synthesized using the same method was smaller in size. These nanoparticles showed a larger variation than the co-encapsulated nanoparticles synthesized using the same method. The particle sizes for blank and mono-encapsulated nanoparticles were present in the sub-micron range however. Similar mean particle sizes were obtained for samples synthesized using ethyl acetate, acetone and acetonitrile.

Particle size can influence the application of the nanoparticles *in vivo* as it can influence the toxicity, targeting and can be internalized by cells at certain particle sizes [184, 229, 283]. The size of the nanoparticles can also potentially affect the release, the drug loading as a result of increased surface area [184] and can also affect stability, for example aggregation during storage [184].

In the current study, even though there were changes in variables result, it was desired that the nanoparticles are present in a submicron range; which was what was achieved. In a study by Song et al (2008) on vincristine and verapamil nanoparticles, despite changes in the variables, the particles remained to be in a submicron range similar to the current study [193, 194]. It has been previously suggested that with changes in the formulation variables, there was mainly an effect on the particle size distribution and was suggested in a study by Wei et al (2008) that it is difficult to control the size distribution, similar to the current study. Wei et al (2008) attempted to reduce the size distribution by extruding the particles through a porous glass membrane to form uniform sized droplets [283]. Overall, it can be suggested that the greatest influence in the particle size was as a result of changing the method of evaporation of the organic solvents from stirring overnight to using reduced pressure. This would allow rapid formation of the nanoparticles by precipitation into the aqueous medium.

2.4.4 DETERMINATION OF THE ZETA POTENTIAL OF THEOPHYLLINE AND BUDESONIDE SYNTHESIZED PLA NANOPARTICLES

Zeta potential measurement is important to determine the stability of the nanoparticles if presented as a suspension. Unstable suspensions can result in uncontrolled particle agglomeration and increase in particle size (Ostwald Ripening) [231]. Surface charge and surface chemistry are also important to determine the interactions between nanoparticles with cell systems [184, 229]. As the polymer, PLA encapsulates the drugs the charge that is expected on the surface of the nanoparticles is negative as a result of the carboxylic acid groups present on the polymer [188, 207, 254, 286]. It is ideal to have a zeta potential charge of ±25mV which indicates that the samples are very stable when present as a suspension system [178, 184, 207, 228, 239, 243]. The zeta potential represents the electrical potential of the particles and is influenced by dispersion medium and particle composition itself [184]. A zeta potential of 20 and 5mV suggests acceptable and short term stability, respectively [178].

A large variation of the zeta potential in the sample can cause some particles to repel each other and some to aggregate and coalesce and therefore affect the overall stability of the formulation.

Overall, the zeta potential obtained for all the samples using a DESD method was negative, as expected. Generally, the variation in the zeta potential obtained for all the samples using different methods was high. Other studies in which the emulsification solvent diffusion method was applied also resulted in an average zeta potential similar to the current study. The DESD method used to formulate nanoparticles of alendronate using various ratios between the organic solvent and aqueous phase resulted in lower zeta potentials (compared to the results obtained in the current study) ranging from -0.52 to -10.4mV. A study on PLA nanoparticles showed that changes in parameters did not remove the negative charge of the nanoparticles, such as changes in the surfactant concentration or volume of the internal phase [294], similar to what was observed in the current study. Despite changes in the variables of the methods, the zeta potential for PLGA nanoparticles encapsulating levofloxacin also remained in the range between -10mV to -30mV using a DESD method. Another study also reported zeta potential values of approximately -10mV using an ESD method, in which it was suggested that the zeta potential of the particles depends on the conformation of the polymer and the medium used for re-precipitation [312]. The dispersion medium for analysing the zeta potential in the current study was water as this is solvent that would be used to nebulize the nanoparticles as a suspension. Other nanoparticles synthesized using an ESD method using PLGA, encapsulating furanodiene, resulted in similar zeta potentials too with values in the range of -20 to -14mV. This observation in the

zeta potential was consistent with PCL and PLGA nanoparticles synthesized using emulsion solvent evaporation method (-15 to -13mV). These results correlate with the results obtained in the current study. Similar zeta potentials for blank and drug encapsulated nanoparticles were obtained, suggesting successful washing of the suspension and removal of excess, un-encapsulated drugs.

Differences were observed in the zeta potential range depending on the method of evaporation of organic solvents in the current study during nanoformulation. Overnight stirring resulted in a large variation in the particle size and also had a similar effect on the zeta potential. Methods 2 and 3 showed zeta potential values with high variation within samples and a large range. Greater zeta potential was observed in the nanoparticles samples (and consistent degree of variation) where pressure was used to remove the organic solvents. A similar effect on the particle size distribution was also observed. This was the case when either a single or mixed organic solvent was used for the formulation of nanoparticles.

Reducing the polymer quantity from 200 mg (Method 2) to 50 mg (Method 4) did not show a large effect on the zeta potential in the current study and still resulted in negatively charged nanoparticles. The effect on reduction of excess aqueous phase was not clear when the polymer concentration was 20 mg/mL and excess aqueous phase reduced to 50 mL, this resulted in an extremely low zeta potential with a large variation. This may potentially suggest unfavorable ratios of polymer and solvents used.

The negative charge obtained on the nanoparticles synthesized using polyesters such as PLA and PLGA was also consistent for when other methods were applied. Similar zeta potentials are obtained for these suggesting that a wide range of zeta potentials are obtained using polyesters. Negatively charged nanoparticles were reported by Nafee et al (2009) which were approximately -8mV [297]. A zeta potential of -16mV was obtained for nicotine encapsulated PLGA nanoparticles [310]. PCL nanoparticles of theophylline were also negatively charged (-12 to -16mV was the range calculated) [260]. Suggesting that the zeta potential obtained in this study is consistent with the zeta potential obtained for various other examples of nanoparticles synthesized using this group of polymers.

2.4.5 Assessment of surface characteristics of theophylline and budesonide nanoparticles using FT-IR spectroscopy

FT-IR spectroscopy was carried out in order to observe the surface properties/characteristics of the nanoparticles and highlight any drug adsorption on the outer surface. Unlike transmission FT-IR, the current investigation is not able to indicate if the drugs are encapsulated and present inside the polymer capsule formed.

Provided that the drugs have been encapsulated in the nanoparticle and not adsorbed on the external surface, the spectra for the nanoparticles would resemble the spectrum for the PLA standard. If the drugs are not encapsulated successfully and still remain in the sample after the washing out steps, or if the formulation of the nanoparticles is not entirely successful, then the peaks of drugs and polymer are expected to be present together on the spectrum. Another reason for not being able to see drug peaks on the spectra could also be as a result of the uneven ratio between the drugs and polymer in the formulation, which could lead to the drug peaks being masked by the polymer spectrum.

The main observation from the FT-IR spectrum is the characteristic ester bond of PLA at ~1750cm^{-1} which was present in all the nanoparticles samples. Similar observations have been made for the polymer [190]. Based on the chemical structure of theophylline, the bonds for an amine, amide, carbonyl and alkene bonds could be seen in the FT-IR spectrum.

Nanoparticles that were synthesized using each method were examined (data not shown). For all the samples, the resemblance of the nanoparticle FT-IR spectrum to the polymer spectrum suggests that the drugs are not adsorbed on to the external surface of the nanoparticles. The lower quantity of drug present in the sample in comparison to the polymer may result in masking of the drug peaks. For example, the ketone peak of budesonide and ester peak of PLA might be overlapping with the ester bond of PLA as all three are seen in the same region on the spectrum. The low loading efficiency calculated for the drugs (Section 2.3.6) further suggests that the low concentration of drugs present in the nanoparticles may be the reason for the low sensitivity. All the different methods carried out to formulate nanoparticles show spectra resembling the polymer and not the drug. This however does not confirm successful encapsulation but mainly suggests that the drugs are not adsorbed on the external surface and any excess (un-encapsulated) drug is washed off. A similar observation has been reported in the literature where nanoparticles characterised by using FT-IR did not show the presence of any drug peaks. It was also further reported that the un-encapsulated drug is removed during the centrifugation step [228].

2.4.6 Assessment of thermal response of co-encapsulated nanoparticles using Differential scanning calorimetry (DSC)

The thermal response of the nanoparticle samples was compared to drug and polymer standards in order to determine any similarities or differences as a result of interactions between the components [178, 286].

The thermogram for the nanoparticles showed the peak at 45°C which represents the glass transition (T_g) of the polymer, which was also observed in the thermogram for PLA standard. The absence of the sharp theophylline and budesonide peaks at their respective melting points suggests potential interaction between the drug and polymer components of the nanoparticles, altering the melting point of the drugs. A large broad peak in the region of 250-400°C is consistent with the polymer thermogram. The differences in the concentration of drug and polymer ratio in the formulation may affect the presence or absence of the peaks akin to the observations made in the FT-IR analysis (Section 2.4.5).

The small shift in the polymer degradation peak suggests possible interactions between the drug and polymer. A similar observation has previously been reported in the literature with budesonide microparticles [263] and with theophylline nanoparticles [260]. It is conceivable that due to the high ratio of polymer to drugs any drug melting peak could also have been masked by the polymer degradation. However, a large transition observed with the nanoparticle melting compared to the PLA standard suggests that chemical interaction between the drugs and polymer to be more likely explanation. This theory would require further investigations using suitable analytical techniques.

It was suggested that the lack of drug peaks in the DSC thermogram suggests the presence of the encapsulated drug in an amorphous state [178, 207, 288]. Thermograms obtained for PLGA and PLA nanoparticles (encapsulating docetaxel) suggested that the polymer inhibits the crystallization of the drug during the formulation of the nanoparticles, resulting in the amorphous state of the drug. The glass transition phase of the polymer was not influenced by the preparation procedure, similar to the current study [207].

2.4.7 Morphological Assessment of theophylline and budesonide nanoparticles

Overall all the samples formulated using different methods showed a wide range of size distribution for the nanoparticles. Particles produced using different methods were all spherical in shape with smooth surfaces. The surface of some the particles show porous features in the form of small perforations on the surface. This feature may be important in the drug release from the nanoparticles. Porosity in the particles may deliver several advantages to drug delivery by these nanoparticles. The perforations present may allow water to enter the particle and cause dissolution of the drug, diffusion of the drug to the outer surface and lead to polymer degradation.

Particle size was observed to be in the submicron range supporting data obtained dynamic light scattering analysis (Section 2.3.1). However, the images do reveal some particles

present in the micrometer range reflecting a wide size distribution. Method 8, which was nanoparticles formulated using acetone, showed a narrow particle size distribution of the nanoparticle sample.

For the samples formulated using Method 14 and 15 that did not include a washing step, it was important to determine if the nanoparticles were present; but just coated by the polymer. For this reason TEM was carried out to obtain more information on the morphological features of the nanoparticles. More importantly, TEM would allow examining the drug encapsulated nanoparticles and to determine and understand how the drug is encapsulated by the polymer. For this characterization method, a co-encapsulated nanoparticle sample was chosen (synthesized using Method 8) and examined. Similar particle size distribution is obtained from the TEM images as observed in the SEM images. Particle size in the TEM images shows greater correlation with the data obtained using dynamic light scattering where particles are present in the submicron range between 200-300nm.

The images and features of the particles were supported by other studies carried out; suggesting nanoparticles synthesized using biodegradable polymers using different methods result in similar products. Common observations made when using SEM or TEM included spherical nanoparticles with smooth surfaces using similar methods of formulation (solvent diffusion methods) to obtain biodegradable polymeric nanoparticles [177, 193, 194, 197, 198, 228, 253, 259, 281, 283, 286-288, 293-295, 311, 313, 314]. Observations were also made to study the size distribution and if it correlated with quantitative size analysis [194, 281, 287]. Similar to the theophylline and budesonide nanoparticles, inclusion of a drug in the formulation did not affect the morphological changes in comparison to the blank PLA nanoparticles synthesized using the same method, Method 8 [207, 287].

The SEM and TEM images obtained for the nanoparticles showed same features for all the different parameters that were changed in the formulation method. Although there were changes in the formulation variables, the particles still remained to be spherical with a smooth surface. This was also noted in studies carried out on PLGA nanoparticles encapsulating praziquantel [293] and PLGA nanoparticles encapsulating levofloxacin [198].

2.4.8 DETERMINATION OF THE LOADING EFFICIENCY OF THEOPHYLLINE AND BUDESONIDE IN PLA NANOPARTICLES SYNTHESIZED USING THE DESD METHOD WITH CHANGES IN FORMULATION VARIABLES

Methods have been developed to increase the encapsulation efficiency of hydrophilic drugs in nanoparticles. Due to high aqueous solubility, the hydrophilic drug partitions to the aqueous phase resulting in low encapsulation efficiency. Several different measures have been taken to increase the encapsulation efficiency, such as changing the organic solvents used, changes in chemical structures the hydrophilic drugs and development of methods such as the double emulsion solvent diffusion (DESD) method, which is used in the current study. Despite the application of this method, it was predicted that the loading efficiency of budesonide would be greater than theophylline. However, it was important to ensure that the loading efficiency of budesonide was not affected when changing method variables. Overall, from the results obtained in the current study, a higher loading efficiency of budesonide was achieved in comparison to theophylline with all the methods.

It has also been previously suggested that the low loading efficiency of hydrophilic drugs is not only caused due to a rapid diffusion of the drug into the aqueous phase but also because of poor interaction between the drug and the polymer. This poor interaction causes an increased diffusion of the drug from the organic to aqueous phase [244, 285, 292]. It was suggested that increasing the concentration of the polymer could increase the encapsulation efficiency [285].

As the DESD method was developed for the encapsulation of hydrophilic drugs, comparison with nanoprecipitation method showed a higher encapsulation efficiency for alendronate sodium using the DESD method (15-34%) compared to 0.36-18.8% achieved with nanoprecipitation [288]. A similar comparison was also made for PLGA nanoparticles containing levofloxacin between methods nanoprecipitation, emulsification solvent diffusion and double emulsification methods, where the loading efficiency was higher using a double emulsification method [198].

The initial method that was tested required the use of one organic solvent, dichloromethane, in the organic phase. It has been described in studies previously, the necessity of dichloromethane in the formulation of particles using an emulsion method. The use of this single organic solvent showed a higher loading of budesonide in comparison to theophylline. It can be suggested that the low solubility results in theophylline not being

able to successfully partition across the organic phase and be successfully encapsulated at high concentrations. For this reason, a method was developed to add a second organic solvent in order to increase the theophylline loading efficiency by increasing the miscibility of the organic phase with the aqueous phase. Theophylline was dissolved in the aqueous phase (containing the surfactant) and therefore this may have had an impact on the loading efficiency of theophylline. However, theophylline's solubility in organic solvents is limited and for this reason it is more suitable for theophylline to be present in the aqueous phase.

Using a mixture of acetone and dichloromethane in a 1:1 ratio along with the aqueous phase resulted in a marginal increase in the loading efficiency at 22% of a hydrophilic drug using the emulsification-solvent evaporation method [198]. Use of the nanoprecipitation method resulted in more rapid diffusion of the hydrophilic drug to the aqueous phase [198]. However, using a mixed organic phase allows for increased miscibility of the organic phase with the aqueous phase thereby enabling the hydrophilic drug to be encapsulated. The drug loading for theophylline and budesonide when using ethyl acetate or acetone as the second organic solvent showed similar results. Variability in drug loading for both the drugs was observed to be less when using acetone. Higher drug loading and variation for both drugs was obtained in samples formulated with acetonitrile. It is important that the variation in the drug loading is limited as it allows more control on the dosing of the drugs and therefore the amount of nanoparticles that would be required for administration. It also allows accurate prediction of the amount of drug encapsulated in the nanoparticles.

In a study conducted by Cheow et al (2010) [198], it was seen that the use of ethyl acetate increased the loading efficiency of the drug compared to acetone in the double emulsion method. However, this study was carried out for the encapsulation of one drug only. A greater solubility of theophylline in acetone consequently may have had a role in the consistent loading efficiency of theophylline (and budesonide) in the nanoparticles. Model hydrophilic drug blue dextran was encapsulated using an emulsion method to form PLGA nanoparticles and showed an encapsulation efficiency of 20% [259]. Approximately 10% loading for an oligonucleotide was obtained when synthesizing PLA nanoparticles [281] and in a study of theophylline PCL nanoparticles encapsulation efficiency was calculated to be 37% [260]. Similar to what was applied here an attempt was made to remove the organic solvents as rapidly as possible in order to allow precipitation of the polymer and synthesis of nanoparticles encapsulating theophylline. However, these nanoparticles had an extremely large particle size in the region of 850nm [260].

In the current study, methods that involved overnight stirring of the sample to remove organic solvent resulted in low encapsulation of theophylline and varied loading efficiency

of budesonide and improved loading efficiency when pressure was applied to remove the solvents. The presence of theophylline in the aqueous medium for longer periods of time (overnight) was thought to be the reason for the reduced encapsulation efficiency of theophylline as it allowed an increased time for theophylline to partition out to the favorable, aqueous medium. Similarly, in a study by Cheow et al (2010), where overnight stirring was used to formulate nanoparticles (using mixed organic phase) encapsulating hydrophilic drugs it also resulted in low loading efficiencies (2.2-2.4%) [198]. It is also possible that due to the slower evaporation of the organic solvents, the nanoparticles would have been formed slower than in comparison to when prepared under pressure due to slower precipitation of the polymer in the aqueous phase. Faster evaporation of organic solvents would therefore reduce partitioning of theophylline and increasing the loading efficiency. Overnight stirring also resulted in large variation in the other characteristics of the nanoparticles, such as particle size and zeta potential suggesting that such a step in the formulation of nanoparticles is not ideal. Even with application of pressure to remove the organic solvents, by reducing the pressure to an even lower amount such as in Method 8 showed an increased improvement in the drug loading of theophylline and budesonide in comparison to Method 5.

Different quantities of theophylline and budesonide were used in the current study in order to increase the drug loading efficiency (Appendix 1: Synthesis and characterization of theophylline and budesonide nanoparticles, Section 10.1.2, Table 10.5). However, it was observed that there was no direct correlation between drug quantity and loading efficiency. By using a larger quantity of drugs in the formulation, it can be suggested that there is a greater probability for it to be encapsulated. However, it was reported in study involving development of procaine hydrochloride nanoparticles synthesized using nanoprecipitation and in PLGA nanoparticles of voriconazole that, such a step led to unnecessary drug wastage as well as drug leakage from the nanoparticles [177, 228]. Although it was a study carried out on PLGA microspheres formulated using a double emulsion method, it was important to consider that an increase in the polymer concentration resulted in an increased loading efficiency of the drug (blue dextran). This was due to the less time required for solidification of the particles but also due to the increased viscosity by increasing the concentration of the polymer [203].

Volume of excess aqueous phase had an effect on the overall success of preparing nanoparticles in the current study. When the excess aqueous phase volume was reduced to 50 mL it was hypothesized that it would lead to an increase in the encapsulation efficiency as a lower aqueous phase will mean a reduction in the quantity of the favorable phase

present for solubilizing theophylline and therefore forcing encapsulation of a higher drug quantity by the polymer.

When the polymer concentration was kept constant (20 mg/mL) but the volume of the excess aqueous phase was reduced (Method 3), there was a small increase in the loading efficiency of theophylline. This result suggests that a reduction in the volume of the excess aqueous phase may have an effect in the amount of drug that is released into the solvent. Reducing the polymer quantity to 50 mg and the excess aqueous phase to 50 mL resulted in a lower loading efficiency for both drugs. The reduced ratio between the drug and polymer can be a reason for the low encapsulation efficiency of theophylline and due to the increased concentration of theophylline in a reduced volume. The reduction in polymer quantity also results in a high variation in the budesonide loading which is not ideal as it results in difficulty with dosing calculations.

Some studies in which the effect of polymer concentration and loading efficiency was observed, it was noted that increasing the concentration of the polymer also increases encapsulation efficiency [285] similar to the current study. The increased concentration of the polymer results in an increased viscosity which reduces the diffusion of the drug to the external phase [285].However, it was visually observed that the suspension formed using 50 mL of the excess aqueous phase resulted in the formation of large aggregates in the suspension after overnight stirring process. This may be as a result of the high concentration of polymer which precipitates out in the smaller volume of excess aqueous phase. For this reason, the method was not ideal for the formulation of nanoparticles.

A study on theophylline microspheres synthesized using double emulsion methods resulted in a 60% loading efficiency in the microspheres [255]. Similar to the current study, it was suggested that the loading efficiency depended on the solubility of the drugs in the solvents and continuous phase along with physicochemical properties of the drugs and polymer. In this study, it was also noted that when the volume of the continuous phase is reduced, it would result in more collisions and cause the particles to fuse resulting in droplets becoming 'white' and solidifying [255].

A multiple emulsion method was applied in this study to understand how it would affect the loading of theophylline and budesonide (Method 6). It was predicted that by forming multiple emulsions, it can result in reduced partitioning of the hydrophilic drug into the favorable, aqueous phase and allow improved loading efficiencies. This method was applied by using acetone to form a double emulsion and then an addition of this to the excess aqueous phase. However, this method resulted in low loading efficiencies for both

hydrophilic and hydrophobic drugs, suggesting this method was not suitable possibly due to the formation of unstable multiple emulsions.

Some studies looked at the relationship between particle size and loading efficiency. In this study, there was no relationship between changes in the methods and particle size. The size remained consistently in the submicron range and the loading efficiency had not altered in relation to the particle size. Although this study showed no relationship between particle size and loading efficiency, several studies reported an increased particle size resulting in an increased loading efficiency [244, 293]. Similar loading efficiencies were obtained for mono-encapsulated and co-encapsulated drugs in the current study. A similar observation was made in a study on PLGA nanoparticles where there was a fixed capacity that could be entrapped in the nanoparticles – but this was for amphiphilic drugs [285].

The drug extraction method that was developed for the current study mainly took into consideration the sustained release of the drugs. Short extraction time methods may result in some drug still entrapped and not released, leading to inaccurate loading efficiency calculations. For this reason, the extraction method developed involved a 24 hour period in which the nanoparticles were present in methanol, allowing the drug to be released from a specific quantity of freeze dried nanoparticles used for analysis.

Loading efficiency of less than a 100% is obtained due to reasons for example disruption of the primary emulsion system and leaching of the material from the inner phase after the encapsulated particles are formed (diffusion) [203]. Drug which is not encapsulated is removed during the washing step in the nanoformulation method before freeze drying. By applying this method, consistent results were obtained for theophylline and budesonide loading in samples formulated using ethyl acetate (Method 7) or acetone (Method 8) and mono-encapsulated nanoparticles using acetone (Method 8).

Some extraction methods used in other studies involve ultracentrifugation for a period of time and assessing the quantity of drugs in the supernatant in relation to what was present in the initial formulation. Times have ranged from 30 minutes [292] to one hour [315]. Other methods involved using a specific quantity of the nanoparticles and placing them in hot acetone (5 mL) which is evaporated and drug dissolved in ethanol for analysis [313]. While other studies used a shorter time period to extract the drugs from the nanoparticles, in another study on hydrophilic drugs (vancomycin) in poly (ortho ester) nanoparticles, a similar extraction method was applied as for theophylline and budesonide. This method also consisted of nanoparticles in solvent for 24 hours [296]. In this extraction method, 10 mg of the nanoparticles were placed in a mixture of DMSO and water and constantly rotated for 24 hours. Several methods did not specify times used for extraction of drug. A method also

involved determining free drug content in a specific quantity of the suspension and then determining the total drug in the nanosuspension [189, 286]. This method was adapted to determine the loading efficiency of vincristine and verapamil but extraction method was only 10 minutes long [193, 194] and for doxorubicin [194, 240]. The loading efficiency of these drugs ranged between 50-69%. Carboxyfluorescin (CF) nanoparticles showed approximately 60% drug loading; but this was determined by measuring the quantity of drugs in the supernatant after centrifugation [253].

Most calculations carried out for loading efficiency were as a ratio between the mass of the drug in the nanoparticles compared to the mass of the drug used in the formulation and presented as a percentage [285, 295, 311]. Some loading efficiencies reported by calculation using this method are reported up to 90% [295]. Quercetrin, loaded in PLGA nanoparticles had an encapsulation efficiency of approximately 40% [311]. Quercetrin has a similar logP value to budesonide, and the loading efficiency of budesonide was measured to be similar in this study (approximately 30%). These nanoparticles were synthesized using a solvent evaporation method. Similar to the current study, a study on lapazine (encapsulated in PLGA and PCL) had loading efficiency calculated based on the theoretical loading (which was based on the initial mass used on the formulation). This was then quantified based on the specific quantity of nanoparticles used for analysis [313]. The loading efficiency calculated for the drug in these nanoparticles was approximately 35-50%. This method of determining loading efficiency was adapted by Miladi et al (2015) for alendronate sodium nanoparticles synthesized using PCL [288]. PLGA nanoparticles encapsulating voriconazole by a multiple emulsification method resulted in approximately 30% drug loading. This was calculated based on a specific quantity of freeze dried nanoparticles used for analysis (3-4 mg) and placed in an organic solvent and centrifuged [228]. Similar quantities of freeze dried nanoparticles were used in the current study. The loading efficiency for a hydrophobic drug prepared in a solid lipid nanoparticle was also calculated determining the concentration of the drug in the specific quantity of freeze dried nanoparticles [315]. By determining the loading efficiency in a specific quantity allows understanding of the variation in the drug loading in the total sample. In the current study, a theoretical loading efficiency was calculated and used in the calculations for determining the loading efficiency. The theoretical loading was also applied in determining the loading efficiency of cholesterol PEG-lyated nanoparticles [316]. As reviewed by Vrignaud et al (2011), measuring the loading efficiency based on the amount of drug entrapped in the nanocapsule in ratio to what was used in the formulation is more representative [251]. Some studies conducted determined encapsulation efficiency by calculating the difference between the total and unbound drug and obtaining a ratio between this difference and the total drug used [290].

2.5 CONCLUSIONS

The aim of the study was to synthesize nanoparticles containing the hydrophilic drug theophylline and the lipophilic drug budesonide using PLA. To achieve this, a suitable method was developed in order to allow encapsulation of both drugs with a suitable loading efficiency. The double emulsification solvent diffusion (DESD) method was applied in this study to encapsulate the drugs as it has been previously used and developed for the encapsulation of hydrophilic drugs and hydrophobic drugs. However, this method has not been previously applied for the co-encapsulation of this combination of drugs.

In order to achieve the aim of the current study, the method was developed by changes in different variables such as drug and polymer quantities, composition of organic solvents and method of evaporation of the organic solvents after which the physicochemical characterization of the nanoparticles was carried out.

It was concluded from the current study that the use of pressure to evaporate organic solvents resulted in a narrower particle size distribution as well as zeta potential and an improved drug loading of both theophylline and budesonide. The ideal formulation quantities were determined to be 200 mg PLA, 50 mg theophylline and 5 mg of budesonide. It was also concluded, that despite the application of a DESD method, the loading efficiency of theophylline was lower than budesonide; but an improved loading efficiency of the hydrophilic drug was achieved.

It is concluded that the most suitable method for the formulation of theophylline and budesonide PLA nanoparticles was with Method 8 and this method was applied to formulate nanoparticles for further characterization. The nanoparticles synthesized using this method resulted in a narrower distribution in the particle size, zeta potential, loading efficiency, which are suitable for the nanoparticles to be developed into a formulation such as nebulized suspension or a dry power. Similar loading efficiency of the drugs was achieved for the co- and mono-encapsulated nanoparticles. This consistency in drug loading would allow accurate calculation of dosage and quantity of nanoparticles required. The nanoparticles showed spherical particles with smooth surfaces. Further characterization of the nanoparticles synthesized using this method was by determining drug release into simulated lung fluid (Chapter 3), cytotoxicity using a human bronchial epithelial cell line (Chapter 4), effect on the tight junctions and transport of the drugs across a human bronchial epithelial cell line (Chapter 5), *in vitro* deposition of a nebulizer and DPI using an MSLI (Chapter 6) and stability study (Chapter 7).

CHAPTER 3 ASSESSMENT OF THE *IN VITRO* RELEASE OF THEOPHYLLINE AND BUDESONIDE FROM PLA NANOPARTICLES USING FRANZ DIFFUSION CELLS

3.1 INTRODUCTION

Pulmonary drug delivery has been used for many years for the treatment of localized disease with several features of the lungs being advantageous for systemic delivery. As described previously, the advantages of local drug delivery include lower risk of systemic adverse effects and higher drug concentration at target site. However, there is little information available on the controlled release of drugs in the lungs. Controlled release drug delivery in the lungs is beneficial for conditions like asthma as it allows control of symptoms over a long duration (for example overnight control of symptoms) [317] with reduced administration frequency therefore potentially improving patient compliance [216-224, 318]. Use of drug-loaded polymeric nanoparticles has been shown to sustain drug release over an extended period of time; drug release from nanoparticles and concurrent or subsequent biodegradation of the polymer are important for developing successful formulations [179].

Formulating drugs within nanoparticles or associated with carriers can help to overcome problems associated with the drug itself such as toxicity (reducing side effects), efficacy, stability, selectivity (targeted delivery) as well as allowing controlled release of the drug [217, 288, 319, 320]. The use of biodegradable polymers also allows reduced adverse effects of the polymers themselves as biodegradable polymers break down to acidic monomers which are further broken down to products which are part of the normal metabolism by the Krebs cycle [223, 293, 321]. Biodegradable polymers such as PLA and PLGA are FDA-approved (for human use) and show versatile degradation kinetics [218]. By incorporating the drug into polymeric biodegradable nanoparticles any extended release will help in reducing the overall dose of the drug that is required for administration [218].

In vitro release studies have been used to determine the rate of drug release from nanoparticles [322]. However, despite the benefits of controlled release drug delivery to the lungs, there is a lack of pharmacopeial methods for the *in vitro* evaluation of the drugs for respiratory [317, 323] and for parenteral applications [324, 325].

In vitro release testing methods are necessary to monitor batch to batch variability in samples produced; but also important to ensure the clinical performance of the drug and its safety, efficacy, quality [237] and to predict and/or determine a relationship between *in vitro* and *in vivo* release data [324]. For the best results, it is important to set standards when studying the release of drugs *in vitro* which include consideration of factors such as apparatus used and its appropriateness/reliability, the media, sampling intervals and temperature [324]. Assessment of the *in vitro* release does not always correlate to what would occur *in vivo* due to differences in the actual volume of fluids present at the target site. Also factors such as uptake of the drug/particles, distribution, biological factors such as enzymes, clearance and physicochemical characteristics can all affect the release of the drugs [322].

There are several technical limitations to assessing the release of drugs from polymeric nanoparticles [322] but no standard or pharmacopeial methods available to assess the release of drugs from nanoparticles or controlled release formulations, except for oral dosage forms [326-328]. As a consequence, a number of methods have been reported in the literature for determining drug release from nanoparticles and controlled release formulations based on their applications in drug delivery.

Methods include the use of side-by-side diffusion cells separated using an artificial or biological membrane, dialysis bag technique, reverse dialysis technique and ultracentrifugation ('sample and separate' technique) and continuous flow [179, 324, 325, 329]. Microdialysis tubing techniques are popular techniques to measure drug concentrations as drugs are released. The tubing/membrane is permeable to water and is connected to impermeable tubing which is put in contact with the donor fluid. Microdialysis membranes act as a filter which removes the need to carry out precise pre-assay separation steps [330]. Miniaturized methods and dialysis sacs have been applied to study release of drugs from controlled release systems [324]. These are particularly useful if low volumes of samples are to be tested as reviewed by Wischke and Schwendeman (2008) [331]. There are several difficulties when analyzing drug release from the nanoparticles using the methods described. These include separation of nanoparticles from the release media; this can be difficult (causing overestimation of drug concentration), and so it can be avoided using a filter such as dialysis tubing. Filtration can also be achieved when using artificial membranes [179]. 'Sample and separate' methods are related to USP Apparatus method 1 and 2 where the sample is dispersed in the medium and samples taken at regular intervals. Use of filters can ensure that nanoparticles are not removed along with the sample [329].

Franz diffusion cells have been used to study the release of drugs from nanoparticles when only a small amount is available or expected drug concentrations are low but frequent time

points are required [317, 325]. It has been suggested that Franz diffusion cells can represent the *in vivo* conditions with addition of agitation [317]. For pulmonary drug delivery, the low volume of liquid in the donor/apical chamber is suggested to represent the air-liquid interface present in the lungs [323, 332]. Franz diffusion cells were originally developed for the study of permeability or transport of drug compounds across the skin and consist of two chambers which are separated by a membrane, allowing drug to diffuse across the membrane once released from the formulation [333].

Different sizes of cell are available which can be used for different concentrations or volumes. The membrane selected for the study can range from artificial membranes or skin when applied for transdermal drug delivery [333]. Membrane binding affinity of the drug is required to be carried out before studying drug release from the formulation [237]. The receiver fluid is also required to be carefully considered in order not to violate sink conditions, i.e., to obtain no more than10% of the donor concentration in the receiver fluid and are commonly constantly stirred over the testing duration in order to maintain sink conditions at the membrane surface. The main disadvantages of using Franz diffusion cells include determining if the release of the drug is affected by its permeability across the membrane or dissolution of the drug in the medium, i.e., determining the rate-limiting step. The dose applied to the donor chamber needs to be considered carefully as well as the duration of the study [317, 332, 334, 335].

Release patterns have commonly been described as biphasic for drugs in controlled release formulations and polymeric nanoparticles. There is an initial 'burst' release where the drug adsorbed near the surface of the particles is released by a diffusion-controlled process [177, 179, 222, 288, 336, 337]. Another explanation for the burst release is thought to be when dispersion medium enters the surface pores of the polymer, it causes dissolution of the drug particles. As the time goes on, erosion of the polymer occurs and there is further release of the drugs that are present within the matrix system. This 'lag phase' release is caused by both diffusion and erosion mechanisms. During the lag phase, the polymer is degraded to its starting chain length [331]. During the entry of the medium into the particles, the particles can swell which can begin the erosion process of the polymer [331] by relaxing the polymer chains [338]. As the ester linkage of the polymer backbone of polyesters such as PLA is hydrolyzed and formation of acidic monomers is increased, the increased acidity of the polymer's surroundings further catalyzes the degradation of the polymer chain by an autocatalytic process [218, 326, 339]. Some studies indicate a final burst release stage towards the end and therefore call the complete release profile – a triphasic release. This final burst phase is an erosion-mediated release of the drug [326, 331, 339-342].

For diffusion-controlled processes, the drug would need to pass through the nanoparticle surface either through the polymer itself or through the pores that would be filled with dispersion medium. Factors such as polymer chain length, flexibility, mobility, swelling behavior, plasticization and the interaction between drug and polymer can affect the diffusion process, reviewed by Wisckhe and Schwendeman (2008) [331]. In comparison to PLGA, PLA is a more hydrophobic polymer and can affect the release of the drugs by preventing diffusion-controlled processes [216]. The loading concentration can also affect the release of the drug; where an increased loading of the drug in consideration (over 10-20%) results in faster release of the drug possibly due to a smaller amount of polymer that could act as a diffusion barrier [331]. An increased concentration also increases the cumulative amount of drug released at any time, including during the burst release [189, 338, 342].

There are five possible mechanisms by which drug can release from the systems, listed below [179, 189]:

1. Desorption of the drug bound to the surface
2. Diffusion through the polymer matrix
3. Diffusion through the polymer walls
4. Nanoparticle matrix erosion
5. Combined erosion and diffusion processes

There are several different profiles of release that can be described such as immediate, modified, delayed, extended and pulsatile release [343].

The release of the drugs from the nanoparticles depends on the nature of the delivery system, for example, a matrix system has drug uniformly distributed/ dissolved throughout the matrix and drug is released by diffusion or erosion of the matrix. The diffusion mechanism is faster than the erosion mechanism as it doesn't depend on the degradation of the matrix system. Nanospheres are matrix-type structures where drug is adsorbed on the surface and entrapped/dissolved in the structure. Nanocapsules contain a polymeric shell and inner core which contains dissolved drug and some drug adsorbed on the surface.

When studying the release of drugs, the dissolution properties of the drugs are also an important concept to understand. The solvent system that is chosen plays an important role in the solubility of the drug and can influence the overall release of the drug. The solution that is attained in these conditions is said to be saturated (C_s) and the concentration less than saturated (i.e. at equilibrium) (C) is said to be 'sub-saturated' [343-345].

If the volume of the solvent is large, or the solute is removed from the bulk of the dissolution medium at a rate faster than it passes into the solution then C becomes a value that is close to 0 and the ΔC which is C_s-C becomes C_s. When applying this concept in practice, the volume of the medium can be such that the value of C is never greater than 10% of the value of C_s, then some approximation can be made on the concentration that should be applied. When these conditions are met, it is said that dissolution is occurring under 'sink' conditions.

There are many factors that can affect the release of drugs from a carrier system and the dissolution rate of a drug particle [343-345]:

- Factors affecting solubility: include the pH of the medium, presence of other compounds or co-solvents and choice of the medium itself. For example, changes in the medium can affect the solubility and stability of the drug in the release medium [322, 329]. The drug also has to be compatible with the release medium (and membrane if used) to allow recovery of the drug for analysis [322]. To study poorly soluble drugs, and also to maintain sink conditions, there can be a requirement of addition of components to make the release medium more suitable, but at the risk of not mimicking biological conditions [322]. Phosphate buffered saline (PBS) is the most common release medium used to study drug release, simulated lung fluid (SLF) has also been used in several studies. An advantage of using medium such as SLF is that it only contains mineral salts and does not contain any protein or mucus components [332]. A surfactant could be added to the SLF in order to improve the solubility of the poorly soluble drugs [332].
- Temperature: can be affected if dissolution is an endothermic or exothermic process from which changes in the temperature of the medium can affect the overall energy required to carry out dissolution process. Higher temperatures may have an effect on the properties of the polymer as it reaches the glass transition temperature. This change in state may potentially affect the way in which the drug can release from the system [326, 331, 340]. It has been reported that the temperature difference between studies conducted at room temperature and those conducted at 37°C did not significantly affect the release of the drugs [217]. Most studies are carried out at 37°C in order to represent body temperature.
- Volume of the medium: if the overall volume is low, then the concentration of the bulk solution (C) increases rapidly and reaches the saturated concentration of the solid (C_s). Large volumes allow the concentration of C to be negligible and allow sink conditions to operate. This is a very important aspect to consider in practice.

For some delivery sites, such as the lungs, rectum and vagina, the volume of liquid at the site is very low. The removal of the dissolved solute from the dissolution medium and replacement of it with fresh dissolution medium can result in a decrease in C and therefore allow an increased rate of dissolution. It has been stated that there is approximately 1μL/cm^2 of fluid available in the lungs [317, 346]. However, using low volumes, while allowing a more accurate representation of the airways, would compromise the chances of maintaining sink conditions [317, 331, 346, 347]. Some studies highlight the importance of maintaining sink conditions in order to obtain accurate release profiles of the drugs, but also discuss that there was no difference noted if non-sink conditions occurred [331]. Miniaturized methods or dialysis sacs used to study the release of drugs from controlled release formulations have been studied using small vials to mimic pharmacopeial methods (USP Apparatus 1 and 2) using 1L volumes, allowing application to the site of delivery to be mimicked [324].

- Porosity: allowing more medium to enter the particle and allow dissolution of the drug via the diffusion-controlled process. If nanoparticles possess porous features in the surface, this may affect the drug release.

There are several mathematical and release kinetic models that can be applied to the drug released from the nanoparticles. Models such as zero order, first order, Higuchi release, Hixson-Crowell cube root plot and Korsmeyer-Peppas models are commonly applied [218, 332, 334, 337, 343, 344, 348-351]. When the drugs are released at a constant rate it can be considered as a zero-order release [218]. Higuchi's model of release describes the release mechanisms largely on the basis of diffusion only [218]. A disadvantage of controlled release formulations is that theoretical models do not fit perfectly to describe the release/dissolution mechanisms and the models do not always take into account polymorphic form, crystallinity, particle size, solubility and other factors which can affect release kinetics [343].

3.1.1 AIM OF STUDY:

The aim of the study was to test the hypothesis that encapsulating the hydrophilic drug, theophylline, and hydrophobic drug, budesonide in PLA nanoparticles would sustain their release. The aim of this chapter was to study the release of both co-encapsulated and mono-encapsulated theophylline and budesonide from nanoparticles using Franz diffusion cells and to compare this release to the diffusion of the un-encapsulated drugs (in solution). The aim of the study was also to determine whether there is a difference between the temperatures used to study the release and the study was carried out at room temperature and at 37°C. In addition, a further aim was to test the release of the drugs from the nanoparticles in different media (methanol, simulated lung fluid (SLF) and water).

3.2 MATERIALS AND METHODS

3.2.1 MATERIALS

Cellulose (dialysis Visking tubing) (DTV.12000.13 Visking Tubing, Size 13, Dia 2", wall thickness 0.05mm, pore size 24Å), Medicell Membranes Ltd, London, UK

1, 2-dipalmitoyl-sn-glycero-3-phosphocholine (DPPC) (≥99%), Sigma-Aldrich, UK (P4329)

Sodium chloride (>99.5%), Sigma-Aldrich, UK (S7653)

Potassium chloride, Ashland Specialty Ingredients, Poole, UK (BCBF3440V)

Magnesium chloride hexahydrate (>99%), Sigma Aldrich, UK (M2670)

Sodium dihydrogen orthophosphate hydrate, VWR Chemicals International, Leuven, Belgium (#10245R)

Anhydrous sodium sulfate, Sigma-Aldrich, UK (239313)

Sodium hydrogen carbonate, Sigma-Aldrich, UK (CAS: 144-55-8)

Sodium citrate dihydrate, Fisher BioReagents, Fisher Scientific, UK (BP327-500, Lot: 114581)

Sodium acetate trihydrate (>99%), Sigma-Aldrich, UK (CAS: 6131-90-4, Code: 5/2040/62)

Calcium chloride dihydrate (>99%), Sigma-Aldrich, UK (CAS: 10035-04-8, Lot#: A0267637)

18.2MOhms water

Methanol, Fisher Scientific, UK (Code: M/4056/17, Lot :1493729)

Dichloromethane, Fisher Scientific, UK (Code : 10458210)

2.5mL Soham Scientific Franz diffusion cells (with clamp, receiver chamber, donor chamber)

Magnetic stirrer rods, Fisherbrand ®, Fisher Scientific, UK (Code: 11587572)

Magnetic stirrer plate (15 place holder), Thermoscientific (50088029)

Magnetic stirrer plate controller (Thermo Electron LED GmbH), Thermoscientific (50094707)

2L volumetric flask

100µL glass Hamilton syringes, SGE Analytical sciences, Australia (Lot: M10-F3973)

2mL sterile syringe, BD Plastipak, Madrid, Spain (Lot: 1312011)

5mL sterile syringe, BD Plastipak, Madrid, Spain (Lot: 11-93C08)

Laboratory Film (Parafilm®), Chicago, Illinois

Chromacol 2mL crimp top vial (clear), Thermoscientific Germany (Lot: 70734807114)

Chromacol Crimp Cap with PTFE/Rubber, Thermoscientific, Germany (Item# 11578150)

3.2.2 METHODS

3.2.2.1 SELECTION OF MEMBRANE FOR USE IN DIFFUSION STUDIES

It is essential that there is minimal binding of the drug to the membrane used in the diffusion studies. Cellulose membrane with a pore size of 24Å (2.4nm) and a thickness of 0.5mm was selected for the study. Three solutions of theophylline and budesonide at 10 µg/mL, 5 µg/mL and 1 µg/mL were prepared in acetonitrile.

A 2 cm^2 piece of membrane was cut and placed in a beaker containing 10 mL of the theophylline and budesonide solutions and stirred at 280 RPM for 24 hours. Samples (1 mL) were taken at time zero and at 24 hours. A control sample of drug solutions without the membrane was also prepared, stirred at 280 RPM for 24 hours and sampled at time zero and 24 hours. All samples were analyzed in triplicate. The HPLC method used is described in detail in Chapter 2, Section 2.2.2.2.5.

3.2.2.2 PREPARATION OF SIMULATED LUNG FLUID (SLF)

SLF was prepared as described in the literature by Marques et al (2011) [352]. Briefly, dipalmitoylphosphatidylcholine (DPPC) (20 mg) was dissolved in 1:1 dichloromethane (10 mL): methanol (10 mL) mixture. This mixture was then transferred into a round bottom flask and the solvents were evaporated at 337mbar. Once a dry film was formed on the inner surface of the round bottom flask, the dry film was dissolved in 20 mL water and stirred at 55°C for two hours. After two hours of stirring, the sample was sonicated at 55°C for one hour. The remaining components (Table 3.1) were weighed and dissolved in 100 mL of deionized water. This solution is then added to the 20 mL of the DPPC solution and mixed thoroughly. The pH of the SLF was 7.4.

Table 3.1 Quantity of contents required to formulate SLF (100 mL volume)

Component	*Quantity (mg)*
Magnesium chloride hexahydrate	20.33
Sodium chloride	601.93
Potassium chloride	29.82
Anhydrous sodium sulfate	7.1
Calcium chloride dihydrate	36.76
Sodium acetate trihydrate	95.26
Sodium hydrogen carbonate	260.43
Sodium citrate dihydrate	9.7
Sodium phosphate monobasic monohydrate	14.2

3.2.2.3 ASSESSMENT OF DRUG RELEASE USING FRANZ DIFFUSION CELLS

Franz diffusion cells consist of three main components; donor chamber, receiver chamber and a membrane. The cellulose membrane was placed in 18.2MOhms deionized water before cutting to a suitable size and placed between the donor and receiver chambers. Franz diffusion cells were assembled by placing a magnetic stirrer bar into the receiver chamber and then covering the surface with the membrane, avoiding any gaps. The donor chamber was aligned with the receiver chamber and wrapped in Parafilm® in order to prevent movement of the two chambers and leakage of any solvents placed into the chambers. The receiver chamber was filled with medium using a 2.5 mL syringe, ensuring no air bubbles were formed under the membrane. The volume of this was 2 mL. For studies conducted at room temperature, the Franz diffusion cell was placed onto a magnetic stirring plate with the use of a clamp. The donor fluid (containing a specific concentration of the test sample in a specific volume) was pipetted directly onto the donor chamber side of the membrane at a specified volume (0.5 mL).

For studies conducted at 37°C the assembled Franz diffusion cells were placed on a magnetic stirrer plate immersed in a water bath and maintained at a temperature of 37°C for 60 minutes before application of the test sample to the donor chamber. A 200 µL aliquot of the samples were withdrawn from the receiver chamber at 0, 1, 2, 3, 4, 5, 6 and 24 hours and the volume removed was replaced with fresh medium at either room temperature or 37^{o}C depending on the experimental conditions. The samples were diluted in 1mL methanol and analyzed using HPLC as previously described (Chapter 2, Section 2.2.2.2.5). The medium in the receiver chamber was 1:1 methanol: SLF mixture. The donor chamber either contained solutions of theophylline (116 µg/mL) or budesonide (23.52 µg/mL) in SLF or nanoparticles suspended in SLF at a concentration of 0.6 mg/mL. The concentration of each drug in solution represents the equivalent encapsulated concentration of the drugs in the nanoparticles. The suspension of nanoparticles was sonicated for a minute to ensure the nanoparticles were dispersed. The solution or suspension (0.5 mL) was pipetted directly onto the donor chamber side of the membrane.

3.2.2.4 ASSESSMENT OF DRUG RELEASE FROM CO-ENCAPSULATED AND MONO-ENCAPSULATED NANOPARTICLES INTO DIFFERENT MEDIA IN THE ABSENCE OF A MEMBRANE

In order to determine drug release from the nanoparticles directly into solution, nanoparticles were suspended in the receiver fluid, which was sampled and analyzed at the same time points as used for the release studies using the Franz diffusion cells (Section

3.2.2.3). This allowed a comparison of the release of theophylline and budesonide from the nanoparticles in the presence and absence of a membrane.

Dispersion medium (2 mL) was accurately pipetted into a tube. At time 0 hours, the nanoparticle suspension (0.5 mL) prepared at the same concentration (0.6 mg/mL) was added to the medium. A sample aliquot (200 μL) was withdrawn at 0, 1, 2, 3, 4, 5, 6 and 24 hours and replaced. The sample was diluted in 1 mL of methanol and analyzed immediately after sampling using HPLC. The method used is described in Chapter 2, Section 2.2.2.2.5. The experiment was carried out in triplicate for each dispersant medium and nanoparticles sample. This study was conducted at room temperature.

3.2.2.5 DATA ANALYSIS

At each time point the concentration of theophylline and budesonide was determined using HPLC analysis and based on the results obtained from a calibration graph. The concentration was corrected for the volume sampled out and area. This was then converted into a percentage at each time point based on the concentration of the two drugs loaded into the nanoparticles (calculated using the equations in Chapter 2, Section 2.2.2.2.6).

3.2.2.6 STATISTICAL ANALYSIS

To determine if the drugs bound to the membranes, the concentrations of theophylline and budesonide remaining in solution at the end of the experiment were compared to the concentration at the start using an independent t-test. The hypothesis was that the concentration obtained would be 100%. $P<0.05$, suggested significant differences.

To determine if the differences in the concentration of theophylline and budesonide released from nanoparticles when suspended directly in different dispersion media was significant, a two way ANOVA was carried out. $P<0.05$, suggested significant differences. Bonferroni post hoc tests were carried out for this statistical analysis.

To test the hypothesis that release would be greater at 37^{o}C, the differences in the release of theophylline and budesonide from mono-encapsulated and co-encapsulated nanoparticles at the same temperature was compared with the release obtained at room temperature and 37°C using a two way ANOVA was carried out. $P<0.05$, suggested significant differences. Bonferroni post hoc tests were carried out for this statistical analysis.

To determine if the percentage of drug released from the nanoparticles at 6 hours and 24 hours was significantly different a paired t-test was carried out. If $P<0.05$, this was significantly different. To determine if the rates of release of drug from the nanoparticles

between 0-6 hours and 6-24 hours were significantly different, a 2way ANOVA was carried out. $P<0.05$, suggested significant differences.

3.3 RESULTS

3.3.1 SELECTION OF MEMBRANE FOR USE IN DIFFUSION STUDIES

The suitability of the cellulose membrane was examined (Table 3.2). Three different drug concentrations were used for this part of the study: 1, 5 and 10 µg/mL which when analyzed by HPLC after 24 hours gave a high percentage recovery. For both drugs percentage recovery was seen to be high at all concentrations and any differences were not observed to be significant ($P>0.05$). This suggested that the drug did not bind to the cellulose membrane. Up to 85-100% of the drug was recovered when using the cellulose membrane for all three concentrations. The concentration of theophylline and budesonide used in this study was 116 µg/mL and 23.52 µg/mL, respectively.

Table 3.2 Percentage recovery of theophylline and budesonide at various concentrations from solutions containing the cellulose membranes over a period of 24 hours (n=3, mean ±SD)

Concentration (µg/mL)	Theophylline	Budesonide
1	86±28	100±7
5	88±6	104±7
10	98±11	92±5

3.3.2 RELEASE OF THEOPHYLLINE AND BUDESONIDE FROM PLA NANOPARTICLES DETERMINED USING FRANZ DIFFUSION CELLS

The release of theophylline and budesonide from nanoparticles was studied using Franz diffusion cells over a period of 24 hours. Drug release from the nanoparticles was compared to diffusion of the drugs from solutions made up of equivalent concentrations of theophylline and budesonide.

Diffusion of theophylline across the membrane from solution showed a biphasic profile, where the rate was reduced in the period between 6-24 hours in comparison to the initial 6 hours of sampling at room temperature (Figure 3.1). This was not observed for the diffusion of budesonide across the membrane from solution (Figure 3.1). Approximately 40% of the theophylline diffused across the membrane within 6 hours, exceeding sink conditions. Approximately 24% of budesonide diffused across the membrane in 24 hours. The difference in the percentage of theophylline/budesonide diffused across the membrane at 6 hours and 24 hours was significantly different for both drugs ($P<0.05$). The average overall percentage recoveries for theophylline and budesonide are 78.69% and 78.66% respectively.

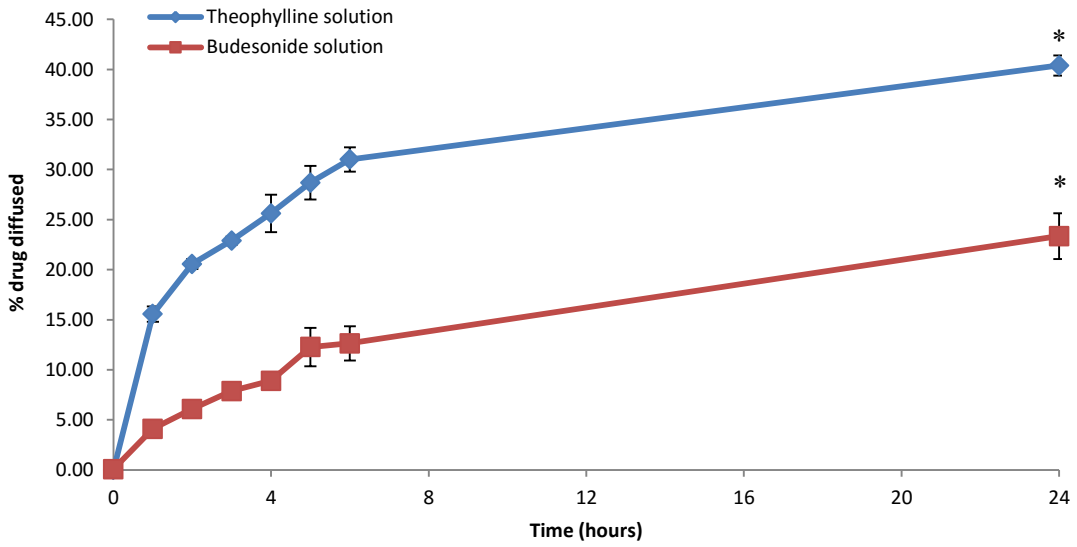

Figure 3.1 Percentage of theophylline and budesonide that had diffused into the receiver chamber of Franz diffusion cells from a solution of equivalent encapsulated concentration of the drugs over a period of 0-24 hours at room temperature. Samples were analyzed using HPLC (*P<0.05) (n=9, mean ±SD)

The percentage of theophylline in the receiver chamber when diffused from the solution is consistently greater than the percentage of theophylline released from the nanoparticles ($P<0.05$). The biphasic profile observed with the solutions was not strongly observed for the nanoparticles and a smaller difference in the gradient between the time period of 0-6 hours and 6-24 hours was observed (Figure 3.2). The release of theophylline from the mono- and co-encapsulated nanoparticles was similar suggesting the release is not affected by the presence of the second drug (in co-encapsulated samples) ($P>0.05$). Less than 10% of theophylline was released from the nanoparticles over the period of 24 hours at room temperature (Figure 3.2). The difference in the percentage of drug released at 6 hours and 24 hours was not significantly different for both mono- and co-encapsulated nanoparticles ($P>0.05$).

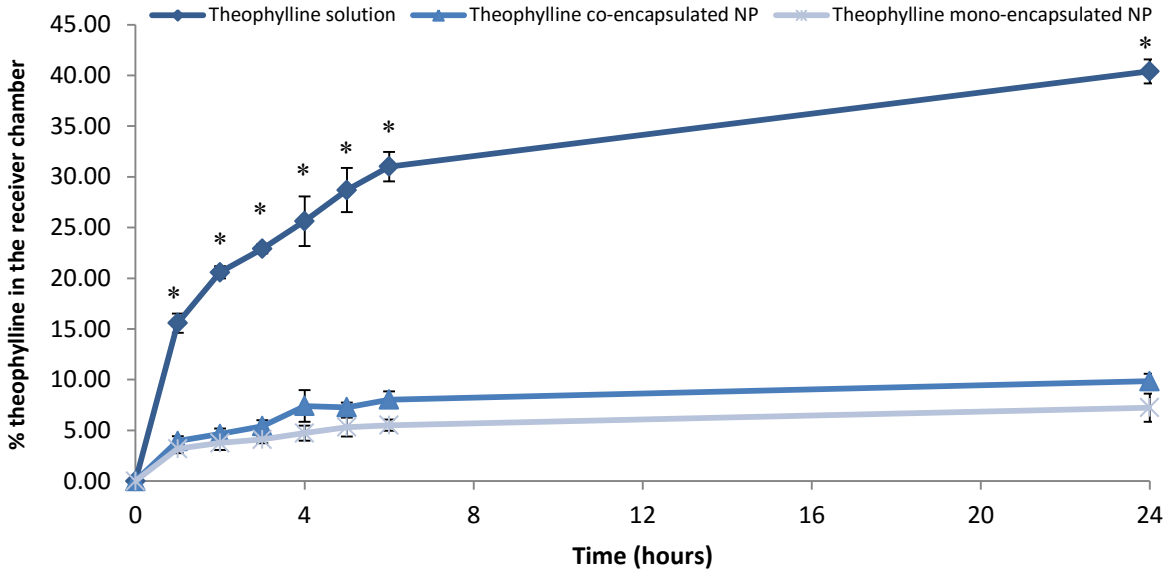

Figure 3.2 Percentage of release theophylline in the receiver chamber from mono- and co-encapsulated nanoparticles in comparison to the percentage of theophylline diffused from the theophylline solution over the period of 24 hours at room temperature. The percentage of theophylline in the receiver chamber from the solution was greater than the percentage of drug released from the nanoparticles (*P<0.05) (Solution: n=9, co-encapsulated: n=21, mono-encapsulated: n=9, mean ±SD) (NP: nanoparticles)

Similar to theophylline, the percentage of budesonide from the solution in the receiver chamber was significantly greater than the percentage of budesonide released from the nanoparticles over the period of 24 hours at room temperature ($P<0.05$)(Figure 3.3). The rate of diffusion of budesonide from the solution in the first 6 hours was greater than from the nanoparticles. Between 0-6 hours and 6-24 hours, the difference in the gradient is smaller. Less than 5% of budesonide was released from the nanoparticles over the period of 24 hours at room temperature. Similar concentrations of budesonide were released from mono- and co-encapsulated nanoparticles ($P>0.05$). The difference in the percentage release at 6 hours and 24 hours was not significantly different for mono- and co-encapsulated nanoparticles ($P>0.05$).

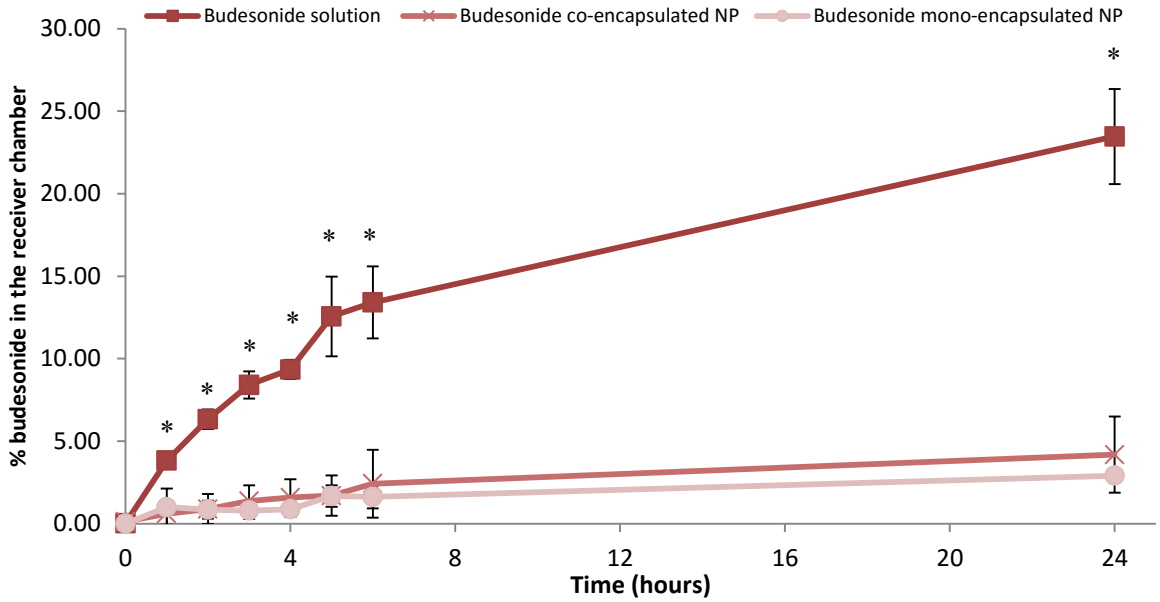

Figure 3.3 Percentage release of budesonide in the receiver chamber from mono- and co-encapsulated nanoparticles in comparison to the concentration of budesonide diffused from the budesonide solution over the period of 24 hours at room temperature (*P<0.05) (Solution: n=9, co-encapsulated: n=21, mono-encapsulated: n=9, mean ±SD) (NP: nanoparticles)

The rate of diffusion of the drugs from the solution at 37°C was greater than the rate of diffusion at room temperature. Up to 50% and 60% of theophylline and budesonide respectively, was present in the receiver chamber after 24 hours (Figure 3.4). At this temperature, both drugs showed a biphasic profile and that sink conditions were exceeded. The difference in the percentage of drug diffused at 6 hours and 24 hours was not significantly different for both theophylline and budesonide (P>0.05).

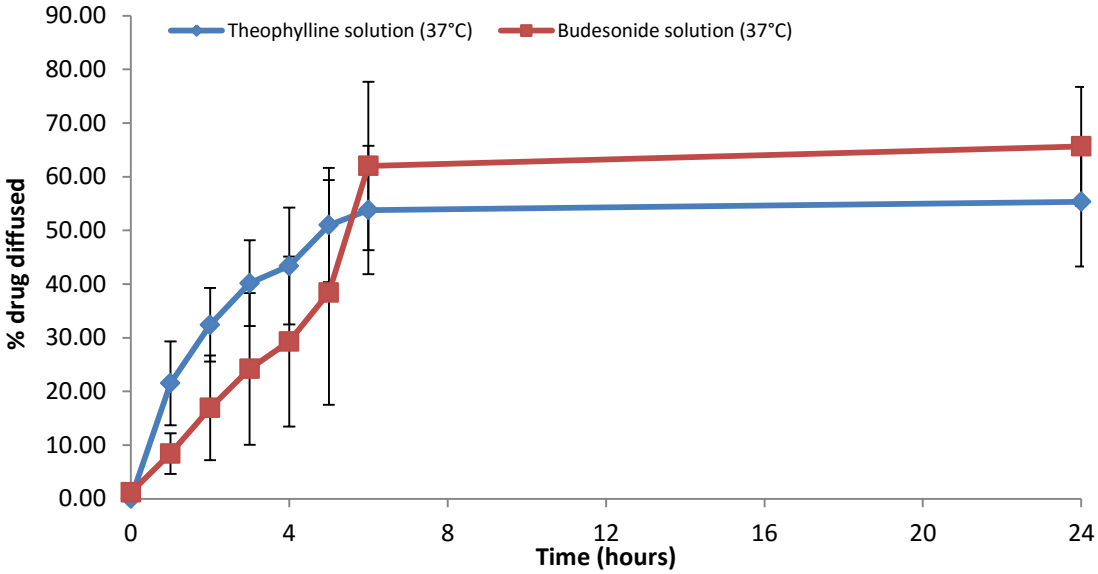

Figure 3.4 Percentage of theophylline and budesonide diffused into the receiver chamber of Franz diffusion cells from a solution of equivalent encapsulated concentration of the drugs over a period of 0-24 hours at 37°C. (n=3, mean ±SD)

Similar to the study carried out at room temperature, at 37°C the percentage of theophylline diffusing across the membrane from the solution was higher than the percentage of theophylline released from the mono- and co-encapsulated nanoparticles over the period of 24 hours. Despite the elevated temperature, only 10%-16% of theophylline was released at the end of 24 hours (Figure 3.5) ($P<0.05$). There was no significant difference in the release of theophylline from the mono- and co-encapsulated nanoparticles ($P>0.05$) except at 24 hours ($P<0.05$). The percentage release of theophylline and 6 hours and 24 hours was not significant for mono-encapsulated nanoparticles ($P<0.05$) but for co-encapsulated nanoparticles ($P>0.05$).

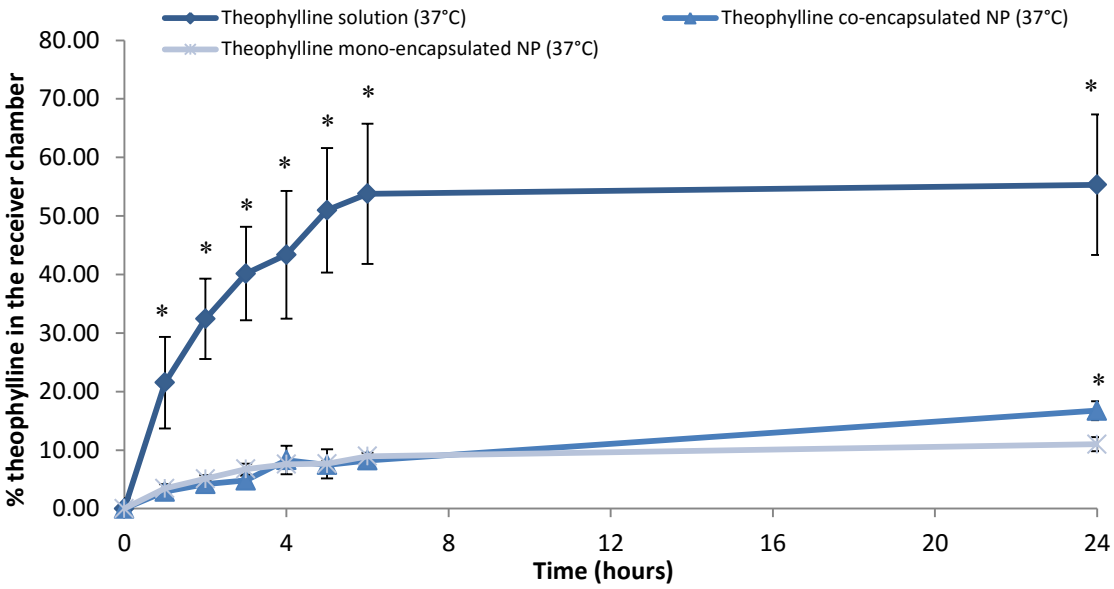

Figure 3.5 Percentage release of theophylline in the receiver chamber released from mono- and co-encapsulated nanoparticles in comparison to the percentage of theophylline diffused from the theophylline solution over the period of 24 hours at 37°C. The percentage of the drug in the receiver chamber from the solution was significantly higher than the percentage released from the nanoparticles (*P<0.05). Similar release was obtained for the theophylline from the nanoparticles except at 24 hours (*P<0.05). (solution: n=3, co-encapsulated: n=6, mono-encapsulated: n=6, mean ±SD) (NP: nanoparticles)

The percentage of budesonide diffusing across the membrane from the solution was also observed to be higher in comparison to the release of budesonide from the nanoparticles ($P<0.05$). Up to 3% and 7% of budesonide was released from the mono- and co-encapsulated nanoparticles over the period of 24 hours at 37°C, respectively (Figure 3.6). The release of budesonide from the mono-encapsulated nanoparticles was significantly lower than from co-encapsulated nanoparticles at 24 hours ($P<0.05$). The difference in the percentage release of budesonide at 6 hours and 24 hours was not significant ($P>0.05$).

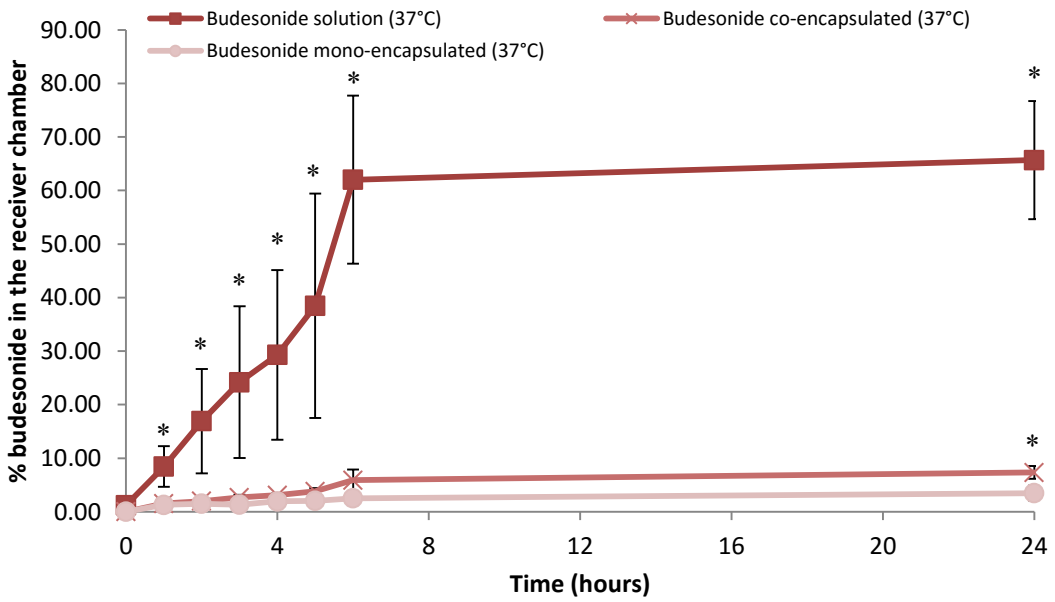

Figure 3.6 Percentage release of budesonide in the receiver chamber from mono- and co-encapsulated nanoparticles in comparison to the percentage of budesonide diffused from the budesonide solution over the period of 24 hours at 37°C. The percentage of the drug in the receiver chamber from the solution was significantly higher than the percentage released from the nanoparticles (*P<0.05). Similar release was obtained for the budesonide from the nanoparticles except at 24 hours (*P<0.05). (solution: n=3, co-encapsulated: n=6, mono-encapsulated: n=6, mean ±SD) (NP: nanoparticles)

Release profiles of theophylline (Figure 3.7) and budesonide (Figure 3.8) from nanoparticles (mono- and co-encapsulated) were compared at the two different temperature conditions. Theophylline release from the co-encapsulated nanoparticles was greater than the remaining nanoparticles samples ($P<0.05$ at 24 hours). The release of both drugs from the remaining samples was not significantly different to each other ($P>0.05$).

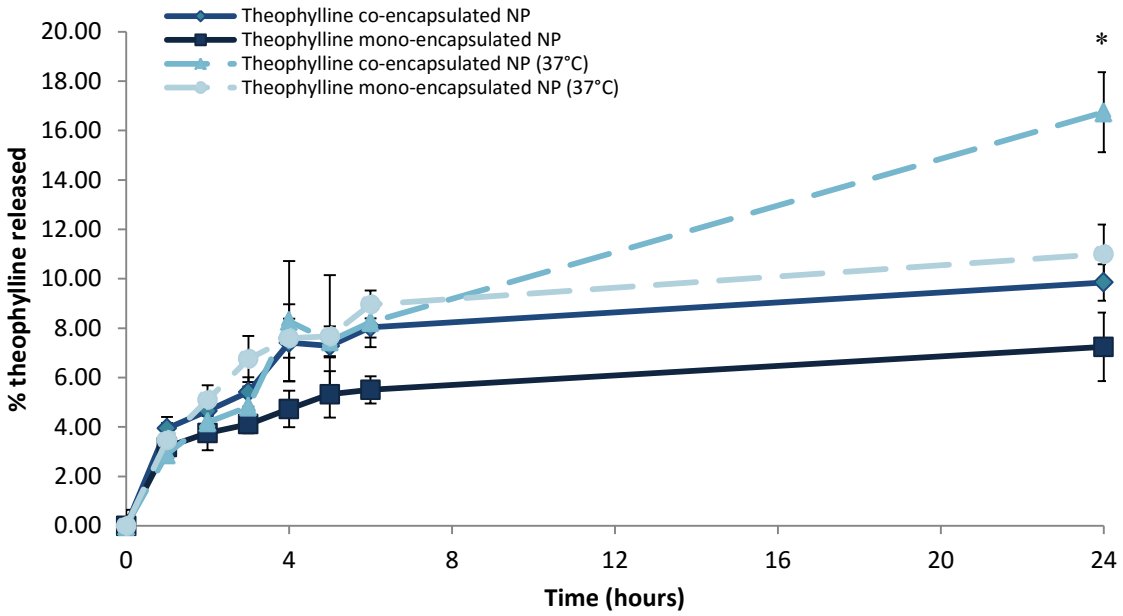

Figure 3.7 Comparing the release of theophylline from mono- and co-encapsulated nanoparticles at room temperature (21-25°C) and 37°C using Franz diffusion cells over a period of 24 hours. The percentage of theophylline released at 24 hours in co-encapsulated nanoparticles at 37°C was higher (*P<0.05) than the remaining samples. (25°C: co-encapsulated: n=21, mono-encapsulated: n=9; 37°C: co-encapsulated: n=6, mono-encapsulated: n=6, mean ±SD) (NP: nanoparticles)

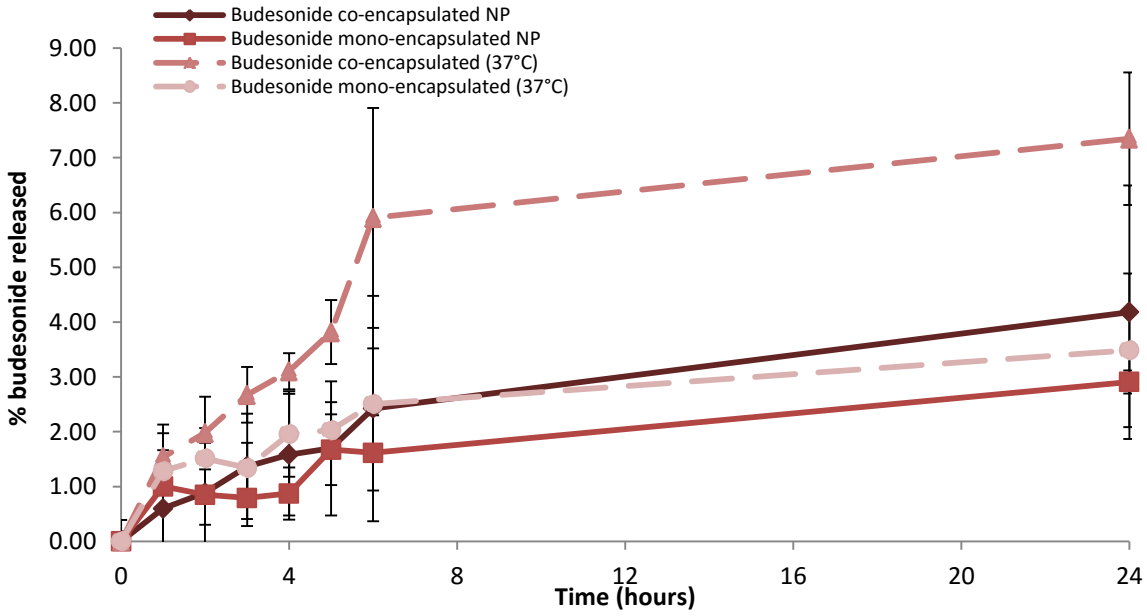

Figure 3.8 Comparing the release of budesonide from mono- and co-encapsulated nanoparticles at room temperature (21-25°C) and 37°C using Franz diffusion cells over a period of 24 hours. (25°C: co-encapsulated: n=21, mono-encapsulated: n=9; 37°C: co-encapsulated: n=6, mono-encapsulated: n=6, mean ±SD) (NP: nanoparticles)

The average diffusion rates of theophylline and budesonide from solutions and nanoparticles over two time periods (between 0-6 hours and 6-24 hours) were calculated (Table 3.3). The rate of diffusion for theophylline and budesonide from solution and mono- and co-encapsulate nanoparticles is greater from 0-6 hours than 6-24 hours at both room temperature and 37°C($P<0.05$). For theophylline the rate of diffusion from solution was almost double at 37^{o}C compared to room temperature and for budesonide the diffusion rate was approximately 4 fold greater at 37^{o}C.

Table 3.3 The average rate of diffusion of theophylline and budesonide across the membrane of the Franz diffusion cells from drug solutions and nanoparticles over the time periods of 0-6 hours and 6-24 hours (NP: nanoparticles) (25°C: solution: n=9, co-encapsulated: n=21, mono-encapsulated: n=9; 37°C: solution: n=3, co-encapsulated: n=6, mono-encapsulated: n=6, mean ±SD)

Time	**0-6 hours**	**6-24 hours**	**0-6 hours**	**6-24 hours**
Drug	*Theophylline rate (µg/hour)*		*Budesonide rate (µg/hour)*	
Room temperature				
Solution	4.21±0.28	0.47±0.02	2.17±0.32	0.56±0.04
Co-encapsulated NP	1.20±0.08	0.10±0.00	0.36±0.23	0.10±0.01
Mono-encapsulated NP	0.78±0.08	0.10±0.05	0.36±0.09	0.07±0.03
37°C				
Solution	7.49±1.44	0.09±0.00	9.10±3.02	0.01±0.26
Co-encapsulated NP	1.36±0.09	0.47±0.05	0.84±0.24	0.08±0.04
Mono-encapsulated NP	1.35±0.18	0.11±0.04	0.34±0.10	0.05±0.02

3.3.3 DRUG RELEASE FROM NANOPARTICLES WHEN SUSPENDED IN DIFFERENT RELEASE MEDIA

Three different release media were studied to determine the release of theophylline and budesonide directly into the solvent. These were methanol, SLF and water. The average percentage release of theophylline and budesonide is given in Figure 3.9.

The percentage release of theophylline was similar from both mono-and co- encapsulated nanoparticles in all media (P>0.05) (Figure 3.9A and B, respectively). Drug release was seen to be biphasic with a sharp increase in concentration from 0 to 6 hours and a reduction in the gradient from 6-24 hours (Figure 3.9). Approximately 100% theophylline release is achieved within the first 6 hours of the experiment time. The difference of the percentage of theophylline released at 6 hours and 24 hours was shown to be non-significantly different for mono- and co-encapsulated nanoparticles (P>0.05).

Budesonide release from mono- and co-encapsulated nanoparticles was similar in the same medium (P>0.05) with only approximately 25-30% of the drug being released (Figure 3.9C and D, respectively). The release of budesonide from nanoparticles in different media was not significantly different from each other (P>0.05). The change in release rate between 0-6 hours and 6-24 hours seen for theophylline was also observed for budesonide (Table 3.4). Similar percentage release of budesonide at 6 and 24 hours was shown for both mono- and co-encapsulated nanoparticles (P>0.05).

Table 3.4 The rate of release of theophylline and budesonide from co- and mono-encapsulated nanoparticles measured over the time period of 0-6 hours and 6-24 hours in the different dispersion media (n=3, mean ±SD).

	Time (hours)	0-6	6-24	0-6	6-24
	Medium	Theophylline rate (µg/hours)		Budesonide rate (µg/hours)	
Co-encapsulated nanoparticles	Methanol	18.13±0.14	0.81±0.47	4.67±0.15	0.41±0.83
	SLF	19.82±0.18	0.46±0.06	5.17±0.16	0.45±0.70
	Water	18.07±0.18	1.18±0.03	4.54±0.33	0.27±1.31
Mono-encapsulated nanoparticles	Methanol	18.11±0.06	1.42±1.25	3.71±0.30	0.12±0.11
	SLF	18.54±0.56	1.55±0.37	3.12±0.27	0.24±0.43
	Water	18.94±0.07	1.17±0.27	3.33±0.28	0.26±0.28

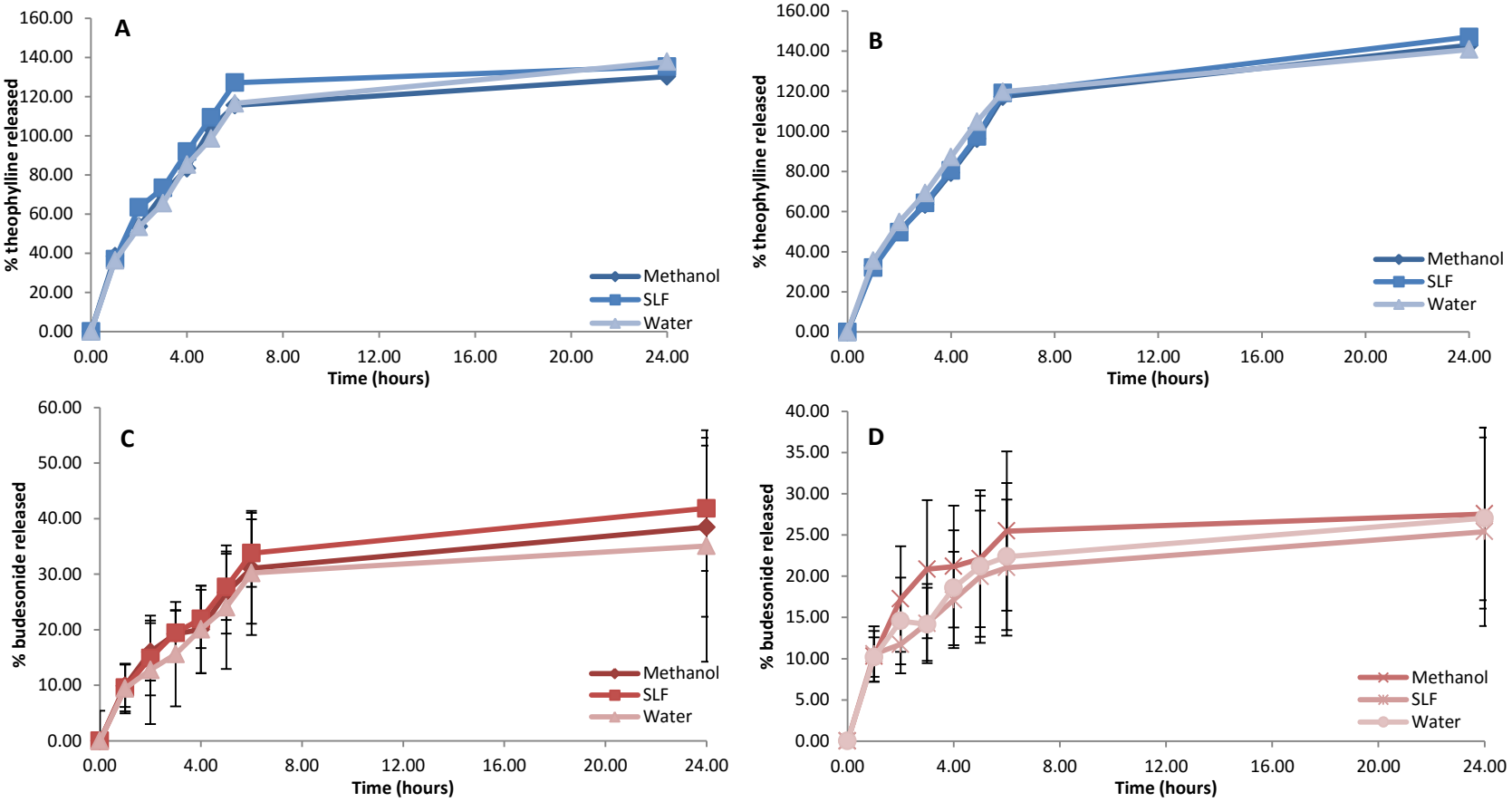

Figure 3.9 The average percentage of theophylline released at each time point when drug release from co- (A) and mono-encapsulated (B) nanoparticles and budesonide from co- (C) and mono-encapsulated (D) nanoparticles is assessed by suspending nanoparticles directly into a dispersion medium. The dispersion media studied were methanol, SLF and water (n=3, mean ±SD)

3.4 DISCUSSION

3.4.1 SELECTION OF MEMBRANE FOR USE IN DIFFUSION STUDIES

There were two aspects that need to be considered when selecting a suitable membrane for use in diffusion studies; these are the pore sizes of the membranes and the chemical binding of the drugs with the membrane. There were a range of membranes available to choose from, such as cellulose acetate, nylon and PTFE which did not show any drug binding to the membrane (data not shown). However, the pore size for these membranes was 0.45μm and was thought that this pore size would result in nanoparticles diffusing across the membrane.

Cellulose membrane (dialysis tubing) is a common membrane used for the release testing of compounds/particles. The advantages include semi-permeability of the membrane and also that, as it acts as a filter, pre-assay separation steps are not required and therefore loss of drug during sampling can be minimized [330]. For the study of theophylline and budesonide release from nanoparticles, cellulose (dialysis) membrane did not show any binding and was deemed to be suitable for use. The small pore sizes (24 Å or 2.4nm) ensured that only the drug crossed the membrane and prevented nanoparticles entering the receiver chamber.

3.4.2 RELEASE OF THEOPHYLLINE AND BUDESONIDE FROM PLA NANOPARTICLES DETERMINED USING FRANZ DIFFUSION CELLS

The aim of formulating theophylline and budesonide nanoparticles using PLA was to sustain their rate of release when encapsulated with a view to obtaining a sustained release product. Drug release was compared to solutions of the drug where the concentration of the drug was equivalent to that present within the nanoparticles.

Franz diffusion cells were chosen as the apparatus for studying the release of theophylline and budesonide from the nanoparticles. This method was chosen as the use of low volumes in the donor chamber allowed a set up similar to the air-liquid interface of the airways to be mimicked. In a study of dissolution techniques for *in vitro* testing of dry powders for inhalation, it was mentioned that Franz diffusion cells were chosen to mimic the diffusion controlled air-liquid interface of the lungs [334]. Depending on the volume of medium that is used, the quantity of test compound should be adjusted accordingly. In the literature a range of different volumes have been used as well as a range of concentrations of drug-loaded

nanoparticles [324]. The main concern with using Franz diffusion cells is being able to distinguish whether the rate of appearance of the drug in the receiver chamber is due to its diffusion across the membrane or the dissolution/release rate of the drug from the nanoparticles [332].

The method used was developed in various ways in order to achieve higher sensitivity in the results allowing accurate representation of the release of theophylline and budesonide from the PLA nanoparticles. Generally, drug release into PBS was reported in a number of studies [324, 325, 353, 354]. Use of PBS ensures that solubility effect due to organic solvents, co-solvents or other components that may be present in the medium interact with the drug release or dissolution rate are absent. Govender et al (1999) studied the release of a water-soluble drug (procaine) from PLGA nanoparticles using HEPES buffer and ultrafiltration technique. It was reported that encapsulating the drug in PLGA nanoparticles, the release of the water-soluble drug was sustained [177].

In the current study release of theophylline and budesonide from PLA nanoparticles into SLF had been studied. This medium was chosen to represent the liquid found in the airways to which the nanoparticles would be delivered. Although it was chosen to mimic the physiological conditions as closely as possible, it is important to understand that there will be other factors (physiological and anatomical changes) that need to be considered when studying drug release. For example, clearance mechanisms that are present in the airway and the presence of mucus can affect the release of drugs [355]. In addition, polymers degrade faster *in vivo* due to the presence of endogenous substances or immunological responses [331].

The use of SLF as the dispersion media and the release of the drugs from the nanoparticles were compared between standard solutions of theophylline and budesonide prepared in equivalent encapsulated concentrations and nanoparticles. The data obtained for the study however was limited due to an extremely low concentration of budesonide (below LOD) that was transported across the cellulose membrane. The method was able to suggest slower release of drugs from the nanoparticles in comparison to the solution as represented by lower concentrations of theophylline (released from the nanoparticles) at the equivalent time points (data not shown). Due to budesonide concentrations being lower than the LOD and LOQ and poor solubility, changes in the medium were required in order to understand the release of the drugs from the nanoparticles [322].

It needs to be appreciated that the inclusion of organic solvents in the setup results in a shift from a representation of the biological system. However, this method was extended and

applied using human airway bronchial cells to determine the transport of theophylline and budesonide across the cells (Chapter 5).

During method development, a variety of solvents for the receiver chamber were explored. These included acetonitrile, methanol, SLF and a 1:1 (v/v) combination of methanol and SLF, as described. The use of organic solvents alone can speed up drug release which would otherwise take days or months in an aqueous environment [331, 339]. The limitation of using organic solvents includes evaporation of the solvent overnight (especially at higher temperatures) and leakage of the organic solvent, causing formation of air bubbles at the underside of the membrane and therefore affecting the release profile [356]. For this reason the use of acetonitrile and methanol alone was not ideal. The most suitable release medium was methanol: SLF (1:1 v/v). This allowed an accurate determination of the concentration of both drugs released and ensured their solubility was not compromised.

Franz diffusion cells show a high dependence on the initial loading dose of the drugs in the nanoparticles and when saturated solubility in the volume has occurred, there is a decreased dissolution and permeability rate [332]. Initially concentrations of 5 mg/mL and 10 mg/mL of nanoparticles suspensions were studied. But high concentration of nanoparticles was also not suitable in such a low volume of medium (data not shown). A higher concentration of the nanoparticles could result in the system operating under non-sink conditions. The use of an organic solvent in the receiver chamber also resulted in evaporation of the solvent and subsequently forming air bubbles and leakage of the solvent. This concentration of the nanoparticles suspensions was thus reduced to 0.6 mg/mL in subsequent experiments.

The volume of release medium used in studies needed to be considered very carefully in order to maintain sink conditions and prevent saturation of the bulk solution during the period of the study. The disadvantage of using small volumes is that sink conditions may not be maintained. However, using low volumes may be required due to the sensitivity of the analytical method [218] or a requirement to mimic the *in vivo* situation. In a study evaluating the different release methods, Salama et al (2008) stated 2mL of receiver fluid can be used and also maintain sink conditions; but it is also important to consider the solubility and concentration of the test sample being used in any particular study [317]. The respiratory tract has low volumes of fluid, approximately 1µL/cm^2 and for this reason it is extremely difficult to develop an *in vitro* model that represents the release accurately [317, 346].

Depending on the volume of medium that is used, the quantity of test compound should be adjusted accordingly. This study used considerably lower volumes in comparison to what is recommended when using USP Apparatus 1 and 2 methods where 1L is used. Using large volumes also results in larger quantity of the samples- for example 40-45 mg of

microparticles in 250mL of PBS [324]. This was not chosen as an option for this study in order to understand the release of the drugs in low volumes which would be present at the site of deposition. Even lower volumes have been applied in other studies of nanoparticles formulated using biodegradable polymers such as PLGA. Volumes as low as 1mL have been used by application of the method such as 'sample and separate' with quantities of nanoparticles as low as 5 mg [357]. This quantity was higher than what is used for theophylline and budesonide nanoparticles in the current study. Another study used a low volume of 5mL but a quantity of up to 500 mg nanoparticles, which may be due to the low loading efficiency of drugs in the nanoparticles [207]. This may allow it to be suitable to study release with such a high quantity of the nanoparticles but also may be chosen as a quantity to consider solubility of the drug in that medium. A similar approach was carried out in a study where 10 mg of nanoparticles were dispersed in 1mL of PBS which was centrifuged for a period of 20 minutes at each time point where the medium was completely replaced to ensure sink conditions were in operation [341]. The low volumes and low concentrations applied in the current study take into consideration sink conditions for the test period, based on the solubility and loading efficiency of the drugs used in this study.

The diffusion of theophylline across the membrane from solution exhibited a biphasic profile which suggested that sink conditions had been violated (Figure 3.1). Over 10% of budesonide from the solution diffused across the membrane at 6 hours.

In comparison to the drug solutions, the release of both drugs from the nanoparticles was sustained over the period of 24 hours and was significantly lower than from the drug solution for both theophylline and budesonide. The biphasic profile was not apparent for theophylline, which is thought to be mainly as a result of the lower concentration of theophylline released from the nanoparticles and sink conditions being maintained. Over the period of 24 hours, approximately 10% of theophylline was released from the nanoparticles. The release from the mono-encapsulated and co-encapsulated nanoparticles was not significantly different, suggesting a similar release pattern of theophylline and budesonide from both mono- and co-encapsulated nanoparticles suggesting that the release is not affected by the presence of the second drug.

As the nanoparticles were intended for pulmonary drug delivery it was important to understand what the release profiles for the drugs would be at physiological temperature (37°C) and this would also allow comparison to the transport of the drugs across human airways epithelial cells (Chapter 5). Most studies of *in vitro* drug release are carried out at 37°C to represent physiological temperature [317, 324, 332]. Studying the release profile at even higher temperatures, although not physiologically relevant, allows a deeper understanding

of the effect of the polymer properties. The glass transition phase of PLA that is used in this study is between 34-39°C (as stated by manufacturers; Appendix 2: Thermal properties data sheet from Manufacturers (Purac Biomaterials)) and by carrying out the release studies at this temperature the effect of changes in polymer properties on release could be observed.

It could be seen that diffusion of both the drugs in the current study from solution was faster at 37^{o}C than at room temperature. Although a more rapid release of the drugs from the nanoparticles was expected at 37°C than at room temperature, only a significantly greater release of theophylline was observed from co-encapsulated nanoparticles in comparison to the release at room temperature. A more rapid release is thought to be due to the changes in the properties of the polymer at higher temperatures. At the glass transition temperature, the polymer changes its state from a glassy to a rubbery state which can allow diffusion processes to be easier [218, 326, 331, 340]. Other factors that are temperature related can also have an influence on faster release of the drugs at an elevated temperature. These include solubility, dissolution and diffusion rate.

A study comparing the release of dexamethasone from hydrophilic matrices using PLGA nanoparticles also showed no significant difference between total release and the rate of release of the drug at 25°C and 37°C [217]. A release study was carried out by Zolnik et al (2006) on PLGA microspheres (containing dexamethasone) at 37, 45, 53, 60 and 70°C which suggested that elevated temperatures was not suitable as a result of the changes which occurred in the polymer [340]. In a study on microspheres of Risperdal Consta® (risperidone) temperatures of 37°C and 45°C were compared where the lag phase of drug release was reduced; but the mechanism of release was not affected [224].

The release profiles of theophylline and budesonide from the nanoparticles were compared to various mathematical models. The values are based on the release of the drug in the first 6 hours of study and when studied using Franz diffusion cells. By calculating R^2 value based on the equation of each model, the correlation between the model and the data obtained from the release testing could be calculated (Table 3.5).

Table 3.5 Determining the mathematical model which best represent the release profile of theophylline and budesonide from PLA nanoparticles.

	Sample	Zero Order R^2	Higuchi Model R^2	Hixson-Crowell R^2
Samples at room temperature	Theophylline co-encapsulated nanoparticle	0.998	0.998	0.935
	Budesonide co-encapsulated nanoparticles	0.969	0.968	0.975
	Theophylline mono-encapsulated nanoparticles	0.891	0.965	0.934
	Budesonide mono-encapsulated nanoparticles	0.926	0.910	0.971
Samples at 37°C	Theophylline co-encapsulated nanoparticle	0.975	0.981	0.961
	Budesonide co-encapsulated nanoparticles	0.752	0.945	0.879
	Theophylline mono-encapsulated nanoparticles	0.977	0.987	0.969
	Budesonide mono-encapsulated nanoparticles	0.898	0.798	0.883

The least correlation was seen with the first order model (data not shown), where on average, low R^2 values (<0.9) were calculated. A high R^2 value (>0.9) was obtained for the models of zero order, Higuchi model and Hixson-Crowell model. However, it is important to look if the models fit differently for budesonide and theophylline as these would have different properties, for example solubility in the solvent system.

The Higuchi model describes release from matrix systems with the following assumptions: that the drug concentration in the matrix is higher than the solubility, edge effects are negligible and diffusion is unidirectional, the thickness of the dosage form is larger than the size of the drug molecules, perfect sink conditions are maintained, swelling is negligible and diffusion is constant. This model is based on Fick's Law. A simplified equation (Equation 3.1) to represent this model is:

$$C = kH\sqrt{t} \qquad \text{Equation 3.1}$$

where C is the amount of drug released at a particular time per unit area, kH is the Higuchi release constant.

Based on this study, it can be understood that the drug concentration in the nanoparticles core is higher than the solubility for budesonide in SLF as theophylline is readily soluble in SLF. In the time scale applied in the study, it can be assumed that the drug release is based on diffusion out of the PLA nanoparticles. It can be suggested that sink conditions are maintained in the time period used for these calculations in the study of the nanoparticles. Due to little information being available on the porosity of the nanoparticles, it can be assumed that particle swelling might be negligible. Porous features are observed in the SEM images of the nanoparticles (Chapter 2, Section 2.3.4); but the effect of these features was not determined in this current study. For this reason, this model can be used to describe the release profiles of theophylline and budesonide from the PLA nanoparticles. The Higuchi model has been reported as the model representing the release of the drugs from different nanoparticle formulations in several studies [288, 358, 359] and release based diffusion [207, 322] suggestive of the Higuchi model.

A good correlation was also observed with the Hixson-Crowell model (Table 3.5). This is a square root model which takes into consideration the surface area and diameter of the drug matrix change over the time period and is based on erosion of the particle. This model is represented by an equation (Equation 3.2):

$$C_0^{1/3} - C_t^{1/3} = kH_c t \qquad \text{Equation 3.2}$$

where C_0 is the initial concentration, C_t is the concentration at a particular time and kHc is the Hixson-Crowell rate constant. However, it must be noted that the erosion process is unlikely to occur in a period of 24 hours and might occur over a longer period of time.

3.4.3 DRUG RELEASE FROM NANOPARTICLES WHEN SUSPENDED IN DIFFERENT RELEASE MEDIA

Three different solvent systems (methanol, SLF and water) were studied in order to further understand the effects of organic solvents and aqueous solvents on the release of the drugs from the nanoparticles. As discussed, the receiver fluid medium was required to be changed from SLF to a mixture of an organic solvent and aqueous medium which although not a reflection of biological system, is suitable for determining *in vitro* drug release as discussed previously, addition of organic solvents to the aqueous layer can result in a rapid release of the drug from the nanoparticles.

When studying the release of drug from nanoparticles using Franz diffusion cells, it is important to establish whether the rate-limiting step is the release of the drug from the nanoparticles or diffusion of the drug across the cellulose membrane, i.e. the permeability (Figure 3.10). For this reason, the release of the drugs from the nanoparticles was also studied when dispersed in a medium in the absence of any membrane. Although this method is based on the 'sample and separate' method which requires centrifugation, in the current study the centrifugation step was not carried out. Ultracentrifugation techniques have been applied successfully for studies of drug release, as reviewed by Wischke and Schwendeman (2008) [331] but they all have several disadvantages.

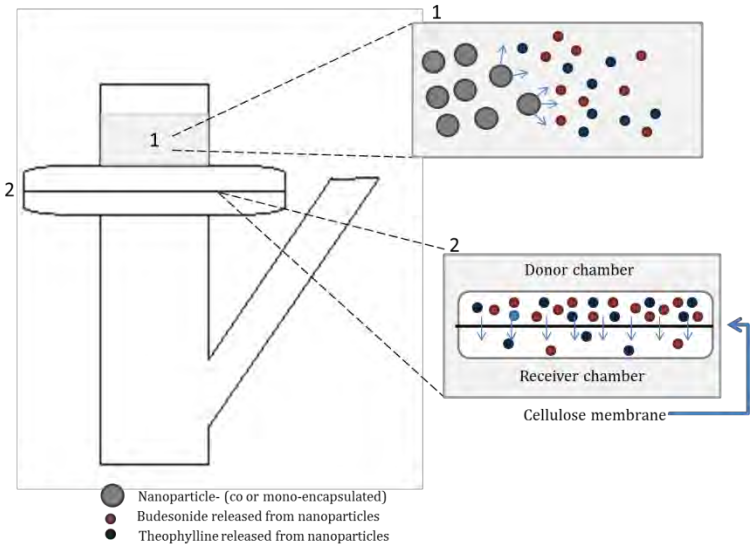

Figure 3.10 The nanoparticles are suspended in SLF and applied to the donor chamber. The drug release occurs in this part of the chamber (1) releasing theophylline and budesonide. The release of the drugs could be the rate-limiting step. Drug diffusion across the membrane occurs in this part of the chamber (2) and could also be the rate-limiting step. The release of the drugs in (1) is comparable to release of the drugs when suspended in release media with no membrane separating chambers.

The disadvantage of this technique is that it is dependent on the particle size/density and how it will settle and separate in the particular testing medium, where can lead to problems when predicting drug release *in vivo* [360]. This technique can also lead to disruption of the particles by causing coalescence [358, 361] and instead of centrifugation, samples can be filtered. Filtration can also result in removal of the drug released and therefore has been suggested that it should be avoided [362]. Another disadvantage of this technique was that centrifugation can cause destabilization of the system [361]. This suggestion was applied in the current project when studying the release of theophylline and budesonide from the nanoparticles by analyzing the samples immediately via HPLC to avoid disruption of particles by centrifugation or by filtration.

In the current study centrifugation was not chosen as a method due to the long duration required for centrifugation of the nanoparticles and other disadvantages discussed. Initially, during method development in the current study, the time points that were chosen for sampling were every 15 minutes and therefore a method such as this would not be suitable. For example, in studies of drug release from paclitaxel-loaded PLA nanoparticles studied over a period of 30 days, the centrifugation time was 15 minutes long, after which the supernatant was analyzed to determine the concentration of the drug [216, 320]. Another study, carried out on coumarin-6-loaded nanoparticles had a similar method, but with a centrifugation time of 8 minutes. This study suggested that centrifugation was not ideal due to leaching and dissociation of the marker in the released medium, suggesting a risk of loss of drug [363]. In a study modelling the encapsulation of a hydrophilic drug (Rose Bengal) the sample was centrifuged for a period of 30 minutes at 13,000 RPM prior to determining the concentration of drug released [318]. A short centrifugation time of 2 minutes was used for indocyanine-loaded nanoparticles [353]. However, a low centrifugation time can only be used if the size and density of the particles are such that they will separate from the solution in the time allowed. Another extreme of time for centrifugation was carried out in a study on paclitaxel-loaded PEGylated PLGA nanoparticles. In this study the sample was centrifuged for 1 hour at 4°C at a high speed of 22,000RPM. Due to various times used and durations, it is difficult to determine what would be appropriate for theophylline and budesonide nanoparticles. For these reasons, it was better not to include an additional centrifugation step. As discussed, the nanoparticles were left to remain in the medium as drugs would be released over time. By application of the method in the current study, it can ensure that disruption of the nanoparticles is avoided and removal of the drug by filtration is also avoided. As there are two drugs included in this study, the settling time may be different and therefore taking samples after the centrifugation process has been carried out may lead to inaccurate representation of the release.

The aim of this portion of the study was to replicate the release of theophylline and budesonide from the nanoparticles in the donor chamber before the drugs diffused across the membrane. For this reason, the total volume used was the same as the total volume of the receiver and donor chamber of the Franz diffusion cell (2.5mL) with the same concentration of nanoparticle suspension being applied.

The decrease in the rate of release of the drug from the sampling period (0-6 hours) compared to the idle period (6-24 hours) suggested that due to there being no change in the volume of the release medium, there was a risk of the system operating in non-sink conditions due to the low volume. This biphasic release was not seen in the release of drugs from the nanoparticles when studied in a Franz diffusion cell.

A biphasic profile was obtained in the diffusion of the drugs across the cellulose membranes when prepared as a solution. It was predicted that the release of the two drugs in the organic solvent was more rapid as a result of the effect of the organic solvent on the polymer; however this was not achieved.

The reason for the difference between release profiles (biphasic release) in the two different setups could be as a result of the presence of a membrane barrier in the Franz diffusion cells. As described previously, the concentration of the drugs obtained in the receiver chamber are dependent on the diffusion across the cellulose membrane, and therefore this depends on a single direction of transport. The membrane also acts as a filter and therefore lower concentration is diffused across the membrane.

The presence of the membrane also causes a reduction in the overall area surrounding the nanoparticle to allow release of the drugs. When nanoparticles are dispersed directly into the media (with no membrane), release can occur in all directions which suggest a larger percentage of drugs released in comparison to when Franz diffusion cells are used. This difference was also observed when 100% SLF was used in the receiver medium. Even at a high concentration of nanoparticles (2 mg/mL), the release of the drugs from the nanoparticles when dispersed in SLF was significantly higher than the amount of drug that diffused across the membrane when studied using Franz diffusion cells, further supporting this suggestion (data not shown).

The importance of maintaining sink conditions was discussed by Wischke and Schwendeman (2008) and stated that only some knowingly break this rule, e.g. by use of small volumes for example 5mL [331]. Further discussion was carried out on comparisons between studies carried out using sink and non-sink conditions and was seen that there was no difference seen between these two conditions. The importance of the dispersion medium and the solubility of drug in the medium were noted to be of more importance [331]. This was supported by an example of when an injection is administered at certain sites which have low perfusion the body fluids will not provide sink conditions (for example with hydrophobic drugs) and this results in the drug not being easily removed from the unstirred boundary layers [331]. However, this difference is observed in theophylline and budesonide concentrations obtained in the two different setups that were used. By studying the release into dispersion medium directly resulted in violation of sink conditions due to the factors discussed (no agitation, low volumes). The violation in sink factors is thought to be the main reason for the reduction in the release rate between sampling time (0-6 hours) and idle time (6-24 hours).

This limitation in the study was also discussed by Zolnik et al (2005), suggesting that the use of miniaturized techniques allows for carrying out release testing of compounds using small dialysis sacs or vials; but this small volume does violate sink conditions, and there is also aggregation of the sample due to limited agitation [324]. For this reason the use of a magnetic stirrer in the Franz diffusion cell apparatus is vital to ensure high concentrations are prevented (near the unstirred layer beneath the membrane) in the receiver chamber, with replacement of the aliquoted methanol: SLF with fresh methanol: SLF at pre-determined time points. No replacement of the SLF: methanol between 6-24 hours further suggests sink conditions were not maintained successfully in this study. Due to the presence of a membrane, lower concentrations are calculated as a result and therefore during the period of 6-24 hours there is no significant change in the rate of drug diffusion, further supporting the sink conditions being maintained.

When drugs are released from microspheres (or nanoparticles) a high concentration of the drug is seen at the boundary layer around the microparticles (or nanoparticle), which is similar to the concept of the diffusion layer model. This can cause saturation of the particles concentration at the boundary layer and hinder further release of the drug. Therefore by constant stirring and replacement of the medium this can be avoided.

The percentage of theophylline released was approximately 100% within 4-5 hours of experiment time. The high solubility of theophylline in the different media suggests the rapid release of theophylline from both mono- and co-encapsulated nanoparticles. Despite the increased solubility of budesonide in methanol, its release into methanol was similar to its release into water. This may be due to the budesonide being encapsulated in the inner core of the nanoparticles resulting in a longer time for it to diffuse out from the nanoparticles in comparison to theophylline. This may be an overestimation due to possible sampling of the nanoparticles as no filtration step is included in this part of the study.

It was observed that the percentage of theophylline and budesonide released from the nanoparticles in the direct release method was higher than the percentage of drugs released using Franz diffusion cells. This suggests that the rate-limiting step is the diffusion of the drug across the cellulose membrane of the Franz diffusion cell. This is supported by the gradients that are calculated for the drugs in the two different setups.

Due to higher concentrations achieved in the method where the nanoparticles are dispersed in media, with no membrane, the method which uses a Franz diffusion cell setup is better. The application of a membrane allows the released drug to diffuse across the membrane and be sampled. As discussed briefly, the application of the membrane can result in limiting the surface area available to the nanoparticles for dissolution of the drugs. Dispersion of the

nanoparticles directly into the media (with no barrier) results in release, diffusion and dissolution of the drug in all directions. This is limited to unidirectional diffusion for the nanoparticles applied in the Franz diffusion cells. As described in Figure 3.10, the rate limiting step can be suggested to be the diffusion of the drugs across the membrane. In addition, nanoparticles may also be sampled and therefore results could be an artefact.

If the release models were to be applied to the release profiles of theophylline and budesonide from the nanoparticles when suspended in the different media, zero order release is observed (R^2>0.9, data not shown) (between 0-6 hours). Zero order release would present a constant rate where release is a function of time and is independent of the concentration. It is represented by the equation (Equation 3.3):

$$C = kt \qquad \text{Equation 3.3}$$

where C is the concentration and k is the rate constant. This is the ideal method of drug release because it is constant at any time. The release profiles measured for the drugs encapsulated in the nanoparticles describe the release that occurs in the donor chamber of the Franz diffusion cells. The release profiles calculated to determine correlation with models (Table 3.5) can be suggestive of the diffusion of the drugs across the membrane into the receiver chamber in the Franz diffusion cells.

As the overall aim of the study was to extend the release of the drugs, the duration of release testing used for theophylline and budesonide nanoparticles was chosen to be 24 hours. This time period was chosen because if the initial release showed lower concentration in comparison to the standard solutions, then the release pattern can be predicted for the remaining time and that successful sustained/extended release is achieved. Increasing time periods would result in longer idle periods (such as between 6-24 hours) which also result in smaller changes in the slope suggestive of violation of sink conditions. With the use of lower volumes in this study, this may not be suitable.

The drug release profile tested in other studies using different systems such as drug carriers, colloidal systems and nanoparticles have ranged from hours to days. Some studies carried out release testing over a period of 80 hours [336]. Studies that used this time period to assess release used higher volumes of medium (PBS). The studies, using semi-permeable mini-dialysis tubes, showed an initial burst release of the drug from PLGA-PEG nanoparticles in the first five days. In the shorter time span of this study, the release of theophylline or budesonide did not show a burst release. Approximately 60% of the drug was released over the period of 80 hours. Another study, on paclitaxel-loaded PLA nanoparticles, was carried out for duration of 30 days [320]. Even after this long duration, the release of paclitaxel was

found to be too low for therapeutic efficacy as a result of the concentration being released was below the therapeutic concentration. For the current study, the concentration released is lower than prescribed dose of inhaled budesonide and the dose of theophylline suggested having an airway effect (Chapter 1). However this concentration can be modified when nanoparticles are being administered in the body. In contrast, another study carried out on paclitaxel nanoparticles formulated using PLGA was carried out for duration of 24 hours using PBS as the release medium. This showed a biphasic and fast release of paclitaxel. The differences in the data obtained could be due to changes in the polymer used (PLA is a more hydrophobic polymer) and the method of formulating nanoparticles (nanoprecipitation was used to formulate paclitaxel-PLGA nanoparticles) [364]. A USP Apparatus 2 method was used to study the release of aciclovir (20 mg) nanoparticles over a period of 24 hours in 5 mL of PBS [358]. This time period was also used in a study of docetaxel loaded PLA/chitosan particles [365]. A dialysis bag technique was used when assessing the release of vincristine and quercetin from PLGA nanoparticles [193]. The release of the free drug (present as a solution) was complete in a period of 3 hours and after a period of 24 hours, 70% of the drug was released from the nanoparticles. A method similar to the one described was carried out by Song et al (2008) for vincristine and verapamil co-encapsulated PLGA nanoparticles showing similar results [194, 195]. The results obtained in the study by Song et al (2009) showed a greater release of the hydrophilic drug in comparison to what was achieved in the current study with theophylline [195].

Other studies that have assessed the release of the drugs from biodegradable polymeric nanoparticles have looked at release over a period of days, up to months. Tobramycin-encapsulated PLGA nanoparticles presented a biphasic release; but sustained release was achieved over a period of a month [210]. Other studies on polymeric nanoparticles have been conducted for an extremely short period of time. For example, release of drug from sildenafil nanoparticles was compared to free drug solution of an equivalent concentration and showed sustained release over a period of 120 minutes. The drug loading of sildenafil was calculated to be 5% [237]. Chitosan nanoparticles of insulin also showed a biphasic release over 100 minutes [366].

The transdermal permeability of xanthine derivatives such as caffeine, theobromine and theophylline was studied using Franz diffusion cells at 37°C and was studied using different release testing media, such as water, propylene glycol and PEG400 [367]. This study showed greater transport in water suggesting preference to a completely aqueous media, supported by the data obtained in the current study. The transdermal delivery of theophylline was also studied by Zhao et al (2006) in a micro-emulsion vehicle using Franz diffusion cells with skin samples as a membrane (barrier) with constant stirring. This study showed a linear

permeability of theophylline as a function of time [170]. Theophylline release from nanoparticles was assessed using 21mL of PBS as the release medium at 37°C with a 0.45µm cellulose acetate membrane. The release of theophylline was compared to all the different drug release mathematical models also showing the release of theophylline with the greatest correlation to the Higuchi model similar to this study [348]. The nanoparticles of theophylline prepared in this study were synthesized directly as a nanosuspension using 250 mg of theophylline so the formulation was different to the one used in the current study.

Budesonide release from powders was studied using Franz diffusion cells and was seen to be released by first order kinetics. Budesonide emulsions were synthesized for topical delivery and skin permeability was studied using Franz diffusion cells. The emulsions were synthesized using triblock polymers which included poly (ethylene glycol), poly (ε-caprolactone) and poly (ethylene oxide/PEG). The release from the emulsions was studied over a period of over 72 hours using PBS in dialysis tubing showing an initial burst release for the first 3 hours with complete release by the end of 72 hours. The initial concentration of budesonide used was 2 mg/mL and large volumes (50mL) were used for analysis to maintain sink conditions [368]. Release of budesonide from Eudragit® microparticles showed sustained release in comparison to the free drug solution when studied in gastric juice at 37°C further suggesting the sustained release achieved by formulation of drug containing particles, supporting the current study [369]. Budesonide nano- and microparticles synthesized for sub-conjunctival delivery showed 25% of budesonide was released in the initial 'burst' release phase and sustained release of budesonide was seen over 2 weeks further showing sustained release of the drugs when present as a nanoformulation. Nanoparticles showed improved release profile compared to the microparticles [223]. There have been no other studies on the release of co-encapsulated theophylline and budesonide from nanoparticles.

3.5 CONCLUSIONS

The aim of this chapter was to study the release of theophylline and budesonide from co-encapsulated and mono-encapsulated nanoparticles using Franz diffusion cells and to compare this release to the diffusion of drug solutions of equivalent encapsulated concentrations.

Release was studied over a period of 24 hours and was seen to be sustained in comparison to the drug solutions of equivalent concentrations. Similar release profiles were obtained for theophylline and budesonide from mono-encapsulated and co-encapsulated nanoparticles at room temperature and at 37°C. The release profiles of the two drugs from the nanoparticles showed the greatest correlation to a Higuchi model from the nanoparticles in the time-scale studied. The release of theophylline and budesonide was also compared at the two different temperatures (room temperature and 37°C) and was concluded to not be significantly different for both drugs, except for theophylline released from co-encapsulated nanoparticles at 37°C. At both temperatures, the rate of release between 6 and 24 hours was reduced significantly than in the first 6 hours of sampling.

CHAPTER 4 EFFECT OF THEOPHYLLINE AND BUDESONIDE ENCAPSULATED NANOPARTICLES ON THE VIABILITY OF A HUMAN BRONCHIAL EPITHELIAL (16HBE14O-) CELL LINE

4.1 INTRODUCTION

The use of nanoparticles has expanded greatly in the recent years [370]. With the potential to use the lungs for systemic or local administration, it is important to understand how nanoparticles interact with the epithelium of the airways; this can be explored by the use of cell lines [371]. Normal respiration allows nanoparticles to deposit throughout the airways; however if factors such as particle dispersion, breathing and particle size are controlled, targeted drug delivery can be achieved [372]. Problems with nanoparticles being delivered, which is not limited to pulmonary drug delivery, is the long term accumulation of the particles or material in the systemic circulation as this can lead to toxic effects [372]. Nanomaterials have a large number of potential applications in different areas and therefore the safety of nanomaterials is a big concern [373-375]. The unique properties of nanoparticles can lead to unknown toxic effects which can potentially present as a great risk when formulation is scaled up [297, 373]. For this reason, the characterization and preparation of the nanoparticles is extremely important [373]. Toxicity of the nanomaterials could be from the polymer used to produce the nanoparticles. One of the main aims in the production of nanomaterials and nanomedicines is the use of biodegradable polymer and excipients [297]. The use of biodegradable materials such as PLGA and PLA is an advantage over the use of materials such as polystyrene as the biodegradable polymers cause a lower inflammatory response [202, 210].

Drugs administered for the treatment of asthma and COPD are mainly locally-acting drugs, limiting side effects mainly to the respiratory system [371, 376]. There are a limited number of drugs and excipients that are approved for use in the respiratory tract and therefore it is important to study the toxic effects of the drugs and excipients which are used for pulmonary drug delivery. Application of a successful *in vitro* cell culture model would be ideal for toxicity screening before further tests on living systems are applied [376].

There are several different assays available to test the viability of cells after exposure to test compounds. Assays are available which differentiate between viable and non-viable cells,

by assessing membrane integrity, apoptosis pathways or enzyme function [376-379]. Commonly used assays to determine toxicity are the 3-(4,5-dimethyl-2-thiazolyl)-2,5-diphenyl-2H-tetrazolium bromide (MTT) assay, neutral red assay and lactate dehydrogenase (LDH) assay.

The MTT assay is based on the reduction of the soluble, yellow MTT tetrazolium ring which cleaves to form an insoluble purple formazan product. This precipitates in the cellular cytosol and is dissolved by the aid of an organic solvent (the most commonly used solvent is DMSO). This reaction is mediated by dehydrogenase enzymes associated with the endoplasmic reticulum and mitochondria [267, 376-378, 380-382]. It can only occur in cells which are viable, and therefore allows differentiation between viable and non-viable cells. The viability of cells exposed to the compound of interest is usually compared to a control, which are untreated cells. Other tetrazolium salts are available to assess viability of cells; these include (2, 3-bis-(2-methoxy-4-nitro-5-sulfophenyl)-2H-tetrazolium-5-carboxanilide) (XTT) and (3-(4, 5-dimethylthiazol-2-yl)-5-(3-carboxymethoxyphenyl)-2-(4-sulfophenyl)-2H-tetrazolium) (MTS) assays.

The neutral red assay also differentiates between viable and non-viable cells where viable cells are able to take up the dye and store it in the inner surface of the lysosomes. This characteristic is not present in dead cells [376].

The LDH assay is a rapid, simple and reliable assay measuring cell membrane damage via the leakage of LDH from the cytosol. LDH converts lactate to pyruvate by reducing NAD+ to NADH/H+. The greater amount of LDH detected indicates greater cell damage and reduced viability [376, 378, 383, 384].

Of these assays, the MTT assay was shown to be the most sensitive [376]. With the LDH assay, it was suggested that conversion could occur in the solution and therefore it may not be reflective of the cell damage [376, 381, 385]. The assessment of toxicity using various different nanomaterials, such as metallic nanoparticles, showed inactivation of LDH molecules non-specifically by possible adsorption on the molecules and therefore not showing true viability results [383].

This study focuses on the respiratory system, and therefore the effect of the nanoparticles on the viability of respiratory epithelial cells was examined using a cell line representative of the expected region of deposition, the upper airways. The human airway epithelium consists of up to six different cell types including ciliated cells, mucus cells and goblet cells. Ciliated cells are the most abundant cell line in the airways [8]. Commonly used and developed cells lines include A549 cells, Calu-3 cells and 16HBE14o- cells. A549 cells are cells derived

from a human pulmonary adenocarcinoma and retain similarity to Type II alveolar epithelial cells [370, 386, 387]. This cell line is used mainly for the study of the lower respiratory tract and the alveolar region, as a model of the alveoli [388]. Cell lines, Calu-3 and 16HBE14o- are cell lines that represent the upper airways. Calu-3 are well developed and commonly used to assess the cytotoxicity of agents. Calu-3 cell line is derived from a human bronchus adenocarcinoma of the lung [388, 389]. They are able to form tight junctions and have been used extensively in the study of drug permeability and transport across the cells [371]. Calu-3 cells also have features of cilia and mucus production [8, 390, 391].

16HBE14o- cells, which were chosen for this study, were developed by transformation of cultured bronchial surface epithelial cells, from a one year old male heart and lung transplant patient. These cells also have the ability to form functional tight junctions when grown under appropriate culture conditions, such as air-liquid interface allowing regulation of ion transport [8, 382, 388, 392-394].

Nanoscale materials have been explored for many biological applications due to their properties. Studies of the effect of polystyrene nanoparticles, metallic nanoparticles, liposomes, nanotubes [375], nanoparticles synthesized with a range of biodegradable polymers including PLA, PLGA, polymer, poly-ε-caprolactone (PCL) [373] and chitosan [381] on cell viability have been carried out.

4.1.1 AIM OF THE STUDY

The aim of this study was to assess the viability of 16HBE14o- cells when treated with mono and co-encapsulated nanoparticles containing theophylline and budesonide and to compare this to cell viability when treated with theophylline and budesonide solutions of equivalent encapsulated concentrations. In addition, the effect of PLA on cell viability was also assessed. This is the first time the cytotoxicity of budesonide, theophylline and PLA toxicity to 16HBE14o- cells has been reported and the first time the cytotoxicity of mono and co-encapsulated nanoparticles containing theophylline and budesonide has been reported in any cell line. It is hypothesized that encapsulation of the drugs within the nanoparticles will reduce their toxicity.

4.2 MATERIALS AND METHODS

4.2.1 MATERIALS

96 well-plates, NunclonTM Delta surface, Thermo Scientific, Denmark (143597)

Cell culture TC flasks (with filter cap), 80 cm^2, Thermo Fisher Scientific, Denmark (Lot: 178905)

Minimum Essential Medium (MEM) with Earle's Salts (with L-glutamine), GE Healthcare- PAA Laboratories, Austria (E15-825)

Fetal Bovine Serum (FBS) 'Gold' PAA Laboratories GmbH, Germany (A15-151)

Trypsin-EDTA (1x) (0.05% w/v and 0.02% w/v in PBS, respectively), GE Healthcare-PAA Laboratories, (L11-004)

Penicillin (10,000 units/mL) / streptomycin (10,000 µg/mL) (Pen Strep), Gibco® by Life Technologies, USA (15140-122)

Trypan Blue Stain (0.4% w/v), Gibco® by Life technologies, USA (15250-061)

Phosphate buffer saline (PBS) tablets (pH 7.3±0.2) - Oxoid Ltd, Basingstoke, Hampshire, United Kingdom (BR0014G)

Dimethylsulfoxide (DMSO) (BioReagent for molecular biology, >99.9%), Sigma-Aldrich, UK (D8418)

Ethanol, absolute (analytical reagent grade), Fisher Scientific, UK (Code: E/0650DF/17, Lot#: 1405343)

3-(4,5-dimethyl-2-thiazolyl)-2,5-diphenyl-2H-tetrazolium bromide (MTT), Sigma-Aldrich, UK (M2128)

10mL disposable serological pipet, Fisherbrand, Fisher Scientific, USA (Cat: 13-676-10J)

25mL disposable serological pipet, Fisherbrand, Fisher Scientific, USA (Cat: 13-676-10K)

Eppendorf- EasyPet 3 Pipette Gun

Transferpette® S Brand – 200, 100 and 20µL Gilson's pipettes

HERA cell incubator (set at 5% CO2, 95% air at 37°C)

4.2.2 METHODS

4.2.2.1 16HBE14O- ROUTINE CELL CULTURE AND PASSAGE

16HBE14o- cells were maintained by culturing as monolayers at a seeding density of 4.0 x 10^3 cells / cm^2 in T-75, surface treated polystyrene cell culture flasks. Cells were cultured at 37°C in a humidified atmosphere of 5% CO_2, 95% air in Minimum Essential Medium (MEM) supplemented with 10% v/v FBS and 1% v/v Penicillin/Streptomycin solution (cell culture medium). Cell culture medium was replaced every two days and the cells were allowed to grow until 80-90% confluence before passaging.

Before cells were passaged, the cells were washed with PBS and then trypsinized using trypsin-EDTA. The trypsin mixture was neutralized by the addition of cell culture medium and the cell suspension centrifuged at 500 x g for 5 minutes. The cells were re-suspended in fresh cell culture medium. The cell pellet was either sub-cultured in flasks with addition of extra cell medium, or a cell count was obtained by use of a Neubauer hemocytometer and the cells seeded on 96 well plates. Live cell count was obtained by dilution of the cell suspension with trypan blue (1:2) on the hemocytometer. All cell studies were carried out under sterile conditions.

4.2.2.2 DETERMINATION OF OPTIMUM CELL SEEDING DENSITY

In order to determine the most appropriate seeding density of the 16HBE14o- cells to test the toxicity of the drugs, polymer and nanoparticles, the cells were seeded at different cell densities in 96 well plates. The cells were passaged as described in the previous section (Section 4.2.2.1). From a stock cell suspension, serial dilutions were made to obtain a diluted cell concentration range. The concentration range that was initially tested was from 10,000 to 300,000 cells/well. This range was then lowered to 156 to 10,000 cells/well. To each well, 100 µL of the cell suspension was added. The plates were then incubated at 37°C (95% air: 5% CO_2) for 48 hours. After the 48 hour period, the medium was removed by aspiration and an MTT assay carried out (Section 4.2.2.4). The background was subtracted from the absorbance values obtained.

4.2.2.3 CYTOTOXICITY OF THEOPHYLLINE, BUDESONIDE, PLA, DMSO AND NANOPARTICLES TO 16HBE14O- CELLS

The 96 well plates were seeded at 4,000 cells/well. The plates were incubated at 37°C (95% air: 5% CO_2) for 24 hours. After the 24 hour period, the medium was removed by aspiration. The test solution/nanoparticles suspension was added (100µL/well) and the cells incubated for 24 hours. After this, the drug solution/nanoparticles suspension was aspirated from the cells and replaced with the MTT solution (5 mg/mL) and the MTT assay was carried out (Section 4.2.2.4). Eight wells were left untreated to provide a control.

4.2.2.3.1 Preparation of theophylline solutions

Theophylline was dissolved in ethanol at a stock concentration of 20 mg/mL which was further diluted in cell culture medium to 2 mg/mL theophylline and 10% v/v ethanol. This solution was serially diluted to obtain theophylline concentrations of: 1 mg/mL, 0.5 mg/mL, 0.25 mg/mL, 0.1 mg/mL, 0.05 mg/mL, 0.025 mg/mL, 0.01 mg/mL and 0.005 mg/mL. The serial dilution also results in dilution of the ethanol concentration present in the solution to give ethanol concentrations of 10 %v/v, 5%v/v, 2.5%v/v, 1.25%v/v, 0.5%v/v, 0.25%v/v, 0.125%v/v, 0.05%v/v and 0.025%v/v, respectively.

Theophylline was also prepared in cell culture medium without the use of ethanol as a co-solvent. The stock concentration was made at 2 mg/mL theophylline and serial dilutions were carried out to give the concentrations: 1 mg/mL, 0.5 mg/mL, 0.25 mg/mL, 0.1 mg/mL, 0.05 mg/mL, 0.025 mg/mL, 0.01 mg/mL and 0.005 mg/mL.

4.2.2.3.2 Preparation of budesonide solutions and suspensions

Budesonide was prepared in three different ways. Budesonide stock prepared in ethanol and further diluted with cell culture medium to form budesonide concentrations in the range from 200 µg/mL to 0.5 µg/mL, with ethanol concentration also ranging from 10% v/v to 0.025%v/v, respectively (Table 4.1).

Budesonide stock prepared in DMSO and further diluted with cell culture medium to form budesonide concentrations in the range of 2 mg/mL to 0.005 mg/mL, with DMSO concentration ranging from 1% v/v to 0.0025% v/v, respectively (Table 4.2).

Finally, budesonide was prepared as a suspension in cell culture medium (without use of any organic solvents). Suspensions of the following concentration were prepared: 2 mg/mL, 1 mg/mL, 0.5 mg/mL, 0.25 mg/mL, 0.1 mg/mL, 0.05 mg/mL, 0.025 mg/mL, 0.01 mg/mL and 0.005 mg/mL (Table 4.2).

Table 4.1 Concentration of budesonide used for the cytotoxicity study when ethanol was used as a co-solvent

Concentration of budesonide (μg/mL)	Concentration of ethanol (%v/v)
200	10
100	5
50	2.5
25	1.25
10	0.5
5	0.25
2.5	0.125
1	0.05
0.5	0.025

Table 4.2 Concentration range of budesonide prepared using DMSO (final concentration of 1%v/v) and serially diluted in cell culture medium or a suspension in cell culture medium (in the absence of DMSO)

Concentration of budesonide (mg/mL)	Concentration of DMSO (%v/v)
2	1
1	0.5
0.5	0.25
0.25	0.125
0.1	0.05
0.05	0.025
0.025	0.0125
0.01	0.005
0.005	0.0025

4.2.2.3.3 Preparation of PLA solutions

PLA stock was prepared in DMSO and serially diluted in cell culture medium. The concentration range that was tested was between 200 μg/mL to 1 μg/mL, in which the DMSO concentration ranged from 1%v/v to 0.005%v/v, respectively (Table 4.3).

Table 4.3 Concentrations of PLA (µg/mL) and DMSO (%v/v) when serially diluted in cell culture medium

Concentration of PLA (µg/mL)	Concentration of DMSO (%v/v)
200	1
100	0.5
50	0.25
25	0.125
10	0.05
5	0.025
2.5	0.0125
1	0.005

4.2.2.3.4 Preparation of DMSO (%v/v) solutions

The effect of DMSO on the viability of 16HBE14o- cells was also tested. Solutions of DMSO only were prepared and serially diluted in cell culture medium at the concentration indicated in Table 4.3.

4.2.2.3.5 Preparation of nanoparticle suspensions

The toxicity of nanoparticles was tested at a range of concentrations. For each concentration, nanoparticles were weighed accurately and suspended in cell culture medium. This process was carried out just before adding the test sample to the seeded cells. The concentrations of nanoparticles prepared are listed in Table 4.4. Dilutions of the nanoparticles were not carried out and each concentration was prepared separately. The maximum theoretical encapsulated concentration is also presented in the table.

Table 4.4 Concentration of nanoparticles and maximum concentration of theophylline and budesonide that could be loaded in the nanoparticles (i.e. if loading was 100%)

Concentration of NP (mg/mL)	**5**	**2.5**	**1**	**0.5**	**0.25**
Theophylline concentration (µg/mL)	980	490	196	98	49
Budesonide concentration (µg/mL)	98	49	20	10	5

4.2.2.4 MTT ASSAY

MTT solution was made to a final concentration of 5 mg/mL in MEM (without FBS and antibiotics). The solution was protected from light, stored at 4°C and used within two weeks. The cell culture medium was aspirated carefully from each well, ensuring no cells would be removed in the process. To each well, 100µL of MTT solution was added and the cells were incubated at 37°C (95% air: 5% CO_2) for 2 hours. After 2 hours had elapsed, the MTT solution was carefully aspirated from the cells and DMSO (100 µL) was added to each well. The cells were left at room temperature for 1 hour and then the absorbance of each well was measured at 595 nm using a microplate reader (Multiskan Ascent, v1.23, serial number: 354000517T, Ascent Software Version 2.6).

4.2.2.5 STATISTICAL ANALYSIS

The absorbance values obtained for treated cells were obtained by subtracting the absorbance for control cells, after applying the MTT solution. The mean for eight wells was obtained and calculated as a percentage of the control which was treated as 100% viability.

A two way ANOVA was carried to compare the absorbance values of cells exposed to the nanoparticles and the drug solutions with the control cells, which was treated as 100% viability. This statistical analysis gave information if any change in viability (in comparison to the control) was significant. When $P<0.05$ suggested significant differences. A Bonferroni post-hoc analysis was carried out. This statistical test was also carried out to compare if the changes in viability were significantly different between the different concentrations of test sample used. If $P<0.05$, this suggested significant differences. A Bonferroni post hoc test was carried out.

An independent (unpaired) t-test was conducted to study if the difference in the viability caused by the nanoparticles and corresponding drug solutions was significant. $P<0.05$ suggested significant differences.

4.3 RESULTS

4.3.1 DETERMINATION OF OPTIMUM SEEDING DENSITY

The lower range of seeding densities studied showed linearity over the range from 156 to 5,000 cells/well (Figure 4.1). A plateau was seen from 10,000 to 40,000 cells/well (data not shown). The optimum seeding density therefore was selected as 4,000 cells/ well, below the upper limit of linearity from 5,000 to 10,000 cells/well.

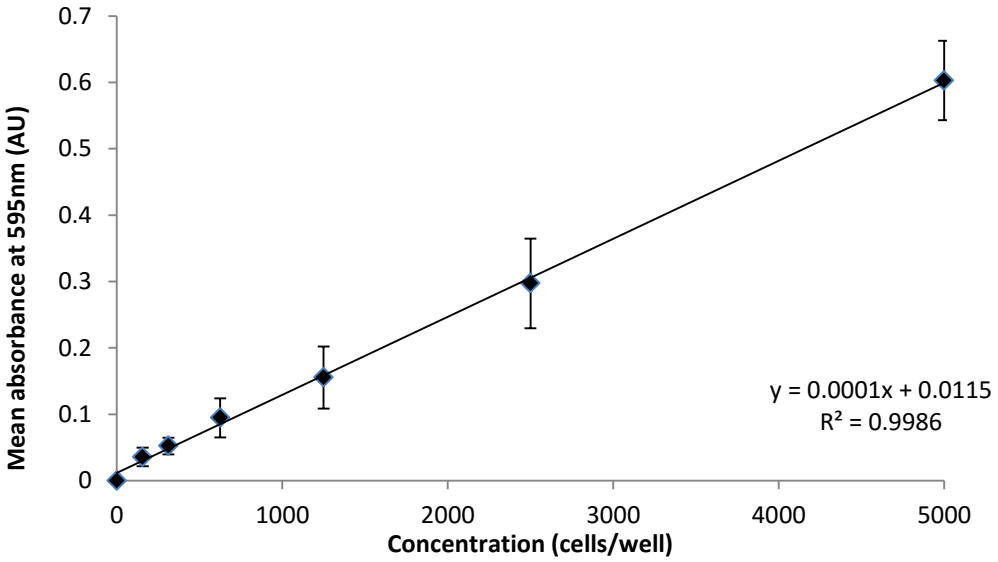

Figure 4.1 The effect of seeding density on absorbance of 16HBE14o- cells 48 hours after seeding cells (n=8, mean±SD, n=8).

4.3.2 THE EFFECT OF DMSO, THEOPHYLLINE, BUDESONIDE AND PLA ON THE VIABILITY OF 16HBE14O- CELLS

4.3.2.1 The effect of DMSO on the viability of 16HBE14o- cells

Initial studies carried out used 10% v/v DMSO or ethanol in medium to prepare the solutions of theophylline, budesonide and PLA. This was then reduced to 1% v/v DMSO as the maximum concentration of DMSO present in the solutions. Therefore the effect of DMSO alone on the 16HBE14o- cell viability was studied over the range of 1% v/v to 0.05% v/v DMSO (Figure 4.2). DMSO had no significant effect on cell viability over this concentration range ($P>0.05$).

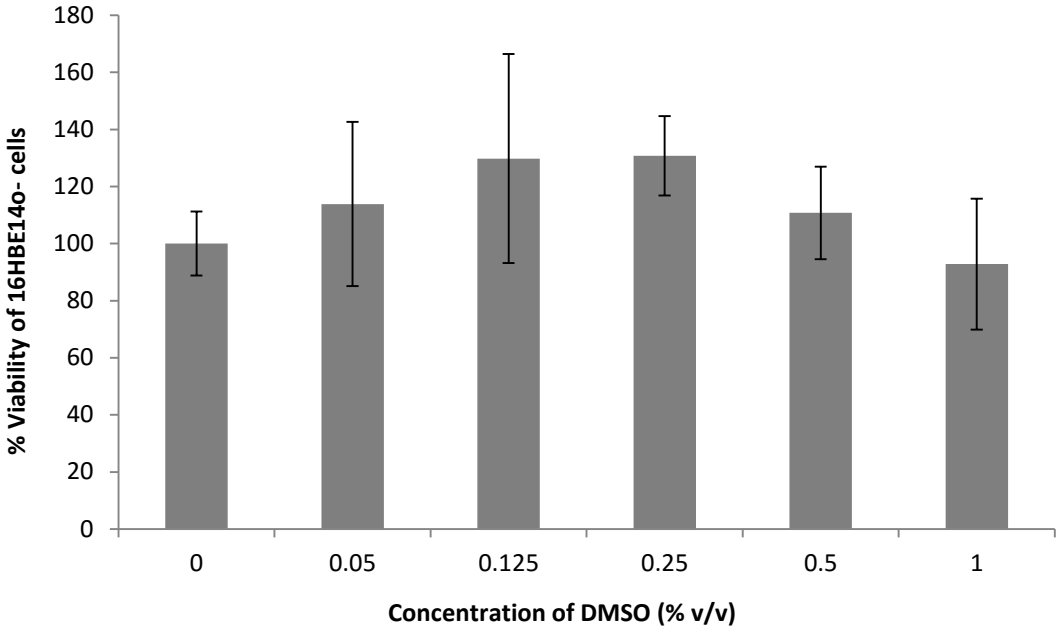

Figure 4.2 The effect of DMSO on the percentage viability of 16HE14o- cells. (n=8, mean±SD)

4.3.2.2 The effect of theophylline on the viability of 16HBE14o- cells

When theophylline was prepared from the stock solution containing ethanol a large reduction in cell viability was observed over the concentration range from 0.25 mg/mL to 2 mg/mL, theophylline (1.25 to 10% v/v ethanol) reducing the cell viability to 14% (1 mg/mL theophylline) and 9% (2 mg/mL theophylline) in comparison to control cells (Figure 4.3) ($P<0.05$). However, when theophylline was prepared in cell culture medium, an improvement in the cell viability was seen. The decrease in cell viability observed when theophylline was applied to the cells in the absence of ethanol was significantly different from the control (untreated cells) only for the concentrations 1 mg/mL and 2 mg/mL, where viability was reduced to 75% and 60%, respectively (Figure 4.4) ($P<0.05$).

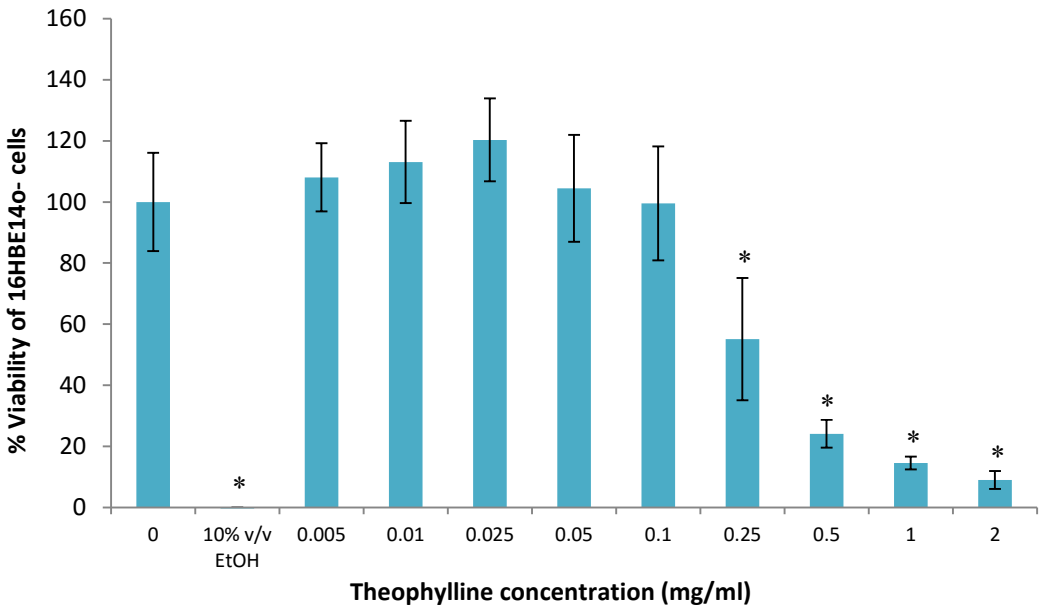

Figure 4.3 The effect of theophylline on the percentage viability of 16HE14o- cells when the theophylline solutions were prepared from a stock solution containing ethanol and serially diluted in cell culture medium. (n=8, mean±SD) (* P<0.05, compared to control and to other test sample concentrations).(EtOH: ethanol)

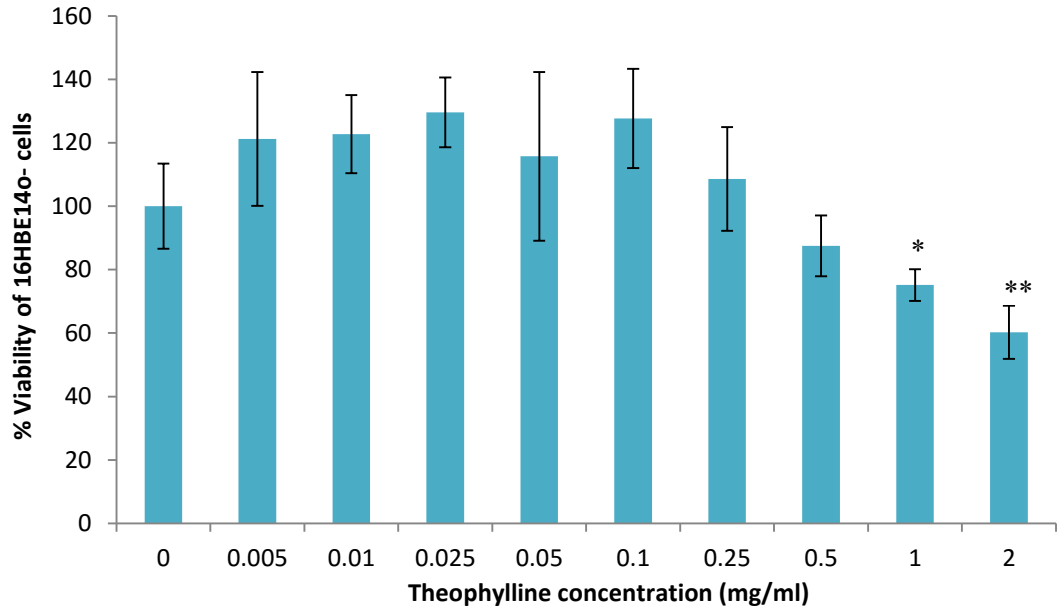

Figure 4.4 The effect of theophylline on the percentage viability of 16HE14o- cells when the theophylline solutions were prepared in cell culture medium (n=8, mean±SD) (* P<0.05, compared to control) (P<0.05, compared to the other test sample concentrations).**

4.3.2.3 The effect of budesonide on the viability of 16HBE14o- cells:

When budesonide was prepared from the stock solution containing ethanol a significant reduction in cell viability was observed when compared to the control cells over the concentration range from 5 to 200 µg/mL. This contained 0.25-10%v/v ethanol ($P<0.05$) (Figure 4.5). When the organic solvent was changed to DMSO and the maximum concentration of DMSO reduced to 1%v/v, the viability remained significantly lower in comparison to the control cells over the concentration range 0.25 mg/mL to 2 mg/mL. These solutions contained 0.125%v/v to 1%v/v DMSO (Figure 4.6) ($P<0.05$). An improvement in the cell viability was observed when budesonide was prepared as an aqueous suspension in cell culture medium in the absence of an organic solvent, and was not significantly different to the control cells (Figure 4.7) ($P>0.05$).

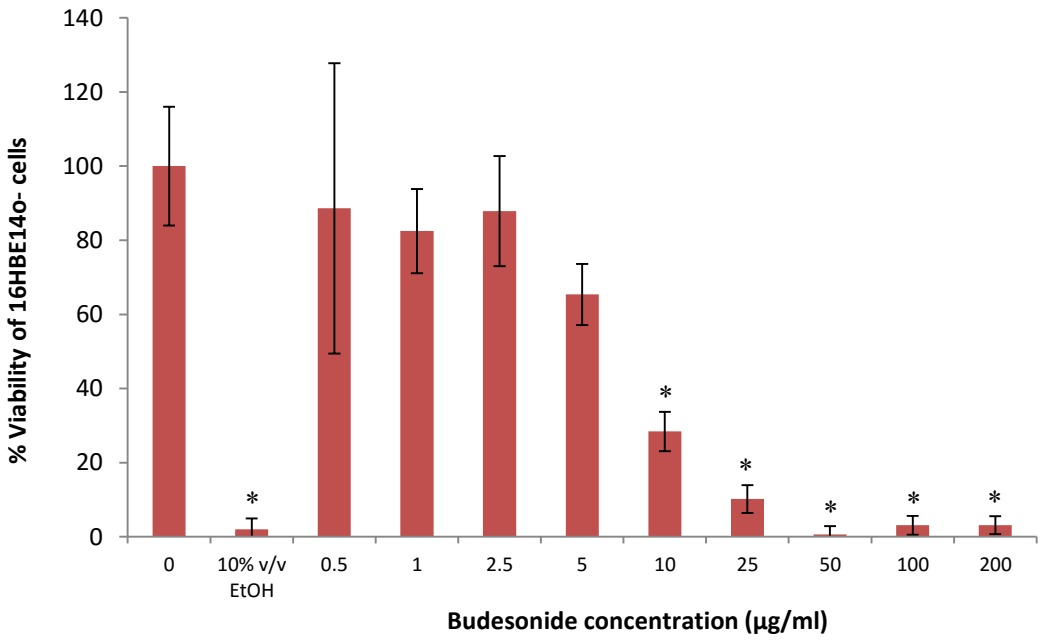

Figure 4.5 The effect of budesonide on the percentage viability of 16HE14o- cells when the budesonide solutions were prepared from a stock solution containing ethanol and serially diluted in cell culture medium (n=8, mean±SD) (* $P<0.05$, compared to control and to other test sample concentrations) (EtOH: ethanol)

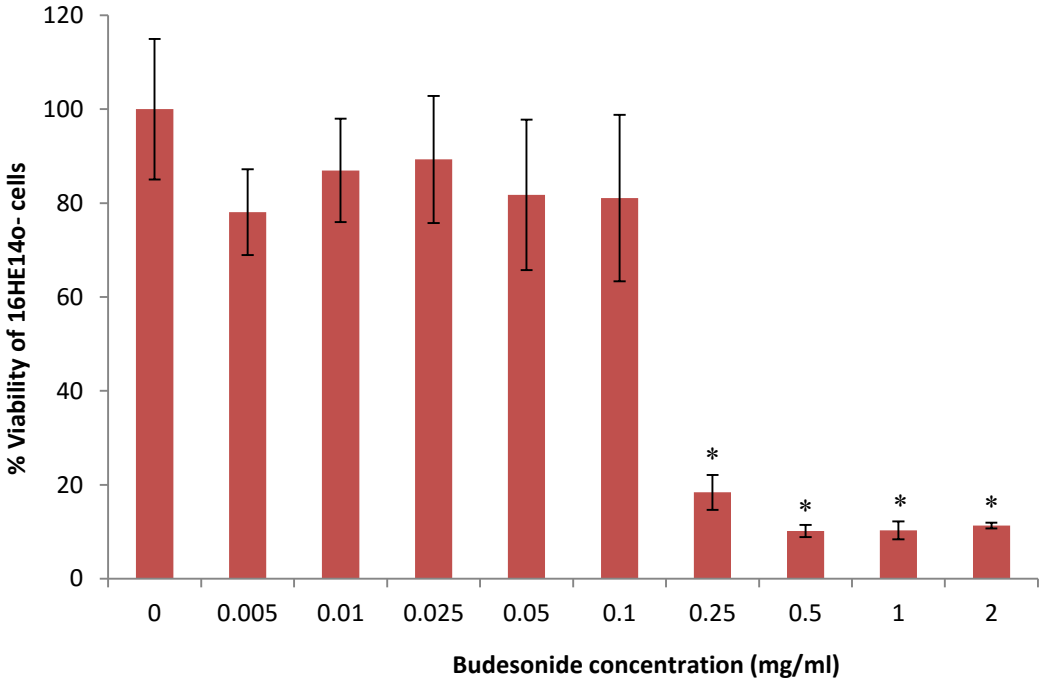

Figure 4.6 The effect of budesonide on the percentage viability of 16HE14o- cells when the budesonide solutions were prepared from a stock solution containing DMSO and serially diluted in cell culture medium. The final concentration of DMSO used was 1% v/v. (n=8, mean±SD) (* P<0.05, compared to control and to other test sample concentrations).

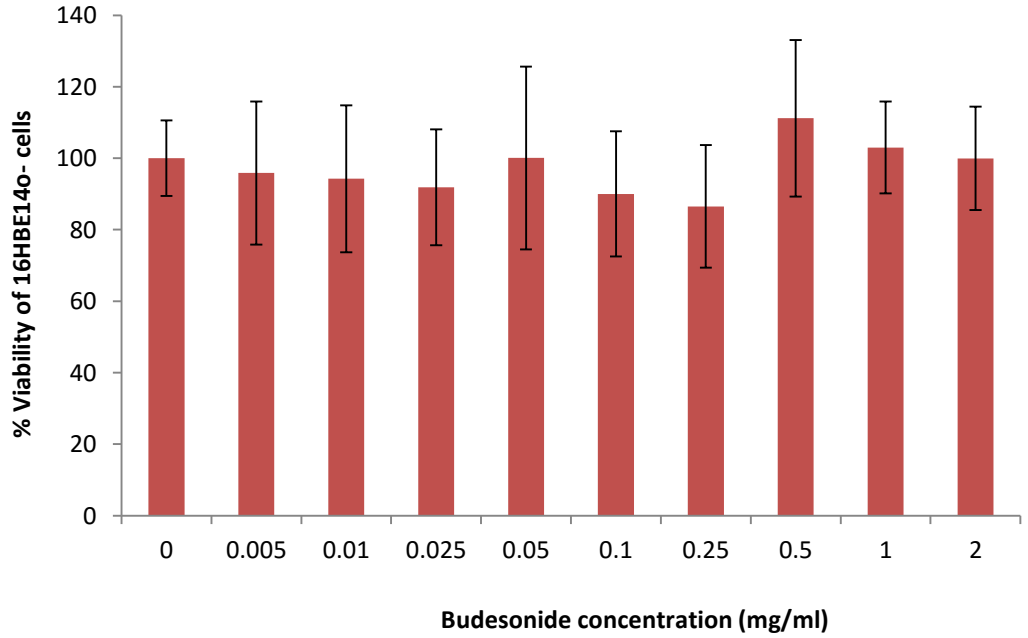

Figure 4.7 The effect of budesonide on the percentage viability of 16HE14o- cells when the budesonide suspensions were prepared in cell culture medium (n=8, mean±SD).

4.3.2.4 The effect of PLA on the viability of 16HBE14o- cells:

PLA formed a major component of the nanoparticles and so various concentrations were examined for their effects on viability. DMSO was used to prepare the solutions of PLA. Cell viability was not affected by PLA (10 to 200 µg/mL) in which the maximum concentration of DMSO was 1%v/v ($P>0.05$) (Figure 4.8).

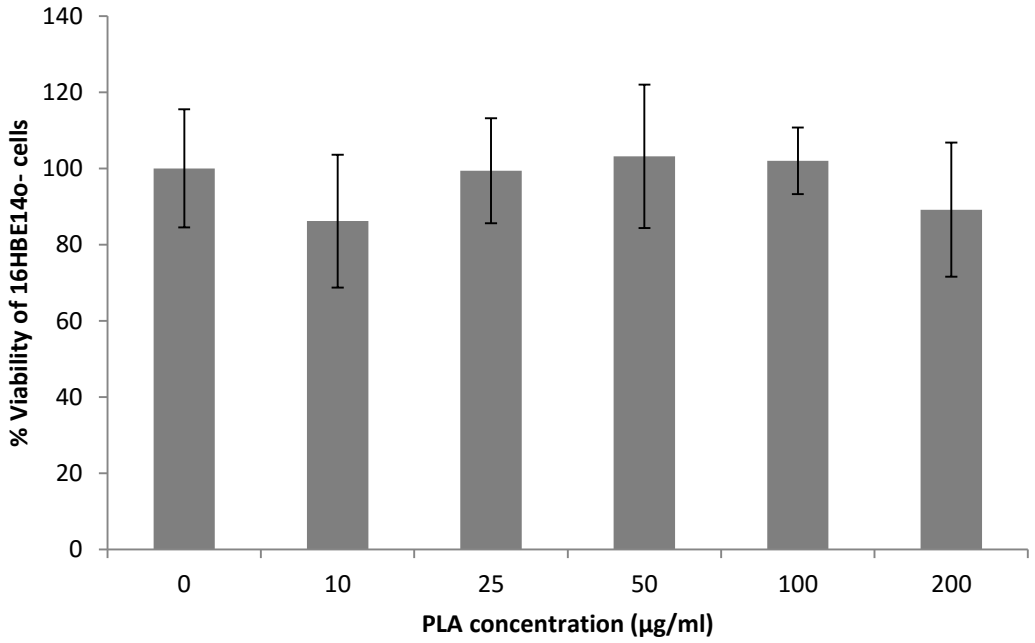

Figure 4.8 The effect of PLA on the percentage viability of 16HE14o- cells when the PLA solutions were prepared from a stock solution containing DMSO and serially diluted in cell culture medium. The concentration of DMSO in the 200 µg/mL PLA solution was 1% v/v (n=8, mean±SD).

4.3.2.5 The effect of the combinations of theophylline, budesonide and PLA on the viability of 16HBE14o- cells:

As co-encapsulated nanoparticles are composed of both drugs and PLA, the effect of theophylline and budesonide combinations in solution on cell viability was also studied. There was no significant effect on the viability of the cells ($P>0.05$) when the drugs were applied at concentrations below 0.5 mg/mL (theophylline and budesonide), even though small concentrations of DMSO were present (Figure 4.9). When PLA was added to the solutions a decrease in cell viability ($P<0.05$) was observed at a concentration of 1.0 mg/mL

(theophylline and budesonide)/ 200 μg/mL PLA (present with a small concentration of DMSO (0.5% v/v)) (Figure 4.10).

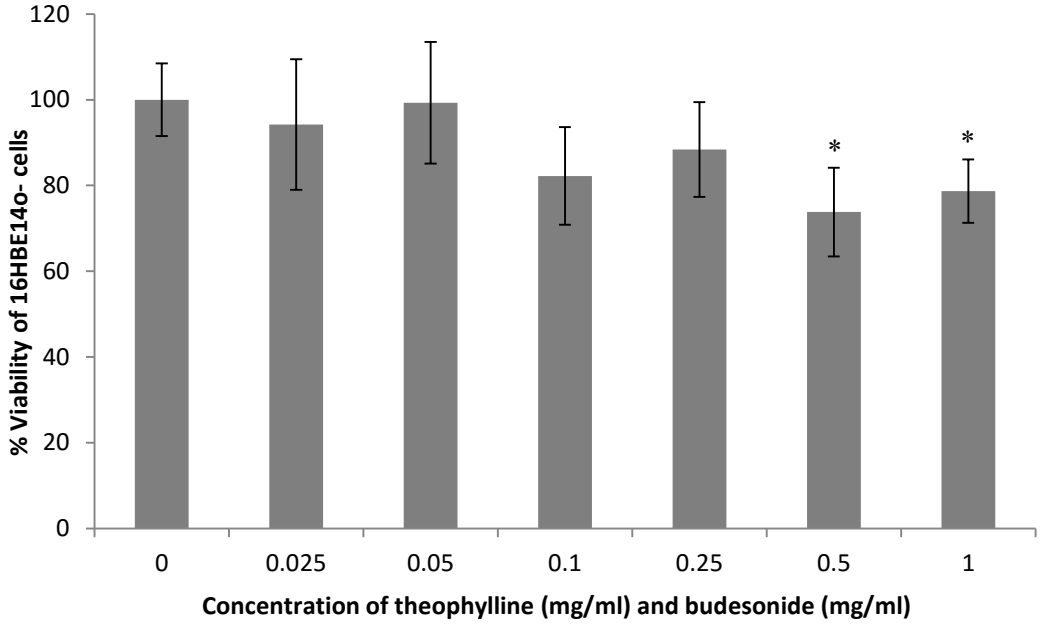

Figure 4.9 The effect of a combination of theophylline and budesonide solutions on the percentage viability of 16HE14o- cells. Budesonide solutions contained DMSO; theophylline was prepared in cell culture medium. The concentration range of DMSO in the combination solutions was between 0.006% v/v to 0.5% v/v (n=8, mean±SD) (* P<0.05, compared to control).

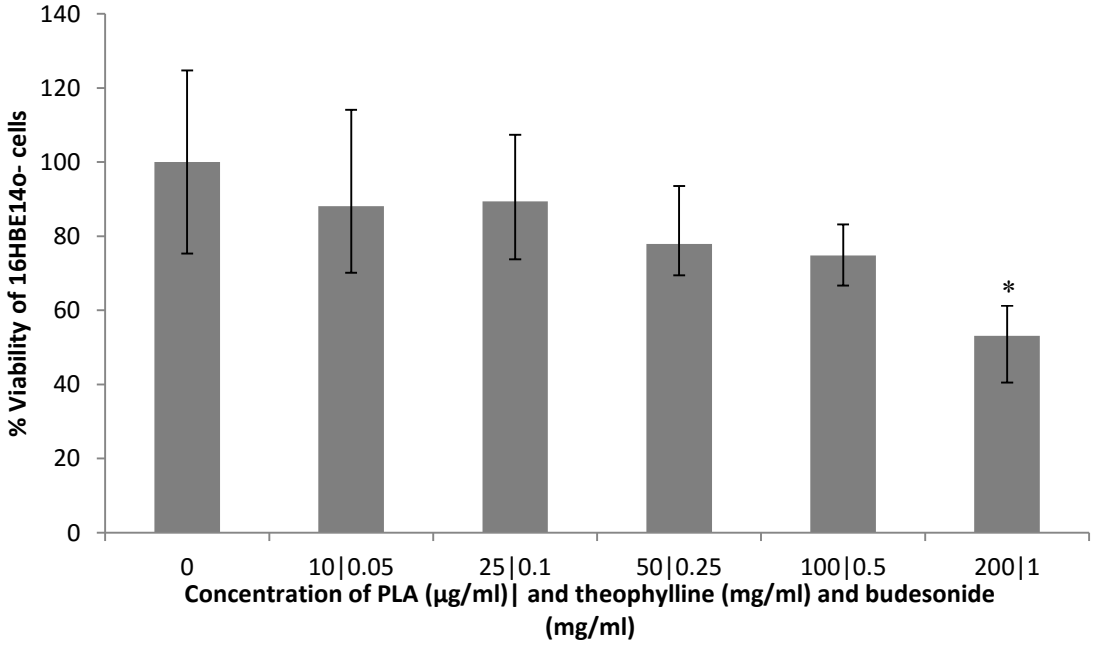

Figure 4.10 The effect of a combination of theophylline solutions, budesonide suspensions and PLA solutions on the percentage viability of 16HE14o- cells. PLA solutions contained DMSO; theophylline was prepared as a solution in cell culture medium and budesonide as a suspension, at equal concentrations. The concentration range of DMSO in the combination solutions was between 0.025% v/v to 0.5% v/v (n=8, mean±SD) (* P<0.05, compared to control and to other test sample concentrations).

4.3.3 THE EFFECT OF BLANK, MONO-ENCAPSULATED THEOPHYLLINE OR BUDESONIDE NANOPARTICLES AND CO- ENCAPSULATED THEOPHYLLINE AND BUDESONIDE NANOPARTICLES ON THE VIABILITY OF 16HBE14O- CELLS

Blank PLA nanoparticles significantly reduced cell viability to approximately 75% of the control cells for all concentrations of blank nanoparticles applied ($P<0.05$) No relationship between concentration and toxicity was observed (Figure 4.11).

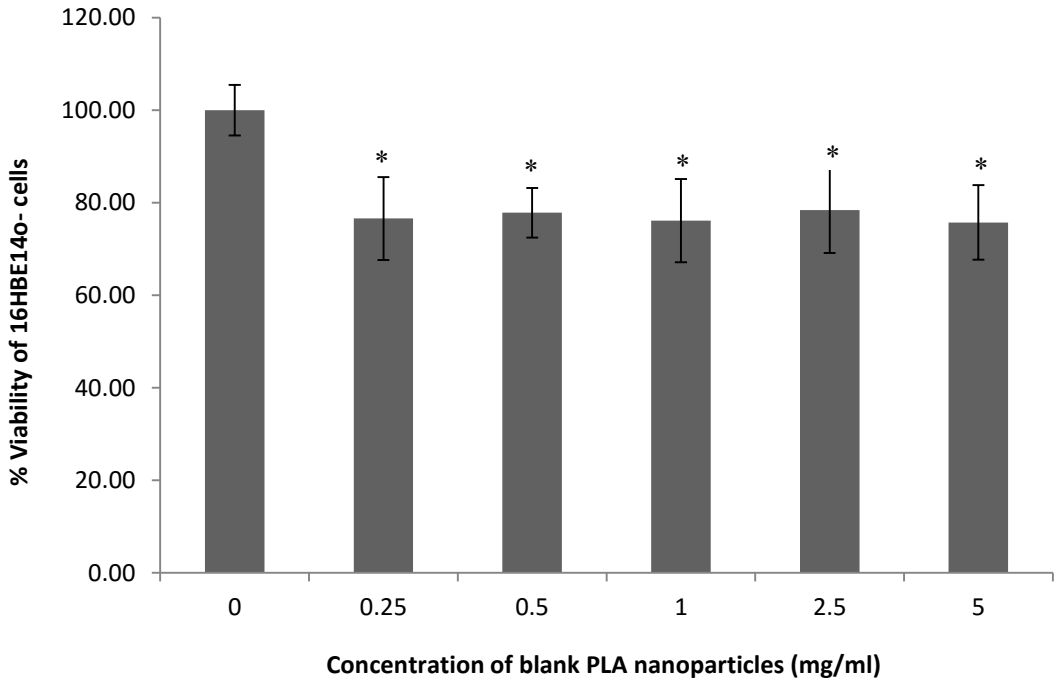

Figure 4.11 The effect of blank PLA nanoparticles on the percentage viability of 16HE14o- cells. The blank PLA nanoparticles are suspended in cell culture medium at the desired concentration (n=16, mean±SD) (* P<0.05, compared to control).

Treatment of cells with theophylline mono-encapsulated nanoparticles had little effect on cell viability except at the highest concentration studied of 5 mg/mL which significantly reduced cell viability by 50% ($P<0.05$) (Figure 4.12).

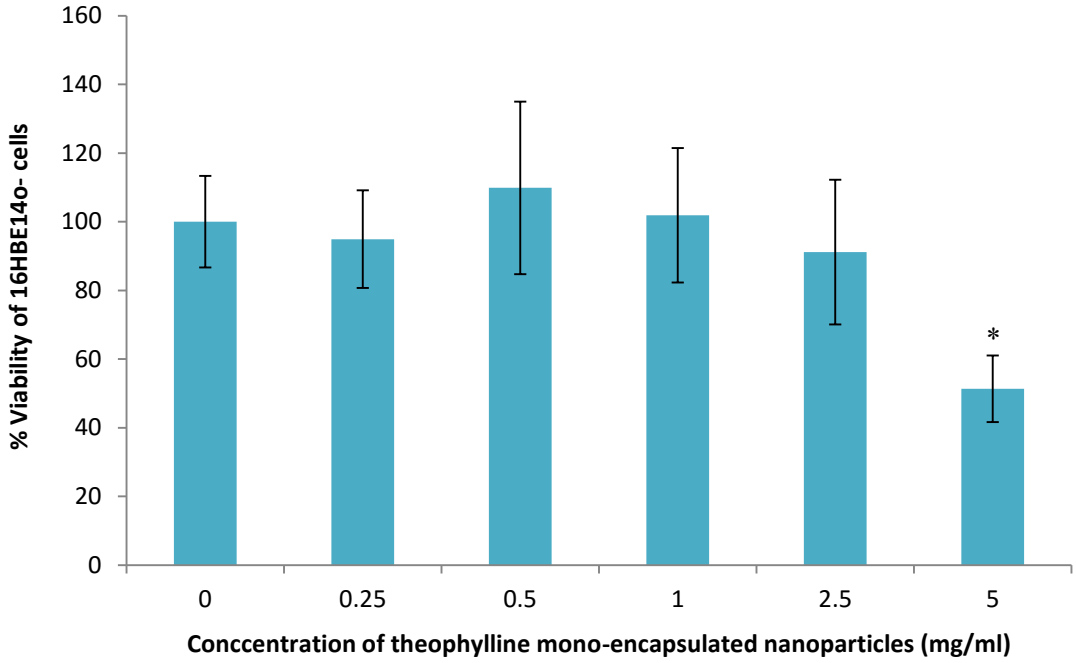

Figure 4.12 The effect of theophylline mono-encapsulated nanoparticles on the percentage viability of 16HE14o- cells. (n=32, mean±SD) (* P<0.05, compared to control and to other test samples).

A similar relationship was observed for cells treated with budesonide mono-encapsulated nanoparticles where a significant reduction in the cell viability was only observed at the highest concentration tested (5 mg/mL nanoparticles) (Figure 4.13) (P<0.05).

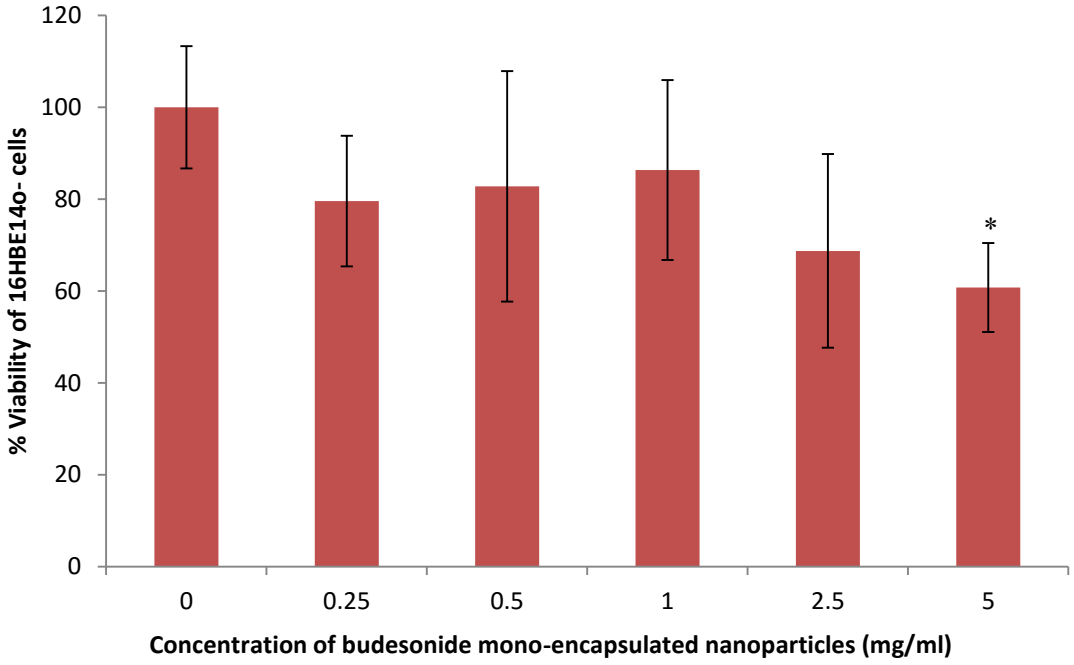

Figure 4.13 The effect of budesonide mono-encapsulated nanoparticles on the percentage viability of 16HE14o- cells. (n=32, mean±SD) (* P<0.05, compared to control).

Theophylline and budesonide co-encapsulated nanoparticles showed a similar pattern to their mono-encapsulated counterparts where the decrease in cell viability caused by the highest concentration (5 mg/mL) (~ 60%) was significantly different to the control cells ($P<0.05$) (Figure 4.14).

There was no significant difference between the effect of the nanoparticles on cell viability and the effect of the drug solutions of equivalent concentrations ($P>0.05$).

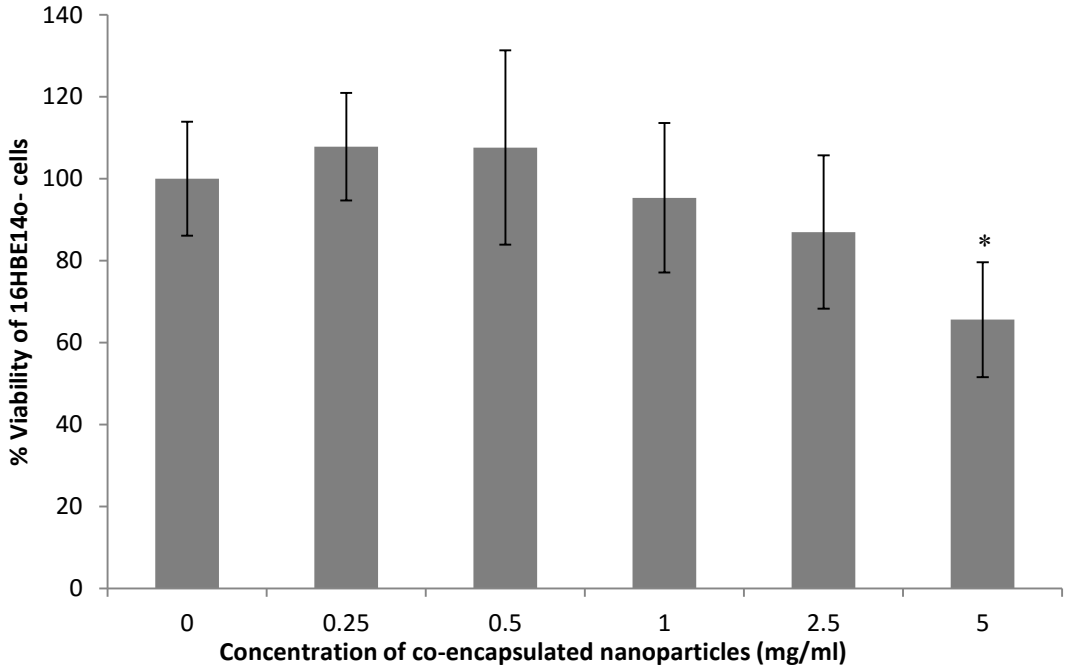

Figure 4.14 The effect of theophylline and budesonide co-encapsulated nanoparticles on the percentage viability of 16HE14o- cells. (n=32, mean±SD) (* P<0.05, compared to control and cells treated with 0.25 and 0.5 mg/ml co-encapsulated nanoparticles).

4.4 DISCUSSION

Several studies on nanoparticles synthesized using biodegradable polymers have been carried out. The points that were considered when designing the current study included concentration of nanoparticles or encapsulated drugs, overall toxicity of biodegradable polymeric nanoparticles and time scale of the study. These variables would allow an understanding of the toxicity of the theophylline and budesonide nanoparticles in the current study when applied on 16HBE14o- cells.

4.4.1 DETERMINATION OF THE OPTIMUM SEEDING DENSITY

In order to carry out the cytotoxicity experiment, a seeding density was required that would give absorbance values towards the top of the linear range with the MTT assay after 48 hours (the full duration of the experiment). Cell seeding densities that were higher than 10,000 cells/well showed deviations from linearity, suggesting confluence of the cells [393]. The linear region that was obtained was for seeding densities less than 10,000 cells/ well. The seeding densities used for the current work were in the range 156 to 10,000 cells/well, as there is a linear relationship between the cell number and absorbance at these seeding densities.

4.4.2 THE EFFECT OF DMSO, THEOPHYLLINE, BUDESONIDE AND PLA ON THE VIABILITY OF 16HBE14O- CELLS

In this study, DMSO significantly reduced cell viability when concentrations of greater than 1% v/v were used (data not shown). Thus DMSO or ethanol (both at 10% v/v) could be used as a positive control to show cytotoxicity was capable of being measured in common with other studies [225, 395, 396]. Reduction of the DMSO concentration to 1% v/v and less was not toxic therefore this was the concentration used to prepare budesonide and PLA solutions to assess their effects on the viability of 16HBE14o- cells.

The concentration range of solutions of theophylline chosen for the assessment of its effect on cell viability included the concentrations likely to be achieved with maximum theoretical loading efficiency of theophylline in the nanoparticles. For instance, a concentration of 5 mg/mL nanoparticles (the maximum used in this study) would be expected to contain approximately 980 μg/mL theophylline and 98 μg/mL budesonide. This allowed a comparison to be made between the effects of the drugs in solution/ suspension and their effects when encapsulated in nanoparticles.

When theophylline solutions were prepared from a stock solution of theophylline dissolved in ethanol a concentration-dependent decrease in the viability of 16HBE14o- cells was observed. A concentration-dependent decrease in the viability of 16HBE14o- cells was also observed for the theophylline solutions prepared at the same concentration in the absence of organic solvent. However, the reduction in viability was greater when ethanol was used to prepare the solutions, indicating that the toxicity was likely to have been caused by the ethanol. It is thought that ethanol is toxic due to its ability to dissolve components of the cellular membrane and denature proteins [376]. Due to the reduction in viability at 1 and 2 mg/mL of theophylline (in the absence of ethanol), it suggests that the concentration of theophylline encapsulated in the PLA nanoparticles would be of low toxicity over the time scale and conditions of the study.

Budesonide solutions containing organic solvents (ethanol or DMSO) caused a concentration dependent decrease in viability and, similar to theophylline, it is thought that the reduction in viability was due to the effect of the organic solvent rather than the drug itself. This is supported by the results obtained for budesonide suspensions prepared in cell culture medium, where cell viability was non-significantly different to the control cells although it should be recognized that the aqueous solubility of budesonide is 45.7 mg/L [85, 140, 397].

One of the main components of the nanoparticles is the polymer encapsulating the drug. Due to the poor solubility of PLA in the cell culture medium, PLA was prepared at required concentrations in DMSO and serially diluted in cell culture medium. At concentrations of DMSO less than 1%v/v, PLA was not toxic to the cells at the concentrations tested.

The co-encapsulated nanoparticles synthesized contain polymer, theophylline and budesonide and this combination was also studied. Generally this combination was not toxic except at the highest concentration studied and similar to the budesonide and PLA solutions; increased toxicity was thought to be due to the presence of the organic solvent, as described previously.

4.4.3 The effect of blank, mono-encapsulated theophylline or budesonide nanoparticles and co-encapsulated theophylline and budesonide nanoparticles on the viability of 16HBE14o- cells

Several studies on the cytotoxicity of nanoparticles synthesized using biodegradable polymers have been carried out. These studies were used in the design of the current study with respect to whether the concentration of nanoparticles was studied or the concentration

of the drugs encapsulated. The current study used concentration of nanoparticles based on the weight of the freeze dried nanoparticles and not the drugs. This is similar to the approach used in a study of temozolomide-loaded PLGA nanoparticles; the concentration range of the drug was 1500-0.1 μg/mL and its effect on cell viability was compared that of the free drug and blank PLGA nanoparticles [398]. PLGA nanoparticles loaded with furanodiene were similarly compared also to blank, drug-containing nanoparticles and free drug solutions; but the concentrations applied in this study were based on the concentration of the drug encapsulated and not the concentration of the nanoparticles [295]. For theophylline and budesonide nanoparticles, the former approach was not chosen as it can result in a highly concentrated suspension of the nanoparticles (due to the low drug loading), which may not be suitable.

In the current study, the range of concentrations that was investigated for the nanoparticles was kept consistent for all the different nanoparticles prepared; it included the concentration used for the release testing study (0.6 mg/mL) (Chapter 3) and a maximum concentration of 5 mg/mL. If 100% loading efficiency was achieved, 5 mg/mL of nanoparticles should contain 980 and 98 μg/mL of theophylline and budesonide, respectively. The inhaled dose of budesonide used clinically is 100-200 μg for the treatment of asthma suggesting this is an appropriate upper limit for the study. However, *in vivo* this dose would be available to the whole lung whereas in the current study the suspension of nanoparticles is applied to cells in a 96 well plate. Due to the area of the wells in a 96 well plate (0.55 cm^2/well) and the volume applied (100μL); 5 mg/mL of nanoparticles would result in a highly concentrated suspension being applied over a small area of cells (4000 cells seeded per well). This may cause a higher toxicity than would be expected *in vivo* and justifies the use of lower concentrations.

The concentration range of nanoparticles used in this study was based on the actual freeze-dried nanoparticle powder weight and a calculated theoretical loading of the two drugs; it was mostly higher than the range used in other studies. While it is possible to calculate theoretical loading of theophylline and budesonide to obtain a comparable range, or a dose that could be considered 'therapeutic'; this can result in a highly concentrated suspension of the nanoparticles in cell culture medium, as described. It was observed that in the highly concentrated suspensions of the nanoparticles; the nanoparticles had settled down on the surface of the cells. As a consequence, it may be possible that the cells were physically deprived of nutrients explaining why the nanoparticles appeared toxic while their equivalent drug solutions were not. However, a similar nanoparticle concentration range as used in the current study was used for mannitol-chitosan nanoparticles [267], freshly dispersed modified

chitosan microparticles [396] and on negatively charged PLGA nanoparticles [399]. This suggests the concentration range and method of nanoparticle preparation is suitable in the current study of theophylline and budesonide nanoparticles. It should also be noted that some concentrations of nanoparticles/nanomaterials assessed for cytotoxicity have been studied at lower and higher concentration ranges; for instance, a concentration range of 25-400 μg/mL was used for heparin nanoparticles when investigating cell viability [297, 373]. Conversely, a study on PLGA-lecithin-PEG core shell nanoparticles used concentrations of up to 25 mg/mL and showed a large reduction in cell viability [287].

The theoretical concentration range calculated in the current study was based on 100% drug loading of both drugs; which may not be the correct representation of the encapsulated dose. However, by determining the 100% loading dose, this also provides an upper limit. This would also allow understanding the effect on viability on 16HBE14o- cells that theophylline and budesonide would have on higher drug concentrations. The concentration range of the drug solutions would cover the concentration of the drugs encapsulated in the nanoparticles.

The effects on the viability on cells of drugs encapsulated in nanoparticles have been compared to drug solutions previously. It was commonly observed that the drugs encapsulated in nanoparticles were less toxic than the free drug solution; but this effect was not significantly different in the current study. Lorazepam nanoparticles synthesized using biodegradable polymers showed that they were less toxic than the free drug solution [380]. In a study of temozolomide loaded PLGA nanoparticles; the concentration range was 1500-0.1 μg/mL of the drug which was compared to the effect on viability caused by free drug and blank PLGA nanoparticles [398]. PLGA nanoparticles loaded with furanodiene were similarly compared also to blank, drug containing nanoparticles and free drug solutions; but the concentrations applied in this study were based on the concentration of the drug encapsulated and not the concentration of the nanoparticles [295]. Both these studies presented improved effect on viability in comparison to the free drug standards.

The current study suggested no significant difference between the nanoparticles and the drug solutions/suspensions at equivalent concentrations. This suggested that the concentrations used in this study are non-toxic; but also can suggest that the concentration of the drug encapsulated in the nanoparticles has a minimal effect on viability. Encapsulation of the drug into polymeric nanoparticles is suggested to present a protective effect and as a result of the sustained release of the drug, the overall concentration of the drug present will be low and show lower effect on toxicity in comparison to the free drug solution/suspension [295, 398].

In order to study the effect on viability of the 16HBE14o- cells that nanoparticles which would equal to 2 mg/mL of drug, this would result in an extremely large reduction in viability due to the highly concentrated suspension of the nanoparticles, which may have a greater effect on the viability in a small area of cells rather than as an effect of the drug itself.

The time period chosen for this study was kept consistent with the release study carried out on the nanoparticles (Chapter 3) and is also consistent with the time used in other studies on the cytotoxicity of nanoparticles [267, 287, 297, 373, 396, 400, 401]. Exposure of the nanoparticles to the cells lines for a period of 24 hours would allow any toxicity due to inhibition of proliferation and/or cell death to be visible in an MTT assay with a definite end point [297, 373]. For this reason, it was also suitable to assess the effects of theophylline and budesonide nanoparticles on the cytotoxicity of 16HBE14o- cells for a period of 24 hours. Studies used different cell lines with different encapsulated drugs [380, 385, 398, 401, 402]. Many studies extended assessment of viability up to 24, 48 and 72 hours; some studies only looked at exposure for 6 hours for example or at frequent time intervals, instead of one definite end time point[297]. PLGA- Doxorubicin nanoparticles formulated were assessed over a period of 48 hours using HepG2 cells [400].

Ideally, it would be beneficial to carry this study out over a longer period of time but this time would be difficult to define as it is not known, nor reported, how long the nanoparticles would remain un-cleared from the lung. PLA breaks down to lactic acid which is further broken down to carbon dioxide and water [189, 385, 398, 403]. This process, however, takes a long period of time (months) [404, 405]. It has been suggested that the degree of toxicity of polymeric nanoparticles is strongly influenced by the conditions of the local environment (such as clearance and metabolism) which further influences the rate of degradation of polymeric nanoparticles [297].

An LDH assay conducted on PCL nanoparticles at varying concentrations (5, 10 and 50 µg/mL) showed no significant cytotoxicity to 16HBE14o- cells [406]. However, a reduction in cell viability has been observed in other studies on biodegradable polymeric nanoparticles [225, 395]. In the current study, the cytotoxicity of the drug loaded nanoparticles was compared to blank PLA nanoparticles. Interestingly, in the absence of drug the blank nanoparticles reduced cell viability by approximately 20% at all concentrations applied but this effect was not observed when the nanoparticles contained drug. For drug-encapsulated nanoparticles a significant decrease in cell viability was only observed at the highest concentrations applied for both mono and co-encapsulated nanoparticles. The reasons for this is unclear but is

possibly an artefact of the smaller variability associated with the experimental data obtained when studying the blank nanoparticles.

PLA (not in nanoparticle form) has been previously assessed for its cytotoxicity using various cell lines and shown that it does not significantly affect cell viability (using CHO-K1 Chinese hamster ovary cells) when assessed using an XTT assay with a duration of up to 72 hours [407] or with increasing concentration of polymer when investigated using an MTT assay showed approximately 80% of viable Calu-3 cells compared to control[408]. This suggests the safety of the polymer when studied *in vitro*. In the current study, when applied in solution, PLA was not toxic to the cells suggesting that any toxicity of the blank nanoparticles was not related to the degradation of the polymer.

Co-polymers of PLA have also been investigated, showing limited toxicity on A549 cells when determined using an MTT assay after exposure to test compounds for 24 hours [409] and other various PLA nanoparticles studied have shown non-significant effects on viability for duration up to 72 hours at a range of concentrations [410, 411] further supporting the safety and limited effect on cell viability when studied *in vitro* as obtained in this current study. Any differences in nanotoxicity were thought to be due to differences in mechanisms of uptake between drug solutions and nanoparticle suspensions [410]. It is generally accepted that PLA and biodegradable polymers have a low toxicity and show good biocompatibility and biodegradability profiles; but their long term toxicity is still required to be assessed [374, 412].

The reduction in viability of the 16HBE14o- cells treated with blank PLA nanoparticles was approximately 75%; and a further reduction for the drug-containing nanoparticles applied at 5 mg/mL nanoparticles to approximately 60% suggests an additive effect of the drug and nanoparticles. Similar comparisons were made between drug loaded nanoparticles and blank PLA nanoparticles (studying the encapsulation of an oligonucleotide) which showed lower toxicity of the blank nanoparticles over the drug nanoparticles. Cytotoxicity was studied after 24 hours using an MTT assay [281].

In a study carried out by Zhu et al (2015), theophylline formulated in a metered dose inhaler was assessed for its effects on Calu-3 cell viability [413]. This was done using an MTS assay in which theophylline was applied to the cells in PBS. The concentration range that was studied was between 19 nM (3.42 ng) to 2 mM (360 µg) and was seen to be tolerated by the Calu-3 cells over a duration of 72 hours [413]. This concentration range is within the concentration range that studied for theophylline nanoparticles and the solutions of theophylline assessed in this study and the results are similar.

Functionalized mesoporous silica nanoparticles of budesonide were tested for cell viability for a period of 24 to 48 hours showing that these were non-cytotoxic when concentrations were in the range of 5-10 μM (2 μg to 4 μg, respectively) [414]. This is a concentration range in the lower range than what is encapsulated in the PLA/budesonide nanoparticles synthesized for this current work, but supports the low toxicity effect on cells treated with budesonide-containing nanoparticles and suspensions in comparison to the control.

Studies have been carried out on budesonide using different cell lines and different concentrations for its effect on cell viability. Bandi and Kompella (2001) studied the cytoxicity of budesonide over a concentration range of 0.01-100μM (4 ng - 40 μg) in Calu-1 and A549 cells for duration of 12 hours [415]. The effect on A549 cells was not significant at 100μM but shown to be significant on Calu-1 cells. These concentrations are within the range of concentrations studied for theophylline and budesonide nanoparticles and suggest the low potential toxicity of budesonide in the conditions and time scale used for this study.

4.5 CONCLUSIONS

The aim of the study was to assess the viability of 16HBE14o- cells when treated with mono- and co-encapsulated theophylline and budesonide in PLA nanoparticles. This was compared to the effect of solutions of theophylline, budesonide and PLA of equivalent encapsulated concentrations on cell viability.

Over the concentration range tested, drug-containing nanoparticles were well tolerated by the cells at and below a nanoparticle concentration of 2.5 mg/mL. At a nanoparticle concentration of 5 mg/mL both mono- and co-encapsulated nanoparticles were toxic to the cells as were the equivalent concentrations of drug applied to the cells in solution. The current study showed that theophylline and budesonide have limited effect on the viability of 16HBE14o- cells over the time-scale and concentration range applied in this study.

CHAPTER 5 THE TRANSPORT OF THEOPHYLLINE AND BUDESONIDE ENCAPSULATED IN PLA NANOPARTICLES ACROSS 16HBE14O- CELLS

5.1 INTRODUCTION

Having formulated and characterized the drug encapsulated nanoparticles it was important to understand their interaction with the airway epithelium. The surface of the airway is lined by a pseudostratified epithelium. The cells are present at an air-liquid interface and cell types include basal cells, ciliated cells, and secretory cells [8, 392, 416-418]. One of the main functions of the airway epithelium is to provide a barrier to prevent inhaled material gaining access to the blood stream [417, 419]; this role would extend to inhaled drugs. Formation and maintenance of this diffusion barrier requires the presence of tight junctions [419] which are dynamic multiprotein structures that are sensitive to certain toxins, pathogens and cytokines [335, 419].

Little is known regarding the effects of drug-loaded nanoparticles after deposition in the lung; with respect to their toxicity, their uptake, drug release and permeability [372]. The use of airway epithelium cell culture models allows the study of the release of drugs *in vitro*, trans-epithelial drug transport, and the health of the cells in contact with drugs [346, 420]. There is wide interest in the pulmonary effects of nanomaterials with research ranging from nanomaterials inhaled as a result of environmental exposure to biodegradable polymeric nanoparticles intended for drug delivery [372].

Immortalized cell lines are useful to study drug permeability, providing they express functional tight junctions, and also the cytotoxic effects of the drug compounds or nanoparticles in the lungs [393]. The airway is divided into the conducting region and respiratory/alveolar region, and there are cell lines that are used to represent these regions of the airways. Briefly, the cell line, A549 is obtained from a human pulmonary adenocarcinoma, retaining a great similarity to Type II alveolar epithelial cells, and has been used to model the alveolar region of the airways in several studies [370, 386, 387].

Human cell lines that have been used to model the upper airways of the lungs and have been developed as models to represent this part of the airways include Calu-3 and 16HBE14o-

cells [388, 392, 417, 418, 421]. Calu-3 cells, which are derived from an adenocarcinoma of the lung, have been used to study drug transport due to their ability to form tight junctions [371, 390-392, 422, 423]. The human bronchial epithelial cell line, 16HBE14o-, has also been used in studies of cytotoxicity and drug transport.

The 16HBE14o- cells readily form tight junctions when cultured to confluency on collagen-coated semi-permeable supports (e.g.Transwells®) at an air-liquid interface [388, 392, 394, 423, 424]. This is more recently termed 3-D culture. The cells are cobblestone in shape and display vectoral ion transport. It is important that the culture conditions of the cells are able to allow differentiation of the cells to form a suitable epithelial barrier. The 16HBE14o- tight junctions stain positively for the tight junctional proteins ZO-1, occludin and intracellular proteins E-cadherin and desmoplakin [393, 425] and also express morphological features such as microvilli [8]. The 'tightness' of the tight junctions is quantified by assessment of the trans-epithelial electrical resistance (TER) of the cells or by measurement of the functional barrier the cells are able to provide to the flux of compounds which diffuse across the cells via the paracellular route [8, 393].

Growing cells on an air-liquid interface or submerged in culture has been studied extensively previously. The air-liquid interface allows differentiation of the cells and morphologically representative of the bronchial epithelium and formation of tight junctions [8, 392, 393, 406, 417, 419, 426-429]. It is important and good to have the air-liquid interface for this purpose [427]. Submerged cultures may compromise of differentiation of the cells, as reviewed by Forbes and Ehrhardt (2005) [392].

While most permeability studies use monolayers of a single cell type, co-culture models have also been developed [417]. A co-culture model of 16HBE14o- cells with fibroblasts was developed by Pohl et al (2009). This model consisted of Transwell® inserts which had bronchial (16HBE14o-) cells present on the apical side and fibroblast cells cultured on the basolateral side of the insert [417]. Co-cultures also allow the study of interactions between endothelial and epithelial cells [335]. Triple co-culture models developed using A549 cells, macrophages and dendritic cells are reviewed by Haghi et al (2014); these have been used to study the effect of exposure to nanotubes [335].

Further development of 3-D models includes the use of fully differentiated epithelial cells (primary cultures) which possess beating cilia and mucus production. Examples of commercially available models are MucilAir™ [335, 428] and Epiairway™ [335, 392]. The limitations of these cells are that they are less convenient and economical. Primary cell cultures also have a limited life span and show great variability in the results obtained, as reviewed by Haghi et al (2014) [335].

As well as using cell culture models to study the release and permeability of drugs encapsulated in nanoparticles, it is possible to study the translocation of the nanoparticles themselves across the cells and supporting matrix. When studying nanoparticles, it is important to ensure the suspension is homogenous and, since most particles pass unhindered across the cell culture support, care should be exercised when selecting the cell culture support [372]. The passage of highly charged particles across the epithelial barrier is prevented due to interactions of nanoparticles with the cell membrane including Van der Waal (VdW) reactions and between polymer and the cell membrane. Translocation is further limited by the presence of the tight junctions between the cells, as described above. Some nanoparticles are able to open tight junctions and increase their delivery; however this is limited to a gap of approximately 13-15nm [430]. Most nanoparticles are able to enter the cells by processes of endocytosis [430]. In translocation studies of nanoparticles, the paracellular permeability of fluorescently-labelled compounds has been used in order to understand the effects the test compounds have on the tight junctions. This functional information is further supported by measurement of the trans-epithelial electrical resistance (TER) of the cells before and after the experiment is carried out [267, 423].

When choosing an airway drug absorption model; the main requirement is that it accurately represents the barrier properties of the bronchial epithelium while being relatively straight forward to culture.

5.1.1 AIM OF THE STUDY

The aim of the study was to assess the transport rate/ permeability of theophylline and budesonide across the 16HBE14o- cells when delivered as mono- and co-encapsulated nanoparticles and to compare this to the transport rate/ permeability of the drugs from theophylline and budesonide solutions of equivalent concentrations. This was to test the hypothesis that encapsulating the drugs within nanoparticles would provide sustained release of the drugs. By characterizing the nanoparticles using 16HBE14o- cells, an additional aim was to obtain further information on the health of the cells by determining the effects on the tight junction of the 16HBE14o- cells using a paracellular marker, fluorescein isothiocyanate–dextran (FD4).

5.2 MATERIALS AND METHODS

5.2.1 MATERIALS

96 well-plates, NunclonTM Delta surface, Thermo Scientific, Denmark (143597)

Cell culture TC flasks (with filter cap), 80 cm^2, Thermo Fisher Scientific, Denmark (Lot: 178905)

Transwell® permeable supports (12 mm diameter inserts with 0.4µm pore size, tissue culture treated polycarbonate membrane), Corning Incorporated (18914033)

96-Well Optical-Bottom Plates with Polymer Base (400µL), Nunc™ MicroWell™ Thermo Scientific, UK (165305)

Minimum Essential Medium (MEM) with Earle's Salts (with L-glutamine), GE Healthcare- PAA Laboratories, Austria (E15-825)

DMEM:Ham's F-12 (1:1) cell culture medium (with L-glutamine), GE Healthcare-PAA Laboratories, Austria (E15-813)

Fetal Bovine Serum (FBS) 'Gold' PAA Laboratories GmbH, Germany (A15-151)

Trypsin-EDTA (1x) (0.05% w/v and 0.02% w/v respectively, in PBS), GE Healthcare-PAA Laboratories, (L11-004)

Penicillin (10,000 units/mL) / streptomycin (10,000 µg/mL) (Pen Strep), Gibco® by Life Technologies, USA (15140-122)

UltroserG®, BioSepra SA, France (15950-017)

Type I Bovine Collagen Solution (3.1 mg/mL), Advanced Biomatrix, San Diego, CA (Part #: 5005-B, Lot#: 7264)

Trypan Blue Stain (0.4% w/v), Gibco® by Life technologies, USA (15250-061)

Fluorescein isothiocynate dextran (Average molecular weight: 3000-5000kDa) (FD4), Sigma-Aldrich, UK (FD4)

Phosphate buffer saline (PBS) tablets (pH 7.3±0.2) - Oxoid Ltd, Basingstoke, Hampshire, United Kingdom (BR0014G)

1.5mL Eppendorf tubes, Fisher Scientific, UK

10mL disposable serological pipet, Fisherbrand, Fisher Scientific, USA (Cat: 13-676-10J)

25mL disposable serological pipet, Fisherbrand, Fisher Scientific, USA (Cat: 13-676-10K)

Eppendorf- EasyPet 3 Pipette Gun

Transferpette® S Brand – 200, 100 and 20µL Gilson pipettes

5.2.2 METHODS

5.2.2.1 GENERAL MAINTENANCE OF 16HBE14O- CELLS

The 16HBE14o- cells were maintained as described in Chapter 4, Section 4.2.2.1.

5.2.2.2 THE CULTURE OF 16HBE14O- CELLS ON PERMEABLE SUPPORTS (TRANSWELL'S®)

Before 16HBE14o- cells could be seeded onto the polycarbonate Transwells®, the Transwells® were coated with collagen (Pure Col). Collagen (200 µL) was pipetted directly onto each insert and these were stored at 2-8°C for at least 24 hours. The apical chamber was then washed at least three times with PBS (1 mL).

After rinsing, 16HBE14o- cells were seeded into the apical chamber of the Transwell at a seeding density of 4.3 x 10^5 cells/well in 500µL of cell culture medium (Dulbecco's Modified Eagles Medium (DMEM) (with L-Glutamine): Ham's F12 medium (1:1) (supplemented with 2% v/v Ultroser G® and 1% v/v penicillin/streptomycin)(cell culture medium) and 1500 µL of cell culture medium was added to the basolateral chamber. The cells were grown at 37°C (95% air, 5% CO_2) in a humidified atmosphere. After 24 hours, the cells were brought to an air-liquid interface by carefully removing the medium from the apical chamber. After this, only the cell culture medium in the basolateral chamber was replaced (every two days). Cells were used on the 7^{th} day from seeding. This was carried out under sterile conditions.

5.2.2.3 MEASUREMENT OF TRANS-EPITHELIAL ELECTRICAL RESISTANCE (TER) OF THE 16HBE14O- CELLS

Prior to commencing a transport experiment (on day 7), the TER of the cells was measured using an EVOM Epithelial Tissue Voltohmeter and 'chopstick' electrodes (World Precision Instruments Inc., Sarasota, FL 34240, USA). The cells were removed from the incubator and the cell culture medium was replaced with pre-warmed transport medium (Dulbecco's Modified Eagles Medium (DMEM) (with L-glutamine): Hams F12 medium (1:1)); 1 mL in the apical chamber and 2 mL in the basolateral chamber. After 60 minutes at 37°C in a humidified atmosphere (95% air: 5% CO_2) the TER of the cells was measured in triplicate and an average value of the TER was obtained for each well. The TER of the blank insert was subtracted from the TER of inserts with cells seeded on them.

5.2.2.4 THE TRANSPORT OF THEOPHYLLINE, BUDESONIDE AND FD4 ACROSS 16HBE14O- CELLS.

After TER measurements were taken the transport medium was removed from the cells. The basolateral chamber transport medium was replaced with fresh transport medium (1500 µL) and the transport medium of the apical chamber was replaced with 500 µL of the drug solution/drug-containing nanoparticle suspension also containing FITC-labelled dextran (FD4) (250 µM). Samples (200 µL) were withdrawn from the basolateral chamber at 0, 1, 2, 3, 4, 5, 6 and 24 hours and from the apical chamber at 24 hours. The volume withdrawn from the basolateral chamber was replaced with fresh transport medium (200 µL).Between sampling, the cells were incubated at 37°C in a humidified atmosphere (95% air: 5% CO_2). Each sample was divided into two portions (100 µL each), one portion was analyzed for the drug content using HPLC (Chapter 2, Section 2.2.2.2.5) and the other portion was analyzed for FD4 content using fluorescence spectroscopy. Measurements were carried out in triplicate and an average was obtained for each well.

Test samples were prepared in transport medium containing no supplements. Co- or mono-encapsulated nanoparticle suspensions were applied to the cells at a concentration of 0.6 mg/mL. Drug solutions were applied to the cells at the equivalent concentration of theophylline and budesonide that would have been encapsulated in 0.6 mg nanoparticles. This was calculated to be 117.65 µg/mL and 39.22 µg/mL for theophylline and budesonide, respectively.

5.2.2.5 ANALYSIS OF FD4 CONTENT OF SAMPLES USING FLUORESCENCE SPECTROSCOPY

Calibration standards of FD4 in transport medium were made in the range 250 µM to 1.56 µM. Specific concentrations that were used were: 50 µM, 25 µM, 10 µM, 5 µM, 2.5 µM, 1 µM, 0.5 µM, 0.25 µM, 0.125 µM, 0.0625 µM. The samples (100 µL) and the standard concentration solutions were transferred to flat, clear bottom, black walled 96 well assay and read on a fluorimeter (Gen5 fluorescence Plate reader). An excitation wavelength of 485/20 nm and emission wavelength of 528/20 nm was set, with a gain of 50. The 20 nm refers to the total band pass at each wavelength.

5.2.2.6 DATA ANALYSIS

An apparent permeability coefficient (Papp) (cm/second) was calculated for all the samples for the period between 0-6 hours, 6-24 hours and 0-24 hours based on the cumulative concentration of theophylline, budesonide and FD4 present in the basolateral chamber. The apparent permeability coefficient was calculated as (Equation 5.1):

$$P_{app} = (\frac{dq}{dt})/(A.C_0) \qquad \text{Equation 5.1}$$

Where (dq/dt) (μM/minutes) is the rate of transport of the test sample, A represents the surface area (cm^2) and C_0 (μM) represents the initial concentration of the FD4 applied to the apical chamber.

5.2.2.7 STATISTICAL ANALYSIS

A one way ANOVA was carried out to compare the TER of the cells with the control cells. $P<0.05$, suggests significant differences.

A 2way ANOVA was carried out to compare the effects on the FD4 transport caused by theophylline and budesonide solutions or nanoparticles to the control. The hypothesis is that there is no significant difference to the effects on FD4 transport across the 16HBE14o- cells as the control treated cells. $P<0.05$, suggests significant differences. A Bonferroni post-hoc test was carried out for this analysis.

A Mann Whitney test was carried out to compare the transport of theophylline and budesonide from the solution to the respective nanoparticle sample across the 16HBE14o- cells. $P<0.05$, suggests significant differences.

5.3 RESULTS

5.3.1 THE EFFECT OF THEOPHYLLINE AND BUDESONIDE SOLUTIONS AND NANOPARTICLES ON TER

The TER of inserts without cells and cell-bearing inserts exposed to control, drug solutions and drug containing nanoparticles suspensions was measured before the transport experiment was commenced (Figure 5.1). The TER of all cells used experimentally exceeded 100 Ω cm^2 when measured before the transport study was commenced making them suitable to use. Similar mean TER values were obtained for the cells before experiment to the control cells ($P>0.05$).

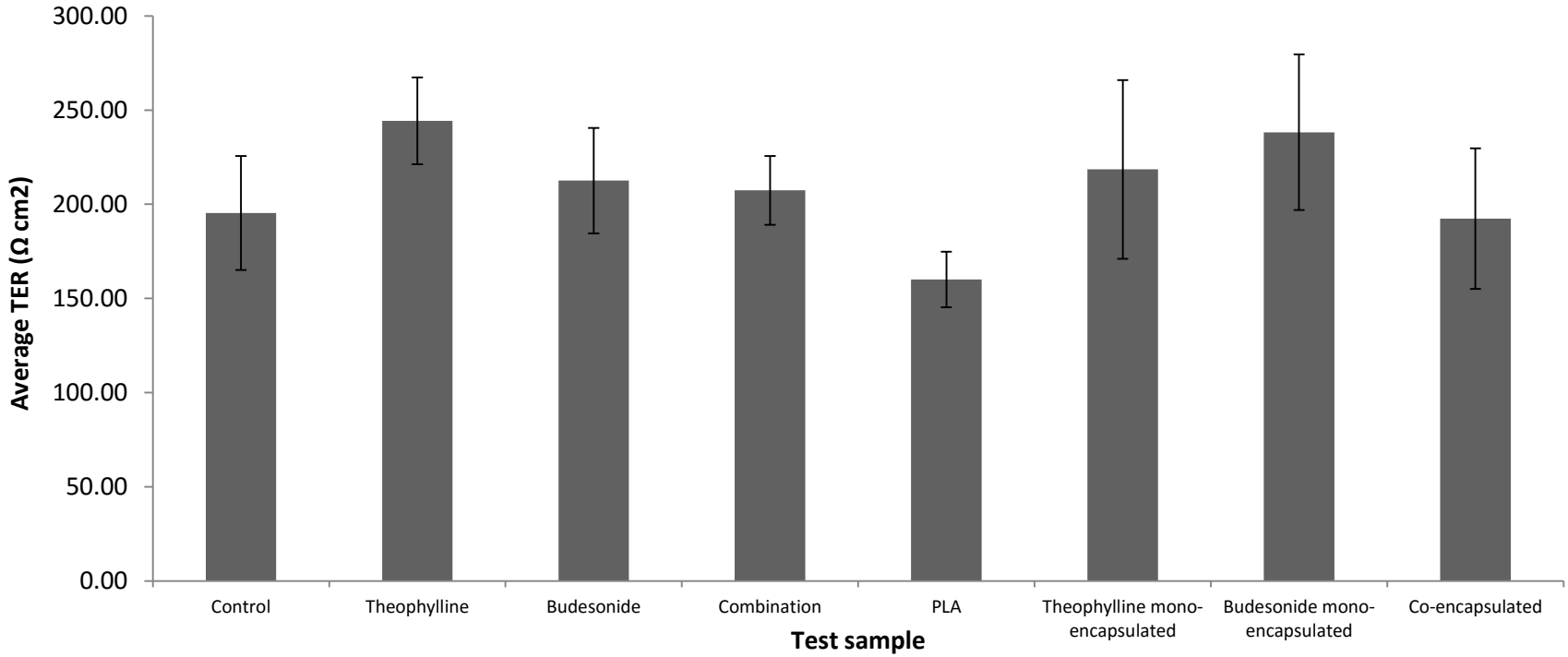

Figure 5.1 The TER of 16HBE14o- cells seeded on collagen-coated Transwell® inserts measured prior to the transport experiment (n=9, mean±SD)

5.3.2 THE EFFECT OF THEOPHYLLINE AND BUDESONIDE SOLUTIONS AND NANOPARTICLES ON FD4 TRANSPORT ACROSS 16HBE14O- CELLS

A calibration graph was plotted for FD4 (prepared in transport medium) in order to determine the concentration of FD4 in the basolateral chambers at various time points (Figure 5.2). A linear region was obtained between 0-5μM with an R^2 of 0.9976. Typical sample concentrations from the transport experiment were in this range.

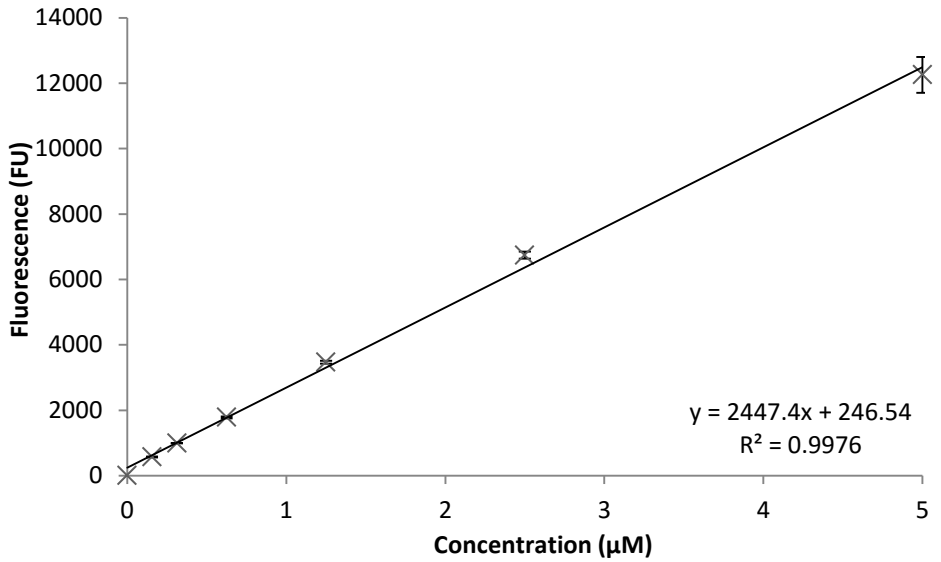

Figure 5.2 Calibration graph of FD4 (n=3, mean±SD)

Over the period of 24 hours, the slope and apparent permeability coefficients of FD4 for cells treated with blank PLA nanoparticles was similar to the control cells (P>0.05). The concentration of FD4 calculated in the basolateral chamber at the end of 24 hours was 2.78 and 2.74 µM for cells treated with blank PLA nanoparticles and control, respectively (Figure 5.3). This was approximately 10 times less than the concentration observed without cells being seeded on the collagen-coated inserts (at 24 hours) showing the cells act as a barrier. The apparent permeability coefficient showing similar transport of FD4 across control cells and cells treated with blank PLA nanoparticles is presented in (Table 5.1). The overall permeability coefficient from 0-24 hours was $0.12x10^{-6}$ cm/seconds for both the conditions.

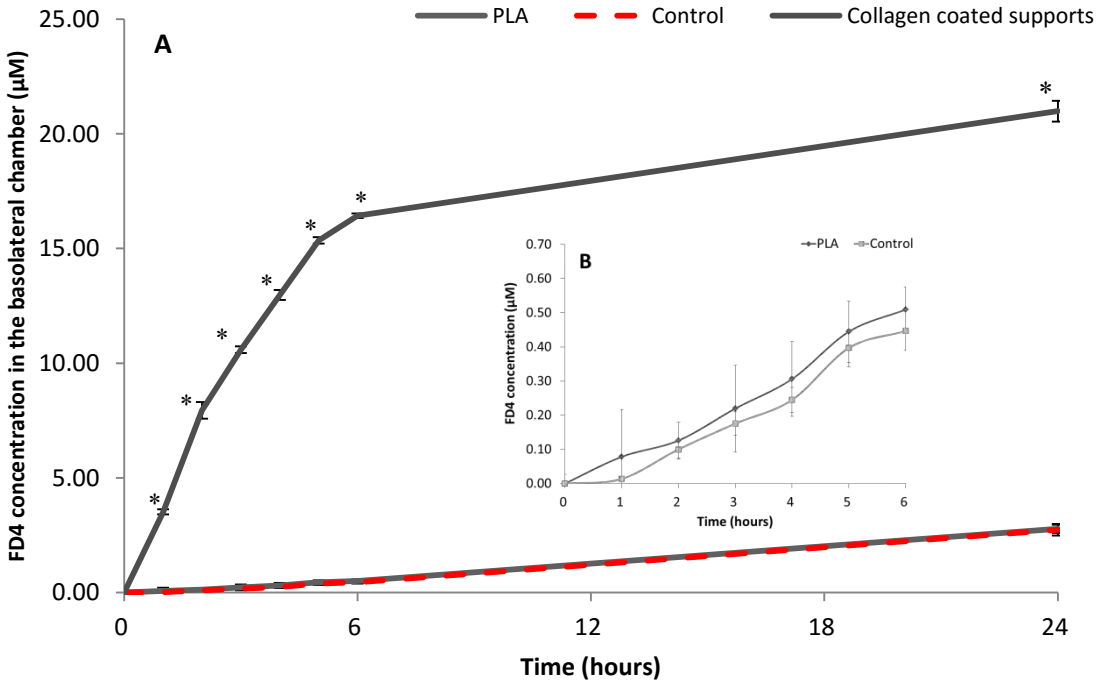

Figure 5.3 (A) The transport of FD4 across collagen-coated inserts without cells, cell-bearing inserts (control cells) and cells treated with the blank PLA nanoparticles (suspended in transport medium), (B) comparison of the transport of FD4 between control cells and cells treated with blank PLA nanoparticles. (mean±SD, n=6 for blank PLA nanoparticles, n=3 for control and collagen-coated supports) (*P<0.05 for FD4 transport in collagen coated supports in comparison to cells treated with blank nanoparticles and control)

Table 5.1 The apparent permeability coefficient of FD4 when transported across the 16HBE14o- cells treated with blank PLA nanoparticles compared to the control and collagen-coated blank inserts (NPs: nanoparticles) (mean±SD, n=6 for blank PLA NP, n=3 for control and collagen-coated supports)(*P<0.05)

Time	0-6 hours	6-24 hours	0-24 hours
	Papp ($x10^{-6}$cm/sec)	Papp ($x10^{-6}$cm/sec)	Papp ($x10^{-6}$cm/sec)
Blank inserts	2.81±0.02*	0.26±0.01*	0.70±0.01*
Cell bearing inserts	0.08±0.01	0.13±0.01	0.12±0.01
Blank PLA NPs	0.09±0.01	0.13±0.00	0.12±0.00

No significant difference was observed in the concentration of FD4 in the basolateral chamber for the 16HBE14o- cells treated with theophylline and/or budesonide and the control (Figure 5.4) (P>0.05). Apparent permeability coefficient values ranged from 0.15-0.19x10^{-6} cm/second (Table 5.2). The change in the apparent permeability co-efficient between 0-6 hours and 6-24 hours was similar for the different test samples (P>0.05).

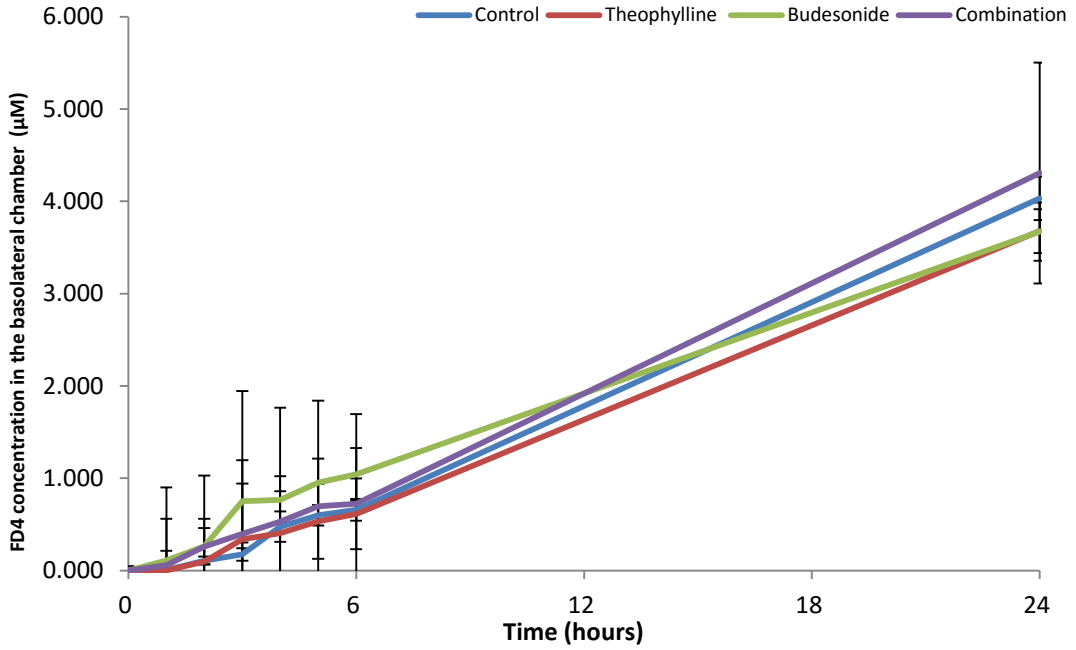

Figure 5.4 The effect of theophylline and budesonide in solution (alone and in combination) (prepared in transport medium) on the transport of FD4 across 16HBE14o- cells in comparison to control cells (n=9, mean±SD) (P>0.05)

Table 5.2 The apparent permeability coefficient of FD4 when transported across the 16HBE14o- cells treated with theophylline and/or budesonide solutions compared to control cells (n=9, mean±SD)

Time	0-6 hours	6-24 hours	0-24 hours
	Papp (x10^{-6}cm/sec)	Papp (x10^{-6}cm/sec)	Papp (x10^{-6}cm/sec)
Control	0.13±0.02	0.19±0.01	0.18±0.01
Theophylline solution	0.12±0.03	0.17±0.01	0.16±0.01
Budesonide solution	0.19±0.01	0.15±0.00	0.15±0.01
Combination solution	0.13±0.14	0.20±0.01	0.19±0.02

The cumulative concentration of FD4 in the basolateral chamber for the 16HBE14o- cells treated with theophylline and budesonide nanoparticles was compared to the control cells (Figure 5.5). There was no significant difference in the cumulative concentration of FD4 in the basolateral chamber of the cells treated with the different test samples. The apparent permeability coefficient for all the test samples and the control was similar, with no significant difference between the control and the nanoparticles. This ranged between 0.14-0.16x10^{-6} cm/second for all the samples (P>0.05). The difference in the apparent permeability co-efficient of FD4 between 0-6 and 6-24 hours was similar (P>0.05) (Table 5.3).

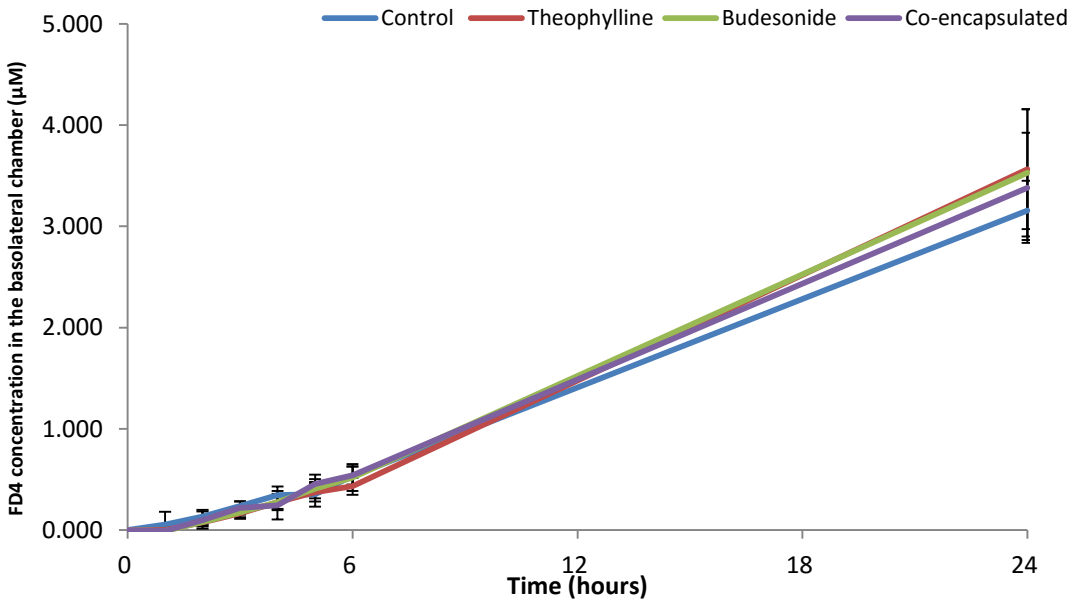

Figure 5.5 The effect of theophylline and budesonide mono- and co-encapsulated nanoparticles (suspended in transport medium) on the transport of FD4 across the 16HBE14o- cells in comparison to the control cells (n=9, mean±SD)(P>0.05)

Table 5.3 The apparent permeability coefficient of FD4 when transported across the 16HBE14o- cells treated with theophylline and budesonide co- and mono-encapsulated nanoparticles compared to the control cells (n=9, mean±SD)

Time	0-6 hours	6-24 hours	0-24 hours
	Papp (x10^{-6}cm/sec)	Papp (x10^{-6}cm/sec)	Papp (x10^{-6}cm/sec)
Control	0.09±0.01	0.15±0.01	0.14±0.01
Theophylline mono-encapsulated	0.08±0.01	0.18±0.03	0.16±0.02
Budesonide mono-encapsulated	0.09±0.02	0.17±0.03	0.16±0.03
Co-encapsulated	0.10±0.02	0.16±0.03	0.15±0.02

5.3.3 COMPARISON OF THE THEOPHYLLINE AND BUDESONIDE TRANSPORT ACROSS THE 16HBE14O- CELLS FROM NANOPARTICLES AND SOLUTIONS OF EQUIVALENT CONCENTRATIONS

The release of theophylline and budesonide from the nanoparticles, and transport across the cells was compared to the transport of drug solutions of equivalent concentrations. This also allowed comparison to results obtained when studying the release profiles of theophylline and budesonide using Franz diffusion cells (Chapter 3).

The transport of theophylline when applied to the cells in solution (both alone and in combination with budesonide) was compared to the transport of theophylline when applied to the cells in the mono- and co-encapsulated nanoparticles (Figure 5.6). The transport rate of theophylline from the two solutions was similar ($P>0.05$) through the period of 24 hours (data not shown). For theophylline in both solutions, approximately 14% was transported across the 16HBE14o- cells. In total approximately 84.64±9.04% (theophylline single solution) and 92.93±5.26% (theophylline mixed solution) was recovered from both, apical and basolateral, chambers. In comparison to the theophylline transported from the solutions, the concentration of theophylline released from the nanoparticles and transported into the basolateral chamber was lower at 24 hours ($P<0.05$). Similar release of theophylline from mono- and co-encapsulated nanoparticles was obtained over the period of 24 hours ($P>0.05$).

The average apparent permeability coefficients for the theophylline solutions from the time period of 6-24 hours show a reduction for all the test samples in comparison to 0-6 hours ($P<0.05$) (Table 5.4). On average, an overall apparent permeability coefficient between 1.16±0.07 and 1.29±0.23x10^{-6} cm/second was obtained for theophylline in the solution (single and mixed, respectively) and between 0.61±0.33 and 0.81±0.23x10^{-6} cm/second for theophylline released from the mono- and co-encapsulated nanoparticles, respectively.

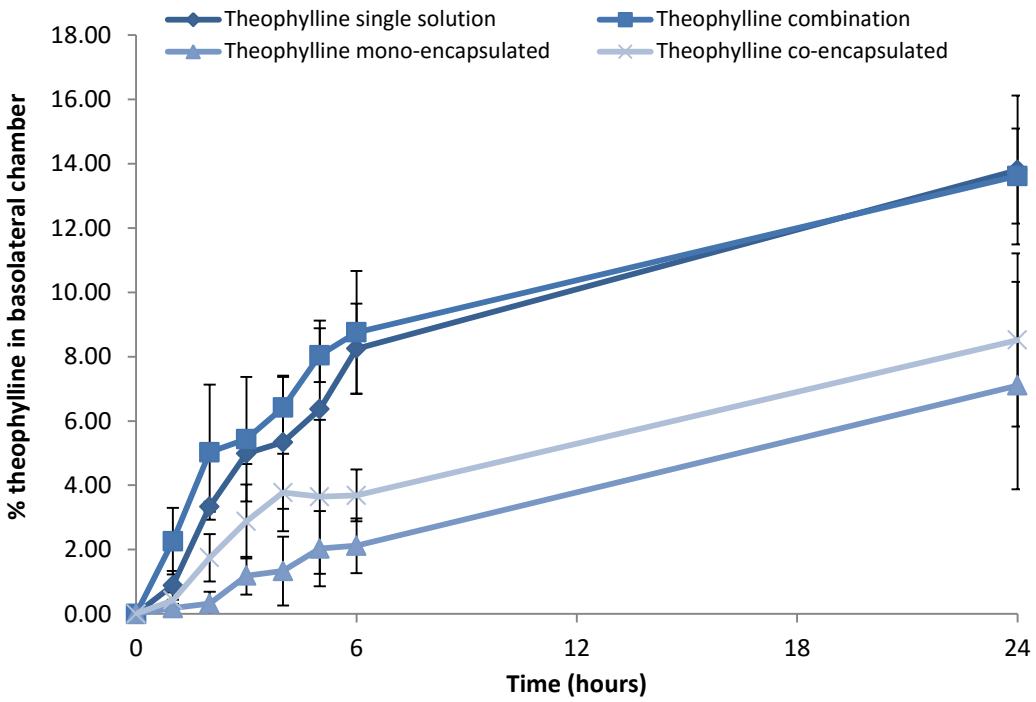

Figure 5.6 The transport of theophylline across the 16HBE14o- cells comparing theophylline solutions with mono- and co-encapsulated nanoparticles (n>3, mean±SD)

Table 5.4 The apparent permeability coefficient of theophylline across the 16HBE14o- cells from solutions and mono- and co-encapsulated nanoparticles (n>3, mean±SD) (*P<0.05 for single and combined counterparts (solutions and nanoparticles)

Time period	0-6 hours	6-24 hours	0-24 hours
	Papp ($x10^{-6}$cm/sec)	Papp ($x10^{-6}$cm/sec)	Papp ($x10^{-6}$cm/sec)
Theophylline solution	3.49±0.51*	0.78±0.13	1.29±0.23
Theophylline and budesonide solution	3.62±0.39*	0.52±0.05	1.16±0.07
Mono-encapsulated theophylline	0.97±0.46	0.54±0.33	0.61±0.33
Co-encapsulated theophylline	1.45±0.74	0.82±0.23	0.81±0.23

The concentration of budesonide in the basolateral chamber when budesonide was applied to the apical surface of the cells in the form of a solution (containing budesonide alone or in combination with theophylline) was compared to the budesonide released from the mono- and co-encapsulated nanoparticles and transported across the 16HBE14o- cells (Figure 5.7). The concentration of budesonide in the basolateral chamber was similar from both solutions ($P>0.05$, except at 2 hours). Less than 2% of the budesonide was transported into the basolateral chamber, however a large variation was observed in the concentration of budesonide at each time point. The overall recovery of budesonide from both, apical and basolateral chambers was calculated to be extremely low and was between 9.84±0.62% and 10.98±1.14% for budesonide in the mixed and single solution, respectively.

The concentration of budesonide released from the nanoparticles and transported across the monolayer into the basolateral chamber was lower than the budesonide from the solutions. The percentage of budesonide in the basolateral chamber was significantly lower from the nanoparticles in comparison to the solutions of budesonide ($P<0.05$ at 24 hours). Budesonide transported and released from the co-encapsulated nanoparticles was higher than the budesonide from the mono-encapsulated nanoparticles ($P<0.05$); which may be as a result of variation in the drug loading during nanoformulation. Less than 1% of the encapsulated budesonide was transported across the 16HBE14o- cells into the basolateral chamber after a period of 24 hours.

Similar to the transport of theophylline, the rates of transport and permeability coefficients obtained for budesonide are lower in the period of 6-24 hours than 0-6 hours (Table 5.5). The reduction in the apparent permeability coefficient was significantly different for the budesonide in a mixed solution ($P<0.05$). The overall apparent permeability coefficient was between 0.12±0.05 and 0.16±0.06 $x10^{-6}$ cm/second for the budesonide present as a single and mixed solution, respectively.

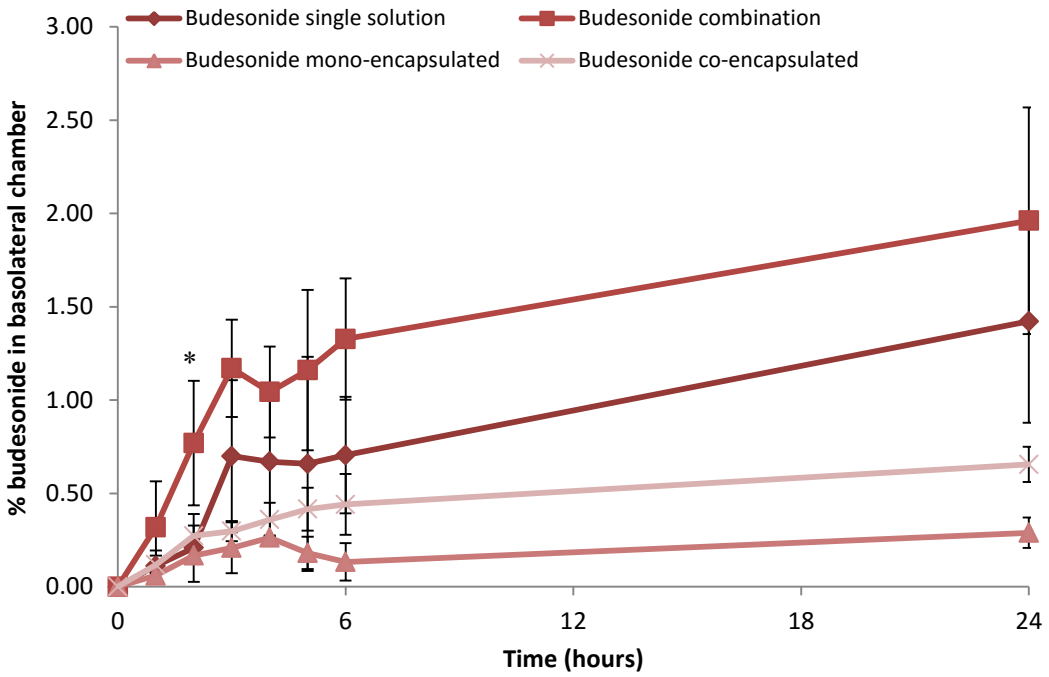

Figure 5.7 The transport of budesonide across the 16HBE14o- cells comparing budesonide solutions with mono- and co-encapsulated nanoparticles (n>3, mean±SD)(*P<0.05 compared to the other test samples).

Table 5.5 The apparent permeability coefficient of budesonide across the 16HBE14o- cells from solutions and mono- and co-encapsulated nanoparticles (n>3, mean±SD)(*P<0.05, for single and combined counterparts (solutions and nanoparticles)

Time period	0-6 hours	6-24 hours	0-24 hours
	Papp ($x10^{-6}$cm/sec)	Papp ($x10^{-6}$cm/sec)	Papp ($x10^{-6}$cm/sec)
Budesonide solution	0.19±0.10	0.10±0.03	0.12±0.05
Budesonide and budesonide solution	0.62±0.17*	0.06±0.02	0.16±0.06
Mono-encapsulated budesonide	0.03±0.03	0.01±0.00	0.02±0.01
Co-encapsulated budesonide	0.15±0.04*	0.02±0.00	0.05±0.00

5.4 DISCUSSION

5.4.1 THE EFFECT OF THEOPHYLLINE AND BUDESONIDE SOLUTIONS AND NANOPARTICLES ON TER

The 16HBE14o- cells were selected for the current study due to the ability of the cells to establish well-defined tight-junctions, which are able to limit the transport of paracellular markers [394]. Intact cell-cell tight junctions are a critical component of any cultured cell absorption model to mimic the *in vivo* conditions which allow studying the transport of the drug [394].

From previous studies the 16HBE14o- cells are best used from day 5 to 7 after seeding on the inserts. In this study, 7 days was kept consistent as there is known to be an effect on the TER of the cells after this time [421]. It is noted that the longer duration the cells present in culture can affect the function of the cells [424]. The air-liquid interface has a large influence on the TER and permeability of the cells to paracellular markers such as mannitol or FITC [392]. Several other factors have been noted to affect the TER such as passage number, surface they are cultured on, medium and seeding density. A seeding density of 10^5 cells/cm^2 is reported to be a typical seeding density [392]. Too low seeding densities (10^3 cells/cm^2) resulted in an incomplete formation of the monolayer [393]. For this study, a seeding density of 4.3×10^5 cells/well was selected.

Measurement of the TER of the cells gives an indication of the health of the cells and the integrity of the tight junctions formed. Overall, the TER values obtained for this study ranged between 100-200 Ωcm^2 for all the cells treated with all the different test solutions and suspensions. Some previous studies carried out using 16HBE14o- cells reported higher TER values than those measured in this study; between 260-360 Ωcm^2, but the cells used in these studies had a lower passage number (33-34). The passage number here was over 69. The TER values of the current study suggest the cells were suitable to use for the transport study experiments. A study on salmeterol absorption characteristics across the 16HBE14o- cells reported similar TER values of between 100-300 Ωcm^2 ; in a review by Lansley (1993), TER values of this range have been described [431, 432]. Higher TER values for 16HBE14o- cells were reported by Westmoreland et al (1999) in a the study of respiratory toxins (approximately 500 Ωcm^2) (passage number not specified) [382]. TER values of greater than 500 Ω cm^2 were also obtained for 16HBE14o- cells by Ahsan et al (2003), suggesting formation of a confluent monolayer [394].

The TER of 16HBE14o- cells has been reported to peak during culture period up to 1000-1200 Ω cm^2 before it reduced [417]. The TER was reduced to 300 Ω cm^2 but in this study the 16HBE14o- cells did not form an organized, differentiated layer. [417]. The TER dropped during day 6-8 after reaching a maximum of 700 Ω cm^2. Similar TER values were obtained for cells at the period of 6 and 7 days and were approximately 250 Ω cm^2 [393, 425, 433].

5.4.2 THE EFFECT OF THEOPHYLLINE AND BUDESONIDE SOLUTIONS AND NANOPARTICLES ON FD4 TRANSPORT ACROSS 16HBE14O- CELLS

The collagen-coated supports, which contain no cells, show the greatest cumulative concentration of FD4 in the basolateral chamber in comparison to the control and the cells treated with nanoparticles and drug solutions. This is expected as there is no cellular barrier to limit the transport of FD4 from the apical to basolateral chamber. With cells seeded on the inserts, the lower apparent permeability coefficients highlight the rate-limiting barrier provided as a result of the cells.

To confirm that drug solutions and nanoparticles had no significant effect on the health and barrier function of the 16HBE14o- cells, the effect on the permeability of FD4 from apical to basolateral chamber was studied. An effect on the tight junctions of the 16HBE14o- cells would result in a change in the permeability of the paracellular marker, FD4, over the period of the experiment. The use of a fluorescent marker along with measurement of the TERs is recommended to confirm whether there is a change in the coherence of the tight junctions of the cells in the study [267, 423].

The rate of transport of FD4 across the cells treated with nanoparticles and drug solutions was not significantly different to the control cells over the period of 24 hours, suggesting that the drugs and nanoparticles did not affect the tight junctions and health of the cells at the concentrations used and the time scale of the study carried out. No additional effect of the drug was observed when comparing the drug encapsulated and blank nanoparticles.

In the current study the nanoparticles synthesized had a zeta potential of approximately -10mV and did not affect the permeability of the cells. This result agrees with that of Salomon and Ehrhardt (2011) in which nanoparticles studied at concentrations ranging from 0.025 to 0.1 mg/mL showed little interaction of the negatively charged nanoparticles with the cell membrane which did not affect the function of the cell membrane nor integrity.

Nanoparticles synthesized with biodegradable polymers for different applications have been studied using various cell lines. Nanoparticles synthesized in the current study are

negatively-charged as a result of the carboxylic acid groups on PLA present on the outer surface of the nanoparticles, which was confirmed when assessing the zeta potential of the nanoparticles. These particles are present in submicron range (approximately 200 nm). Although the uptake of the nanoparticles has not been studied here, for other nanomaterials such as PEG/PLA nanoparticles which are in the size range of 150-200 nm and also negatively-charged, it has been suggested that translocation occurs across the epithelial barriers [422, 434]. It was suggested that paracellular transport of nanoparticles which are greater than 20 nm was not feasible because intercellular spaces open up to 15 nm only [422, 435]. This suggests that, in the current study, the nanoparticles (average particle size range approximately 200 nm) do not cross the cell barrier and that only the drugs are able to cross the cells as a result of the small gap between the intracellular spaces.

Previous studies on the translocation of nanoparticles across cells also noted the use of an appropriate pore size of the cell supports. While the most common pore size is 0.4 μm (used in the current study); this is thought to be unsuitable to allow translocation of the nanoparticles. A study used 1.0 μm pore supports for particles that were present in a size range of 200-300 nm [372].

Other studies on nanoparticles included polystyrene nanoparticles present in a size of 50 nm and 100 nm. In order to study their transport and uptake across Calu-3 cells, these nanoparticles were fluorescently-tagged but a setup on Transwell® inserts using Calu-3 cells was carried out. The final concentration used was 0.4 mg/mL and showed limited effect on the tight junctions in unmodified nanoparticles and a greater uptake of the (unmodified) nanoparticles which were below 50 nm [436].

Cell uptake of negatively-charged nanoparticles would also be limited due to the negative charge on the cell membranes however a study carried out on PLGA nanoparticles reported that the cellular uptake of the negatively-charged nanoparticles would be high due to the strong, non-specific interaction with the positively-charged sites on the plasma membrane causing bending of the membrane favoring the formation of endocytosis invaginations [297, 380, 437]. The mechanisms that are thought to allow uptake of the nanoparticles in the cells include phagocytosis and pinocytosis. It has been suggested by Madlova et al (2009), that nanoparticles are readily retained inside the cell and don't translocate easily [372].

The effect of positively-charged chitosan nanoparticles has been a topic of great interest. Research on nanomaterials has shown interaction between positively-charged substances and the negatively-charged membrane. The positively-charged nanoparticles have also shown the highest cytotoxicity; with minimal cell death induced by negatively-charged nanoparticles, which suggests an effect on cell membrane integrity [370]. In several studies,

this positive charge of chitosan, conferred by the amino groups, interacts with the negative sialic group on the mucus membranes opening the tight junctions [381, 422, 423, 438].

Various methods have been applied to study the effects of uptake and translocation of biodegradable polymers. The current study used FD4, a fluorescent, paracellular marker to indicate if there was any effect on the tight junctions of the cells; other studies have synthesized fluorescence-tagged nanoparticles to study their effect on 16HBE14o- cells at different concentrations in order to study the uptake and translocation [406].

To understand the uptake of polycaprolactone (PCL) nanoparticles instead of using the drugs, FITC encapsulated into the nanoparticles. This approach could have been taken with PLA nanoparticles synthesized in the current study to study the uptake to or follow translocation, but nanoparticles encapsulating a compound other than the one of interest can potentially possess different physicochemical properties such as the loading efficiency, size, surface charge and release potential. Therefore, if a model compound such as FITC is encapsulated in nanoparticles to study the uptake of the drugs, the additional effects of the drugs may not be fully understood [439]. A similar method was chosen for PLGA-PEG nanoparticles (where a fluorescent marker was used instead of drug) [440]. Polystyrene nanobeads have also been assessed which contained a fluorescent tag. The size of the nanobeads was 51nm; and these were seen to be translocated through the co-culture model developed by Dekali et al (2014) [441].

The current study suggests that that although FD4 will be transported paracellularly, due to the size of the nanoparticles, only the FD4 will be transported across the cell layer or as suggested, nanoparticles may, by certain processes, be taken up by the cell. If the nanoparticles had an effect on the tight junctions of the 16HBE14o- cells, then a change in the concentration of FD4 accumulated in the basolateral chamber would have been seen. No such change was observed that was considered a significant effect caused by treatment of the cells with nanoparticles or drugs. However, to understand the uptake of the nanoparticles in the cells, it would require tagging the nanoparticles with a fluorescent marker or encapsulating the fluorescent marker in the nanoparticles instead of the drugs; however both these changes can potentially alter the properties of the nanoparticles. Based on the studies carried out, it suggests that, as a result of the tight junctions and due to the negative charge of the nanoparticles and submicron particle size, only drug was transported across the cell layers in the current study.

5.4.3 COMPARISON OF THE THEOPHYLLINE AND BUDESONIDE TRANSPORT ACROSS THE 16HBE14O- CELLS FROM NANOPARTICLES AND SOLUTIONS OF EQUIVALENT CONCENTRATIONS

Along with FD4, the drug concentration in the basolateral chamber was also determined. The release and transport of the drugs from the nanoparticles was compared to theophylline and budesonide standard solutions applied at equivalent concentrations. By determining the release profiles and transport profiles, it enables an understanding of the potential mechanisms the two drugs in the current study use to cross the cell monolayer. It is extremely difficult and challenging to determine the concentration of drug reached in the lung fluid after inhalation [335, 427].

Both lipophilic and hydrophilic compounds are absorbed by passive diffusion the former transcellularly and latter paracellularly; these processes are reviewed by Haghi et al (2014) [335]. For compounds with a logP of less than 1.9, a similar permeability to mannitol (used as a paracellular marker) was obtained. Compounds with a logP of greater than 2 showed a high permeability coefficient ($20x10^{-6}$ cm/second)[393].

The concentration of theophylline in the basolateral chamber of cells treated with drug solutions is greater than that of cells treated with nanoparticles. Approximately 14% of theophylline is transported across to the basolateral chamber from the solutions prepared. The lower concentration of theophylline in the basolateral chamber for cells treated with nanoparticles (and lower apparent permeability coefficients) can suggest that the rate limiting step in the process was the release of the drug from the nanoparticles and not the transport across the cell monolayer.

Theophylline (logP: -0.02) and FD4 (logP: -2.0) are hydrophilic molecules and as a result transport may be similar by the paracellular route [8]. Theophylline has been studied by Zhu et al (2015) using Calu-3 cells where approximately 97.9% of the drug deposited was transported across. This study however, did not mention any potential transport mechanisms [413]. Caffeine is similar in structure to theophylline and has logP of -0.07, which is similar to theophylline [442]. Due to limited information available on the transport of theophylline across a cell monolayer, the information on the transport of caffeine was studied. In a study using a 3D model of the respiratory epithelium, it was reported that the transport of caffeine was by passive, transcellular, transport [428]. McCall also reported the transport of caffeine to be by simple diffusion [443]. Extremely high apparent permeability coefficients have been reported for the transport of caffeine (approximately $20x10^{-6}$ cm/second) [428, 444]. High

apparent permeability coefficients for theophylline are obtained in the current study in the time period of 0-6 hours suggestive of a passive, transcellular mechanism, similar to caffeine.

In a study by Mukherjee et al (2012), it was suggested that the maximum dose of bronchodilators was 5 μM and 100 μM for corticosteroids [427]. The concentration was reduced to 50 μM for corticosteroids due to the limited solubility [427]. These concentrations have been reviewed by Haghi et al (2014) [335]. These concentrations are similar to what is used in this study (for budesonide): but further increasing the concentration of the drug would, as described, be limited as a result of the poor solubility of budesonide in the cell culture medium.

The transport of budesonide across the 16HBE14o- cells was more rapid from the solutions than the budesonide released from the nanoparticles, consistent with the results obtained for theophylline. Similarly, this is thought to be due to transport of budesonide being dependent on release of budesonide from the nanoparticles (rate limiting step). By being present in an un-favorable aqueous environment, the release of budesonide from mono- and co-encapsulated nanoparticles may be further reduced and was less than 1% after a period of 24 hours.

Corticosteroids are reported to be transported by use of the transporter protein, P-glycoprotein and compete with passive diffusion. The high lipophilicity can lead to an increased uptake and retention leading to an increased effect of glucocorticoids in the airways [445]. The transport of budesonide across epithelial cells has been studied and reviewed extensively.

Budesonide is moderately lipophilic (logP: 2.17) [445]. In airway tissue, budesonide becomes esterified and conjugated to fatty acids intracellularly resulting in retention of the compound in the cells and can result in apical release for over a period of 10 hours [335, 392, 445, 446]. The conjugation of budesonide resulted in creating an intracellular depot. The conjugated form of budesonide is highly lipophilic (2-4 greater lipophilicity) [445, 447]. Approximately 50% of the inhaled budesonide is esterified at C21 hydroxyl group of budesonide [447, 448]. The prolonged airway retention is as a result of the increased selectivity [445] and occurs ten times greater in the airways than peripheral tissues [449]. The conjugate itself is inactive in form [446]. Upon replacement of the medium *in vitro* or presence of lipases, the conjugation is reversed and the non-conjugated form of the steroid is released [446, 447]; this is a rate-limiting step [450]. When the concentration of budesonide is reduced, the ester form is reversed back to the active drug [449]. The prolonged action of budesonide in the airways as a result of the esterification suggests that budesonide is as effective as or more effective than other inhaled

corticosteroids [450]. The process of conjugation is selective to budesonide as it is dependent on the structure [451].

In a study by Borchard et al (2002) on budesonide and fluticasone transport across Calu-3 cells, showed gradual release over the period of 10 hours; these results are similar to what is obtained in the current study [452]. This study suggested concentration-dependent transport of budesonide when using Calu-3 cells. In order to determine the intracellular fatty acid conjugation of budesonide, which results in a gradual release of active budesonide, the Calu-3 cells were incubated for 2 hours with 30μM of budesonide and washed on both apical and basolateral side. After 10 hours, it was noted that 68.5% of the initial concentration was present on the apical chamber, but only 14.2% present on the basolateral chamber. In the current study, an overall recovery of only approximately 10% of budesonide (total from both apical and basolateral chambers) was obtained, which can potentially suggest intracellular conversion of budesonide to the inactive form; however to confirm this, further work would be required to be carried out. Higher apparent permeability coefficients (approximately $5x10^{-6}$ cm/second) have been reported for budesonide than the current study and differences maybe be as a result of a different cell line being used in the current study [452, 453]. Additionally, a higher concentration of the budesonide used in the current study may potentially result in a greater conversion of the drug to the inactive form resulting in less active drug available/transported across the cells.

However, in a study by Manford et al (2005) using 16HBE14o- cells, a higher apparent permeability coefficient for budesonide ($10x10^{-6}$ cm/second) than that obtained in the current study was reported [425]. The use of DMSO (0.1%v/v) in the test solutions was suggested to affect the integrity of the tight junctions and which suggests a more rapid transport of the drug and drop in the initial TERs of the cells [425].

The current study on the drug transport of theophylline and budesonide is mainly limited due to a single concentration of nanoparticles (0.6 mg/mL) being used for analysis. As discussed, there have been studies reported where a single concentration has been used to understand the effect on the health of the cells. A study carried out on chitosan-PLGA nanoparticles was studied a single concentration of 0.9 mg/mL of the nanoparticles [297]. The concentration of test samples selected by other studies was based on the information obtained from the cytotoxic assessment of the compounds being analyzed similar to the current study [381, 422]. Other studies carried out have based the concentration of drugs used on the therapeutic doses of the drugs in consideration [386]. The disadvantage of using higher concentrations of drugs includes an effect on cell. As the current study allows understanding of the transport of theophylline and budesonide across 16HBE14o- cells, further information

can be obtained by developing a suitable method to study the uptake of the nanoparticles and the effects intracellularly.

A further limitation to the current study was the sensitivity of the analytical technique (HPLC) used. The use of HPLC resulted in some peaks not being detected and therefore resulting in large variations in the results and therefore in order to improve the method and analysis, it would be important to use a more sensitive technique. Low recovery values of budesonide can also suggest adsorption of budesonide to the plastics of the wells resulting loss of the drug, which can potentially lead to inaccurate calculations of the apparent permeability coefficient as a result of the lower concentration than what is used in the actual calculations.

5.5 CONCLUSIONS

The main aim of the study was to assess the transport of theophylline and budesonide across the 16HBE14o- cells when delivered as mono- and co-encapsulated nanoparticles and compare this to drug solutions of equivalent encapsulated concentrations. The results were able to show successful sustained released of the drug from nanoparticles represented by a lower drug concentration in the basolateral chamber of cells treated with nanoparticles in comparison to the solutions. Budesonide showed a lower apparent permeability coefficient and was suggested from previous results that this may potentially be as a result of the intracellular esterification and fatty acid conjugation on budesonide or due to binding of the budesonide to the plastic of the Transwells® which can lead to a low overall recovery.

An additional aim was to obtain further information on the health of the cells by determining any changes in the transport of a paracellular marker, FD4. Treatment of the 16HBE14o- cells with theophylline and budesonide present as solutions or released from the nanoparticles showed no significant effect on the tight junctions compared to the control which was measured by similar cumulative concentration of FD4 in the basolateral chamber.

CHAPTER 6 *IN VITRO* DEPOSITION OF THEOPHYLLINE AND BUDESONIDE MONO- AND CO- ENCAPSULATED PLA NANOPARTICLES

6.1 INTRODUCTION

Pulmonary administration of drugs to treat local diseases and the challenges of pulmonary drug delivery has been discussed in Chapter 1 [25, 235, 253, 454-459]. There are three principal formulations that are used to deliver drugs to the lungs which include pressurized metered dose inhalers (pMDIs), nebulizers and dry powder inhalers (DPIs), which are all equally efficacious if used correctly [25]. All the devices have been discussed in detail in Chapter 1. Formulation factors are tightly controlled to ensure that a reproducible and efficient dose is obtained after actuation.

Nebulizers are very efficient in creating mists of extremely fine droplets of active containing particles with good pulmonary deposition [460]. The types of nebulizers include jet nebulizers, ultrasonic nebulizers and vibrating mesh nebulizers [25, 41]. Jet nebulizers use a compressed source of gas and ultrasonic nebulizers make use of a piezo-electric crystal vibrating at a high frequency, which allows production of inhalable aerosol [27, 40]. Vibrating mesh nebulizers also reduce the droplet size by the use of apertures in the device and come in an active and passive form. Advantages of using nebulizers are that a breathing effort is not required and the patient can continue with a normal breathing cycle while the dose is being nebulized. The main disadvantages of using nebulizers include the time required to administer the drugs and that they are generally large, and not portable [4, 25, 289, 457]. Formulations made for nebulization should be sterile products and could require the use of excipients such as surfactants e.g. polysorbates, sorbitans or use of preservatives such as parabens or even salts (NaCl) for optimum osmolality [11, 457].

Significant research and effort is taken to develop and improve DPIs and aiming to improve the efficiency of drug delivery [461]. DPIs are seen to be a more favorable choice than pMDIs mainly due to the long term stability in their solid state and bioavailability of the drugs in comparison to drugs present in a solution [235]. DPIs have also shown better patient compliance due to being breath-actuated in comparison to the other formulations [460, 462]. Devices currently available are portable, propellant-free, easy to operate and low cost [289, 455, 463-466]. They are potentially available for a wider range of drugs than pMDIs as a result of

their increased stability [460]. However, some disadvantages include loss of drug if exhaled into the device, dependence on the inspiratory effort put in by the patients, strict formulation characterization and optimization [25]. Deposition of drugs from DPI formulations depends on the actual powder formulation, the device, technique adopted by patient and the metering system [11, 467-469].

DPIs mainly consist of adhesive 'ordered' mixtures of the active ingredient which is adhered to the surface of a coarse carrier particle to form binary formulations [11, 455, 457, 460, 461, 463, 467, 470-473]. In general, the active particles will detach from the coarse carrier particles by overcoming the inter-particulate (adhesion) forces in order to deposit at the target site; inefficient detachment results in inefficient delivery of the drug [11, 289, 455, 457]. It is important that the DPI dose delivered is reproducible and consistent, obtaining a high pulmonary deposition. This can be achieved by carefully selecting carriers as aerosolization efficiency is highly dependent on carrier characteristics [455, 474]. Carrier particles help improve the drug particle flowability and improve the dosing accuracy by reducing the variation between drug formulations alone [455]. Particle size range for the carriers vary and can vary from 50-100μm [457]. Carrier molecules act as a bulking agent, allowing handling, dispensing and metering of the dose easier, potentially improving the deposition profile [455, 471, 475]. Ideal properties of carrier particles include physicochemical stability, inert, compatibility with the active ingredient, economical and biocompatible [457, 463, 476]. The use of computational fluid dynamics (CFD) suggest that complete dispersion of the powder never occurs but is more important to obtain flow rates and turbulence as a result to allow maximum dispersion [477]. Variation in the formulation can lead to changes in the deposition profile of the product and affect its overall efficiency [478].

Lactose is a commonly used excipient and a carrier used in preparing DPI formulations [455, 461]. Lactose is present in two isomeric forms as α- or β- lactose monohydrate as well as in an amorphous form. Lactose has a well investigated toxicity profile, good physical and chemical stability, high compatibility, is readily available and economical [455]. Properties of lactose that are considered when selecting a grade include morphology and surface chemistry [233, 472]. The roughness of the surface of the lactose carrier particles and formation of cavities in which drug particles can adhere to can affect uniformity of dose and deposition as these can play a role in the attachment and detachment of active and carrier particles [289, 460, 470].

There has been a large debate on the effect of the addition of 'fines' to the mixtures of actives and lactose particles, and their role in increasing the fine particle fraction (FPF) [471]. 'Fines' are small particles which act as spacer or flow enhancers instead of fulfilling a role

as a carrier particle and may have a role in minimizing agglomeration [470]. 'Fines' are classified as particles between a size range of 0.1-2μm and 'ultrafines' as <0.1μm [5]. The particle size distribution of the carrier particles can lead to presence of 'fines', which can fit into voids encouraging packing of the particles. Addition of other ternary components such as magnesium stearate also help reduce the cohesive forces and improve flow by binding to sites on the surface of the carrier particles to which active ingredients may not adhere to [455, 460]. Coating of carrier excipients has also been studied as an option to improve the aerosol performance of products [479]. In some studies, the drug itself was micronized in order to be suitable for delivery to the lungs. Problems of dispersion and uniformity of content can be alleviated by adapting this technique [460].

The main aim of drug delivery using a DPI is that the dose delivered is consistent and reliable therefore requiring sufficient energy to overcome inter-particulate forces and de-agglomeration of the mixture to deliver the respirable fraction [233]. Less than 20% of the emitted dose is present as a respirable fraction due to poor aerolization efficiencies of the DPI device [233].

Particles can resist flow due to solid-solid particle friction [480]. Cohesion between lactose particles can occur due to van der Waals (VdWs) forces [457, 481]. Other forces that must be overcome in order to detach the active and the carrier particles include electrostatic charges, which are due to frictional movement of the particles called 'triboelectric charging' [457, 480] and capillary forces [11]. Ternary compounds added to the mixture can affect the electrostatic charges and even affect the interaction between the drug, carrier and surrounding environment [460]. For the efficient delivery of the drug and reproducibility of the dose, it is important to overcome the cohesive and adhesive forces but also important to achieve a balance between cohesive and adhesive forces in the powder mixture [289, 460, 467, 474, 482, 483]. Decrease in particle size and increase in surface area leads to increased cohesion. This is further affected by changes in shape, surface roughness (irregular surfaces lead to more contact points, decreasing powder fluidity), density and porosity [463]. It is important to maximize the fraction of the powder that is emitted upon inhalation by the patient which is of a respirable size [482].

Several methods are applied in order to formulate dry powders suitable for pulmonary delivery including spray drying. Spray drying can be carried out alone with the drug particles or in combination with the carrier particles [460].Spray drying allows particles to be present in a narrow size distribution with a higher purity, compared to other techniques such as jet milling [462, 484-486]. However, not all particles can be treated in the high temperatures used in spray drying. Main disadvantage is the production of low yield of samples [462].

Lactose can also be prepared by milling or sieving; this process can also be used for the active drug if used alone. Milling produces more 'fines' increasing the FPF but in comparison to this method, a greater emitted dose is produced with sieving technique [480]. The particle size obtained when the milling technique is applied is more varied. Another method, air jet milling, produces particles within a respiratory range, but there is limited control of physicochemical characteristics, such as particle size, using this technique. Further to this, air jet milling can produce particles with an electrostatic force resulting in increased cohesiveness and poor flow [460]. Supercritical fluid precipitations (SCF) also aid in the production of uniform particles in terms of morphology, crystallinity, size distribution and produce a less electrostatic charge [474].

Along with formulation characteristics, the role of the device chosen for DPIs is equally important [460, 463, 474]. Devices are available as single unit or multiple unit dosing devices. Currently all devices are 'passive' devices [474]. Single unit devices require patient's ability to place capsule in the device, pierce it successfully and inhale the drug. Multiple dosing devices have an advantage of less contamination and less technique required from patients (who might be less able to insert/pierce capsules successfully). Devices also have a role in the deagglomeration of particles, which also relate to the adhesive and cohesive forces between the drug and the carrier [483]. Device factors that can play a role in deagglomeration include grid structure, mouth piece length, air-inlet size and resistance of the device [487]. Factors such as humidity and hygroscopicity of the formulations also need to be considered, as it can lead to instability and alteration in the deposition profile due to uptake of water [460, 463]. Devices chosen should be sealed and prevent moisture uptake by the formulation during storage [474].

In general, no matter how good the DPI design and powder formulation characteristics are the efficacy depends on patient compliance and training to use the device correctly. Patient education is critical and plays a large role in the successful treatment of asthma and COPD [23, 36, 112, 474].

Measurement of aerosol efficiency, or deposition, can be measured using cascade impactors or impingers. Each stage contains a single or a series of nozzles or jets through which the aerosolized sample laden air is drawn directing airborne particles towards the surface of collection plate but impacting on a particular stage depending on the aerodynamic diameter. The particles stay entrained in the airstream until it impacts on the particular stage. The stages in the cascade impactor are assembled together in a stack of decreasing particle size. As the diameter decreases, the air velocity increases and finer particles are collected through each stage [455, 463, 471]. Fine particle dose (FPD) is calculated in relation to the total emitted

dose that has deposited in the respiratory region. Fine particle fraction (FPF) is a percentage of the FPD [11, 456, 457, 477]. Other calculations also include Mass Median aerodynamic diameter (MMAD) which relates the particle aerodynamic diameter to the diameter of a sphere of a unit density that would have the same settling velocity as the particle in consideration [11, 455, 457]. In this study, the multi-stage liquid impinger (Figure 6.1) was used to investigate at which stage the formulated nanoparticles would deposit.

6.1.1 AIM OF THE STUDY

The aim of this portion of the study was to investigate the *in vitro* deposition profiles of the theophylline and budesonide co- and mono-encapsulated nanoparticles using different inhaler formulations. The two most suitable formulations to administer nanoparticles successfully are thought to be a nebulized suspension of the nanoparticles and dry powder formulations using lactose as a carrier in the mixture. In order to formulate dry powder formulations, four different grades of commercial lactose will be selected and characterized to understand differences in the deposition profiles and which lactose grade provides improved deposition. It is hypothesized that the deposition of theophylline and budesonide nanoparticles from dry powder inhalers will depend on the characteristics of the lactose used.

6.2 MATERIALS AND METHODS

6.2.1 MATERIALS

Copley Scientific Glass (Twin) Stage Impinger, Copley Scientific Ltd, Nottingham, UK

Copley Scientific Multi stage liquid impinger (aluminum type), Copley Scientific Ltd, Nottingham, UK

Copley High Capacity Vacuum Pump (HCP5), Copley Scientific Ltd, Nottingham, UK

Copley Flow meter (Model: DFM3), Copley Scientific Ltd, Nottingham, UK

Mouthpiece adapter for nebulizer, Copley Scientific, UK

Mouthpiece adapter for Cyclohaler®, Copley Scientific, UK

Omron COMP AIR compressor nebulizer (Model: NE-C28P), OMRON HEALTHCARE UK LTD, Milton Keynes, UK

Cyclohaler/Aerolizer® device,

18.2MOhms deionized water

Methanol (HPLC grade), Fisher Scientific, UK: Lot: 1493729 (Code: M/4056/17)

Filter paper, Fisherbrand QL 100, 70mm (diameter), Fisher Scientific, UK (Code: FB59017)

Centrifuge tubes (30 mL), Fisher Scientific, UK

Size 3 hard gelatin capsules, Capsugel, UK

Lactohale® 201, DFE Pharma, Germany (Product code: 585791)

Lactohale® 300, DFE Pharma, Germany (Product code: 585814)

Respitose® ML001, DFE Pharma, Germany (Lot: 10759897)

Respitose® ML006, DFE Pharma, Germany (Lot: 10767946)

SEM Specimen Stubs (aluminium), 12.5mm diameter, 3.2 x 6mm pin, AGAR Scientific, United Kingdom (AGG301F)

Carbon adhesive double sided disc/tape (Leit Adhesive Carbon Tabs) for SEM stubs, AGAR Scientific, United Kingdom (AGG3347N)

2mL crimp top clear Chromacol Vials- Autosampler Vials crimped (2CV-P220)(Lot: 70734807114), Thermoscientific, Germany

Chromacol 11mm crimp cap- Rubber/ PTFE Type 7 Rubber Lot 9132010752

6.2.2 METHODS

6.2.2.1 ASSESSING THE DEPOSITION OF THEOPHYLLINE AND BUDESONIDE FROM A NEBULIZED SUSPENSION OF NANOPARTICLES USING A MULTI STAGE LIQUID IMPINGER (MSLI)

6.2.2.1.1 Preparation of the nanoparticle suspension

To deliver the nanoparticles in a nebulized formulation, the nanoparticles were suspended in 18.2MOhms deionized water. The nanoparticles were weighed accurately (5 mg) and suspended in 5mL of 18.2MOhms deionized water and sonicated for 60 seconds. The suspension was transferred into the chamber of the nebulizer and the weight of the chamber plus suspension was recorded.

6.2.2.1.2 Set up of the MSLI for assessment of nebulizer suspension

A schematic diagram of the multistage liquid impinger is shown in Figure 6.1. An Omron COMP AIR compressor nebulizer (Model: NE-C28P) was used in the current study. This nebulizer consisted of an air tube connecting to the nebulizer device and mouthpiece. The solvent system that was used in the MSLI was 70:30 methanol: water (mobile phase). In stages 1-4, 20 mL of the mobile phase was added. A filter paper (70mm pore sizes 450 μm (Fisherbrand®) was placed at Stage 5. The mouthpiece adapter was placed at the end of the induction port where the nebulizer mouthpiece would be placed. In order to study nebulized solutions and suspensions using the MSLI the recommended flow rate was 60 L/minute. Before operating the nebulizer, the flow pump was run for a period of 10 seconds. After 10 seconds had elapsed, the nebulizer pump was switched on and run for a duration of 5 minutes. After the period of five minutes, the nebulizer pump was switched off, but the flow pump of the MSLI was run for an additional 5 seconds. The flow rate was pre-calibrated before each run using a flow meter (Copley Scientific Ltd) to ensure the flow rate is 60 (±5) L/minute. After completion of the run, each stage of the MSLI was washed in order to obtain the entire sample. The 20 mL dispensed in Stages 1-4 was collected, and each stage further washed with 5 mL of 70:30 methanol: water. The throat and mouth piece was washed with 10 mL 70:30 methanol: water. The nebulizer chamber was washed carefully with 10 mL of methanol. The filter paper placed in Stage 5 of the device was washed with 10 mL of methanol. Each sample was incubated at room temperature for 24 hours for

complete extraction of the drugs into solution and analyzed by HPLC to determine the concentration.

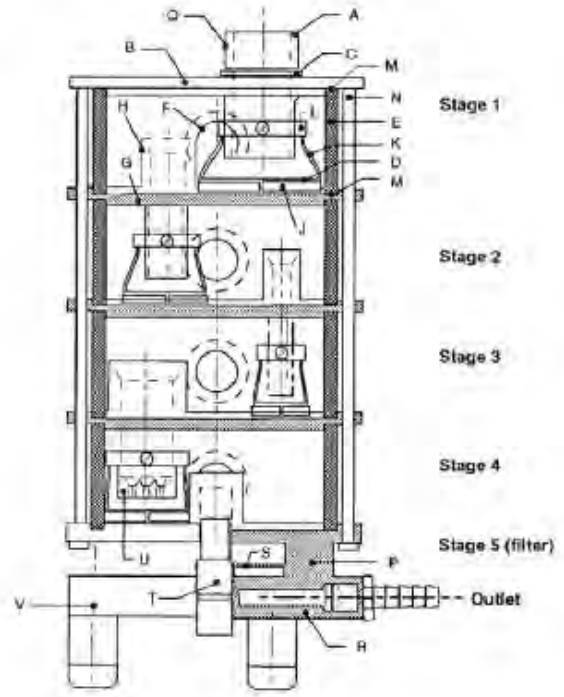

Figure 6.1 Schematic diagram of multi-stage liquid impinger (MSLI). Each stage presents a cut off diameter when operated at a specified flow rate. Image is from Copley Scientific Ltd Brochure for Inhaler testing [488]

6.2.2.2 ASSESSING THE DEPOSITION OF THEOPHYLLINE AND BUDESONIDE FROM DRY POWDER INHALER (DPI) FORMULATIONS OF NANOPARTICLES USING A MSLI

6.2.2.2.1 Grades of inhalable lactose used

Four different commercially available carrier grades of inhalable lactose were used and compared in the current study (Table 6.1). Their particle size and preparation of techniques were different and the methods carried out by the manufacturer were supplied in certificate of analysis of these excipients.

Table 6.1 Properties and particle size of the different grades of lactose used to formulate dry powder mixtures for inhalation provided in the certificate of analysis by commercial supplier [33]

Lactose grade	Characteristics	D50 (µm)
Lactohale® 201	Hard milled lactose Irregular shaped particles with various amounts of fine particles	<50
Lactohale® 300	Micronized lactose Size comparable with particle size of the active Highly cohesive material	<5
Respitose® ML001	Milled inhalation grade lactose Broad particle size distribution	<55
Respitose® ML006	Fine milled inhalation grade lactose with narrow particle size distribution	<17

6.2.2.2.2 Preparation of the dry powder inhaler formulations of PLA nanoparticles and lactose

A 5 mg quantity of nanoparticles was mixed with 40 mg of lactose added stepwise and mixed as summarized in Figure 6.2. The resulting mixture was filled into size 3 hard shell gelatin capsules (Capsugel®).

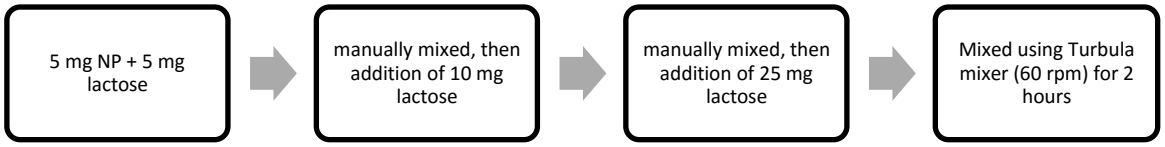

Figure 6.2 Method of preparing dry powder mixtures of nanoparticles (co and mono-encapsulated) and lactose (NP= nanoparticles)

6.2.2.2.3 Characterization of the dry powder formulations

Uniformity of mixing

To measure the uniformity of mixing of the nanoparticles, determined as a measure of theophylline and budesonide concentration in the mixture prepared, three random samples of the mixture (5 mg±0.25 mg) were weighed into an extraction tube and 3 mL of methanol was added. The samples were then left in methanol for a period of 24 hours to extract the drugs and the concentration determined using HPLC analysis (Chapter 2, Section 2.2.2.2.6).

Scanning electron microscopy (SEM)

SEM was used for morphological assessment of the dry powders and determination of particle size. From each powder, <1 mg was taken and placed on an adhesive on an

aluminum stub for particle morphology characterization. The method followed is described in detail in Chapter 2, Section 2.2.2.2.2.

6.2.2.2.4 Assessment of aerodynamic characterization of dry powder formulations

The DPI device used for assessment was a Cyclohaler (Aerolizer)® device. This device requires insertion of a size 3 hard shell gelatin capsule, filled with the powder. After placing it in the device and attaching the appropriate mouthpiece (Copley Scientific, Ltd), the capsule was pierced to release its contents. The weight of the capsule (with powder) was recorded before and after a run was carried out, in order to determine how much powder was emitted from the device. The MSLI was prepared as described previously (Section 6.2.2.1.2). The mouthpiece adapter was placed at the end of the induction port, in which the Cyclohaler® device was inserted. The flow rate was 60 (±5) L/minute which would produce a drop of 4.0 kPa over the inhaler device when testing the deposition of the test compounds using the MSLI [489]. The duration of the run was 4 seconds. The flow rate, solvent and the volume in each stage and extraction of sample from the MSLI was carried out in the same manner as described in Section 6.2.2.1.2. In addition, the capsule and the Cyclohaler® device were also rinsed with methanol (10 mL).

6.2.2.3 STATISTICAL ANALYSIS

To determine if any changes in the deposition were significant between replicates of dry powders and between co- and mono-encapsulated nanoparticles nebulized suspensions of nanoparticles, a two way ANOVA was carried out. $P<0.05$ suggests a significant difference. Bonferroni post hoc tests were carried out for this statistical analysis.

6.3 RESULTS

6.3.1 DEPOSITION OF THEOPHYLLINE AND BUDESONIDE FROM A NEBULIZED SUSPENSION OF MONO AND CO-ENCAPSULATED NANOPARTICLES MEASURED USING A MSLI

A large percentage of nanoparticles (and therefore drugs) remained in the chamber of the nebulizer when the suspension was nebulized. This amounted to approximately 40% for theophylline, whether delivered as co- or mono-encapsulated nanoparticle suspension (Figure 6.3). It was observed that high percentages for theophylline were recovered from all stages of the MSLI; approximately 20% of theophylline deposited in stage 5. A high percentage of theophylline was also recovered from stages 2-4. The amount of theophylline recovered from the various stages of the MSLI for both types of nanoparticles was not significantly different ($P>0.05$), suggesting a similar deposition profile of the nanoparticles. Lower percentage deposition is obtained in the throat and stage 1 of the MSLI. Extremely large variation in the concentrations at each stage suggests variation in drug loading during nanoformulation. The fine particle fraction was calculated to be 69.26±19.23% and 60.02±20.69% for theophylline mono- and co-encapsulated nanoparticles, respectively.

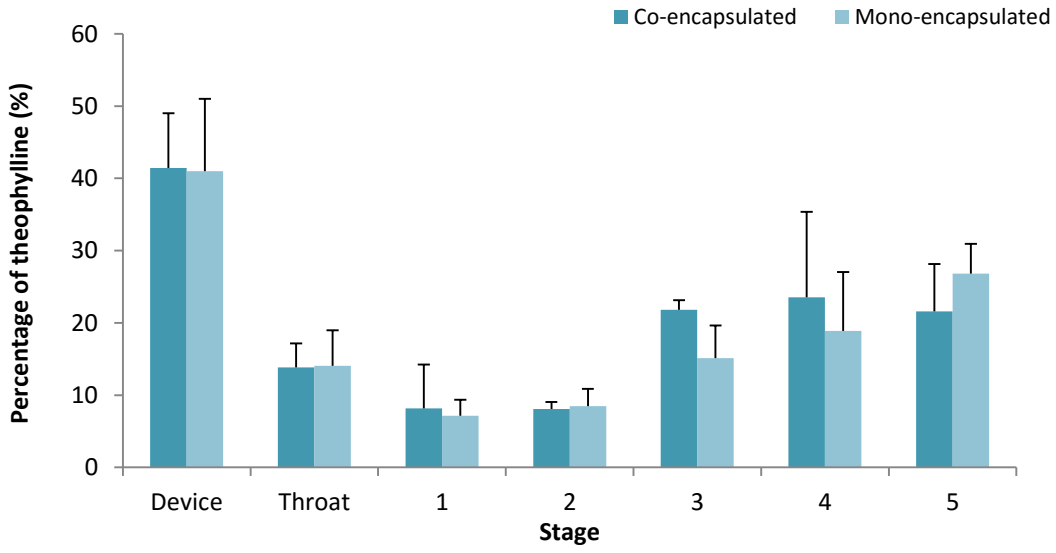

Figure 6.3 Comparison of the deposition profiles of theophylline from co- and mono-encapsulated nanoparticles in the different stages of the MSLI when delivered as a nebulized suspension (n=3, mean±SD) (P>0.05 for theophylline co- and mono-encapsulated nanoparticles)

A similar deposition profile to encapsulated theophylline was observed for budesonide (Figure 6.4). But approximately 25% of budesonide was recovered from the nebulizer chamber. With a large variation in the mono-encapsulated sample, this showed a range from 10-40% of budesonide present in the chamber of the nebulizer. The differences between the percentage of budesonide calculated in the mono and co-encapsulated nanoparticles could be as a result of different loading concentrations of the budesonide from the synthesis stage. Apart from the concentration calculated at Stage 5, these differences were not significant ($P>0.05$). Overall, a lower total concentration of budesonide was recovered from both mono- and co- encapsulated nanoparticles (56% and 85%, respectively).A lower deposition percentage of drugs are obtained in the throat and stage 1 and a greater percentage is obtained where the cut off diameter is 6.8µm (from stage 3 to 5). This is in the range of recommended particle size for pulmonary deposition. The fine particle fraction was calculated to be 20.31±4.18% and 48.90±14.94% for budesonide mono- and co-encapsulated nanoparticles, respectively.

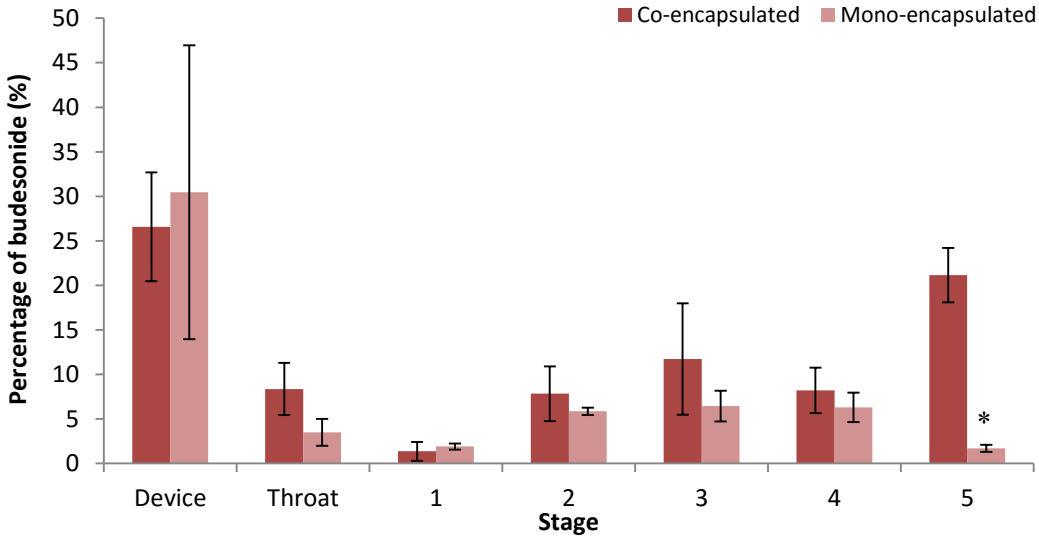

Figure 6.4 Comparison of the deposition profiles of budesonide from co- and mono-encapsulated nanoparticles in the different stages of the MSLI when delivered as a nebulized suspension (n=3, mean±SD) (*=P<0.05)

6.3.2 CHARACTERIZATION OF THEOPHYLLINE AND BUDESONIDE CO- AND MONO-ENCAPSULATED NANOPARTICLES AND DPI MIXTURE

6.3.2.1 Uniformity of Mixing of mono- and co-encapsulated nanoparticles

Uniformity of mixing of the drugs was measured for each of the different types of the DPI formulations prepared. The limits for the uniformity of content between samples should be between 75-125% of the original concentration [489]. The concentration of theophylline and budesonide in the nanoparticles used to formulate dry powders with lactose was calculated prior to using the nanoparticle sample. Analysis was carried out using HPLC using the method described in Chapter 2, Section 2.2.2.2.6. For this part of the study, the initial loading concentration of theophylline (13-18%) and budesonide (50-55%) was determined for what would be present in 5 mg of the nanoparticles. The initial drug loading value would be represented as 100% and therefore concentration of the drug concentration obtained in the random aliquots are percentage of the initial loading concentration. An average loading concentration is obtained for both the drugs in each dry powder formulation using different grades of lactose as the carrier. Percentage of theophylline and budesonide calculated after mixing with lactose carrier powders are shown in Table 6.2.

Ideally, a similar concentration of theophylline and budesonide in the random aliquots would suggest uniformity in the mixture after mixing processes (and encapsulation). This would be represented by smaller percentage relative standard deviation for the concentration calculated in the lactose grade. The data shows the average budesonide or theophylline loading calculated in the random aliquots

From the powder mixtures formulated using Lactohale® 201 the variation ranged between 10-22% in all the samples with a greater variation in the concentration obtained in the co-encapsulated samples. The greatest variation in the percentage of theophylline and budesonide calculated was obtained for nanoparticles mixed with Lactohale® 300 in particular, the co-encapsulated nanoparticles. The high variation suggests the inefficient mixing or adherence between nanoparticles and the 'fines' and suggests that some regions may contain a high concentration of nanoparticles and some a lower concentration.

The least variation was obtained in the dry powder mixtures formulated using Respitose® ML001 samples. From all the different dry powder mixtures the variation was calculated between 2.51 to 9.52%. This was the smallest range from all the different dry powder mixtures showing good mixing of the samples and uniformity in the dose. Respitose® ML001 lactose particles contain a broad size distribution and this could result in

nanoparticle freeze dried agglomerates being able to bind to some 'fines' and to larger coarse particles. A bigger range, but similar percentage variations were obtained for the samples formulated using Respitose® ML006 as for Lactohale®201 (except budesonide mono-encapsulated nanoparticles which were seen to be very low).

In summary, Respitose® ML001 showed better uniformity of content of the nanoparticles and the greatest variation was produced in the DPI mixtures formulated using Lactohale® 300. Although variation could be mainly due to the mixing properties, it could also be accounted for the variation in loading concentration. From the data obtained on the average variation, it is suggested that the differences in the variation in Respitose® ML001 is significantly lower than the remaining samples ($P<0.05$).

Table 6.2 Average percentage of theophylline and budesonide calculated in random aliquots of dry powder samples

Lactose grade	Sample	Budesonide mono-encapsulated	Budesonide co-encapsulated	Theophylline mono-encapsulated	Theophylline co-encapsulated
Lactohale® 201	Average	18.28	34.73	5.79	8.74
	SD	1.91	6.09	0.77	1.94
	% RSD	10.47	17.54	13.23	22.20
Lactohale® 300	Average	12.95	23.19	5.93	5.21
	SD	0.84	8.92	0.91	3.21
	% RSD	6.46	38.44	15.37	61.70
Respitose® ML001	Average	6.97	4.13	2.79	9.97
	SD	0.18	0.23	0.14	0.95
	% RSD	2.51	5.50	5.12	9.52
Respitose® ML006	Average	11.86	17.08	7.69	4.14
	SD	0.14	3.91	1.51	0.93
	% RSD	1.17	22.91	19.61	22.48

6.3.2.2 Morphological examination of the dry powders

Powders synthesized with Lactohale® 201 showed large particles of lactose (D50 given by the commercial supplier is 50μm) with nanoparticles adhered onto the lactose (Figure 6.5). In support of the uniformity of content data showing large variation in the concentration (Section 6.3.2.1), there are regions concentrated with nanoparticles, and regions with an absence of nanoparticles. Similar observations were made for all mono- and co-encapsulated nanoparticles. The SEM images also showed 'fine' particles adhered to the irregular surface of the larger coarse lactose carrier particles, which can affect the binding of the nanoparticles.

Lactohale® 300 is a micronized form of inhalable lactose which is comparable in particle size to the active (Figure 6.6). The SEM images show differences in the appearance of this formulation in comparison to other lactose powders studied and the sample shows the presence of a large amount of 'fines', which this lactose grade mainly consists of. Due to the particle size of the lactose, it is extremely difficult to see nanoparticles mixed in the sample. Similar to Lactohale® 201, there are regions of only lactose with the absence of any nanoparticle sample. Nanoparticles were identified due to their characteristic morphological features described in Chapter 2, Section 2.3.4, which are spherical in shape and present in a sub-micron range.

Lactose grade Respitose® ML001 is similar to Lactohale® 201 (D50 given by the commercial supplier is 55μm) but has a broad size distribution (Figure 6.7). The samples show very good distribution of the nanoparticles (both mono- and co-encapsulated) within the lactose similar to Lactohale® 201.

Morphological assessment of the Respitose® ML006 lactose grade (D50 is 17μm), containing a narrow size distribution, was also carried out (Figure 6.8). Similar to previous observations, there are regions where nanoparticles are present and absent and large aggregates of nanoparticles can be observed.

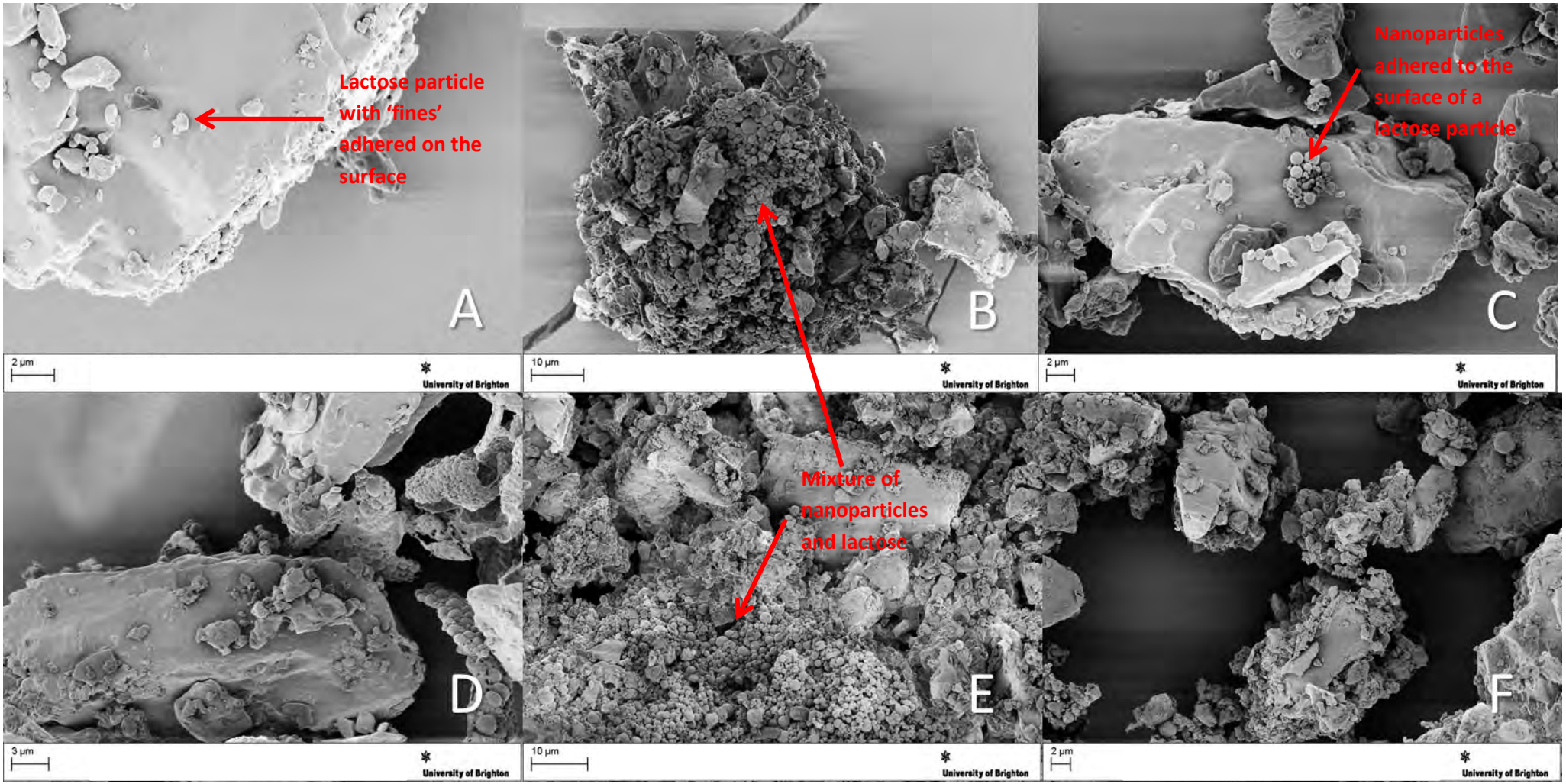

Figure 6.5 Dry powder mixtures formulated mixing nanoparticles (co and mono-encapsulated) and Lactohale® 201. Lactohale® 201 particles are large, with a broad size distribution. The images are of dry powder mixtures of Lactohale® 201 and A-B: co-encapsulated nanoparticles, C-D: theophylline mono-encapsulated nanoparticles, E-F: budesonide mono-encapsulated nanoparticles

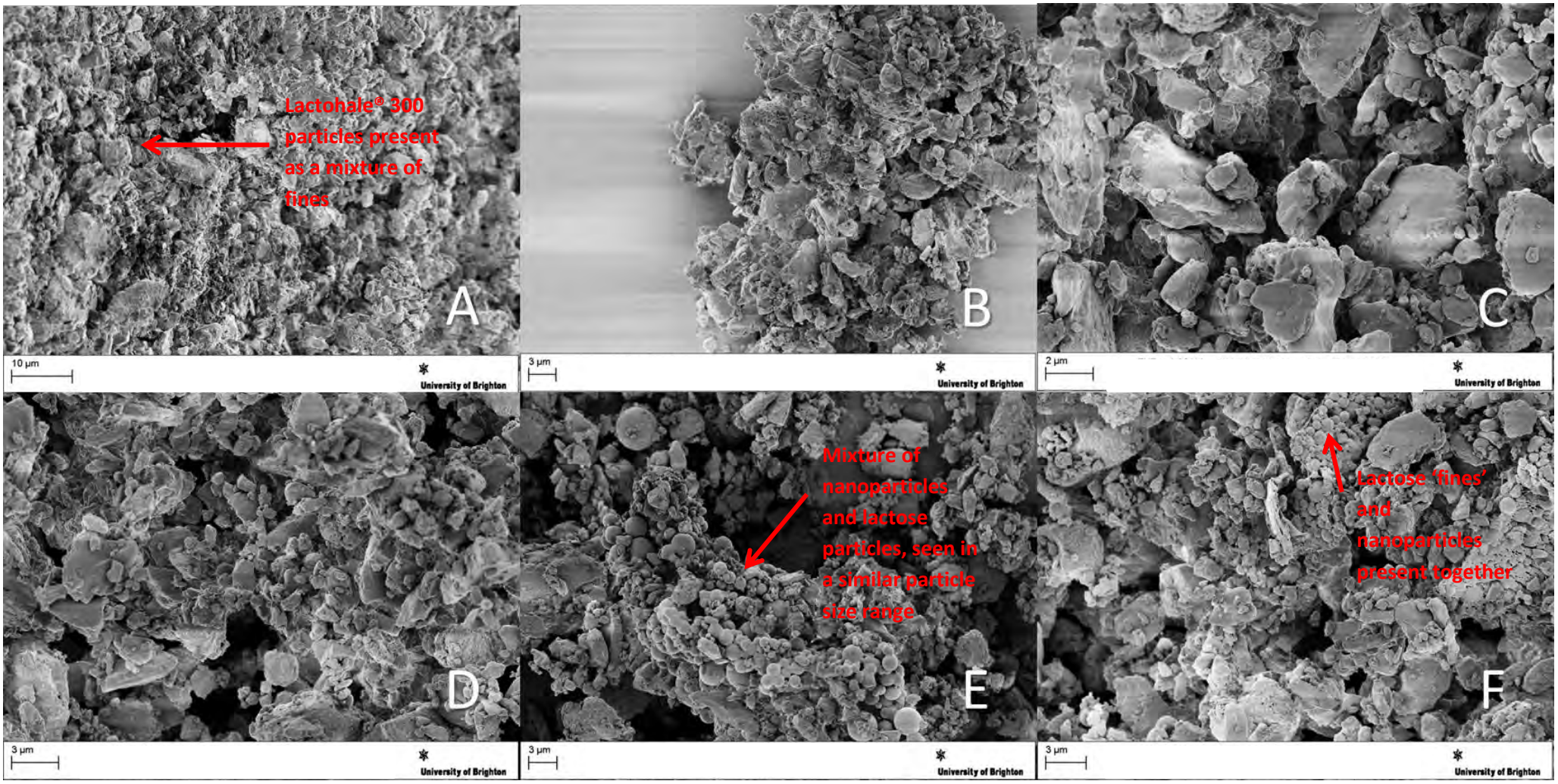

Figure 6.6 Dry powder mixtures formulated mixing nanoparticles (co and mono-encapsulated) and Lactohale® 300. Lactohale® 300 particles are classified as 'fines' with small particle size. The images are of dry powder mixtures of Lactohale® 300 and A-B: co-encapsulated nanoparticles, C-D: theophylline mono-encapsulated nanoparticles, E-F: budesonide mono-encapsulated nanoparticles

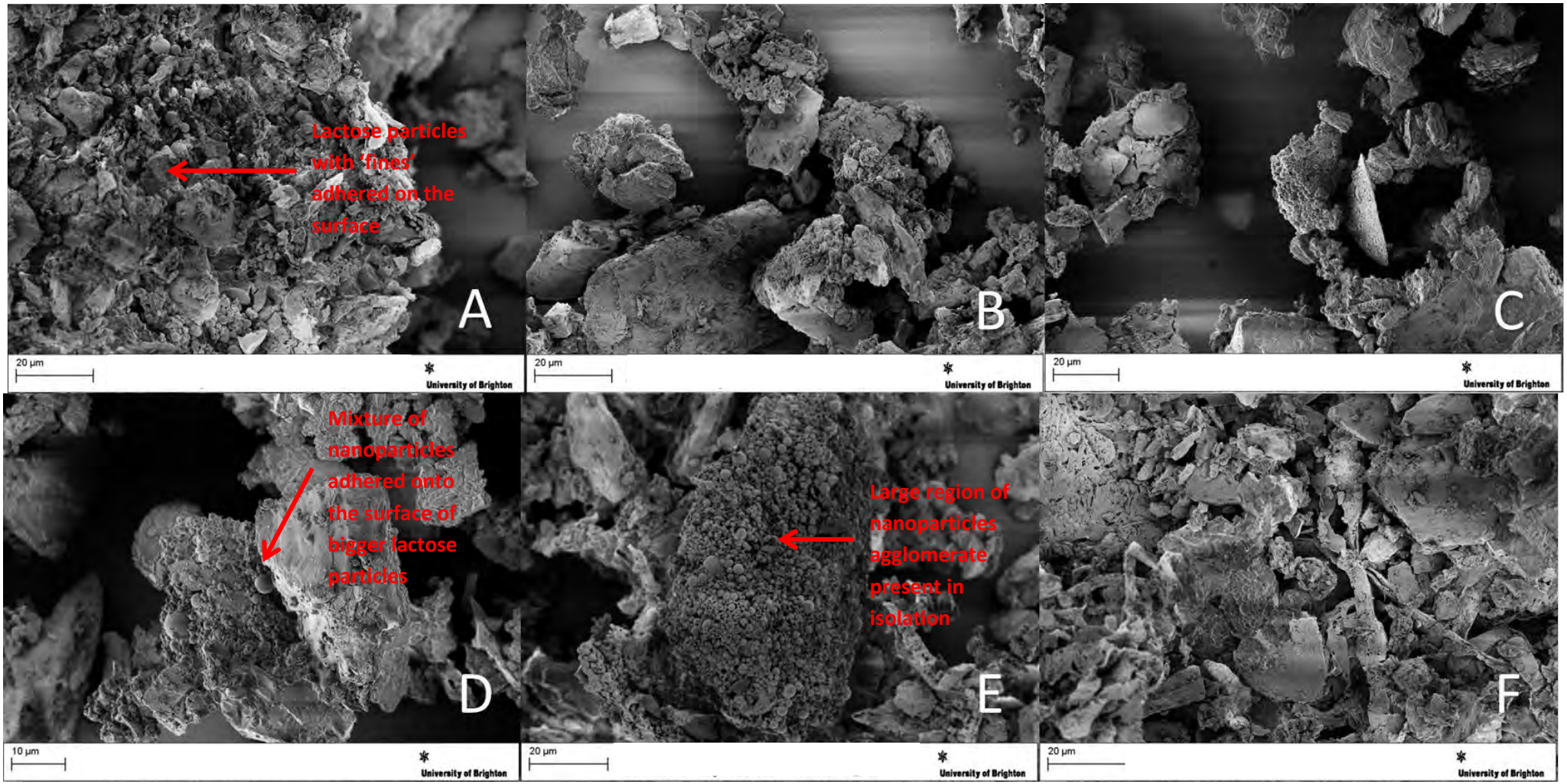

Figure 6.7 Dry powder mixtures formulated mixing nanoparticles (co and mono-encapsulated) and Respitose® ML001. Respitose® ML001 particles are large, with a broad size distribution, similar to Lactohale® 201. The images are of dry powder mixtures of Respitose ® ML001 and A-B: co-encapsulated nanoparticles, C-D: theophylline mono-encapsulated nanoparticles, E-F: budesonide mono-encapsulated nanoparticles

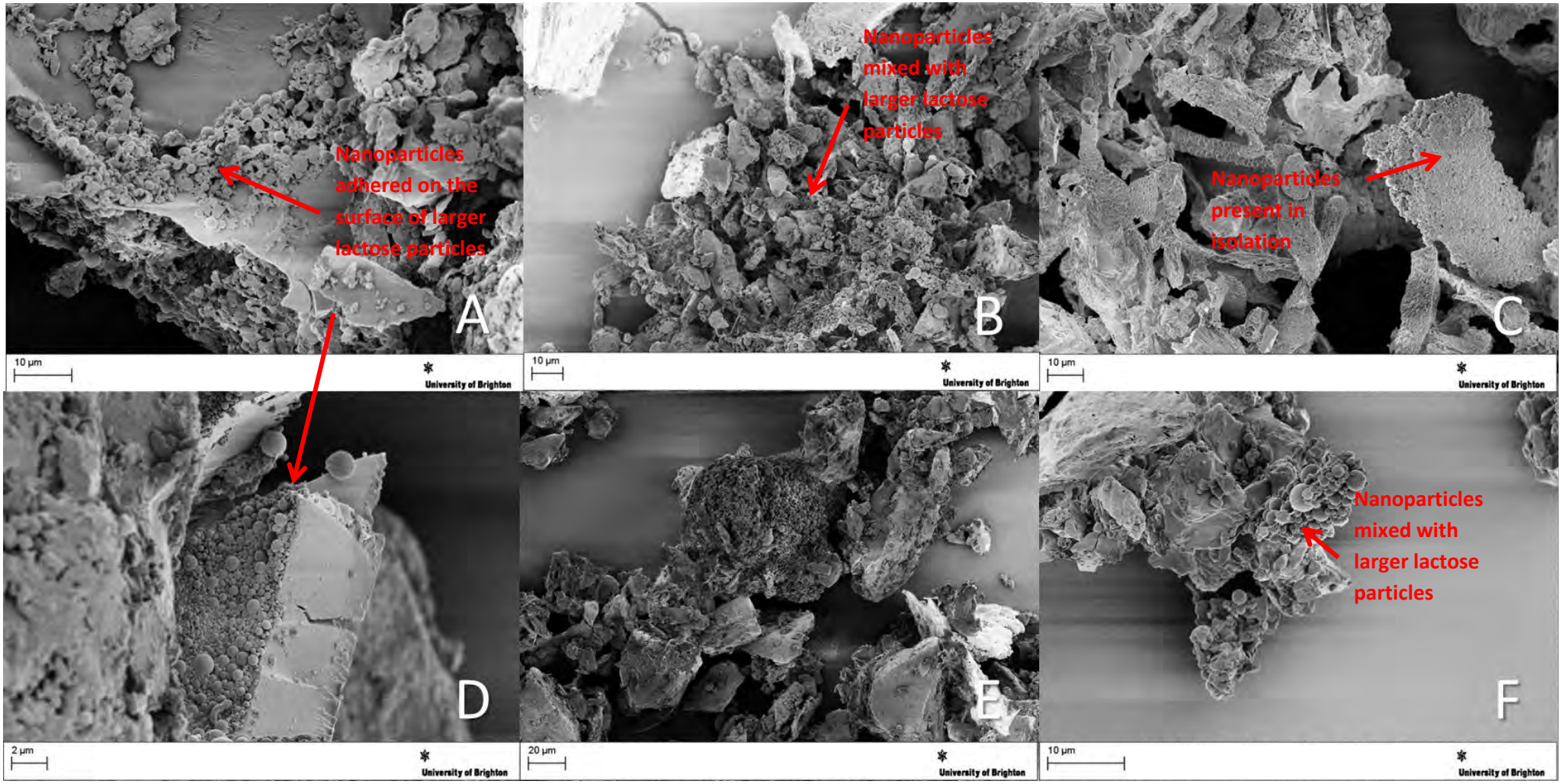

Figure 6.8 Dry powder mixtures formulated mixing nanoparticles (co and mono-encapsulated) and Respitose® ML006. Respitose® ML006 particles are large in size, but with a narrow size distribution. The images are of dry powder mixtures of Respitose® ML006 and A-B: co-encapsulated nanoparticles, C-D: theophylline mono-encapsulated nanoparticles, E-F: budesonide mono-encapsulated nanoparticles

6.3.3 Effect of lactose grade on the Deposition of budesonide mono-encapsulated nanoparticles determined using MSLI delivered using a DPI

The general pattern of deposition for the nanoparticles using the different grades of lactose showed a greater deposition in the throat and stage 1 of the MSLI. This corresponds to particles present in a size greater than 13µm.

The total percentage recovery obtained from the samples also varied with a higher percentage recovery of budesonide in nanoparticles mixed with Lactohale® (201 and 300) grade lactose in comparison to the Respitose® (ML001 and ML006) grade lactose. On average, less than 50% of budesonide was recovered from the Respitose® lactose grade samples.

Budesonide mono-encapsulated nanoparticles delivered with Lactohale® 201 showed a total average recovery of 60.21% calculated from deposition at all stages, device and capsule (Figure 6.9A). In determining the uniformity of mixing, the greatest variation in the concentration of drugs selected from random sites was from samples formulated using Lactohale® 300 (Figure 6.9B). This high variation between samples is also observed when analysis was carried out on the MSLI at the different stages. Total average percentage recovery of over 75% was obtained for budesonide nanoparticles formulated using Lactohale® 300. A low total average recovery (42%) of budesonide was recovered from the samples prepared using Respitose® ML006 (Figure 6.9C), and approximately 50% average recovery using Respitose® ML001 was obtained (Figure 6.9D).

Overall, from all the different formulations produced using different grades of lactose, the greatest deposition was observed in the throat and stage 1 of the MSLI. Variability between the repeats for powders formulated using Lactohale® 201 was not significantly different except for a high concentration of budesonide recorded for stage 1 in the second repeat ($P>0.05$). For the budesonide nanoparticles mixed with Lactohale® 300, it was difficult to determine a particular pattern of deposition due to the presence of large variation obtained within samples. The large variation resulted in significant differences between each replicate carried out ($P<0.05$). The greatest concentration of budesonide was recovered in the capsule for these powders. For the budesonide nanoparticles mixed with Respitose® ML006, the variations between the replicates was not significantly different ($P>0.05$). Although the greatest concentration of budesonide was obtained from the sample present in the capsule (15-18%), a high deposition was also obtained in the throat and stage 1 of the MSLI

(approximately 7-10%). Deposition profile of budesonide nanoparticles mixed with Respitose® ML001 are similar to that of Lactohale® 201, where a low concentration of drug was calculated in the capsule and device, but a large deposition was observed in the throat and stage 1 of the MSLI. On average 15% and 22% was deposited in the throat and stage 1, respectively. The differences in the concentration recovered were not significantly different ($P>0.05$).

A low percentage recovery of the nanoparticles was recovered from the capsules and devices suggesting good flow properties of the powders formulated with Lactohale® 201 and Respitose® ML001. Percentage recovery was less than 5% for both these powders which was not significantly different in each replicate ($P>0.05$). An extremely high percentage recovery was calculated from the capsule for budesonide nanoparticles formulated using Lactohale® 300 which was on average 47%. Over 15% of the budesonide nanoparticles were recovered in the capsule for powders formulated using Respitose® ML006.

As a larger concentration of nanoparticles was recovered in the throat and stage 1, collectively from stages 3-5, a low amount was recovered. This content is referred to as the 'fine particle fraction' and was less than 15% for all the powders formulated using different lactose grades. Between 5-10% of the nanoparticles were recovered in stages 2-5.

For powders formulated using Lactohale® 201 the FPF was calculated to be approximately 11.76%. The FPF calculated for the powders formulated using Respitose® ML006 was approximately 8%. Similar to the previous results, a larger variation was observed in samples synthesized using Lactohale® 300. The variation between replicates was shown to be significantly different ($P>0.05$). The FPF for powders synthesized using Lactohale® 201 and Respitose ® ML001 were also present in the range from 8-11%.

Budesonide nanoparticles were also observed to deposit in the 5^{th} stage of the MSLI for all the formulations produced which was less than 1.5% for all the different formulations. Although Lactohale® 300 consists of 'fines' and therefore would aid the deposition of the particles in the lower stages of the MSLI, the amount of nanoparticles recovered in the fifth stage was not significantly different to the other powders formulated ($P>0.05$).

Apart from Lactohale® 300, clearer deposition profiles were obtained for budesonide from nanoparticle-lactose mixtures. The greatest deposition was achieved in the throat and stage 1. The FPF was calculated from stage 3 (where particle size is less than 6.8µm) and was seen to be the greatest (and most varied) for samples formulated using Lactohale® 300. Similar FPF were calculated for the remaining lactose grades.

The deposition profiles for the two different grades of Lactohale® were shown to be significantly different from each other at all stages of the MSLI, including the capsule and device ($P>0.05$). The powders formulated using Respitose® ML001 and ML006 are shown to be significantly different for the percentage of nanoparticles recovered in the capsule ($P<0.05$). Lactohale® 201 and Respitose® ML001 were shown to have similar deposition profiles ($P>0.05$).

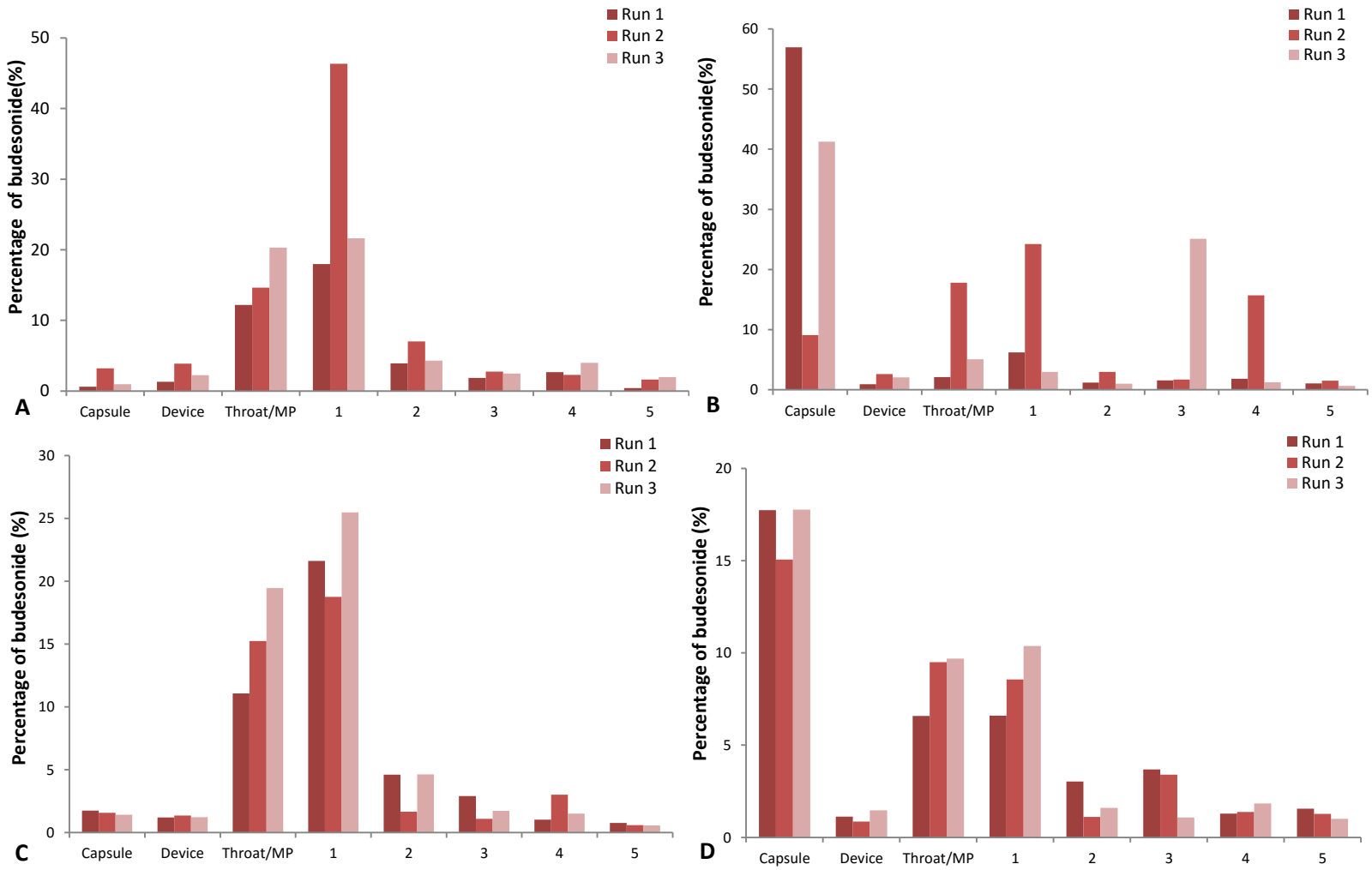

Figure 6.9 The effect of lactose grade on the percentage of budesonide mono-encapsulated nanoparticles depositing at each stage of the MSLI when delivered from a DPI. (A) Lactohale® 201, (B) Lactohale® 300, (C) Respitose® ML001 and (D) Respitose® ML006 are administered using a Aerolizer® device. Each bar represents an individual run and 3 runs were conducted. The x-axis represents the stage of the MSLI. (MP:Mouthpiece)

6.3.4 *Effect of lactose grade on the Deposition of theophylline mono-encapsulated nanoparticles determined using MSLI delivered using a DPI*

Lactohale® 201 powders of theophylline nanoparticles showed a total average recovery of 82.67% theophylline. However, in the individual runs carried out, this ranged between 66.23-109.99%, which was not significantly different from each other ($P>0.05$) (Figure 6.10A). For Lactohale® 300 powders mixed with theophylline mono-encapsulated nanoparticles the total recovery was calculated to be 116%; which may be as a variation in the loading efficiencies of theophylline. The total average percentage recovery obtained for the samples formulated using Respitose® ML001 was 60%. For theophylline nanoparticles mixed with Respitose® ML006 the total percentage recovery ranged between 60-140% (approximately).

For Lactohale® 201 an overall low concentration was obtained in the device; except for Run 2. Unlike budesonide nanoparticles mixed with lactose grades, a large variation was present in all the different lactose grades in the assessment of theophylline nanoparticles deposition. Approximately 15% of the nanoparticles are recovered in the capsule after actuation for theophylline nanoparticles mixed with Lactohale® 201. The greatest amount of nanoparticle was recovered in capsule for theophylline nanoparticles mixed with Lactohale® 300 (approximately 40%). Approximately 10% of theophylline nanoparticles were present in the capsule after actuation for powders formulated using Respitose® ML006. Although a large, significantly different variation is obtained, the lowest quantity of theophylline nanoparticles were recovered from the capsule for powders formulated using Respitose® ML001.

In general, deposition in stage 5 was obtained but greatest deposition was in the throat and stage 1, similar to the deposition of budesonide. But each lactose grade presented a large variation in the percentage of theophylline calculated from the nanoparticles recovered resulting in some significant differences in the deposition profile. For powders formulated using Lactohale® 201, a large concentration of nanoparticles were recovered in the throat and stage 1. This was similar to powders synthesized using Lactohale® 300 (Figure 6.10B). Theophylline nanoparticles mixed with Respitose® ML001 presented an extremely high variation and was observed for the samples, which was seen to be statistically different for some of the experimental replicates: run 3 (Figure 6.10C). Deposition of theophylline from powders formulated using Respitose® ML006 also showed a similar pattern where the

deposition was the greatest in the throat and stage 1 of the MSLI (Figure 6.10D). The deposition profile was similar to that obtained with the nanoparticles deposited using Lactohale® 201. Approximately 30-50% of the dose was calculated in stage 1 of the MSLI. Due to this variation, it is difficult to determine a clear deposition profile, but on average the greatest deposition was calculated for these stages.

Similar to budesonide nanoparticles, lower deposition occurred in stages 2-5. On average, for all four different powders formulated, the quantity deposited in these stages was significantly lower than that in stage 1 ($P<0.05$), except Lactohale® 201 stage 5 ($P>0.05$).

Theophylline nanoparticles mixed with Lactohale® 201 showed a FPF of 10% which was similar to the budesonide nanoparticles mixed with Lactohale® 201. Similar FPF was obtained for Respitose® ML001 (16%) and Respitose® ML006 (14.49%). But for both samples large significant differences were observed in the replicates ($P<0.05$). Low concentration of theophylline nanoparticles were recovered from stages 2-5 when mixed with Lactohale® 300, suggesting that there would be poor deposition of the theophylline mono-encapsulated nanoparticles in the lower region of the airways. The FPF calculated was 5.60%.

Although a large amount of variation was observed in the individual replicates that were carried out, on average; similar to the budesonide nanoparticles mixed with lactose, a large deposition of the nanoparticles was recovered from the throat and stage 1. The quantity of nanoparticles recovered in the capsule in Respitose® ML001 was significantly lower than in the other lactose grades ($P<0.05$). The quantity of theophylline nanoparticles recovered from the fifth stage of the MSLI when mixed with Lactohale® 201 was significantly higher than the other powders ($P<0.05$).

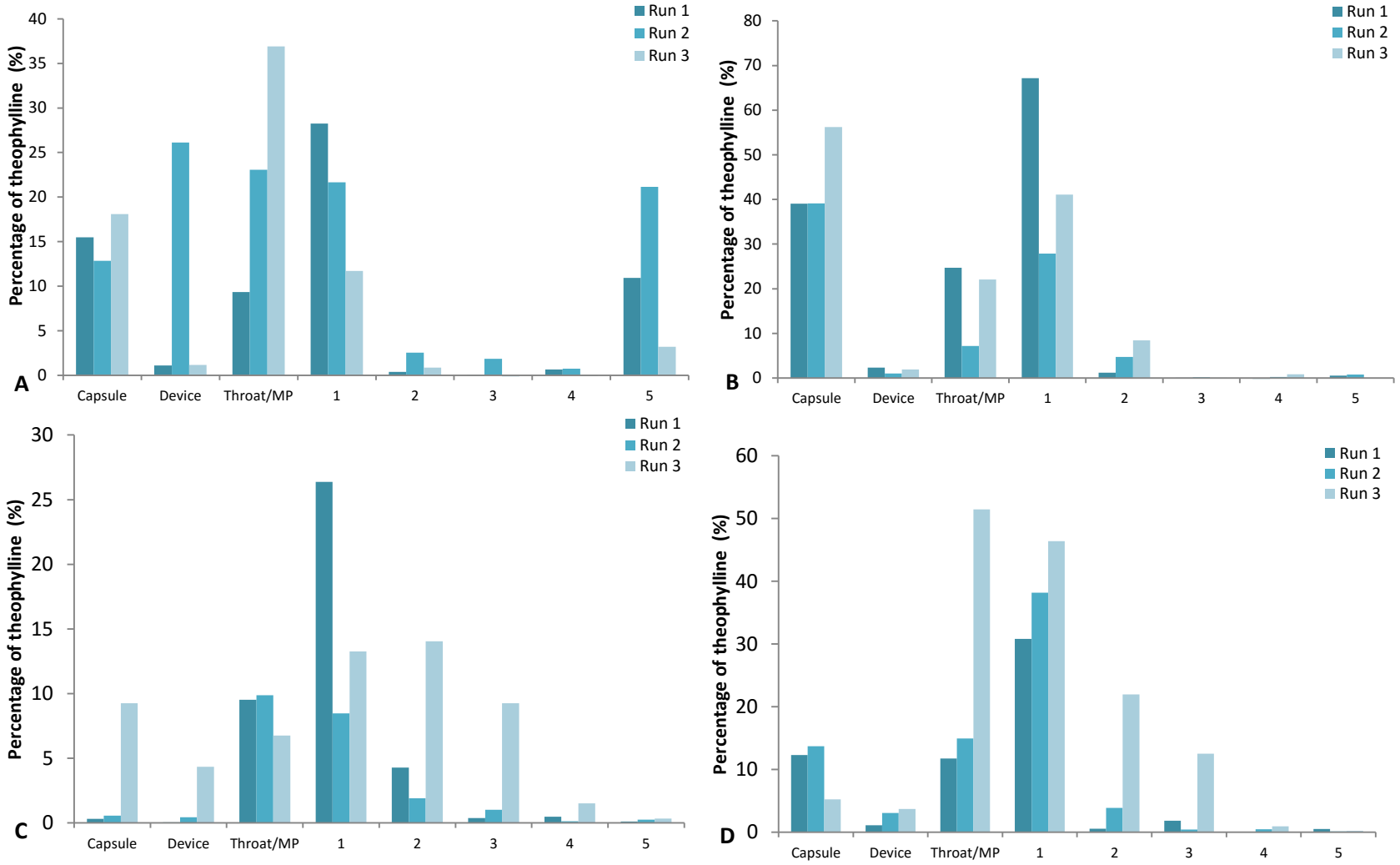

Figure 6.10 The effect of lactose grade on the percentage of theophylline mono-encapsulated nanoparticles depositing at each stage of the MSLI when delivered from a DPI. (A) Lactohale® 201, (B) Lactohale® 300, (C) Respitose® ML001 and (D) Respitose® ML006 are administered using a Aerolizer® device. Each bar represents an individual run and 3 runs were conducted. The x-axis represents the stage of the MSLI. (MP: mouthpiece)

6.3.5 *Effect of lactose grade on the Deposition of theophylline and budesonide co-encapsulated nanoparticles determined using MSLI delivered using a DPI*

When produced as mixtures of mono-encapsulated nanoparticles and the different lactose grades, theophylline and budesonide presented (on average) the greatest deposition in the throat and stage 1 of the MSLI. When delivering both drugs together, it is important to understand if the deposition for both drugs is similar or independent of each other. In this study it is predicted that the deposition profiles of theophylline and budesonide will be dependent on the nanoparticles, rather than the two drugs.

Low percentage recoveries were obtained for theophylline in the mixtures for Lactohale® 201. High percentage recoveries were obtained for budesonide (Figure 6.11A) but theophylline recovery (Figure 6.12A) was calculated to be low for powders formulated using Lactohale® 201. This could be due to the variation in the loading concentration of the drugs in the samples. Deposition profile for theophylline and budesonide is similar to budesonide mono-encapsulated nanoparticles, where the greatest concentration was deposited in the throat or stage 1. Large variation was obtained for powders formulated using Lactohale® 300 and consistent with the greatest deposition at the throat and stage 1. The percentage recoveries were similar for both drugs when formulated using Lactohale® 300 (ranging from approximately 70-115%) (Figure 6.11B and Figure 6.12B). The greatest percentage of dose emitted was obtained for the powders formulated with Respitose® ML001 where approximately 80.65% of the powder was emitted (Figure 6.11C and Figure 6.12C); and was consistent with the mono-encapsulated nanoparticles. Unlike the recoveries obtained for the drugs in the mono-encapsulated nanoparticles, the percentage recovery for theophylline and budesonide was extremely high for powdered mixtures formulated with Respitose® ML006 (Figure 6.11D and Figure 6.12D) and over 100% recovery was achieved. Similar deposition profile to mono-encapsulated samples revealed a large quantity of nanoparticles recovered in the capsule.

Concentration of theophylline and budesonide calculated in the capsule is varied and as suggested may be as a result of the differences in loading efficiency of the two drugs. Similar results were obtained for both Lactohale® grade powders. In comparison to the other stages, the percentage of drugs was seen to be the highest in the capsule (after actuation) for powders formulated using Respitose® ML006. Similar results were obtained

for budesonide nanoparticles. The concentration of the drug remaining in the capsule correlated with the quantity of powder remaining in the capsule after inhalation. Approximately 70% of the theophylline concentration was calculated to be in the capsule. The concentration of budesonide ranged from 30% to over 70%. Approximately 16-27% of the powder remained in the capsule for the nanoparticles mixed with Respitose® ML001.

Consistent with the previous results, the greatest percentage of nanoparticles was calculated in the throat and stage 1 of the MSLI where, for nanoparticles mixed with Lactohale® 201, approximately 20% of theophylline and over 50% for budesonide was calculated. The highly cohesive Lactohale® 300 formulated powders show a degree of variation in the data which is similar to both the drugs when studying the deposition profiles from mono-encapsulated nanoparticles. Despite the anomalies obtained, a general note is made to observe that the concentration of the two drugs is still greatest in the throat and stage 1. For powders formulated using Respitose® ML006, 20-40% of the nanoparticles were recovered in these stages, which was the second highest after the percentage recovered in the capsule. Deposition of both the drugs was similar, further suggesting that the deposition profile is related to the characteristics of the nanoparticles and not the drugs, and was seen to be greater in the throat and stage 1 of the MSLI. Respitose® ML001 showed deposition with the least variation, suggesting the ability of the nanoparticles and the lactose powders to mix well. However, the greatest deposition was obtained in the throat (ranging from 60-80%) and stage 1 (ranging from 30-40%).

Stage 2 also shows approximately 10% of both drugs present at this stage. A low FPF was calculated from both drugs which ranged from 0.85-9% from powders formulated using Lactohale® 201. This was much lower than the mono-encapsulated nanoparticles. For powders formulated using Lactohale® 300, approximately 10% was deposited on stage 2. A low FPF ranging from 2-4% was calculated. This was lower than the mono-encapsulated samples. A similar FPF was calculated for the powders mixed with Respitose® grades. For powders mixed with Respitose® ML006, a percentage of the two drugs deposited in the lower airways were seen to be slightly higher (FPF: 6.77% for theophylline, 10.92% for budesonide). This was similar for Respitose® ML001 (FPF: 8.71% for theophylline, 8.86% for budesonide).

Despite a consistency in the deposition of nanoparticles in the throat and stage 1, as a result of the variation within the samples, the differences were significant ($P<0.05$).

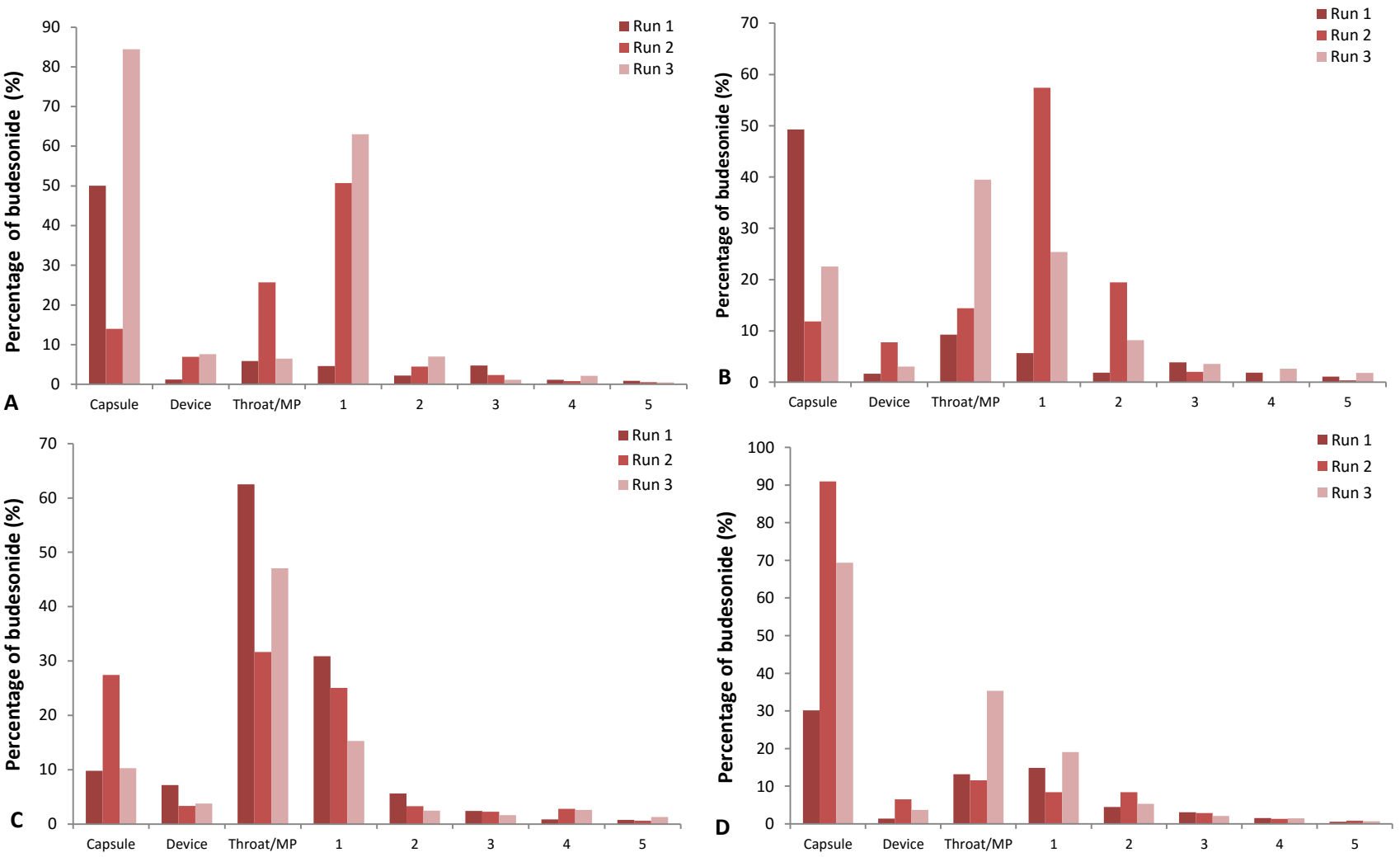

Figure 6.11 The effect of lactose grade on the percentage of budesonide co-encapsulated nanoparticles depositing at each stage of the MSLI when delivered from a DPI. (A) Lactohale® 201, (B) Lactohale® 300, (C) Respitose® ML001 and (D) Respitose® ML006 are administered using a Aerolizer® device. Each bar represents an individual run and 3 runs were conducted. The x-axis represents the stage of the MSLI. (MP: mouthpiece)

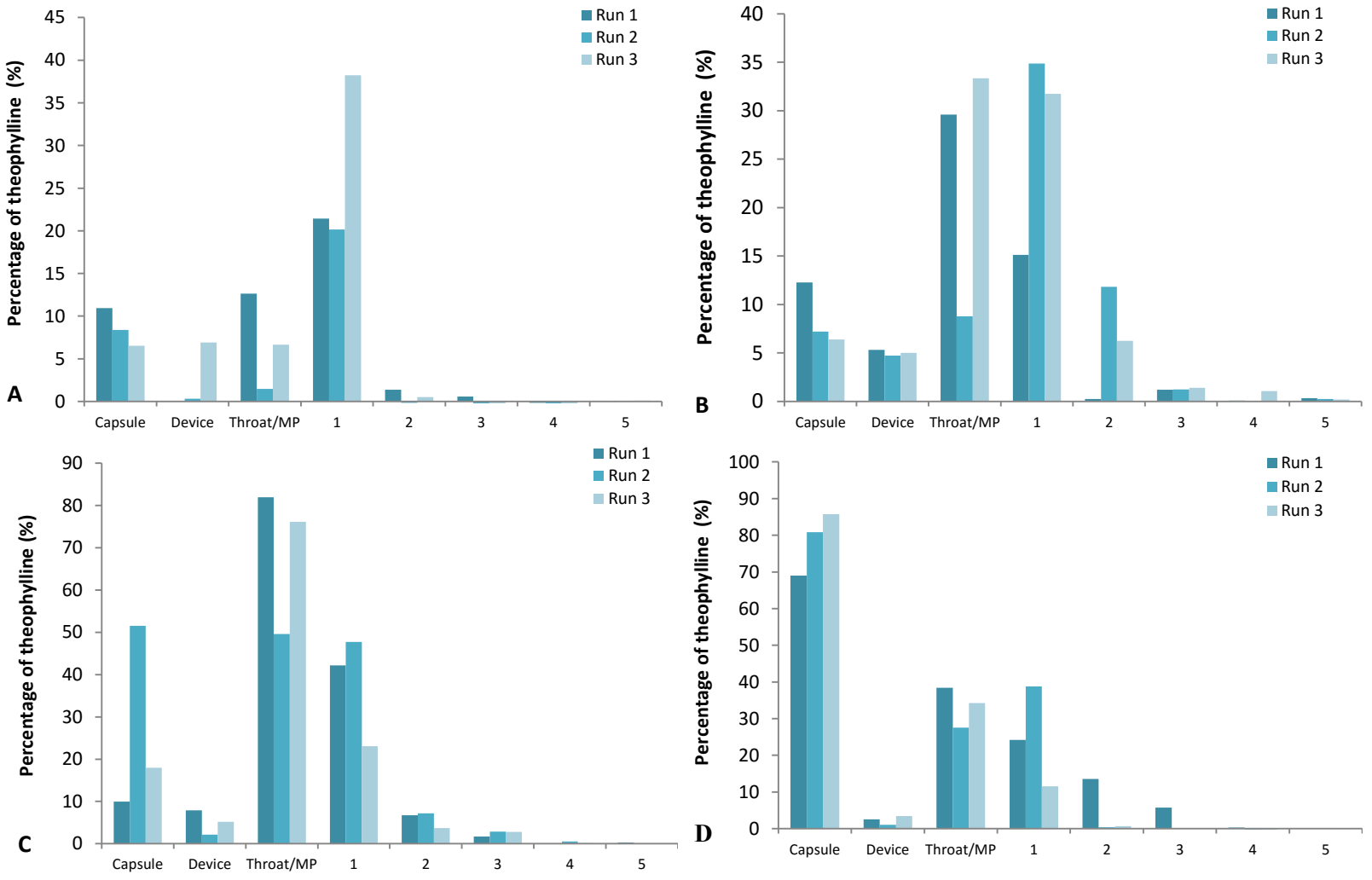

Figure 6.12 The effect of lactose grade on the percentage of theophylline co-encapsulated nanoparticles depositing at each stage of the MSLI when delivered from a DPI. (A) Lactohale® 201, (B) Lactohale® 300, (C) Respitose® ML001 and (D) Respitose® ML006 are administered using a Aerolizer® device. Each bar represents an individual run and 3 runs were conducted. The x-axis represents the stage of the MSLI. (MP: mouthpiece)

6.4 DISCUSSION

6.4.1 THE USE OF IMPINGERS

Impingers and impactors are instruments that are used in order to determine the particle size distribution and deposition of drugs in lungs. There are various studies used to study the inhalation of aerosols and to understand their deposition in the airways when delivered alone, or in combination with other drugs or with excipients. *In vitro* aerodynamic assessment of the size and size distribution of the particles, the fine particle fraction (FPF), and/or mass that can reach the lungs provides a measure of the consistency of the inhaler in drug delivery and the deposition pattern in the lungs.

In this study, impingers have been used to study the deposition of nanoparticles with a view to predicting their deposition in the lungs. Impingers, unlike impactors, require use of solvents and therefore allow particles to deposit in a liquid surface. When particles are inhaled, they are driven by the airflow, but due to inertial impaction, particles will deposit at various sites in the impinger as they lose their momentum. Small particles possess a lower level of momentum and are not collected, but large particles are seen to deposit when there is sufficient airflow. The delivery of nanoparticles to the lungs is challenging due to their small size, which causes the particles to be exhaled [210]. Different approaches have been taken in order to successfully deliver nanoparticles to the lungs.

The main problem with assessing controlled release formulations is the disadvantage/limitation that not all drugs can be analyzed immediately after the run has taken place as this would not be representative of the total amount of drug present in the controlled release formulation. In order to determine the concentration as accurately as possible, the samples were kept in the solvent system for 24 hours for complete drug extraction and then analyzed using the analytical method. The time period of 24 hours was kept consistent with the release testing of the nanoparticles (Chapter 3).

Previously, a twin stage liquid impinger (TSLI) was used to obtain preliminary results with the solvent system consisting of only water (data not shown). This resulted in low recovery of budesonide which was thought to be due to the poor solubility of budesonide in water. The resultant recovery of theophylline was high and was thought to be due to the high solubility of theophylline in water and aqueous media, allowing for a more rapid release of theophylline from the nanoparticles. This observation was supported by a quicker release of theophylline in SLF in comparison to budesonide (Chapter 3, Section 3.3). The results obtained when TSLI was used suggested successful deposition in the airways where particle size is less than 6.4μm, which is ideal for pulmonary deposition.

As a result of the low recoveries it is thought that it would be ideal and more important to include an organic solvent in the impinger. The use of a MSLI with more stages would also allow a greater understanding of the deposition of nanoparticles. It has been commonly seen that the extraction of drug is carried out by use of the mobile phase or organic solvent as the solvent system to be dispensed in the impinger [238, 490].

The MSLI is a cascade impinger allowing assessment of several types of formulations, including dry powders, pressurized metered dose inhalers and nebulizer formulations. The MSLI consists of five stages in total: four stages containing glass walls and a suitable solvent system which ensures the glass walls inside are moist to aid in deposition of the drugs. The fifth stage is an integral filter stage capturing all other particles.

A range of flow rates can be applied to use in the MSLI. The nominal flow rate (Q_n) used is 60 L/minute in which the cut off diameters are shown in the Table 6.3.

Table 6.3 Cut off diameters at each stage of the MSLI when the flow rate is set to as the nominal flow rate (60L/minute)

Stage	Cut off diameter at 60 L/min (µm)
1	13
2	6.8
3	3.1
4	1.7

6.4.2 FORMULATION OF DRY POWDER INHALER FORMULATIONS AND CHARACTERIZATION USING THE MSLI

For the nanoparticles, it would be ideal to develop a formulation where the nanoparticles are in a dry powder state. This would ensure that the drug is not released in their dispersion medium. Should the formulation need to be nebulized, it is important the nanoparticles remain as the lyophilized powder which can be suspended in water just before administration. This would ensure drugs are not released from the nanoparticles when suspended in an aqueous medium.

Dry powder formulations can consist of the drug component and an inert carrier particle, such as lactose or mannitol. For the theophylline and budesonide nanoparticles synthesized, it would be ideal to use dry powders as a formulation to deliver the nanoparticles. The carrier that was chosen was the commonly used lactose. Lactose is available in several different grades produced with changes in the processing method and particle size as a result. Lactose has also been used for the successful formulation of spray-dried PLGA nano-

embedded microparticles (containing tobramycin) [210, 491]. PLGA nanoparticles, loaded with siRNA, have also been tested for the deposition in the lungs[208]. Mannitol has also been used for the formulation of dry powder mixtures of nanoparticles for pulmonary delivery [208, 366]. Many techniques have used spray drying suggesting that this technique did not affect the properties of the nanoparticles in attempt to synthesize dry powder mixtures of lactose and nanoparticles [208].

Pharmacopeial methods and guidelines specify a 4kPa pressure drop across the device or a flow rate of 60L/minute when testing the deposition of drugs from DPIs [492] resulting in 4L over 4 seconds [493] when using a 60L/minute flow rate using a Cyclohaler (Aerolizer)® device [494]. Each device has a particular flow rate at which the experiment should be conducted at in order to achieve the 4kPa pressure drop. The flow rates are different due to the differences in the resistance of the device and the turbulence caused by the device features which can affect the FPF (which are mainly dependent on the device) [36]. However, it was noted from several studies the option of 60L/minute (which is specific to Cyclohaler® device) was used, irrespective of the device.

In a review by Hoppentotch et al (2014), it was stated that this flow rate or pressure drop is not needed to be achieved because other studies have been able to show the same fine particle fraction (FPF) when the pressure drop across the device is 2-3kPa, which means that the deposition was suggested to be independent of the pressure drop [474]. Patients who are suffering from COPD generate a 2-4kPa drop, i.e. too much inspiratory effort is not required if attempting to mimic the physiological situation [25, 459, 474, 493]. Another review by Ashurst et al (2000) further suggested that the requirement of the 4kPa pressure drop at a specific flow rate is not required as long as the experiment is validated at a particular flow rate [464]. This specific flow rate of 60L/minute producing a 4kPa pressure drop over 4 seconds is appropriate for the Cyclohaler (Aerolizer®) device and was chosen as the settings for testing the deposition of theophylline and budesonide nanoparticles in the current study. By using these settings, the size ranges at each stage (Table 6.3) are constant as well. It was observed that the FPF for the different lactose grades was varied when this pressure was kept constant suggesting the differences in the properties of the powders.

There are several examples of studies where these conditions were followed in order to test the deposition of dry powders in impactors and impingers. The deposition of spray dried disodium cromoglycate using a Marple Miller Impactor (MMI) was studied at a 4kPa pressure drop across the device [233, 495]. Inhalation delivery of peptides was studied using an MSLI using a Novolizer® Device. In order to obtain a 4kPa pressure drop across the device, the flow rate was increased to 70L/minute, appropriate for the device [484]. A study carried

out on spray dried tobramycin used different settings on the MSLI which included a higher flow rate (100L/minute) and a shorter duration (2.4 seconds). This was said to obtain a 4kPa pressure drop across the inhaler device, which was the same as when operated at 60L/minute for 4 seconds to achieve a 4kPa drop (Aerolizer®) [456]. Although this study used the spray dried formulation of the API, the flow rate and duration were different to what has been used for the Aerolizer® device in the current study. Although the same pressure drop is overall achieved, the differences in the deposition may be as a result of the increased flow rate causing an increased turbulence. A study carried out on PEGylated alginate nanoparticles, characterized using the Next Generation Impactor (NGI), and was carried out at 60L/minute for duration of 6 seconds and also by placing 15 mL of a specified buffer in each stage of the NGI. It can be suggested that this study may not be able to determine the accurate deposition profile of the nanoparticles due to the incorrect flow rate and duration of inhalation and presence of liquids in an impactor [234]. It was recommended by manufacturers and protocols provided that impingers contain solvents dispensed at the different stages, but this was not required in impactors. Studies have also been carried out to see the effect of different flow rates on the deposition of particles and the FPF, for example with salbutamol particles using polystyrene as carriers [473]. An inhalable form of rifapentine was studied using high flow rates of 100L/minute using an Aerolizer® device over the 4 second duration [496]. An increased flow rate showed an increased detachment of the active from the carrier, which may be due to the increased turbulence and velocity, as described.

The Aerolizer® device used in this study consists of two pins in the dosing chamber which, when pressed, pierce the capsule after which inhalation can cause high velocity collisions from which turbulence is further increased by the presence of a grid [469]. This is a simple, single dose device which was suitable for the powders formulated for this study. As specified, the flow rate is required to be 60L/minute for the duration of 4 seconds in order to achieve the 4kPa pressure drop across the device, as recommended by manufacturer and pharmacopeial guidelines [488, 489]. An alternative flow rate that can be used was 100L/min for 2.4 seconds which also causes a 4kPa pressure drop. The flow rate of 60L/minute was used as a constant flow rate for when nebulized suspensions were studied using the MSLI. This allows direct comparisons between the depositions of the nanoparticles using the two different formulations. There are many studies which use the Aerolizer® device and conduct the studies at a flow rate of 60L/minute.

The validity of these settings (60L/minute over 4 seconds using a Cyclohaler/Aerolizer® device to achieve a 4kPa drop) was supported by several studies. A deposition study carried out by Ong et al (2014) [454] on combined salbutamol and mannitol therapy was conducted

using an MSLI run at 60L/minute for 4 seconds using an Cyclohaler® device, in which FPF was calculated as cumulative content of drug deposited in the respiratory region (<6.4μm) studied using 40 mg of the powder [454]. The current study uses a similar quantity of dry drug powder (45 mg) for assessment of deposition. Another study on the deposition of a combination powder of fluticasone and salmeterol (with no carrier) from the same device was also carried out (using cell culture inserts) on a twin stage impinger at 60L/minute [497]. This flow rate and test duration was also applied when studying the deposition profile using an NGI and quercetin solid-lipid microparticles using an Aerolizer® device [498]. The MSLI apparatus was used to study the cellular uptake of the same microparticles using A549 cells using the same device, duration and flow rate [490]. Spray dried mannitol and ciprofloxacin powders were studied using an MSLI at 60L/minute for 4 seconds using an Cyclohaler (Aerolizer)® device [499, 500]. This study showed that the two drugs did not act as a binary formulation and acted as an independent system where the deposition profile of one drug did not affect the other drug [499, 500]. When delivering theophylline and budesonide together as co-encapsulated nanoparticles or as mono-encapsulated nanoparticles, it was important to understand if the deposition was affected by the presence of two drugs or one. In the current study it is predicted that the deposition profiles of theophylline and budesonide will be similar due to the two drugs being encapsulated in the nanoparticles together and not separately and therefore the deposition will be dependent on the nanoparticles, rather than the two drugs. This was observed from the results obtained in the current study using all the different grades of lactose. From the results obtained, it was understood that the deposition is mainly dependent on the type of lactose used and not the nanoparticles incorporated, i.e., it was independent of being a mono- or co-encapsulated nanoparticles sample. Similar to the results obtained for the nebulized suspensions.

Previous studies used different settings and conditions to characterize dry powders which can result in differences in the results obtained in comparison to the current study. In the current study of theophylline and budesonide nanoparticles, there were limitations when studying the deposition profile and therefore certain methods, such as, preparation of the nanoparticles as a dry powder mixture, was just carried out by tumble blending instead of a commonly used method, spray drying. Spray drying has been previously applied for sensitive molecules such as insulin and chitosan nanoparticles [235]. Tumbling blending has been previously suggested to allow achieving homogeneity and breaking of agglomerates. However, this method can lead to the formation of 'fines' which may affect deposition of the particles [460]. The particle size range of the nanoparticles in the current study of theophylline and budesonide nanoparticles would be considered as 'fines' as they are in a sub-micron range (between 200-500nm), and by carrying out the mixing process, the 'fines'

can adhere to coarse particles as a result of VdW's forces, electrostatic forces or capillary action, especially onto the active sites of the lactose carrier [466, 501]. SEM images however revealed that the agglomerates of the freeze dried nanoparticles were not fully separated for most mixtures, suggesting poor adherence between the carrier and nanoparticles. This however, was not seen in the mixtures produced by Lactohale® 300 and budesonide nanoparticles, suggesting a stronger interparticulate forces between the 'fines' of the lactose and nanoparticles. This suggests that in order to improve the mixtures, it is important to incorporate 'fines' of the carrier particles with coarse particles to obtain uniformity by adherence of the nanoparticles to the larger coarse carrier particles and 'fines' of the lactose. This can also be suggested by seeing the uniformity of mixing of the nanoparticles and Respitose® ML001 samples which contains a broad size distribution.

In the current study, limited characterization was carried out on the nanoparticles. The doses were preferred to be individually prepared for each capsule as it was a preliminary study to understand the deposition of the nanoparticles and for this reason the concentration was based on the nanoparticles and not the drugs. Dosing based on the drugs encapsulated would result in extremely large concentration of freeze dried nanoparticles required. The concentration of 1 mg/mL as the nebulized suspension was chosen as it was also shown to be safe when 16HBE14o- cells were treated (Chapter 4). As the doses were individually prepared to fill the capsules, the total quantity of the DPI formulation was only 45 mg for each capsule. This amount was too small to do characterization on the flow properties of the powder mixture. Due to the properties of the nanoparticles, it was also very difficult to determine the size using established methods and techniques such as DLS, sieve analysis and time of flight. Some of these techniques involve the use of organic solvents, which as a result would affect the polymer, PLA, leading to the drugs being released. The lactose grades that were used in this study had powder flow tests conducted by the commercial suppliers. These tests showed that Respitose® ML001 and ML006 had poor flow. Lactohale® 300 was reported to have the poorest flow properties [461, 502]. It was selected in the current study due to the small particle size of the carrier molecules which may have been suitable when mixed with the submicron sized theophylline and budesonide PLA nanoparticles.

The concentration of 5 mg of nanoparticles (1 mg/mL for nebulized suspension) was thought to be suitable for the current study. It is thought that delivery of drugs by the pulmonary route to act locally and be effective, concentrations administered can be low and with the use of sustained release of the drugs from nanoparticles, an increase in concentration at deposited site can be obtained over the time period [41, 463]. The total

quantity of dry powder used in the current study was 45 mg (lactose and nanoparticles). Quantities of dry powders (of pure drug, mixed in carrier or colloidal particles) that were used in previous studies ranged from 10 mg (of microparticles [498]) to 30 mg [490, 499, 500, 503]. Inhaled rifapentine was studied using 10 mg of powder suggesting that inhalable antibiotics required higher concentrations [496].

Due to the differences in the initial loading concentrations of the drugs in mono- and co-encapsulated nanoparticles, the data was expressed as percentage of the initial loading concentration. For the uniformity of mixture, an average was obtained for each, and the percentage variation was calculated to show how uniform the samples were. It is difficult to follow the strict guidelines of the pharmacopeial requirements for the uniformity of mixture due to several reasons. For example the drugs are encapsulated in nanoparticles, and not present as a free drug form mixed in the carrier mixture, and therefore it is expected that the concentration of theophylline and budesonide calculated will be lower than the original concentration. The reason being it depends on how much drug is released and how much drug is encapsulated. For this reason, the percentage variation is used as an indicator to determine variation within a sample. The uniformity of mixing depends on the powder flow properties and for this current study it is thought that samples presenting variation over 50% would suggest that there is difficulty in obtaining a uniform mixture of the nanoparticles and the lactose powders and they do not mix well. It is important to take into consideration that the loading concentration of theophylline and budesonide will also have a certain amount of variation which would affect the concentration obtained in a random aliquot.

From the different lactose grades used, Lactohale® 300 presented the greatest amount of variation in the samples. The large presence of 'fines' in this sample can suggest inefficient mixing and adherence between nanoparticles and the lactose powders, resulting in regions with a high concentration of nanoparticles and regions with drug absent. The powder is highly cohesive with a particle size range similar to actives agents and for this reason; adherence of the nanoparticles uniformly would be difficult. As discussed, this lactose grade has previously shown to have the poorest flow properties.

The variation in Respitose® ML001 samples was the lowest in comparison to the other lactose and nanoparticles powder mixtures studied. Respitose® ML001 lactose particles contain a broad size distribution and this could result in the freeze dried nanoparticle agglomerates being able to adhere to the different sized lactose particles.

Lactohale® 201 and Respitose® ML001 both contain a broad size distribution with presence of 'fines' and this as a result can affect the adherence of the nanoparticles to the

lactose powders. Furthermore, Lactohale® 201 also has irregular shaped particles which can also affect how nanoparticles adhere to the surface of lactose. Variation in the uniformity of content was observed when assessing the powders using SEM with regions concentrated in nanoparticles and regions containing no nanoparticles. Presence of irregular surfaces also provides an increased number of regions where nanoparticles can adhere to the lactose carrier.

Poor flow properties of lactose can affect the amount of drug that is discharged from the capsule after actuation. This theory was observed in powder mixtures prepared using Lactohale® 300, where a large quantity of nanoparticles remained in the capsule after actuation. This explanation is further supported when a low quantity of nanoparticles were detected in the capsule after actuation of the dry powder mixtures containing Respitose® ML001 (approximately 80% of the powder was emitted from the capsule). The uniformity of mixing, which was also presented to be favorable, further suggests good flow properties for Respitose® ML001 in comparison to the cohesive, Lactohale® 300.

From the results obtained using the dry powder mixtures, the greatest deposition of the powders was achieved in the throat and stage 1 of the MSLI, where the particle size of the dry powders would be greater than 6.8µm (cut off diameter for stage 1 is 13.0µm). The target site for the treatment of asthma and COPD is the upper airways, and therefore this would be beneficial to have a greater deposition of particles in the stages 3-4 allowing treatment locally, where desired particle size is between than 6.8-1.7µm, for successful airway deposition. COPD however does affect the alveoli too. Some replicates show a low amount of deposition to the 5th stage of the MSLI (where particle size is <1.7µm). In comparison to the nebulized suspension of theophylline and budesonide nanoparticles, the deposition of the dry powders is mainly in the upper airways. It was noted that the deposition profile of ciprofloxacin and mannitol showed high deposition in the throat stage of the MSLI suggesting the unsuccessful de-agglomeration of the powder as could be the case with theophylline and budesonide nanoparticles [499].

When the particles are delivered as a nebulized suspension, they deposit in the stages 3-4, but the unsuccessful deposition of the dry powders (in stages 2-4) due to the large quantity recovered in the throat and stage 1 of the MSLI suggest unsuccessful detachment of the nanoparticles from lactose. The study showed that 5 minutes of nebulization shows a large distribution of the drug in all stages of the MSLI with minimum deposition in the throat and stage 1. A large quantity (approximately 50%) of drug calculated is in the device which was mainly due to not all the 5mL being tested was nebulized in the time the experiment was run. To overcome loss of drug as a result of it remaining in the device after nebulization

time, the concentration of the nanoparticles in the suspension can be increased. From previous cytotoxicity study, up to 2.5 mg/mL showed non-significant reduction in viability (compared to the control cells) (Chapter 4), and therefore this concentration can be increased, and the volume of the suspension can be reduced. The prescribed dose of budesonide ranges from 100-200 μg per metered dose actuation and therefore, suggestions on increasing concentration would be appropriate to carry out as a low concentration was deposited below stage 2 (approximately 10 μg). The time for nebulizing the suspension would be required to be optimized in order to understand how to achieve targeted drug delivery (to the upper respiratory tract).

In some of the replicates carried out for the dry powders formulated with lactose carrier particles, the total percentage recoveries are low. A possible explanation for this could be incomplete release of drugs from the nanoparticles or the presence of lactose in the powder mixture affecting the release of drugs from the nanoparticles. Drug loss in transfer of the samples may lead to low recoveries. In some cases, where over 100% of the drug is calculated, this could be as a result of the variation in drug loading of the samples; which was observed in Chapter 2 when the loading efficiency of theophylline and budesonide was calculated.

To improve the formulation of the nanoparticle-lactose powders, it would be ideal to include 'fines' in the mixture with larger particles of lactose and study the deposition profiles of these particles. The method can be further improved by forming a large, bulk quantity of the powder which can be optimized and studied for deposition profile. By producing a bulk powder in a large quantity, it allows the powders to be characterized by the various powder flow tests that would be essential. By knowledge of the different characteristics of lactose and nanoparticles mixed powders, the flow properties of these powder mixtures can be modified either by the addition of 'fine' carrier particles or by the addition of glidants such as magnesium stearate. As discussed earlier, it can be seen that the deposition of the nanoparticles is independent of the drugs encapsulated and mainly depends on the properties of the lactose as a consistency is observed where the deposition of the nanoparticles is greatest in the throat and stage 1 and not in the lower stages of the MSLI. Lactohale® 201 and Respitose® ML006 presented similar results suggesting the similarity in the lactose grades as a result of the broad particle size distribution of the lactose carrier. High concentration of drug calculated in the capsule for Respitose® ML006 can also suggest poor flow properties of this lactose grade and poor mixing. The variation in uniformity of mixing was high for the dry powder mixtures synthesized using this lactose grade.

It is important to understand the flow characteristics of the lactose or carrier particles that are used. Some studies of dry powders for use in inhalers measure tapped density, bulk density, Carr's Index and flow angles [210, 470]. These tests suggested that large sized lactose particles of different shapes had poor flow properties, which could affect the uniformity of dose in the drug-carrier particle. However, it was later observed that large particles had good uniformity of dose due to drug being embedded into crevices which resulted in improvement in the deposition profile [470]. A similar observation was made in the current study with Respitose® ML001 and Lactohale® 201. As suspected, the nanoparticles were embedded into crevices which suggested poor detachment efficiency. As the nanoparticles are embedded in crevices, this may affect the release of the drug and therefore lead to low recoveries of the drug as was seen for some samples formulated using Respitose® ML001(approximately 50%). Therefore, this situation may not be ideal in delivering consistent doses. Lactohale® 300 powder mixtures showed increased de-agglomeration when flow rate was increased in a study by Behara et al (2011) [483]. But in the current study the flow rate was kept constant at 60 L/min to meet pharmacopeial requirements. Due to the low recovery rates obtained for theophylline and budesonide from some of the powder mixtures this method could be further improved by determining the content of lactose deposited in each stage of the MSLI too. This has previously been investigated using gamma scintigraphy [457].

In studies reported in the literature, the effect of the addition of 'fines' of carrier particles to the deposition of active was shown to be unclear. The work carried out by Kho et al (2013) suggested that addition of 'fines' caused no improvement in the deposition and FPF [470]. From the Lactohale® and Respitose® grades chosen, some grades had a narrow size distribution. Wider size distribution would result in a larger proportion of 'fines' potentially affecting the deposition of the nanoparticles [460]. However it is difficult to determine this effect accurately from the current study due to the low recovery dose obtained for some of the samples and the grades of lactose used. As discussed by Kinnunen et al (2014), the inclusion of 'fines' showed that the deposition of active was seen to be improved using Lactohale® 300 and milled Lactohale® 210. For theophylline and budesonide nanoparticles, in the current study, the deposition was greatest in the upper stages of MSLI (>6.8µm) [471]. It is seen that 'fines' are usually added as ternary agent rather than using a lactose grade consisting of only 'fines' [504, 505]. For this reason, theophylline and budesonide nanoparticles deposition and formulation of a successful powder mixture was not achieved fully with Lactohale® 300. As mentioned previously, the use of computational fluid dynamics (CFD) is able to show that there is never complete dispersion of the powder into the airways, as obtained for the current study [477].

6.4.3 FORMULATION OF A NEBULIZED SUSPENSION AND CHARACTERIZATION USING THE MSLI

While many studies have utilized the DPI formulation due to the advantages provided, for example stability, to deliver nanoparticles by the pulmonary route, Pandey et al (2003) formulated PLGA nanoparticles encapsulating anti-TB drugs and delivered them via a nebulizer formulation [506]. Azarmi et al (2008) reviewed the successful deposition of drugs encapsulated in nanoparticles when delivered by a nebulized suspension [374]. This review highlighted the use of (biodegradable) polymeric nanoparticles delivered via a surfactant free nebulized suspension [374]. This suggested the use of minimal use of excipients to prepare suspensions similar to the current study, where reconstitution of the freeze dried nanoparticles before administration was thought to be ideal. Chitosan-modified surface PLGA nanoparticles (containing calcitonin) were also delivered using a nebulizer formulation showing therapeutic effects [212, 374]. SiRNA- chitosan nanoparticles were prepared as a nebulized suspension were studied using a twin stage liquid impinger showing successful deposition of nanoparticles (>50%) in stage 2, where particle size is <6.4μm [314]. In the current study, theophylline and budesonide nanoparticles did show a difference in the deposition profiles when delivered as a dry powder compared to a nebulized suspension. As discussed, dry powders showed a large deposition in the throat and stage 1 of the MSLI where the particle size of the deposited particles would be greater than 6.8μm suggesting unsuccessful deposition to the target site of asthma and COPD. The use of the nebulizer showed successful deposition where the particle size is less than 6.8μm. However, as a large quantity of the nebulizer suspension remains in the device, the concentration of the suspension can be increased in order to obtain a suitable therapeutic dose. As approximately 50% of the suspension remained in the device after nebulization had taken place, the volume can also be reduced to prevent drug wastage.

Successful deposition and sustained release of the drugs can be achieved with nebulized suspensions of nanoparticles, but it is important to obtain a chemically and physically stable suspension which can be used for pulmonary drug delivery.

The FPF for budesonide was reported to be 22.7% when included in a dry powder mixture of Lactohale® 210 and Lactohale® 300 [471]. Most of this was reported to deposit on stage 2 of the NGI (operated at 90L/minute for 2.7 seconds). It was suggested that the agglomeration of budesonide and 'fine' particles was greater in improving the DPI performance. In another study carried out using the Aerolizer® as a device, containing budesonide and formoterol in a single capsule showed a FPF of 54% (at 90L/minute using an Anderson cascade impactor) [507]. Budesonide was seen to have stronger cohesive forces

than lactose in a study, as stated by Jaffari et al (2013) [482]; which may also suggest possible reasons for the low recovery of budesonide.

Although it is possible to deliver nanoparticles (and encapsulated drugs) to the lung, it is important to note the limitations of using nanotechnology in drug delivery via the pulmonary route. This includes difficulty of large scale production, variability and reproducibility between batches which can lead to variable lung deposition profiles [508].

From the deposition profile of theophylline and budesonide observed in this study, it is important to keep in mind that for the treatment of asthma and COPD, the deposition of inhaled corticosteroids should be in the peripheral region and for bronchodilators in the smooth muscle region [465]. *In vitro* studies give a good indication of the deposition profiles, but do not reflect any airway changes caused due to diseased states (e.g. collapsed airways in COPD patients).

6.5 CONCLUSIONS

The aim of this portion of the study was to investigate the *in vitro* deposition profiles of theophylline and budesonide co- and mono-encapsulated nanoparticles using a nebulized suspension and dry powders as the choice of the formulations. The deposition profiles were obtained using an MSLI. With nebulized suspensions of the nanoparticles, successful deposition was achieved in the region of stages 3-4 (where particle size was required to be 6.8-1.7μm) with a good overall recovery of the nanoparticles obtained. Dry powder formulations were synthesized using different grades of lactose. In conclusion, successful deposition in the stages 3-5 was not achieved. The greatest deposition of the nanoparticles was instead observed in the throat and stage 1 of the MSLI. A fine particle fraction (FPF) of approximately 10-15% was obtained for these powders, further suggesting poor deposition of the particles when particle size is <6.8μm. It is thought that with the addition of 'fine' carrier particles, the properties of the powder could be improved; Respitose® ML001 showed the best uniformity of mixing which was reflected calculating the percentage dose emitted (over 80%). From the deposition profiles obtained, it can be concluded that the deposition profile was dependent on the lactose properties.

There were several limitations in this part of the study. The methodology applied here was a preliminary study but would require many aspects to be improved in order to obtain a more accurate deposition profile. This would include changing the solvent being dispensed in the MSLI to pure organic solvents, for example 100% methanol which could improve the detection limits for budesonide, as the recovery in some samples was shown to be low. Additionally, formulating a bulk powder would be preferred which would require dosing to be based on the concentration of the drugs encapsulated and not the quantity of nanoparticles used. Forming a bulk powder would allow improved characterization of the dry powders for inhalers, e.g. powder flow testing and particle size testing. The effect of different flow rates and different inhalers could also be studied.

Overall, it can be concluded that the nebulized suspension of the nanoparticles was the most suitable formulation for theophylline and budesonide encapsulated PLA nanoparticles. In order to improve the concentration of the drugs deposited, a higher concentration of nanoparticle suspension could be used as well as increased duration of inhalation.

CHAPTER 7 STABILITY TESTING OF THEOPHYLLINE AND BUDESONIDE PLA NANOPARTICLES

7.1 INTRODUCTION

The use of nanoparticles can be extended to numerous applications and in various formulation types. In order to use the nanoparticles as a formulation for pulmonary drug delivery it is important to evaluate their long term stability. This is necessary to determine the shelf life of the product, which is mandatory for active pharmaceutical ingredients as well as for the final formulation. Based on the ICH (International Conference on Harmonization) guidelines, determining the long term stability of a product is '*to provide evidence on how the quality of a drug substance or product varies with time under the influence of a variety of environmental factors such as temperature, humidity, and light*' [509].

The ICH guidelines for long term stability testing are based on the analysis of the effects of the drug substance or product in different climatic conditions and are based on three principle regions. For long term studies, the frequency of testing is recommended to be sufficient to determine the stability profile of the drug substance. The guidelines specify conditions for 12 months testing (with a re-testing period) and accelerated study to be carried out for 6 months. The accelerated storage conditions require a minimum of three time points. Intermediate conditions are applied if a significant change occurs during accelerated study.

The storage conditions that are recommended for evaluation of stability are those that are able to test the thermal stability of the product (and, if applicable, the sensitivity to moisture/humidity). The conditions recommended by the ICH guidelines are shown in Table 7.1.

Table 7.1 Storage conditions of a drug substance and the time period that should be covered. Table is reproduced from the ICH guidelines on Stability testing of new drug substances and products (RH: relative humidity) [509]

Study	Storage condition	Recommended testing period
Long term	25°C ± 2°C/60% RH± 5% RH and/or 30°C ± 2°C/65% RH± 5% RH	12 months
Intermediate	30°C ± 2°C/60% RH± 5% RH	6 months
Accelerated	40°C ± 2°C/75% RH± 5% RH	6 months

There are also recommendations on the storage conditions if the drug substance is intended for storage in at 2-8°C. The time period of study should be 12 months for a long term stability testing at 5°C ± 3°C/60% RH± 5% RH but an accelerated study of this would be for a duration of 6 months at 25°C ± 2°C/60% RH± 5% RH[509].

Limited information is available on the 'long term' stability study of nanomaterials. It was also noted that the definition of long term and duration of studies on nanoparticles was different. According to the ICH guidelines, 'long term' was defined as 12 months. In this current study, 6 months was used as 'long term' and in several studies reported, 6 months was classified as long term [510, 511]. As nanoparticles have a wide range of potential applications, it is important to ensure that nanoparticles retain their stability in their application-associated environment [512].

The application of stability studies has been noted to be different for nanoparticles. While some studies consider the stability of the nanoparticles in suspension in comparison to the freeze-dried nanoparticles [513-515], other studies have considered the stability of nanoparticles as freeze-dried formulations and improving the stability by addition of cyro-protectants during the freeze drying process [513, 514]. However, some stability studies have been conducted to determine the long term stability of the nanoparticles over a period of time with characterization of the nanoparticles at time zero (t=0) and at the pre-determined storage time point. Disadvantages of nanoparticles present in suspensions include drug release and hydrolysis of the polymer. Acidification of the medium (as a result of polymer hydrolysis) can lead to catalytic hydrolysis of the polymer backbone [516]. Freeze drying of nanoparticles ensures long term stability of the nanoparticles [517, 518].

Stability of the nanoformulation can be determined by studying its physical stability. For example, if nanosuspensions are used then to study the coalescence and agglomeration over a period of time. Stability studies can also include examining the chemical stability, which accounts for degradation of the drug or polymer (depending on the storage conditions, e.g. changes in temperature or pH).

In a review by Abdelwahed et al (2006), long term stability was described as studying the chemical and physical stability of the nanoparticles [515]. The review states the ICH guidelines of storage conditions and duration to be ideal. For the nanoparticles, determination of particle size, zeta potential and drug loading should be evaluated in order to determine any instability [515].

7.1.1 AIM OF THE STUDY

The aim of the study was to evaluate the stability of the nanoparticles over a period of 6 months at different storage conditions, which were: 2-8°C, room temperature (21-25°C) and 40°C and to subsequently determine the most suitable storage conditions for the synthesized theophylline and budesonide nanoparticles. In order to achieve this, the nanoparticles were characterized at regular time points in order to establish whether any changes had occurred during the storage period. Characterization tests performed were particle size, surface characterization by zeta potential analysis and FT-IR spectroscopy, morphological assessment using SEM, thermal analysis using DSC and determination of loading efficiency. Any variation obtained in the data would affect the confidence in the sample [509]
.

7.2 MATERIALS AND METHODS

7.2.1 MATERIALS

18.2MOhms deionized water

Dichloromethane, Fisher Scientific, UK (D/1856/17)

Acetone, Fisher Scientific, UK (A/0606/17)

Ethanol (absolute), Fisher Scientific, UK (E/0650DF/17)

Morphological assessment:

SEM Specimen Stubs (aluminum), 12.5mm diameter, 3.2 x 6mm pin, AGAR Scientific, United Kingdom (AGG301F)

Carbon adhesive double sided disc/tape (Leit Adhesive Carbon Tabs) for SEM stubs, AGAR Scientific, United Kingdom (AGG3347N)

Particle size and zeta potential analysis:

Disposable plastic UV cuvettes, Plastibrand (2.5-4.5mL), Fisher Scientific, UK (Product code: 10046731)

Folded capillary Malvern Zetasizer 'Zeta cell' , Malvern Instruments, UK (DTS 1061)

Differential scanning calorimetry (DSC):

Aluminum crucibles (without pin) (40µL) (case containing pan and lids), Mettler Toledo, UK (ME-26763)

High performance liquid chromatography (HPLC):

2mL crimp top clear Chromacol Vials- Autosampler Vials crimped (2CV-P220)(Lot: 70734807114), Thermoscientific, Germany

Chromacol 11mm crimp cap- Rubber/ PTFE Type 7 Rubber Lot 9132010752

Acetonitrile (HPLC grade), Fisher Scientific, UK: Lot 1346198

Formic acid (90%), BDH Laboratory supplies, England: Lot 2442640729

Methanol (HPLC grade), Fisher Scientific, UK: Lot: 1493729 (Code: M/4056/17)

7.2.2 METHODS

7.2.2.1 SYNTHESIS AND CHARACTERIZATION OF THEOPHYLLINE AND BUDESONIDE MONO- AND CO-ENCAPSULATED NANOPARTICLES

The nanoparticles were prepared using Method 8 described in Chapter 2, Section 2.2.2.1. At each time point, the nanoparticles were characterized. Complete details for the characterization methods are provided in Chapter 2, Section 2.2.2.2. The characterization tests that were carried out are:

- Particle size measurement (Chapter 2, Section 2.2.2.2.1)
- Zeta potential measurement (Chapter 2, Section 2.2.2.2.1)
- Morphological assessment using SEM (Chapter 2, Section 2.2.2.2.2)
- Surface characterization using FT-IR (Chapter 2, Section 2.2.2.2.3)
- Thermal analysis using DSC (Chapter 2, Section 2.2.2.2.4)
- Determination of loading efficiency of theophylline and budesonide using HPLC (Chapter 2, Section 2.2.2.2.6)

7.2.2.2 SAMPLE PREPARATION FOR STABILITY TESTING OF NANOPARTICLES

Three different conditions were chosen for the stability testing of the nanoparticles which were: room temperature (21-25°C), refrigerator (2-8°C) and oven (40°C). Aliquots (5-10 mg of freeze dried nanoparticles) were prepared for both co- and mono-encapsulated nanoparticles and weighed accurately into beakers and placed in the different storage conditions, undisturbed for the required time periods. The samples were sealed with the use of Parafilm® (and foil for storage at 40°C) and stored away from light. The samples were characterized at time 0 (0 months) (t=0), 1 month (t=1), 3 months (t=3) and 6 months (t=6). Samples stored at 2-8°C or at 40°C were removed from their storage conditions to take an aliquot for a specific characterization test and returned immediately to their storage conditions.

7.2.2.3 STATISTICAL ANALYSIS

To determine if the changes in the particle size, zeta potential and loading efficiency as a result of storage temperature and the duration of the storage were significantly different from the data obtained at t=0 , 2way ANOVA was carried out. $P<0.05$ suggests a significant difference. A Bonferroni post hoc test was carried out for this statistical analysis.

7.3 RESULTS

7.3.1 MORPHOLOGICAL ASSESSMENT USING SEM

Morphological assessment of mono-encapsulated theophylline and budesonide nanoparticles was carried out using SEM. SEM images for all the nanoparticles are shown in Figure 7.1, 7.2 and 7.3. Samples analyzed at t=1, 3 and 6 months after storage at 2-8°C and room temperature did not show any remarkable difference from the features of the nanoparticles at t=0. These features include the spherical shape and smooth surface. Samples stored at 40°C showed a loss of these features, and suggest that the polymer has lost its integrity.

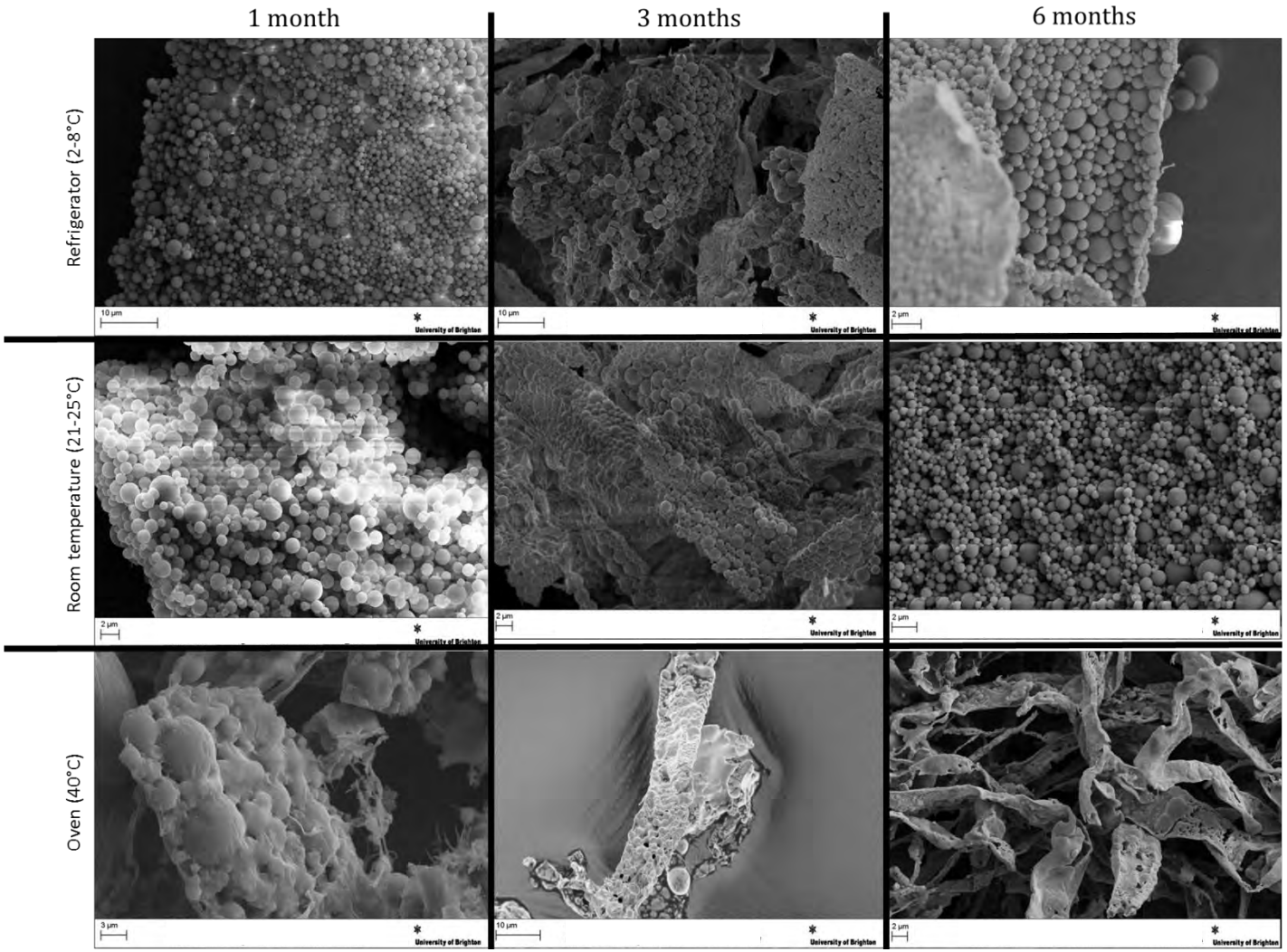

Figure 7.1 SEM images of theophylline mono-encapsulated nanoparticles stored at 2-8°C, room temperature and 40°C obtained at 1 month, 3 months and 6 months to understand changes in the morphological features of the nanoparticles

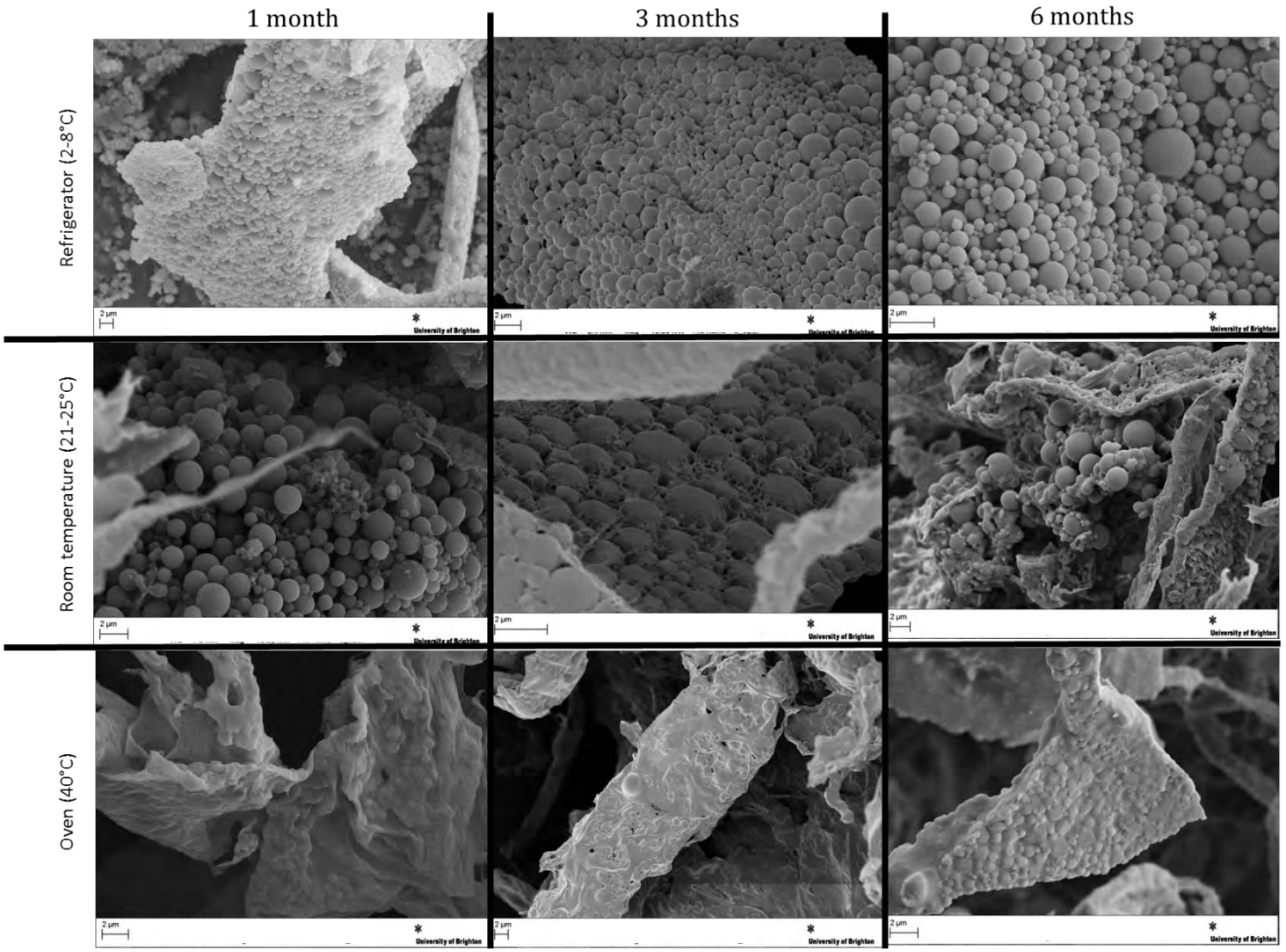

Figure 7.2 SEM images of budesonide mono-encapsulated nanoparticles stored at 2-8°C, room temperature and 40°C obtained at 1 month, 3 months and 6 months to understand changes in the morphological features of the nanoparticles

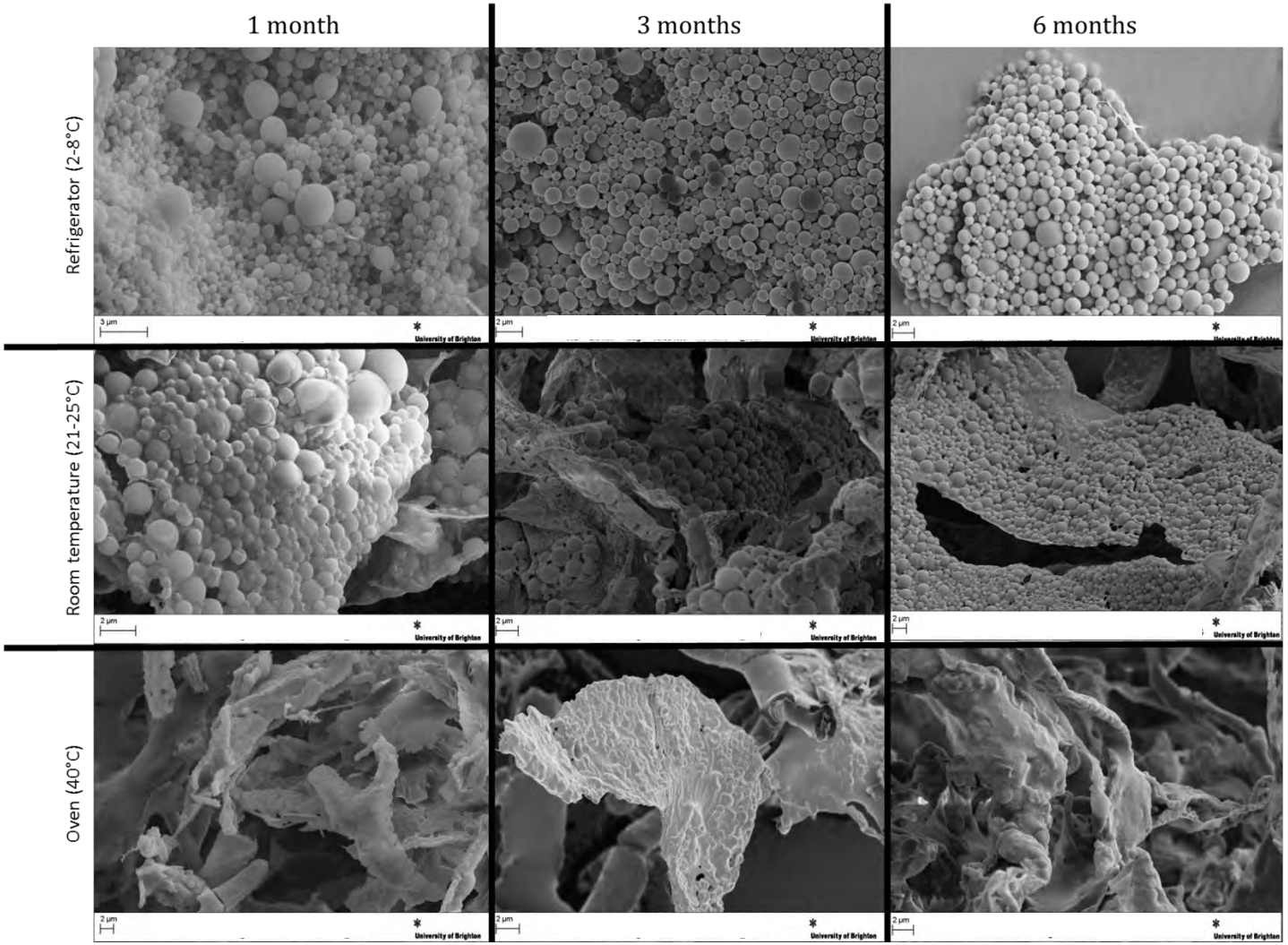

Figure 7.3 SEM images of co-encapsulated nanoparticles stored at 2-8°C, room temperature and 40°C obtained at 1 month, 3 months and 6 months to understand changes in the morphological features of the nanoparticle

7.3.2 SURFACE CHARACTERIZATION USING FT-IR

FT-IR allows determining if there is any drug adsorbed on the surface of the nanoparticles. Characterization of the nanoparticles by FT-IR at t=0 suggested that there was no drug adsorbed on the surface of the nanoparticles. This was indicated by the absence of characteristic drug peaks in the spectra for the nanoparticles and resemblance only to the PLA spectrum. The polyester, PLA, has an ester bond in the region of 1746cm^{-1}. C-O stretches are also seen in the region of 1100-1400cm^{-1}. Peaks at 3500cm^{-1} represent OH bonds present and a broad peak at 2960cm^{-1} are representative of the C-H bonds present in the structure of PLA (Chapter 2, Figure 2.1A). Figure presented here is for the co-encapsulated nanoparticles over the period of 6 months under different storage conditions (Figure 7.4). Mono-encapsulated nanoparticles are shown in Appendix 3: Chapter 7: Stability testing of theophylline and budesonide PLA nanoparticles .

Samples stored at 2-8°C for 1 month show similarity to the FT-IR spectra of nanoparticles at t=0. A large broad peak at 3303cm^{-1} suggests background reading of CO_2 and H_2O. An ester stretch at 1750cm^{-1} is characteristic of the polymer and there are no drug peaks present in the spectra. Similar spectra to t=0 was obtained for samples stored at room temperature and assessed after 1 month. In the spectrum for co-encapsulated nanoparticles, there is an additional peak at 1666.66cm^{-1} which is a peak present in both theophylline and budesonide drug standards (representing the C=C bond). In Chapter 2 (Figure 2.1D), this peak is present in the free drug and polymer mixed standards.

For samples stored for t=3 months the nanoparticles stored at three different storage conditions shows resemblance to the PLA spectra. However, a reduction in the intensity of the ester peak of PLA is observed for the samples stored at room temperature and at 40°C. Samples stored at 2-8°C for t=6 months show no difference in the spectra over the period of time and resemble the PLA spectrum. A large difference in spectrum is observed for the samples stored at room temperature where the intensity of the PLA ester bond is reduced and peaks representing both theophylline and budesonide appear in this spectrum (Chapter 2) at t=6 months. Spectra largely resembling the PLA spectrum are observed for the samples stored at 40°C.

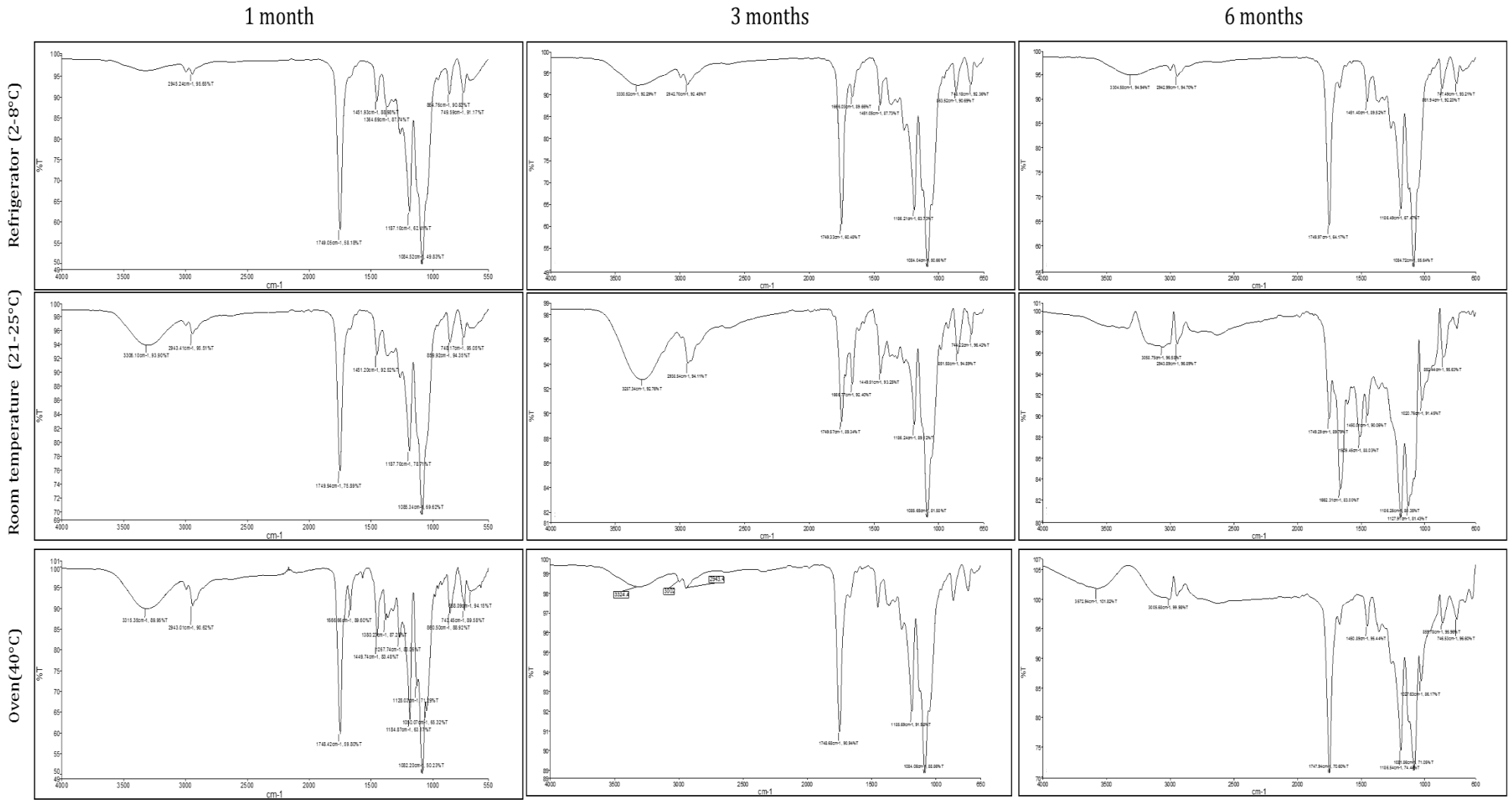

Figure 7.4 FT-IR spectra of co-encapsulated theophylline and budesonide nanoparticles stored at 2-8°C, room temperature and 40°C at 1 month, 3 months and 6 months period to observe any changes in the surface characteristics of the nanoparticles

7.3.3 THERMAL ANALYSIS USING DIFFERENTIAL SCANNING CALORIMETRY (DSC)

Differential scanning calorimetry (DSC) was used to determine if there are any changes in the nanoparticles over the period of 6 months when placed at different storage conditions. Melting points for theophylline (Chapter 2, Figure 2.3A) and budesonide (Chapter 2, Figure 2.3B) are observed at 271.46°C and 260.48°C, respectively. Thermogram for the PLA shows an exothermic peak in the region of 44.87°C which represents the glass transition phase (Chapter 2, Figure 2.3C). PLA changes its state from a glass to rubbery state at this temperature increasing the temperature to over 200°C results in a large, broad exothermic peak at approximately 360°C which represents degradation of the polymer. At t=0, the thermogram obtained for drug encapsulated nanoparticles (Chapter 2, Figure 2.3D) indicated an absence of the drug peaks and only resemblance to the polymer peak's thermogram. The thermograms presented are for co-encapsulated nanoparticles at various time points at the different storage conditions (Figure 7.5).

At t=1 month, the nanoparticles stored at all the different storage conditions showed the presence of a glass transition state of the polymer, PLA. In comparison to the nanoparticles stored at lower temperatures, nanoparticles stored at 40°C showed a peak of less intensity at the glass transition temperature peak. At t=3 months, similar (to t=1) thermograms are obtained for the samples at different storage conditions. The glass transition peaks are seen to be smaller than the other samples in comparison to the t=0 data and for samples stored at 40°C. For nanoparticles stored for 6 months (t=6), samples showed an even smaller peak for the glass transition phase for the PLA especially for nanoparticles stored at 40°C in comparison to the other temperatures and at t=0. The large degradation peak is present in the samples stored at 2-8°C over the period of 6 months, but is varied for the samples stored at room temperature and at 40°C.

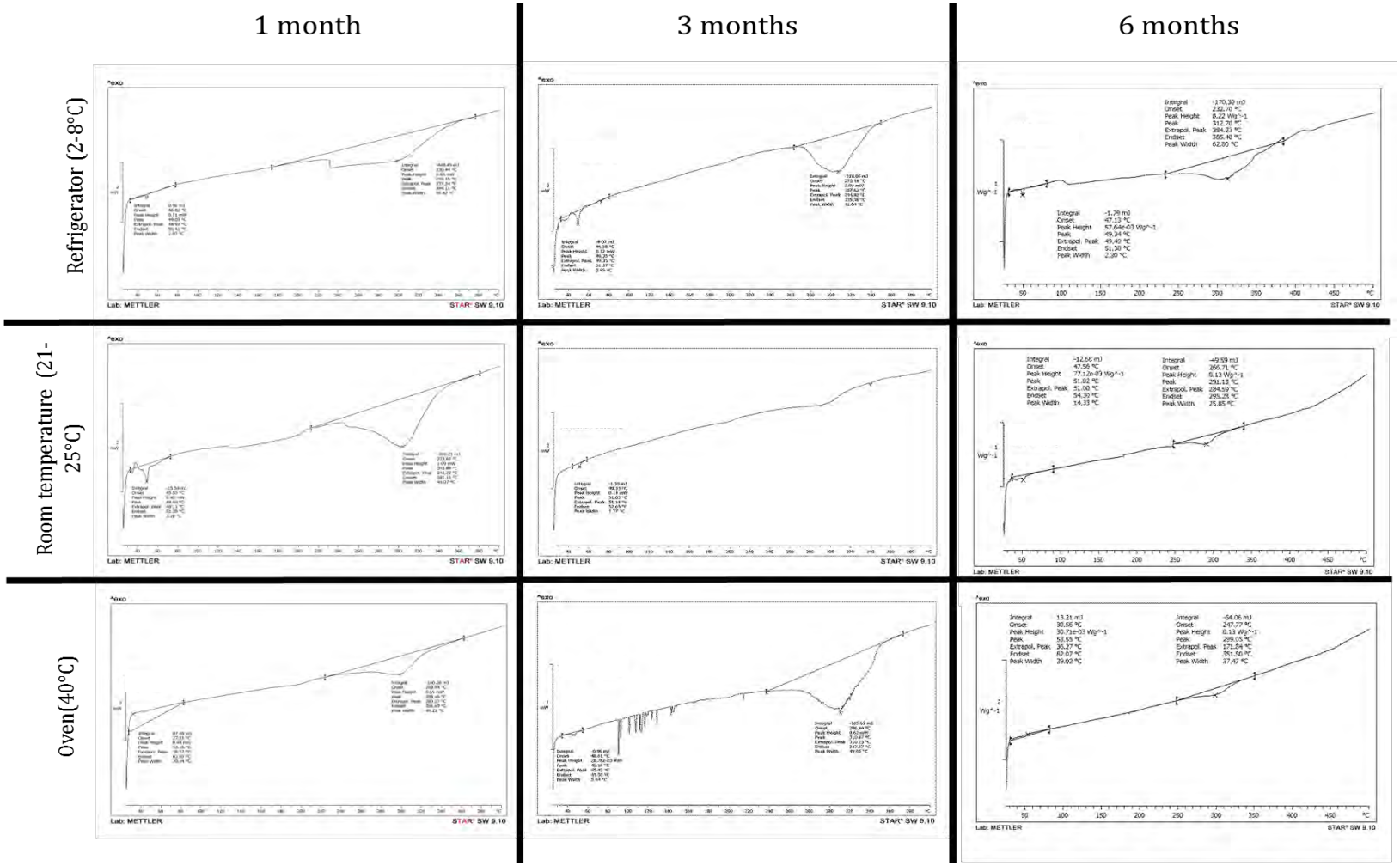

Figure 7.5 DSC thermograms of co-encapsulated theophylline and budesonide nanoparticles stored at 2-8°C, room temperature and 40°C samples for 1 month, 3 months and 6 months.

7.3.4 DETERMINATION OF PARTICLE SIZE AND ZETA POTENTIAL

The average particle size and zeta potential of theophylline and budesonide mono- and co-encapsulated nanoparticles was measured at t=0 (Table 7.2). Overall, for all the drug encapsulated nanoparticles, there was no pattern in the change in particle size over the period of 6 months from t=0. Although the average particle size obtained for theophylline nanoparticles showed some significant differences to t=0 (for example when stored at room temperature) there was overall no increase in the average particle size at t=6 ($P>0.05$) (Table 7.3). Similarly, for budesonide mono-encapsulated nanoparticles (Table 7.4), there was no significant change in the size of the nanoparticles when stored at 2-8°C and room temperature over 6 months in comparison to t=0 ($P>0.05$). With the exception of co-encapsulated nanoparticles stored at 40°C ($P<0.05$), similar results to the mono-encapsulated counterparts were obtained at the different temperature compared to t=0 ($P>0.05$) (Table 7.5).

Similar to the changes in particle size, there was also no pattern in the changes of zeta potential over the period of 6 months compared to t=0. Due to the small amount of variation for the zeta potential obtained, the differences in the average zeta potential over the period of 6 months was seen to be significantly different for theophylline mono-encapsulated nanoparticles stored at the three different storage conditions ($P<0.05$) (Table 7.3). The differences in the zeta potential obtained for the different storage conditions were also on average seen to be significantly different ($P<0.05$). Despite these significantly different values obtained, there is no pattern in the changes of the average zeta potential over the period of 6 months but all the average zeta potentials measured are negatively charged as t=0. Similar results are obtained for budesonide mono-encapsulated nanoparticles (Table 7.4) and co-encapsulated nanoparticles (Table 7.5). It is observed that the variation in the zeta potential for the samples stored at 40°C shows a greater variation in comparison to the nanoparticles stored at 2-8°C and at room temperature.

Table 7.2 Average particle size and zeta potential of theophylline and budesonide mono- and co-encapsulated nanoparticles at t=0

Sample	Theophylline mono-encapsulated nanoparticles	Budesonide mono-encapsulated nanoparticles	Co-encapsulated nanoparticles
Average particle size ±SD (nm)	210.25±56.57	208.13±100.43	191.25±23.72
% RSD	26.91	48.25	12.40
Average zeta potential ± SD (mV)	-15.38±5.85	-16.25±4.86	-13.12±3.27
% RSD	38.07	29.92	24.92

Table 7.3 Particle size and zeta potential obtained for theophylline mono-encapsulated nanoparticles stored at 2-8°C, room temperature and 40°C and measured at 1 month, 3 months and 6 months (n=9, mean±SD) (*P<0.05)

Theophylline nanoparticles Month	Temperature	2-8 (°C)		25 (°C)		40 (°C)	
		Size (nm)	**Zeta potential (mV)**	**Size (nm)**	**Zeta potential (mV)**	**Size (nm)**	**Zeta potential (mV)**
1	Average± SD	177.07±15.91	-8.57±2.55*	95.07±52.59*	-9.55±1.87*	141.70±32.39*	-9.38±0.12*
	%RSD	8.98	29.75	55.32	19.58	22.85	1.24
3	Average± SD	111.76±46.58*	-8.70±1.05*	470.15±51.00*	-6.10±0.70*	145.80±34.37*	-3.49±0.85*
	%RSD	41.68	12.10	26.86	11.51	23.57	24.49
6	Average± SD	185.65±62.01	-7.53±1.24*	156.43±49.41*	-8.18±0.54*	179.77±83.39	-13.83±1.57
	%RSD	33.40	16.52	31.58	6.57	46.39	11.35

Table 7.4 Particle size and zeta potential obtained for budesonide mono-encapsulated nanoparticles stored at 2-8°C, room temperature and 40°C and measured at 1 month, 3 months and 6 months (n=9, mean±SD) (*P<0.05)

Budesonide nanoparticles Month	Temperature (°C)	2-8 (°C)		25 (°C)		40 (°C)	
		Size (nm)	**Zeta potential (mV)**	**Size (nm)**	**Zeta potential (mV)**	**Size (nm)**	**Zeta potential (mV)**
1	Average± SD	127.97±17.15*	-8.70±1.83*	149.93±18.43*	-7.72±1.72*	103.05±3.75*	-16.10±0.85
	%RSD	13.40	21.02	12.29	22.23	3.64	5.31
3	Average± SD	126.75±14.64*	-6.01±1.05*	139.22±6.95*	-8.69±0.74*	161.43±6.88	-3.68±0.72*
	%RSD	11.55	17.40	4.99	8.54	4.26	19.57
6	Average± SD	177.57±39.47	-11.03±1.08*	153.65±28.07*	-7.82±1.02*	160.15±42.78	-7.84±0.95*
	%RSD	22.23	9.83	18.27	13.02	26.71	12.10

Table 7.5 Particle size and zeta potential obtained for co-encapsulated nanoparticles stored at 2-8°C, room temperature and 40°C and measured at 1 month, 3 months and 6 months (n=9, mean±SD) (*P<0.05)

Co-encapsulated nanoparticles Month	Temperature (°C)	2-8 (°C)		25 (°C)		40 (°C)	
		Size (nm)	**Zeta potential (mV)**	**Size (nm)**	**Zeta potential (mV)**	**Size (nm)**	**Zeta potential (mV)**
1	Average± SD	116.78±65.32*	-12.63±0.86	109.69±18.77*	-8.04±0.86*	125.12±53.24*	-5.79±2.67*
	%RSD	55.93	6.82	17.11	10.64	42.56	46.06
3	Average± SD	228.40±59.29	-9.19±1.29*	119.86±38.01*	-11.70±2.02	176.57±33.04	-3.05±0.18*
	%RSD	25.96	14.03	31.71	17.29	18.71	6.06
6	Average± SD	168.63±18.59	-10.38±1.07	151.00±29.70	-4.11±0.15*	380.60±53.88*	-6.41±0.19*
	%RSD	11.02	10.30	19.67	3.72	14.16	2.98

7.3.5 DETERMINATION OF THE LOADING EFFICIENCY OF THEOPHYLLINE AND BUDESONIDE IN SYNTHESIZED NANOPARTICLES

The loading efficiency of the nanoparticles was calculated in the same way as described in Chapter 2, Section 2.2.2.2.6. In this part of the study, the loading efficiency of theophylline and budesonide in the nanoparticles stored in the different storage conditions is presented as ratio to the loading efficiency of the two drugs at t=0 (100%)(Figure 7.6).

Variations in the loading for theophylline mono-encapsulated nanoparticles was observed (Figure 7.6A). For samples obtained at t=3 months and t=6 months show a greater consistency in the loading efficiency, compared to the samples at t=1 month. The changes in the loading efficiency are shown to be significantly different at the different temperatures ($P<0.05$). As a result of the large variation, no consistent change is observed over the different storage conditions. There is no clear effect of the storage condition on the loading efficiency of theophylline in the nanoparticles.

Similar results were obtained for theophylline loading in the co-encapsulated nanoparticles (Figure 7.6B). Although the differences in the loading efficiency calculated over the period of 6 months were significant, there was no clear effect of the storage condition on the loading efficiency of theophylline ($P<0.05$). This suggests that the storage condition has limited effect on the loading efficiency of theophylline over the period of 6 months.

Similar effects were seen for the loading efficiency of budesonide in mono-encapsulated nanoparticles (Figure 7.6C) and co-encapsulated nanoparticles (Figure 7.6D). However, there is no correlation between storage conditions and the length of storage. A large variation is observed in the loading efficiency of budesonide which resulted in the differences being significant ($P<0.05$).

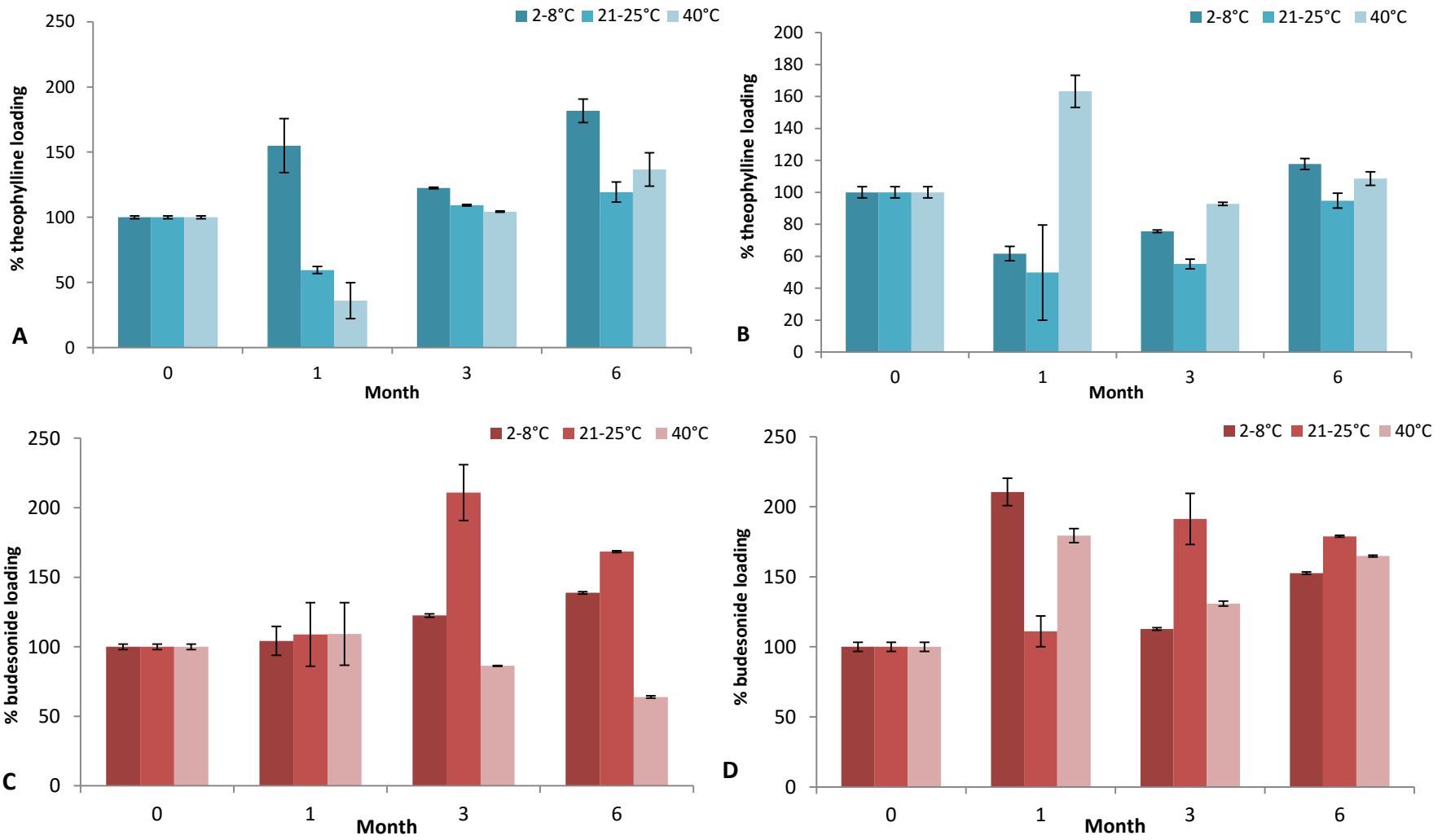

Figure 7.6 Effect of storage temperature and time on the loading efficiency of theophylline mono-encapsulated (A) and co-encapsulated (B) nanoparticles and budesonide mono-encapsulated (C) and co-encapsulated nanoparticles (D) (2-8°C, room temperature and 40°C) measured at 1 month, 3 months and 6 months (n=3, mean±SD)

7.4 DISCUSSION

The aim of the long term stability study was to evaluate the stability of the drug substance in the nanoparticles over a period of time at different conditions and determine the most suitable storage conditions for the nanoparticles. Guidelines and requirements are specified by ICH which recommend the use of different temperatures (and humidity) in order to determine the effect it would have on the product/substance. In the current study, the overall duration was reduced to 6 months but at the recommended storage conditions based on the guidelines. Studies have been reported for duration of 1-3 months [513, 516, 519, 520], 6 months [510, 511], 1 year [521] up to 4 years [519] and 10 years [519].

Time points in long term stability studies were varied. In the current study, three time points were chosen as it allowed determining where and when, if, any changes in the physicochemical properties of the nanoparticles would occur. Some studies used time points that are more frequent. For example, silver nanoparticles were studied at weekly intervals to ensure their stability in a suspension formulation [522]. The stability of PLGA nanoparticles and freeze-dried albumin nanoparticles were also assessed at three different storage conditions: 4°C, 25°C and 40°C similar to the current study, but at more frequent time points: 1, 2 and 3 months (and a shorter duration of study) [513, 516].

From the results of the current study, it can be suggested that greatest stability of the nanoparticles was obtained for the samples stored at 2-8°C over the period of 6 months. This is supported by several other studies [359, 514, 515, 519, 521]. For example, the stability of polysorbate nanoparticles was compared at two temperatures (4°C and room temperature). The study was carried out over a period of one year and showed that particle size increased slightly at room temperature but only marginally changed at 4°C even after 4 years. In the same study, a suspension of drug-encapsulated nanoparticles (Nile Red and loperamide were used as model drugs) were studied for a period of two months and showed no significant change in the physicochemical properties of the nanoparticles [519].

A similar study was carried out to compare the stability of silver nanoparticles at 4°C and room temperature showing an increased stability at 4°C reducing the rate of changes in the particles in terms of their shape and size [521]. In a review by Abdelwahed et al (2013), PLA-PCL nanoparticles formulated as nanosuspensions were stable for 350 days at 5°C but for only 4 months at 25°C [515]. Haloperidol in solid lipid nanoparticles (SLN) formulations was also studied in the same manner as described above with same time points where the effect on size, zeta potential and loading efficiency was determined, this study also showed better stability at 4°C [359].

Changes in the morphological features of the theophylline and budesonide nanoparticles were observed when stored at 40°C which may be as a result of the polymer changes at a higher temperature. This temperature is in the glass transition temperature range which may cause these changes in the polymer. Suspensions of solid-lipid nanoparticles (SLN) were also studied at different temperatures suggesting that 4°C was the more suitable storage temperature. Characterization of the nanoparticles was also carried out by observing the morphological changes, where it had also been suggested at 40°C there was polymorphic transition (from a glass to a rubbery state) [510]. It has been recommended that the higher the glass transition temperature is in relation to the storage temperature, the more stable a system will be i.e. approximately 20°C differences between these two [230, 516]. For this reason it can be suggested that the PLA is not stable causing changes in the morphology when stored at 40°C as it is in the glass transition temperature of the polymer (which is between 34-39°C). It is better to store the nanoparticles at a temperature that is below the glass transition temperature to allow increased stability of the particles, as reviewed by Abdelwahed et al (2013) [515]. Although, some spherical particles were observed, a large degree of coalescence was also observed. Similar characterization tests as conducted in this work were carried out on doxorubicin nanoparticles, which were assessed for their stability in a suspension formulation, and stored at 40°C for a period of 1 month. This study showed changes in the particle size and zeta potential, but also chemical degradation during this period [520].

Budesonide and theophylline melting points were observed at 260.48°C and 271.46°C, respectively, as reported in literature [230, 523-525]. As described in Chapter 2, Section 2.4.6 resemblance of the nanoparticles thermogram to the polymer thermogram was suggested to be due to several reasons. Greater polymer quantity in ratio to the two drugs present, possible interactions between the drug and polymer masking the drug peaks or drug peaks not being detected as a result of the large degradation peak of the PLA at the same temperature range are all possible factors. As a common observation, the peak representing the degradation of the polymer at approximately 360°C showed a shift to approximately 300°C (overall). This shift in the peak suggests possible interaction between drugs and polymer, for which the melting point for both drugs is less than 300°C.

In some samples stored at 40°C, a reduction in the intensity of the glass transition phase was observed. This reduction in intensity could be as a result of the polymer affected by the temperature during storage such that the heat transfer during this process does not release as much energy. Glass transition phase for the polymer for samples stored at 2-8°C was seen to be of a greater intensity in comparison to the samples stored at higher temperatures, which can suggest that the stability of the particles was higher at 2-8°C. The peaks that represent

the polymer degradation were smaller for all the samples, especially for samples stored at 40°C. This could be a result of the extended time period when stored at 40°C, which would have affected the physical properties of the polymer as it is present in the temperature range for the glass transition phase.

Based on the observations of SEM images it can be predicted that some drug might be detected in samples that were stored at 40°C due to the disruption of the structure of the synthesized nanoparticles as a result of the change in state that the polymer would undergo at higher temperatures which can lead to possible leakage of the drug. From previous observations discussed in Chapter 2, drug peaks were not detected on the FT-IR spectra suggesting that the drug had not adsorbed on to the surface of the nanoparticles. For the samples stored at 2-8°C for a period of 6 months, spectra similar to t=0 were obtained, which indicates better stability when stored at these conditions. Changes in the spectrum for drug encapsulated nanoparticles was observed at t=6 months for samples stored at room temperature and 40°C. Lower intensity for the PLA ester bond suggests this could possibly be as a result of physical changes in the polymer leading to some drug peaks appearing on the spectrum.

In the current study, although an increase in particle size was observed for the samples stored at 40°C, this size increase was not significantly different over the period of 6 months or when compared to the other two storage conditions (except for co-encapsulated nanoparticles). Similar observations were reported for freeze-dried albumin nanoparticles encapsulating HI-6 protein (studied at different temperatures over a duration of 3 months), which showed an increase in the particle size for the samples stored at 40°C but minimal degradation at 4°C [513]. In contrast, a study on polybutylcyanoacrylate (PBCA) nanoparticles showed a reduction in the particle size at 42°C along with decomposition of the product after only 4 weeks of storage [517]. A slight increase in particle size of curcumin nanoparticles was observed, but not seen to be significant [511].

A greater consistency with minimal changes in the zeta potential were observed for samples stored at 2-8°C and at room temperature in the current study. Similar observations were reported in a study on curcumin PLGA nanoparticles, in which the study was also conducted over a period of 6 months at 4°C. The samples were seen to be stable for this duration where no collapse or aggregation of the nanoparticles being observed. It was also observed in the SEM images for theophylline and budesonide nanoparticles stored at 2-8°C, that the properties of the nanoparticles (spherical shape and smooth surface) were retained for the duration of 6 months.

In a study by Holzer et al (2009), it was noted that there was difficulty in re-dispersing freeze dried nanoparticles at 40°C at 1-2 months, but not at room temperature until 3 months. This study on PLGA nanoparticles also supported the greatest stability of the nanoparticles was achieved at 4°C with no significant changes in the properties of the nanoparticles [516]. In the current study, there was no difficulty in re-disersibility of theophylline and budesonide nanoparticles at any time points during the 6 month stability study for all the storage conditions.

As both the drugs were encapsulated in the formulation process (at t=0), it can be predicted that there may not be a change in the actual concentration of drug present in the particular sample being analyzed, regardless of storage condition. However, changes that occur to the polymer (at 40°C) may potentially occur at different storage conditions for budesonide and theophylline, which can affect the concentration calculated. The loading efficiency at t=0 was calculated and presented as 100%. For this part of the analysis it is difficult to determine if the changes in the loading efficiency over the period of time are due to the large variation as part of the nanoformulation process at t=0 or if it was as an effect of the temperature. Due to a lack of relationship between the storage condition and drug loading obtained in the current study (Section 7.3.5); it can be assumed the variation in the loading is mainly as a result of the nanoformulation process. Changes as an effect of the temperature would be supported by on changes in the DSC thermograms or FT-IR.

Limited information is available on the two drugs that are used in this study for their long term stability. Theophylline (and citric acid) were studied as co-crystals and was seen that theophylline was stable after a period of up to 60 days at 55±0.5°C/40±2% RH [524]. In a study on the different physicochemical forms of theophylline it was noted that after 1 week, theophylline absorbed water at 40°C at 79 and 82% RH [525]. Nanoporous-microparticles of budesonide prepared using spray drying were found to be stable after 1 year, at room temperature [230].

It was noted that a lot of studies on nanoparticles stability studies referred to changing the formulation of the nanoparticles from a suspension formulation to a freeze-dried formulation and comparisons were made between these two formulations [513-515]. In the current study, suspensions of the nanoparticles was not appropriate as a formulation due to theophylline (and budesonide) being able to diffuse out of the particles into the aqueous medium rapidly leading to a loss of the drug encapsulated, which was observed during nanoformulation method development. Other stability studies on nano-suspensions were to determine the importance of electrostatic charge around the nanoparticles to improve the stability of the nanoparticles when suspended in a medium as it would prevent coalescence

and aggregation of the nanoparticles [512, 515, 526, 527]. Other forms of stability studies of nanoparticles included to determine the effects of cyro-protectants and its effect during freeze-drying process, where it was shown to reduce the nanoparticle size distribution [513, 514].

An important observation from the stability studies of the nanoparticles in suspensions was in polyesters such as PLGA and PLA, the hydrolytic instability of the polymer in aqueous suspension is the main problem. Drugs can also leak from the nanoparticles leading to further instability of the nanoparticles and for this reason freeze-dried nanoparticles are able to provide greater stability [516]. PCL, PLA and PLGA nanoparticles were studied at four different temperatures for 1 year in a suspension suggested that the nanoparticles degraded by hydrolysis of the polymer and further catalyzed by the carboxylic acid groups. In a study reported in the literature, it was suggested that there is a direct relationship between the degradation rate and temperature (with improved stability at 4°C) and as a result of polymer hydrolysis, the nanoparticles which were freeze-dried were suggested to be more stable than when suspended in water [528]. In the current study, theophylline and budesonide nanoparticles suspensions cannot be stored for a long duration of time due to problems such as leakage of theophylline and hydrolysis of the polymer, as discussed. For this reason, if the nanoparticles were to be administered as a nebulized formulation, the freeze-dried nanoparticles would be mixed with a suitable aqueous solution at the time of use and then administered immediately to minimize any drug release into the solution.

7.5 CONCLUSIONS

The aim of the study was to evaluate the stability of the nanoparticles over a period of 6 months under different storage conditions and to subsequently determine the most suitable storage conditions for the synthesized theophylline and budesonide nanoparticles. Three different storage conditions, based on the ICH guidelines, were used in order to determine the most suitable storage conditions. These were 2-8°C, room temperature (21-25°C) and 40°C.

Based on the results obtained in the current study, the best storage conditions for theophylline and budesonide nanoparticles were 2-8°C over the period of 6 months. The greatest retention of the properties of nanoparticles from t=0 was achieved at this temperature. Storage of the nanoparticles at 40°C resulted in morphological changes on the surface of the nanoparticles which were thought to be due to the changes in the polymer properties as the temperature is close to its glass transition temperature. Storage at 40°C also showed effects on the particle size, zeta potential variation and appearance of drug peaks on the FT-IR spectra.

CHAPTER 8 GENERAL DISCUSSION AND CONCLUSIONS

8.1. GENERAL DISCUSSION

Nanoparticles can be in the form of polymeric nanoparticles, nanocapsules, micelles, liposomes and carbon nanotubes. Various polymers have been used for the synthesis of nanoparticles, examples include naturally occurring chitosan, or synthetic biodegradable polymers, poly (lactic-co-glycolic acid) (PLGA) and poly (lactic acid) (PLA) [243, 247]. PLGA and PLA are the most commonly used biodegradable polymers [181, 185, 190, 198-200, 214, 253], and have advantages such as biocompatibility and degradation by naturally occurring metabolism processes to end products present in the body (carbon dioxide and water) [189, 223, 293, 321, 385, 398, 403]. There are several examples of drugs that have been encapsulated using these polymers and several methods exist to synthesize drug encapsulated nanoparticles. The current study looked at two anti-asthmatic and COPD drugs, theophylline and budesonide which differ in their lipophilicity. Both drugs have been shown to be effective when used as a combination in the treatment of the airway inflammatory diseases. Theophylline, a drug that has been relegated to third-line therapy due to safer, inhaled alternatives available, has been shown to prevent the resistance to corticosteroids in patients suffering from COPD [6, 16, 143, 151, 153-158]. Budesonide is a corticosteroid with a safe side effect profile, is widely prescribed and used as a first line inhaler preventer therapy in asthma [127, 145].

In order to synthesize theophylline and budesonide co-encapsulated nanoparticles using the biodegradable polymer, PLA, a suitable method was required to be developed in order to achieve successful encapsulation. The overall aim of this study was therefore, to successfully formulate co-encapsulated polymeric nanoparticles encapsulating a hydrophilic (theophylline) and hydrophobic (budesonide) drug.

Subsequently, the nanoparticles need to be characterized for their physicochemical characteristics in order to determine which method provided the most optimal characteristics of the nanoparticles based not only on the loading efficiency, but also consistency with other factors such as size, surface charge and morphology. The effect of different temperatures allows understanding of the optimum conditions of storage in an attempt to retain properties of the nanoparticles over long term.

For drugs such as theophylline, which have a narrow therapeutic range, sustained release products can provide advantages in therapy by reducing the risk of side effects.

Additionally, advantages such as reduced dosing frequency, lower overall concentration of drug and potential improved compliance can aid in the treatment of asthma and COPD; but is also applicable to other conditions where frequent dosing may be required [179, 216-224, 317, 318]. Further characterization of the drug encapsulated PLA nanoparticles on human bronchial airway cell lines can allow understanding of the acute effects of PLA nanoparticles. Characterization of *in vitro* pulmonary deposition profile would allow determining whether nanoparticles are suitable for the treatment of airway disease when administered as a dry powder or a nebulized suspension. Pulmonary drug delivery is preferred not only in the treatment of asthma and COPD, but the deposition of polymeric nanoparticles can also be extended for applications in other pulmonary conditions such as tuberculosis and cancer where sustained release can be beneficial.

8.1.1. NANOFORMULATION AND CHARACTERIZATION

Existing nanoformulation methods were developed and allow increased encapsulation for hydrophobic drugs, but experience high rates of partitioning for hydrophilic drugs [188, 194, 199, 259, 260]. The double emulsion method has been applied in several studies to improve the encapsulation efficiencies of drugs in particular for hydrophilic drugs [247, 251]. For this reason, a modified version of this method was applied in the current study. Variables such as organic solvent combinations, quantity of drug and polymer, rate of evaporation and method of evaporation of organic solvents were all investigated.

Improvement in the overall physicochemical characteristics of the nanoparticles was obtained when the organic solvents were evaporated using pressure in comparison to overnight stirring and a higher ratio between polymer and drug quantity used [288]. The quantities of 50 mg theophylline, 5 mg budesonide used with 200 mg of PLA were found to be the most suitable combination/ratio of drug and polymer based on the characterization results obtained [285].This change in the method showed improvement in the loading efficiency of theophylline and budesonide with lower variation (Table 2.6). Lower variation in drug loading is essential as it allows quantifying the nanoparticles for dose calculation accurately. The use of overnight stirring also resulted in larger variation in the particle size and zeta potential of the nanoparticles (Table 2.3). However, despite the changes in the variables of the method, the particle size of the drug encapsulated PLA nanoparticles remained to be in the sub-micron range (200-500nm) and negatively charged as a result of the carboxylic acid groups on PLA.

Greatest improvement in the physicochemical characteristics (such as particle size, zeta potential and loading efficiency) of the nanoparticles was obtained when acetone and

dichloromethane were used as the organic solvents (Method 8). Acetone was reported as the solvent of choice in several studies [193, 198, 199, 253, 296, 297] and is a solvent in which theophylline was readily soluble. The use of this mixed organic phase would allow reduced partitioning of the hydrophilic drug to the external phase and therefore improve the loading efficiency [193, 194, 198, 298].

Storage of the nanoparticles at over the period of 6 months at three different storage conditions however revealed that storage at 40°C resulted in an increased variation in the particle size and zeta potential (Table 7.3-7.4).An increase in the average particle size of nanoparticles was observed in the current study and reported in previous studies carried out on nanoparticles stored at 40°C [513]. Samples stored at 2-8°C were least affected and can be suggested that this is an ideal temperature to store the nanoparticles for long term stability. The nanoparticles stored in this temperature showed reduced variation in the particle size and zeta potential. The results obtained in the current study correlate with previous stability studies carried out on nanoparticles supporting the storage of drug encapsulated PLA nanoparticles at this temperature [359, 514, 515, 519, 521].

Reproducibility in the loading efficiency of theophylline and budesonide in mono- and co-encapsulated nanoparticles allows an increased confidence in the reproducibility of the method and ability to determine the concentration of drugs encapsulated in a particular quantity of nanoparticles (Table 2.7). Despite changes in the method to improve the loading efficiency of the hydrophilic drug, the nanoformulation method demonstrated the preference in encapsulation of hydrophobic drugs which is reported in other studies [197]. Stability studies of the nanoparticles revealed that there was no change in the drug content related to the effect of the temperature when stored over a period of 6 months and was suggestive that the changes in the drug content was due to the nanoformulation method (Figure 7.6).

FT-IR of the nanoparticles obtained resembled the PLA spectrum suggesting no drug adsorbed on the outer surface of the nanoparticles (Figure 2.2); which is expected due to (i) nanoformulation method developed was for encapsulation of the drugs and (ii) washing off any un-encapsulated drug or surfactant by centrifugation steps [225]. The DSC thermograms of the nanoparticles also suggested successful encapsulation of the drugs. The glass transition phase of the polymer at approximately 45°C was present in the nanoparticles samples and a shift in the polymer degradation peak, closer to the melting point of both drugs suggested an interaction between the drugs and the polymer (Figure 2.3). An effect on the intensity of the glass transition temperature peak was observed in DSC thermograms for nanoparticles stored at 40°C the duration of 6 months (Figure 7.5).

Morphology of the nanoparticles revealed smooth surfaces (Figure 2.4), supporting other studies on nanoparticles synthesized using biodegradable polymers and correlation to particle size analysis carried out using dynamic light scattering. Loss of morphological features of the nanoparticles present at t=0 was observed consistently for the duration of 6 months for the nanoparticles stored at 40°C (Figure 7.1-7.3) [510]. This was thought to be due to the temperatures being in the glass transition temperature range of the polymer, which can lead to changes in the PLA from a glass to a rubbery state. The nanoparticles stored at 2-8°C retained morphological features (spherical shape, smooth surface) over the course of 6 months (Chapter 7).

As a result of the improved physicochemical properties, nanoparticles synthesized using Method 8 was selected for further characterization. Freeze dried nanoparticles were used for further characterization of the nanoparticles by studying the drug release profiles (Chapter 3 and Chapter 5), effects on a human bronchial epithelial cell line (Chapter 4 and Chapter 5) and *in vitro* deposition (Chapter 6).

8.1.2. *IN VITRO DRUG RELEASE STUDY*

By formulating theophylline and budesonide encapsulated nanoparticles, the aim was to achieve sustained release of the two drugs. The release of theophylline and budesonide from the PLA nanoparticles was studied using Franz diffusion cells (Chapter 3) and this model was extended to Transwell® inserts seeded with human bronchial epithelial cells (Chapter 5). The features of the Franz diffusion cells show suitability for the study of the nanoparticles [317, 323, 325, 332, 334]. These include the use of low volumes and a membrane. These features can be also applied to the setup using 16HBE14o- cells seeded on Transwell® inserts.

Both setups showed a greater concentration of drug in the basolateral/receiver chamber when drug solution (of equivalent concentration) was applied to the apical/donor chamber in comparison to drug released from mono-encapsulated and co-encapsulated nanoparticles. Both setups showed successful sustained release of the drug from the nanoparticles. Similar release profiles of theophylline and budesonide were obtained from both mono- and co-encapsulated nanoparticles in both setups (Figure 3.1-Figure 3.6, Figure 5.6 and Figure 5.7).

Comparable concentration of theophylline in the basolateral chamber of the Franz diffusion cells (studied at 37°C) and Transwells® were obtained. These ranged from 10-16% in total (Figure 3.7 and Figure 5.6). Theophylline is readily soluble in methanol, SLF and transport

medium and this can be suggested as a potential reason that the release of theophylline is similar in the two setups.

Lower concentration of budesonide was released from the nanoparticles and obtained in the basolateral chamber of the Transwells® treated with the budesonide mono- and co-encapsulated nanoparticles (Figure 5.7) in comparison to the concentration of budesonide in the receiver chamber of Franz diffusion cells (Figure 3.8). This may be due to the aqueous medium used in the study of transport of drug across the 16HBE14o- cells (Chapter 5), resulting in a largely unfavorable environment for budesonide in comparison to the receiver medium used in the Franz diffusion studies which included the use of an organic solvent (methanol).

A large difference in the total recovery (from apical and basolateral chamber) of budesonide was shown in the two different setups. Approximately 78% of budesonide was recovered from the Franz cell experiments (Chapter 3), but only approximately 10% of budesonide was recovered from the apical and basolateral chambers of cells treated with budesonide solutions of equivalent encapsulated concentrations (Chapter 5). Possible reasons for this difference are thought to be due to a possible fatty acid conjugation of budesonide which results in conversion of budesonide to an inactive form resulting in prolonged retention [335, 392, 445-447]. Additionally, it is possible that binding of budesonide to the plastics of the Transwell® may have resulted in a poor recovery of the drug. The possible binding of budesonide to the Transwell® plastic can also lead to potential inaccurate calculation of apparent permeability coefficients (Table 5.5).

The pore sizes of the cellular supports were 0.4μm when conducting transport experiments using 16HBE14o- cells; but tight junctions formed by the human bronchial epithelial cell line are thought to be approximately 13-15nm resulting in a potential transport of only drugs and not nanoparticles across the cell monolayer. Similarly, the cellulose membrane used in the Franz diffusion cells was 24Å (2.4nm) which also results in transport of the drugs only and not nanoparticles, acting as a filter[330]. The importance of the filter was highlighted when nanoparticles were suspended in release media and faster release of the drugs from the nanoparticles was obtained in comparison to the Franz diffusion cells (Figure 3.9). However, it is thought that this may also be due to the overestimation of drug as a result of sampling nanoparticles during analysis.

It is thought that the drugs diffuse out of the PLA nanoparticles and showed high correlation to the Higuchi model which demonstrates release by diffusion mechanism [218, 288, 357-359]. The rate limiting step was thought to be the release of the drugs from the nanoparticles rather

than the diffusion of the drug across the cell monolayer or cellulose membrane (Figure 3.10) [332].

Additionally, from the Franz diffusion cell experiments, it was observed that the release of drugs from the nanoparticles at physiological temperature was not significantly different to the release at room temperature (Figure 3.7-3.8) [217]. The similar release concentrations obtained in the transport study experiments conducted using 16HBE14o- cells also demonstrate the little effect of the increased temperature on the release of the drugs from the nanoparticles in the current study (Chapter 5).This was noted in several other studies as well. It was thought that the release of the drugs at physiological temperature may be affected by changes in the polymer state from glass to rubbery state due to the presence of the nanoparticles in the glass transition temperature range. Changes in the polymer were also observed for nanoparticles stored at 40°C (Chapter 7) where an effect on morphology was observed and a larger variation in other physicochemical characteristics such as particle size and loading efficiency [218, 326, 331, 340]

8.1.3. Characterization using human bronchial epithelial cell line (16HBE14o-)

The effects of the nanoparticles on viability and integrity of tight junctions was studied using a human bronchial epithelial cell line, 16HBE14o- cells [8, 382, 388, 392-394]. This cell line was selected as it is able to represent the upper airways, which is the target site and affected site of the airways in patients suffering from chronic inflammatory diseases, asthma and COPD. The cell line expresses tight junctions when cultured at an air-liquid interface [388, 392, 394, 423, 424].

Concentrations of nanoparticles studied in the various experiments in the current study were overall shown to be safe and non-toxic to 16HBE14o- cells in time scale applied. Nanoparticles studied at a range of concentrations in the assessment on their effect on the viability of 16HBE14o- cells and only showed a significant reduction only at the maximum concentration used in the current study (5 mg/mL) over a period of 24 hours (Figure 4.11-4.14). It was thought that the reduction in viability was due to the highly concentrated nanosuspension and not due to the concentration of drugs encapsulated, as the drugs were shown to cause non-significant effects on viability in comparison to the control (Chapter 4).

At concentrations of the nanoparticles (between 0.5-1 mg/mL) where there was no significant effect on the viability, the nanoparticles also showed no significant effect on the

tight junctions expressed by the 16HBE14o- cells. This was measured by determination of the concentration of paracellular marker, FD4, in the basolateral chambers of cells treated with drug solutions and nanoparticle suspensions in comparison to the control (Figure 5.4 and Figure 5.5). It has been suggested that submicron sized nanoparticles are not able to translocate across the cells monolayer due to the small intracellular spaces (15nm) [422, 435]. As a result of the negatively charged membranes, it is thought that the effect of negatively charged nanoparticles is limited therefore resulting in a limited effect on the cell viability and tight junctions [370].

Further to this, the concentration of nanoparticles used for *in vitro* deposition studies (1 mg/mL in the nebulized suspension) was also shown to be non-toxic to cells. This can therefore be suitable for potential experiments of *in vitro* deposition of the nanoparticles in impingers or impactors where cell lines can be placed in the various stages at an air-liquid interface and deposition and subsequent transport of the encapsulated drugs can be studied using combination of the release study, transport study and *in vitro* deposition methods at non-toxic concentrations.

8.1.4. IN VITRO AEROSOL DEPOSITION STUDIES

The *in vitro* deposition of the nanoparticles was characterized using a multistage liquid impinger (MSLI). In the current study, freeze dried theophylline and budesonide nanoparticles were prepared as a dry powder formulation or suspension to be nebulized. Dry powders are preferred due to the increased stability (when stored correctly) of the product and was observed to be a common method adapted for the successful delivery of polymeric nanoparticles via the pulmonary route [208, 210, 235, 366, 460, 491]. For the current study, freeze-dried nanoparticles would be required to be re-constituted to prepare a nebulized suspension at the time of inhalation in order to prevent un-wanted release of drug and reduced stability. Nanoparticle suspensions have been used previously to deliver drugs via the pulmonary route [212, 374, 506].

Nebulizer formulations showed deposition in the target area (Figure 6.5-6.4) but a large percentage of the dose remained in the nebulizer chamber. With minimal requirements of preparation, appropriate dose adjustments and duration of nebulization can result in optimum deposition at target site.

Dry powder inhalers were prepared using different grades of inhaled lactose. The dry powders were deposited using a single dose, Aerolizer® device. It was consistent with all

the different lactose grades and mono- or co-encapsulated nanoparticles that greatest deposition occurred in the upper stages of the MSLI where particle size is approximately over 6.8µm (Chapter 6, Section 6.3). In the respiratory system, this would lead to an un-successful deposition and therefore dry powders would need further modifications or increased mixing times in order to allow successful deposition at target site.

The minimal use of excipients is ideal as it allows ease in preparation and limited effects of inhaled excipients. Dry powder inhaler formulations have been used for the administration of nanoparticles via the pulmonary route in various studies and prepared using several techniques including milling, tumbling blending or spray drying or with a combination of 'fines' and larger carrier particles. Lactose grades which consisted of a wide particle size distribution showed better deposition profiles than ones with only 'fines' or larger particles as it would allow nanoparticles to adhere to greater range of particles. The use of Lactohale® 201 and Respitose® ML001 showed improved mixing and deposition of the nanoparticles which may be due to the presence of 'fines' and a combination of larger, coarser carrier particles.

As this was a preliminary study on the deposition of the nanoparticles in the airways, there were limitations which would be addressed in order to improve the deposition of the nanoparticles in the lungs. The powders formulated in this study were made as individual doses, but it would be more ideal to make a bulk powder and have the dosing of the nanoparticles based on the concentration of the two drugs and not nanoparticles. The formulation of a bulk powder would allow assessment of the powder flow properties and improve formulation processes and selection of the most appropriate lactose grade to allow increased and improved deposition

By achieving greater deposition in the appropriate/target stages of the MSLI the dose of the drugs/ nanoparticles can be adjusted according to the loading dose calculated. As approximately 50% of the volume remained in the nebulizer chamber, this volume can also be adjusted accordingly to avoid drug wastage. Successful deposition of the nanoparticles in the correct site, it would lead to increased bioavailability of the drug by sustained release at the target site. By delivering sustained release nanoparticles, the frequency of dosing can be reduced, which can potentially increase patient compliance and reduction in toxic adverse effects. The negative surface charge of the synthesized PLA nanoparticles (Chapter 2) and reconstitution of the nanoparticles in water at the time of administration would lead to an increased stability further supporting the use of nebulized suspensions. By developing suitable models of release (Chapter 3) with or without the use of cells at an air-liquid interface (Chapter 5) in the impinger, the concentration of drug released after a period of 24

hours can also be predicted at each stage of the MSLI which can lead to development of an accurate and reproducible dosing system. The confidence in the reproducibility is further increased by achieving loading efficiencies of the encapsulated drugs (theophylline and budesonide) in a consistent range (Chapter 2). Dosing of the nanoparticles can be based on the drug concentration rather than the nanoparticles, where a potential greater concentration of drugs can be used due to the non-toxic effects shown the 16HBE14o- cells (Chapter 4 and 5).

It is important to note that the quantities and concentration of the nanoparticles used in the current study were sub-therapeutic. In order to have any effect, the concentration of the nanoparticles would have to be increased significantly. From the results obtained for the deposition studies using dry powders, only 10% of the initial dose is the FPF. With the current quantity/concentration of nanoparticles used and based on the release profiles, approximately only 1.76 µg of theophylline and less than 1 µg of budesonide of the deposited 10% would be released in the target region; both sub-therapeutic doses. In comparison, a greater FPF was obtained when nebulized suspensions of the nanoparticles were tested. The FPF for theophylline was calculated to be approximately 60% which would result in approximately 10 µg of theophylline released in the 24 hour period in the target site. This would be in the therapeutic range and safe in terms of toxicity levels. However, the concentration of budesonide deposited and released in 24 hours would be approximately 0.272 µg which would be sub-therapeutic. For this purpose, it would be important to use a concentration of nanoparticles that would result in sufficient release of both theophylline and budesonide over the period of 24 hours. In addition, by delivering the drugs locally, the concentration of theophylline can be further increased if required.

8.2. CONCLUSIONS

Theophylline and budesonide nanoparticles have been successfully formulated using a double emulsion solvent diffusion (DESD) method. The method was developed and modified in order to increase the loading efficiency of both the drugs which differ in their lipophilicity. Despite the changes in the nanoformulation methods, the loading efficiency of the hydrophobic drug (budesonide) was higher than the hydrophilic drug (theophylline). Nanoparticles synthesized using acetone and dichloromethane in the organic phase, which when removed under pressure, showed lower variation in the particle size, zeta potential and drug loading. Reproducibility of loading efficiency of theophylline and budesonide was obtained in mono- and co-encapsulated theophylline and budesonide nanoparticles which

can be an advantage to determine concentration of drug encapsulated and in dosing. Spherical, smooth surfaced, sub-micron and negatively charged nanoparticles showing no adsorption of the drugs was shown consistently in the nanoparticles.

Encapsulating theophylline and budesonide in the polymeric nanoparticles achieved sustained release of the drugs over 24 hours. Similar release profiles of theophylline and budesonide from mono-encapsulated and co-encapsulated nanoparticles were observed. The release was thought to follow the Higuchi model, which is based on the diffusion of the drugs from the nanoparticles.

When the transport of the drugs across the 16HBE14o- cell monolayer was assessed, similar results to when the Franz diffusion cells were used was obtained and thought to be that the release of the drugs from the nanoparticles was the rate limiting step. Sustained release was achieved when compared to the drug solutions of equivalent concentrations.

The nanoparticles significantly reduced the viability of the 16HBE14o- cells when a concentration of 5 mg/mL was used (compared to the control); however this was thought to be due to an effect of the highly concentrated suspension of the freeze dried nanoparticles on a smaller area rather than an effect of the drug. Similarly, the negatively charged nanoparticles (studied at a concentration where viability of 16HBE14o- cells was not significantly reduced) did not affect the integrity of the tight junctions of the 16HBE14o- cells indicated by a similar permeability of the exposed cells to the paracellular marker, FD4, as control cells.

In vitro deposition studies showed a wide deposition profile of the nebulized suspensions of theophylline and budesonide nanoparticles. Dry powder formulations of the nanoparticles mixed with lactose showed greater deposition in the throat section of MSLI suggesting unsuccessful deposition profile. For stability purposes, freeze dried nanoparticles would be required to be reconstituted as a suspension at the time of administration if the medication were to be administered using a nebulizer. Optimization in the dose and time to nebulize the suspensions can lead to greater deposition in the target site.

To achieve prolonged stability of the nanoparticles, it was suggested from the current study that freeze dried nanoparticles stored at 2-8°C retained their physicochemical properties from t=0 over the period of 6 months. The least favorable conditions were at 40°C, which showed changes in the shape and morphology of the nanoparticles as a result of the polymer changing state from glass to a rubbery state near the glass transition temperature. Along with an increased variation in the particle size and zeta potential in comparison to the nanoparticles stored at 2-8°C and room temperature.

8.3. FUTURE WORK

For future work, it would be important to further optimize the encapsulation of hydrophilic drugs in polymeric nanoparticles. The current study demonstrated variables in the method development that should be carried out in order to improve not only the drug loading of both hydrophilic and hydrophobic drugs, but also other aspects of the nanoparticles including particle size and zeta potential. Despite improvements in drug loading, higher drug loading of the hydrophobic drug was obtained and therefore future work can be performed to achieve further improvements in the method which can lead to equal encapsulation efficiencies of both hydrophilic and hydrophobic drugs. Additionally, scaling up of the method of nanoparticle synthesis would be ideal. This would allow potential larger yields of nanoparticles and ease in the synthesis method.

Theophylline and budesonide can be used as model drugs for the encapsulation of hydrophilic and hydrophobic drugs and/or co-encapsulation of drugs in polymeric nanoparticles. For future work, this application can be extended to other conditions which are not necessarily specific to pulmonary diseases. Treatment of infections such as tuberculosis (TB) requires multiple medications coupled with longer treatment regimens and it would be ideal to attempt the treatment of tuberculosis using polymeric nanoparticles encapsulating anti-TB medication.

Future work on the release profile can be carried out and extended for a longer duration. Some studies have carried out the release study of the drugs encapsulated for periods of up to 4 weeks or longer. However the disadvantage of the method used in the current study if applied over a longer period of time can potentially include compromising on sink conditions if small volumes are to be used. For this reason, higher volumes and larger concentrations of the nanoparticles could be used to study the release of the drugs from the nanoparticles over a longer period of time. Larger volumes ensure that the sink conditions are not compromised therefore concentrations are accurate. Greater concentrations also allow the use of an aqueous based receiver medium which would allow an accurate representation of the airways *in vitro*.

Further work can be carried out on the cytotoxicity study; comparisons by carrying out an LDH assay would be able to give more information on the cytotoxicity of the nanoparticles. Cytotoxicity can also be studied over an extended period of time, for example up to 48 hours or longer time periods. The effect of PLA nanoparticles on the tight junctions of cell

lines can also be studied at higher concentrations. Application of an alternative cell line can allow seeing if the effects of the nanoparticles are reproducible. By using a mucus-secreting cell line, the effect of the mucus on the nanoparticles can also be studied this way. Addition of mucus can further allow knowledge on the effect of mucus on the nanoparticles and the permeability of drugs across the membrane. The nanoparticles can be delivered as aerosols with cells present at an air-liquid interface and the concentration of drugs transported across the cell monolayer or taken up can be determined.

For the *in vitro* deposition of the nanoparticles, it would be important, and very useful, to further develop a suitable formulation for pulmonary drug delivery. As part of this study, only preliminary work was carried out to obtain an understanding of the deposition of nanoparticles in the airways when delivered with the use of minimum excipients. It is more important to formulate a bulk powder of the nanoparticles and a carrier and to base the concentration not on the amount of nanoparticle, but the concentration of the drugs that are required. This would allow the dosing to be more accurate and can be related to the therapeutic efficacy of the drugs. Formulating bulk powders in this manner also allow study on the flow characteristics of the formulation and therefore adjustment to the powders accordingly.

By using the inhalation formulations (dry powders and nebulized suspension of freeze dried nanoparticles) the clearance in the airways can be assessed. The clearance of the nanoparticles in the upper airways and response of macrophages to the nanoparticles deposited in the lower airways can be assessed. Although the target site is the upper airways, it is very likely that a small concentration of nanoparticles will deposit in the lower airways. Although there is also a large possibility that these will not be engulfed by macrophages due to their small particle size; this response can be considered. Clearance of the nanoparticles in the upper airways would be by the mucociliary clearance system and by using an appropriate cell line or model to show this, would allow determination of the clearance of the nanoparticles in the upper airways.

A future study that can be carried out on the theophylline and budesonide PLA nanoparticles synthesized in the current study can begin at the optimization of the pulmonary formulation. This can be both, nebulized suspension or dry powder formulation, or one of them. The deposition profiles can be assessed using a next generation impactor (NGI) and by characterization of the actual formulation too. Cell lines can be added onto an impinger and therefore the deposition and subsequent effect on the cell lines can also be assessed. Further to this, the effect of the formulation on a primary cell line can be assessed for the short life span that primary cell lines have. After characterization on primary cells,

the study can be carried out *in vivo* or *ex vivo* (using isolated perfused lungs) where the response to the drugs can be measured. This can be measurement by determining the changes in the airway diameter when drugs are inhaled and measurement of markers in the bronchial alveolar lavage (BAL) fluid.

CHAPTER 9 REFERENCES

1. Labiris, N.R. and M.B. Dolovich, *Pulmonary drug delivery. Part I: physiological factors affecting therapeutic effectiveness of aerosolized medications.* Br J Clin Pharmacol, 2003. **56**(6): p. 588-99.
2. *National Institute of Health and Care Excellence (NICE)*, in *Human insulin powder for inhalation (Afrezza) for treating type 1 and type 2 diabetes*. 2014.
3. Traini, D., *Inhalation Drug Delivery*, in *Inhalation drug delivery- Techniques and products*. 2013, John Wiley & Sons, Ltd: West Sussex.
4. Taylor, K.M.G., *Pulmonary Drug Delivery*, in *Aulton's Pharmaceutics- the design and manufacture of medicines*, Aulton, M.E. and K.M.G. Taylor, Editors. 2013, Churchill Livingstone Elsevier: UK.
5. Smola, M., T. Vandamme, and A. Sokolowski, *Nanocarriers as pulmonary drug delivery systems to treat and to diagnose respiratory and non respiratory diseases.* Int J Nanomedicine, 2008. **3**(1): p. 1-19.
6. Ward, J.P.T., J. Ward, R.M. Leach, and C.M. Weiner, *The Respiratory System at a Glance*. 2nd Edition ed. 2006, Massachusetts, USA: Blackwell Publishing Ltd.
7. Levitzky, M.G., *Pulmonary Physiology*, in *Pulmonary Physiology*. 1999, The McGraw-Hill Companies: United States of America.
8. Forbes, B., *Human airway epithelial cell lines for in vitro drug transport and metabolism studies.* Pharm Sci Tech Today, 2000. **3**(1): p. 18-27.
9. Haughney, J., D. Price, N.C. Barnes, J.C. Virchow, N. Roche, and H. Chrystyn, *Choosing inhaler devices for people with asthma: current knowledge and outstanding research needs.* Respir Med, 2010. **104**(9): p. 1237-45.
10. Cegla, U.H., *Pressure and inspiratory flow characteristics of dry powder inhalers.* Respir Med, 2004. **98**: p. S22-S28.
11. Pilcer, G. and K. Amighi, *Formulation strategy and use of excipients in pulmonary drug delivery.* Int J Pharm, 2010. **392**(1-2): p. 1-19.
12. Kwok, P.C. and H.K. Chan, *Delivery of inhalation drugs to children for asthma and other respiratory diseases.* Adv Drug Deliv Rev, 2014. **73**: p. 83-8.
13. Amirav, I. and M.T. Newhouse, *Deposition of small particles in the developing lung.* Paediatr Respir Rev, 2012. **13**(2): p. 73-8.
14. Virchow, J.C., G.K. Crompton, R. Dal Negro, S. Pedersen, A. Magnan, J. Seidenberg, and P.J. Barnes, *Importance of inhaler devices in the management of airway disease.* Respir Med, 2008. **102**(1): p. 10-9.
15. Virchow, J.C., V. Backer, F. de Blay, P. Kuna, C. Ljorring, J.L. Prieto, and H.H. Villesen, *Defining moderate asthma exacerbations in clinical trials based on ATS/ERS joint statement.* Respir Med, 2015. **109**(5): p. 547-56.
16. Rang, H.P., J.M. Ritter, R.J. Flower, and G. Henderson, *Rang & Dale's Pharmacology*. 8th Edition ed. 2016, UK: Elsevier Churchill Livingstone.
17. Kaplan, A. and D. Ryan, *The role of budesonide/formoterol for maintenance and relief in the management of asthma.* Pulm Pharmacol Ther, 2010. **23**(2): p. 88-96.
18. Lavorini, F., A. Magnan, J.C. Dubus, T. Voshaar, L. Corbetta, M. Broeders, R. Dekhuijzen, J. Sanchis, J.L. Viejo, P. Barnes, C. Corrigan, M. Levy, and G.K. Crompton, *Effect of incorrect use of dry powder inhalers on management of patients with asthma and COPD.* Respir Med, 2008. **102**(4): p. 593-604.
19. Barnes, P.J., *Asthma management: can we further improve compliance and outcomes?* Respir Med, 2004. **98**: p. S8-S9.
20. Aydemir, Y., *Assessment of the factors affecting the failure to use inhaler devices before and after training.* Respir Med, 2015. **109**(4): p. 451-8.

21. Fink, J.B. and B.K. Rubin, *Problems With Inhaler Use: A Call for Improved Clinician and Patient Education.* Respir Care, 2005. **50**(10): p. 1360-1375.
22. Rau, J.L., *The Inhalation of Drugs: Advantages and Problems.* Respir Care, 2005. **2005**(3): p. 367-382.
23. Arora, P., L. Kumar, V. Vohra, R. Sarin, A. Jaiswal, M.M. Puri, D. Rathee, and P. Chakraborty, *Evaluating the technique of using inhalation device in COPD and bronchial asthma patients.* Respir Med, 2014. **108**(7): p. 992-8.
24. Weers, J., *Inhaled antimicrobial therapy - barriers to effective treatment.* Adv Drug Deliv Rev, 2015. **85**: p. 24-43.
25. Dolovich, M.B. and R. Dhand, *Aerosol drug delivery: developments in device design and clinical use.* Lancet, 2011. **377**: p. 1032-1045.
26. Rau, J.L., *Practical Problems With Aerosol Therapy in COPD.* Respir Care, 2006. **51**(2): p. 158-172.
27. Labiris, N.R. and M.B. Dolovich, *Pulmonary drug delivery. Part II: the role of inhalant delivery devices and drug formulations in therapeutic effectiveness of aerosolized medications.* Br J Clin Pharmacol, 2003. **56**(6): p. 600-12.
28. Geller, D.E., *Comparing Clinical Features of the Nebulizer, Metered-Dose Inhaler, and Dry Powder Inhaler.* Respir Care, 2005. **50**(10): p. 1313-1322.
29. O'Connor, B.J., *The ideal inhaler: design and characteristics to improve outcomes.* Respir Med, 2004. **98**: p. S10-S16.
30. Newman, S.P., *Inhaler treatment options in COPD.* Eur Respir Rev, 2005. **14**(96): p. 102-108.
31. Gupta, S., *How to ensure the correct inhaler device is selected for each patient.* Pharm J, 2009. **1**: p. 322-323.
32. Keller, M., *Innovations and perspectives of metered dose inhalers in pulmonary drug delivery.* Int J Pharm, 1999. **186**: p. 81-90.
33. *DFE Pharma Inhalation: The custom-made solutions of DFE Pharma Inhalation*.
34. *Inhalation Drug Delivery*, ed. Colombo, P., D. Traini, and F. Buttini. Vol. 1. 2013, UK: Wiley-Blackwell.
35. M.P. Timsina, G.P. Martin, C. Marriott, D. Ganderton, and M. Yianneskis, *Drug delivery to the respiratory tract using dry powder inhalers.* Int J Pharm, 1994. **101**: p. 1-13.
36. Newman, S.P. and W.W. Busse, *Evolution of dry powder inhaler design, formulation, and performance.* Respir Med, 2002. **96**: p. 293-304.
37. Chan, H.-K., *Dry powder aerosol drug delivery—Opportunities for colloid and surface scientists.* Colloids Surf A Physiochem Eng Asp, 2006. **284–285**: p. 50-55.
38. *British National Formulary (BNF): Chapter 3: Respiratory System*. 2015 [cited 2015 24.11.15]; Available from: http://www.bnf.org/products/bnf-online/.
39. Dalby, R. and J. Suman, *Inhalation therapy: technological milestones in asthma treatment.* Adv Drug Deliv Rev, 2003. **55**(7): p. 779-791.
40. Najlah, M., A. Vali, M. Taylor, B.T. Arafat, W. Ahmed, D.A. Phoenix, K.M. Taylor, and A. Elhissi, *A study of the effects of sodium halides on the performance of air-jet and vibrating-mesh nebulizers.* Int J Pharm, 2013. **456**(2): p. 520-7.
41. Zhou, Q.T., P. Tang, S.S. Leung, J.G. Chan, and H.K. Chan, *Emerging inhalation aerosol devices and strategies: where are we headed?* Adv Drug Deliv Rev, 2014. **75**: p. 3-17.
42. Hickey, A.J., P.G. Durham, A. Dharmadhikari, and E.A. Nardell, *Inhaled drug treatment for tuberculosis: Past progress and future prospects.* J Control Release, 2015.
43. *National Institute of Health and Care Excellence (NICE) Guidelines: Chronic obstructive pulmonary disease in over 16s: diagnosis and management*. 2010.
44. British-Thoracic-Society. *BTS/SIGN Asthma Guideline 2014*. 2014 [cited 2015 24.11.15]; Available from: https://www.brit-thoracic.org.uk/document-library/clinical-information/asthma/btssign-asthma-guideline-2014/.

45. Button, B., L.H. Cai, C. Ehre, M. Kesimer, D.B. Hill, J.K. Sheehan, R.C. Boucher, and M. Rubinstein, *A periciliary brush promotes the lung health by separating the mucus layer from airway epithelia.* Science, 2012. **337**(6097): p. 937-41.
46. Smith, D.J., E.A. Gaffney, and J.R. Blake, *Modelling mucociliary clearance.* Respir Physiol Neurobiol, 2008. **163**(1–3): p. 178-188.
47. Ding, X. and L.S. Kaminsky, *Human extrahepatic cytochromes P450: function in xenobiotic metabolism and tissue-selective chemical toxicity in the respiratory and gastrointestinal tracts.* Annu Rev Pharmacol Toxicol, 2003. **43**: p. 149-73.
48. Tattersfield, A.E., A.J. Knox, J.R. Britton, and I.P. Hall, *Asthma.* Lancet, 2002. **360**(9342): p. 1313-22.
49. Donohue, J.F., *Therapeutic Responses in Asthma and COPD.* Chest, 2004. **126**(2): p. 125S-137S.
50. de Miguel-Diez, J., R. Jimenez-Garcia, V. Hernandez-Barrera, A. Lopez de Andres, J.R. Villa-Asensi, V. Plaza, and P. Carrasco-Garrido, *National trends in hospital admissions for asthma exacerbations among pediatric and young adult population in Spain (2002-2010).* Respir Med, 2014. **108**(7): p. 983-91.
51. Barnes, P.J., *Asthma guidelines: recommendations versus reality.* Respir Med, 2004. **98**: p. S1-S7.
52. Burns, J., C. Mason, N. Mueller, J. Ohlander, J.P. Zock, F. Drobnic, B. Wolfarth, J. Heinrich, E. Omenaas, T. Stensrud, D. Nowak, K. Radon, G.A.L.-O. Study-Team, and S. European Community Respiratory Health, *Asthma prevalence in Olympic summer athletes and the general population: An analysis of three European countries.* Respir Med, 2015. **109**(7): p. 813-20.
53. Baldacci, S., S. Maio, S. Cerrai, G. Sarno, N. Baiz, M. Simoni, I. Annesi-Maesano, G. Viegi, and H. Study, *Allergy and asthma: Effects of the exposure to particulate matter and biological allergens.* Respir Med, 2015.
54. Peters, S.P., G. Ferguson, Y. Deniz, and C. Reisner, *Uncontrolled asthma: A review of the prevalence, disease burden and options for treatment.* Respir Med, 2006. **100**(7): p. 1139-1151.
55. Jain, V.V., R. Allison, S.J. Beck, R. Jain, P.K. Mills, J.W. McCurley, K.P. Van Gundy, and M.W. Peterson, *Impact of an integrated disease management program in reducing exacerbations in patients with severe asthma and COPD.* Respir Med, 2014. **108**(12): p. 1794-800.
56. Holgate, S.T., *Pathophysiology of asthma: What has our current understanding taught us about new therapeutic approaches?* J Allergy Clin Immunol, 2011. **128**(3): p. 495-505.
57. Holgate, S.T., *Cytokine and anti-cytokine therapy for the treatment of asthma and allergic disease.* Cytokine, 2004. **28**(4-5): p. 152-7.
58. Holgate, S.T. and D.E. Davies, *Rethinking the pathogenesis of asthma.* Immunity, 2009. **31**(3): p. 362-7.
59. Holgate, S.T., *Pathogenesis of asthma.* Clin Exp Allergy, 2008. **38**(6): p. 872-97.
60. Holgate, S.T., *The sentinel role of the airway epithelium in asthma pathogenesis.* Immunol Rev, 2011. **242**(1): p. 205-19.
61. Linzer Sr, J.F., *Review of Asthma: Pathophysiology and Current Treatment Options.* Clin Pediatr Emerg Med, 2007. **8**(2): p. 87-95.
62. Chanez, P., S.E. Wenzel, G.P. Anderson, J.M. Anto, E.H. Bel, L.-P. Boulet, C.E. Brightling, W.W. Busse, M. Castro, B. Dahlen, S.E. Dahlen, L.M. Fabbri, S.T. Holgate, M. Humbert, M. Gaga, G.F. Joos, B. Levy, K.F. Rabe, P.J. Sterk, S.J. Wilson, and I. Vachier, *Severe asthma in adults: What are the important questions?* J Allergy Clin Immunol. **119**(6): p. 1337-1348.
63. Tuomisto, L.E., P. Ilmarinen, and H. Kankaanranta, *Prognosis of new-onset asthma diagnosed at adult age.* Respir Med, 2015. **109**(8): p. 944-54.
64. Munoz, X., M. Viladrich, L. Manso, V. del Pozo, S. Quirce, M.J. Cruz, F. Carmona, A. Sanchez-Pla, and J. Sastre, *Evolution of occupational asthma: does cessation of exposure really improve prognosis?* Respir Med, 2014. **108**(9): p. 1363-70.

65. Apter, A.J., *Advances in adult asthma diagnosis and treatment in 2014.* J Allergy Clin Immunol. **135**(1): p. 46-53.
66. Holgate, S.T. and R. Polosa, *The mechanisms, diagnosis, and management of severe asthma in adults.* Lancet, 2006. **368**(9537): p. 780-93.
67. Bjerg, A., J. Eriksson, I.S. Olafsdottir, R. Middelveld, K. Franklin, B. Forsberg, K. Larsson, K. Toren, S.E. Dahlen, and C. Janson, *The association between asthma and rhinitis is stable over time despite diverging trends in prevalence.* Respir Med, 2015. **109**(3): p. 312-9.
68. Crowe, A. and A.M. Tan, *Oral and inhaled corticosteroids: Differences in P-glycoprotein (ABCB1) mediated efflux.* Toxicol Appl Pharmacol, 2012. **260**(3): p. 294-302.
69. Mayhew, M., *Asthma medications and the new FDA public health advisory.* J Nurse Pract, 2006. **2**(2): p. 120-121.
70. Karakaya, G., E. Celebioglu, and A.F. Kalyoncu, *Non-steroidal anti-inflammatory drug hypersensitivity in adults and the factors associated with asthma.* Respir Med, 2013. **107**(7): p. 967-74.
71. Holgate, S.T., *Asthma therapy in the new millennium.* Allergol Int, 2000. **49**(4): p. 231-236.
72. Renauld, J.C., *New insights into the role of cytokines in asthma.* J Clin Pathol, 2001. **54**(8): p. 577-89.
73. Kelly, H.W., *Inhaled corticosteroid dosing: double for nothing?* J Allergy Clin Immunol, 2011. **128**(2): p. 278-281.e2.
74. Khan, M.A., M.R. Nicolls, B. Surguladze, and I. Saadoun, *Complement components as potential therapeutic targets for asthma treatment.* Respir Med, 2014. **108**(4): p. 543-9.
75. Sugihara, N., S. Kanada, M. Haida, M. Ichinose, M. Adachi, M. Hosoe, C. Emery, M. Higgins, and B. Kramer, *24-h bronchodilator efficacy of single doses of indacaterol in Japanese patients with asthma: a comparison with placebo and salmeterol.* Respir Med, 2010. **104**(11): p. 1629-37.
76. Davidsen, J.R., J. Sondergaard, J. Hallas, H.C. Siersted, T.B. Knudsen, J. Lykkegaard, and M. Andersen, *Impact of socioeconomic status on the use of inhaled corticosteroids in young adult asthmatics.* Respir Med, 2011. **105**(5): p. 683-90.
77. Lotvall, J., *Pharmacology of bronchodilators used in the treatment of COPD.* Respir Med, 2000. **94**: p. S6-S10.
78. Mason, N., N. Roberts, N. Yard, and M.R. Partridge, *Nebulisers or spacers for the administration of bronchodilators to those with asthma attending emergency departments?* Respir Med, 2008. **102**(7): p. 993-8.
79. Adams, N.P. and P.W. Jones, *The dose-response characteristics of inhaled corticosteroids when used to treat asthma: an overview of Cochrane systematic reviews.* Respir Med, 2006. **100**(8): p. 1297-306.
80. Schueepp, K.G., S.G. Devadason, C. Roller, S. Minocchieri, A. Moeller, J. Hamacher, and J.H. Wildhaber, *Aerosol delivery of nebulised budesonide in young children with asthma.* Respir Med, 2009. **103**(11): p. 1738-45.
81. Frois, C., E.Q. Wu, S. Ray, and G.L. Colice, *Inhaled corticosteroids or long-acting β-agonists alone or in fixed-dose combinations in asthma treatment: A systematic review of fluticasone/budesonide and formoterol/salmeterol.* Clin Ther, 2009. **31**(12): p. 2779-2803.
82. Sadatsafavi, M., L.D. Lynd, M.A. De Vera, Z. Zafari, and J.M. FitzGerald, *One-year outcomes of inhaled controller therapies added to systemic corticosteroids after asthma-related hospital discharge.* Respir Med, 2015. **109**(3): p. 320-8.
83. Korsgaard, J. and M. Ledet, *Potential side effects in patients treated with inhaled corticosteroids and long-acting beta2-agonists.* Respir Med, 2009. **103**(4): p. 566-73.

84. Tamm, M., D.H. Richards, B. Beghé, and L. Fabbri, *Inhaled corticosteroid and long-acting β2-agonist pharmacological profiles: effective asthma therapy in practice.* Respir Med, 2012. **106**: p. S9-S19.
85. Szefler, S.J. and H. Eigen, *Budesonide inhalation suspension: a nebulized corticosteroid for persistent asthma.* J Allergy Clin Immunol, 2002. **109**(4): p. 730-42.
86. Holgate, S.T., J. Holloway, S. Wilson, P.H. Howarth, H.M. Haitchi, S. Babu, and D.E. Davies, *Understanding the pathophysiology of severe asthma to generate new therapeutic opportunities.* J Allergy Clin Immunol, 2006. **117**(3): p. 496-506.
87. Kim, J., K. Kim, Y. Kim, K.H. Yoo, C.K. Lee, H.K. Yoon, Y.S. Kim, Y.B. Park, J.H. Lee, Y.M. Oh, S.D. Lee, and S.W. Lee, *The association between inhaled long-acting bronchodilators and less in-hospital care in newly-diagnosed COPD patients.* Respir Med, 2014. **108**(1): p. 153-61.
88. Halpin, D.M. and M. Miravitlles, *Chronic obstructive pulmonary disease: the disease and its burden to society.* Proc Am Thorac Soc, 2006. **3**(7): p. 619-23.
89. Cazzola, M., C.F. Donner, and N.A. Hanania, *One hundred years of chronic obstructive pulmonary disease (COPD).* Respir Med, 2007. **101**(6): p. 1049-65.
90. Cazzola, M., A. Segreti, E. Stirpe, M. Appodia, L. Senis, and M.G. Matera, *Energy expenditure and impact of bronchodilators in COPD patients.* Respir Med, 2010. **104**(10): p. 1490-4.
91. Pauwels, R.A. and K.F. Rabe, *Burden and clinical features of chronic obstructive pulmonary disease (COPD).* Lancet, 2004. **364**(9434): p. 613-620.
92. Musafiri, S., J. van Meerbeeck, L. Musango, G. Brusselle, G. Joos, B. Seminega, and C. Rutayisire, *Prevalence of atopy, asthma and COPD in an urban and a rural area of an African country.* Respir Med, 2011. **105**(11): p. 1596-605.
93. Gratziou, C., A. Florou, E. Ischaki, K. Eleftheriou, A. Sachlas, S. Bersimis, and S. Zakynthinos, *Smoking cessation effectiveness in smokers with COPD and asthma under real life conditions.* Respir Med, 2014. **108**(4): p. 577-83.
94. Rabe, K.F., S. Hurd, A. Anzueto, P.J. Barnes, S.A. Buist, P. Calverley, Y. Fukuchi, C. Jenkins, R. Rodriguez-Roisin, C. van Weel, J. Zielinski, and D. Global Initiative for Chronic Obstructive Lung, *Global strategy for the diagnosis, management, and prevention of chronic obstructive pulmonary disease: GOLD executive summary.* Am J Respir Crit Care Med, 2007. **176**(6): p. 532-55.
95. Barnes, P.J., *COPD: is there light at the end of the tunnel?* Curr Opin Pharmacol, 2004. **4**(3): p. 263-72.
96. Fitzgerald, M.F. and J.C. Fox, *Emerging trends in the therapy of COPD: bronchodilators as mono- and combination therapies.* Drug Discov Today, 2007. **12**(11–12): p. 472-478.
97. Fitzgerald, M.F. and J.C. Fox, *Emerging trends in the therapy of COPD: novel anti-inflammatory agents in clinical development.* Drug Discov Today, 2007. **12**(11-12): p. 479-86.
98. Edebnan, N.H., Robert M. Kaplan, A.B. Cohen, L.A. Hoffman, M.E. Kleinhenz, G.L. Snider, and Frank E. Speizer, *Chronic Obstructive Pulmonary Disease.* CHEST, 1992. **102**(3): p. 243S-256S.
99. Cosio, B.G., A. Iglesias, A. Rios, A. Noguera, E. Sala, K. Ito, P.J. Barnes, and A. Agusti, *Low-dose theophylline enhances the anti-inflammatory effects of steroids during exacerbations of COPD.* Thorax, 2009. **64**(5): p. 424-9.
100. Kanervisto, M., T. Vasankari, T. Laitinen, M. Heliovaara, P. Jousilahti, and S. Saarelainen, *Low socioeconomic status is associated with chronic obstructive airway diseases.* Respir Med, 2011. **105**(8): p. 1140-6.
101. Hanania, N.A., N. Ambrosino, P. Calverley, M. Cazzola, C.F. Donner, and B. Make, *Treatments for COPD.* Respir Med, 2005. **99 Suppl B**: p. S28-40.
102. Pauwels, R.A., A.S. Buist, P.M.A. Calverley, C.R. Jenkins, and S.S. Hurd, *Global Strategy for the Diagnosis, Management, and Prevention of Chronic Obstructive Pulmonary Disease- NHLBI/WHO Global Initiative for Chronic Obstructive Lung*

Disease (GOLD) Workshop Summary. Am J Respir Crit Care Med, 2001. **163**: p. 1256-1276.
103. Wouters, E.F.M., *Management of severe COPD.* Lancet, 2004. **364**(9437): p. 883-895.
104. Celli, B.R., W. MacNee, A. Agusti, A. Anzueto, B. Berg, A.S. Buist, P.M.A. Calverley, N. Chavannes, T. Dillard, B. Fahy, A. Fein, J. Heffner, S. Lareau, P. Meek, F. Martinez, W. McNicholas, J. Muris, E. Austegard, R. Pauwels, S. Rennard, A. Rossi, N. Siafakas, B. Tiep, J. Vestbo, E. Wouters, and R. ZuWallack, *Standards for the diagnosis and treatment of patients with COPD: a summary of the ATS/ERS position paper.* Eur Respir J, 2004. **23**(6): p. 932-946.
105. Tamimi, A., D. Serdarevic, and N.A. Hanania, *The effects of cigarette smoke on airway inflammation in asthma and COPD: therapeutic implications.* Respir Med, 2012. **106**(3): p. 319-28.
106. Mannino, D.M. and A.S. Buist, *Global burden of COPD: risk factors, prevalence, and future trends.* Lancet, 2007. **370**(9589): p. 765-773.
107. Anzueto, A., S. Sethi, and F.J. Martinez, *Exacerbations of chronic obstructive pulmonary disease.* Proc Am Thorac Soc, 2007. **4**(7): p. 554-64.
108. Cosio, B.G., L. Tsaprouni, K. Ito, E. Jazrawi, I.M. Adcock, and P.J. Barnes, *Theophylline restores histone deacetylase activity and steroid responses in COPD macrophages.* J Exp Med, 2004. **200**(5): p. 689-95.
109. Iiboshi, H., J. Ashitani, S. Katoh, A. Sano, N. Matsumoto, H. Mukae, and M. Nakazato, *Long-term treatment with theophylline reduces neutrophils, interleukin-8 and tumor necrosis factor-alpha in the sputum of patients with chronic obstructive pulmonary disease.* Pulm Pharmacol Ther, 2007. **20**(1): p. 46-51.
110. Dekhuijzen, P.N., W. Vincken, J.C. Virchow, N. Roche, A. Agusti, F. Lavorini, W.M. van Aalderen, and D. Price, *Prescription of inhalers in asthma and COPD: towards a rational, rapid and effective approach.* Respir Med, 2013. **107**(12): p. 1817-21.
111. Dekhuijzen, P.N., L. Bjermer, F. Lavorini, V. Ninane, M. Molimard, and J. Haughney, *Guidance on handheld inhalers in asthma and COPD guidelines.* Respir Med, 2014. **108**(5): p. 694-700.
112. Chorao, P., A.M. Pereira, and J.A. Fonseca, *Inhaler devices in asthma and COPD--an assessment of inhaler technique and patient preferences.* Respir Med, 2014. **108**(7): p. 968-75.
113. Kobayashi, M., Y. Nasuhara, T. Betsuyaku, E. Shibuya, Y. Tanino, M. Tanino, K. Takamura, K. Nagai, T. Hosokawa, and M. Nishimura, *Effect of low-dose theophylline on airway inflammation in COPD.* Respirology, 2004. **9**: p. 249-254.
114. Barnes, P.J., *Frontrunners in novel pharmacotherapy of COPD.* Curr Opin Pharmacol, 2008. **8**(3): p. 300-7.
115. Barnes, P.J. and T.T. Hansel, *Prospects for new drugs for chronic obstructive pulmonary disease.* Lancet, 2004. **364**(9438): p. 985-996.
116. Magnussen, H., H. Watz, A. Kirsten, M. Decramer, R. Dahl, P.M. Calverley, L. Towse, H. Finnigan, K. Tetzlaff, and B. Disse, *Stepwise withdrawal of inhaled corticosteroids in COPD patients receiving dual bronchodilation: WISDOM study design and rationale.* Respir Med, 2014. **108**(4): p. 593-9.
117. Rennard, S.I., *Treatment of stable chronic obstructive pulmonary disease.* Lancet, 2004. **364**(9436): p. 791-802.
118. Joos, G.F., *Are B2-Agonists Safe in Patients with Acute Exacerbations of COPD?* Am J Respir Crit Care Med, 2007. **176**: p. 322-323.
119. Katajisto, M., J. Koskela, A. Lindqvist, M. Kilpelainen, and T. Laitinen, *Physical activity in COPD patients decreases short-acting bronchodilator use and the number of exacerbations.* Respir Med, 2015.
120. Butland, B.K., H.R. Anderson, and C.J. Cates, *Bronchodilator treatment and asthma death: a new analysis of a British case-control study.* Respir Med, 2011. **105**(4): p. 549-57.

121. Ford, P.A., A.L. Durham, R.E. Russell, F. Gordon, I.M. Adcock, and P.J. Barnes, *Treatment effects of low-dose theophylline combined with an inhaled corticosteroid in COPD.* Chest, 2010. **137**(6): p. 1338-44.
122. Calverley, P.M., W. Boonsawat, Z. Cseke, N. Zhong, S. Peterson, and H. Olsson, *Maintenance therapy with budesonide and formoterol in chronicobstructive pulmonary disease.* Eur Respir J, 2003. **22**(6): p. 912-919.
123. Szafranski, W., A. Cukier, A. Ramirez, G. Menga, R. Sansores, S. Nahabedian, S. Peterson, and H. Olsson, *Efficacy and safety of budesonide/formoterol in the management of chronic obstructive pulmonary disease.* Eur Respir J, 2003. **21**(1): p. 74-81.
124. Holownia, A., R.M. Mroz, A. Kolodziejczyk, E. Chyczewska, and J.J. Braszko, *Increased FKBP51 in induced sputum cells of chronic obstructive pulmonary disease patients after therapy.* Eur J Med Res, 2009. **14**(Suppl. IV): p. 108-111.
125. Barnes, P.J., *Immunology of asthma and chronic obstructive pulmonary disease.* Nat Rev Immunol, 2008. **8**(3): p. 183-92.
126. ZuWallack, R.L., D.A. Mahler, D. Reilly, N. Church, A. Emmett, K. Rickard, and K. Knobil, *Salmeterol Plus Theophylline Combination Therapy in the Treatment of COPD.* Chest, 2001. **119**(6): p. 1661-1670.
127. Oh, Y.J., J. Lee, J.Y. Seo, T. Rhim, S.-H. Kim, H.J. Yoon, and K.Y. Lee, *Preparation of budesonide-loaded porous PLGA microparticles and their therapeutic efficacy in a murine asthma model.* J Control Release, 2011. **150**(1): p. 56-62.
128. Yang, Y., N. Bajaj, P. Xu, K. Ohn, M.D. Tsifansky, and Y. Yeo, *Development of highly porous large PLGA microparticles for pulmonary drug delivery.* Biomaterials, 2009. **30**(10): p. 1947-53.
129. Rodrigo, G.J. and J.A. Castro-Rodriguez, *Daily vs. intermittent inhaled corticosteroids for recurrent wheezing and mild persistent asthma: a systematic review with meta-analysis.* Respir Med, 2013. **107**(8): p. 1133-40.
130. Boulet, L.P., M.E. Boulay, G. Gauthier, L. Battisti, V. Chabot, M.F. Beauchesne, D. Villeneuve, and P. Cote, *Benefits of an asthma education program provided at primary care sites on asthma outcomes.* Respir Med, 2015. **109**(8): p. 991-1000.
131. Porsbjerg, C., P. Lange, and C.S. Ulrik, *Lung function impairment increases with age of diagnosis in adult onset asthma.* Respir Med, 2015. **109**(7): p. 821-7.
132. Bochenek, G., K. Szafraniec, J. Kuschill-Dziurda, and E. Nizankowska-Mogilnicka, *Factors associated with asthma control in patients with aspirin-exacerbated respiratory disease.* Respir Med, 2015. **109**(5): p. 588-95.
133. *Theophylline*. 2013 19/6/13]; http://www.drugbank.ca/drugs/DB00277.].
134. Andrews, K.L., S.C. Jones, and J. Mullan, *Asthma self management in adults: A review of current literature.* Collegian, 2014. **21**(1): p. 33-41.
135. van Dellen, Q.M., K. Stronks, P.J. Bindels, F.G. Ory, W.M. van Aalderen, and P.S. Group, *Adherence to inhaled corticosteroids in children with asthma and their parents.* Respir Med, 2008. **102**(5): p. 755-63.
136. Pauwels, R.A., C. Lofdahl, L.A. Laitinen, J.P. Schouten, D.S. Postma., N.B. Pride, and S.V. Ohlsson, *Long-term treatment with inhaled budesonide in persons with mild chronic obstructive pulmonary disease who continue smoking.* N Engl J Med, 1999. **340**(25): p. 1948-1953.
137. Lisspers, K., G. Johansson, C. Jansson, K. Larsson, G. Stratelis, M. Hedegaard, and B. Stallberg, *Improvement in COPD management by access to asthma/COPD clinics in primary care: data from the observational PATHOS study.* Respir Med, 2014. **108**(9): p. 1345-54.
138. Barnes, P.J., *Anti-inflammatory actions of glucocorticoids: molecular mechanisms.* Clin Sci (Lond), 1998. **94**(6): p. 557-72.
139. Fahey, T.D. *Anabolic-androgenic steroids: Mechanism of action and effects on performance* Encyclopedia of Sports medicine and science 1998 05/02/2016]; Available from: http://www.sportsci.org/encyc/anabster/anabster.html.

140. Szefler, S.J., *Pharmacodynamics and pharmacokinetics of budesonide: a new nebulized corticosteroid.* J Allergy Clin Immunol, 1999. **104**(4 Pt 2): p. 175-83.
141. *Budesonide*. http://www.drugbank.ca/drugs/DB01222. 2013 [cited 2013 19/6/13]; http://www.drugbank.ca/drugs/DB01222.].
142. Edsbacker, S. and T. Andersson, *Pharmacokinetics of budesonide (Entocort EC) capsules for Crohn's disease.* Clin Pharmacokinet, 2004. **43**(12): p. 803-21.
143. Clark, T.J.H., S. Godfrey, and T.H. Lee, *Asthma*. Vol. 3. 1992, London, UK: Chapman & Hall.
144. Montuschi, P. and P.J. Barnes, *New perspectives in pharmacological treatment of mild persistent asthma.* Drug Discov Today, 2011. **16**(23–24): p. 1084-1091.
145. Price, D. and J. Bousquet, *Real-world perceptions of inhaled corticosteroid/long-acting β2-agonist combinations in the treatment of asthma.* Respir Med, 2012. **106**: p. S4-S8.
146. Wells, K.E., E.L. Peterson, B.K. Ahmedani, R.K. Severson, J. Gleason-Comstock, and L.K. Williams, *The relationship between combination inhaled corticosteroid and long-acting beta-agonist use and severe asthma exacerbations in a diverse population.* J Allergy Clin Immunol, 2012. **129**(5): p. 1274-1279.e2.
147. Walters, J.A.E., R. Wood-Baker, and E.H. Walters, *Long-acting -agonists in asthma: an overview of Cochrane systematic reviews.* Respir Med, 2005. **99**(4): p. 384-395.
148. O'Byrne, P.M., *Acute asthma intervention: insights from the STAY study.* J Allergy Clin Immunol, 2007. **119**(6): p. 1332-6.
149. Durrani, S.R., R.K. Viswanathan, and W.W. Busse, *What effect does asthma treatment have on airway remodeling? Current perspectives.* J Allergy Clin Immunol, 2011. **128**(3): p. 439-48; quiz 449-50.
150. Barnes, P.J., *Theophylline: new perspectives for an old drug.* Am J Respir Crit Care Med, 2003. **167**(6): p. 813-8.
151. Barnes, P.J., *Theophylline in chronic obstructive pulmonary disease: new horizons.* Proc Am Thorac Soc, 2005. **2**(4): p. 334-9; discussion 340-1.
152. Barnes, P.J., *Theophylline for COPD.* Thorax, 2006. **61**: p. 742-743.
153. Evans, D.J., D.A. Taylor, O. Zetterstrom, K.F. Chung, B.J. O'Connor, and P.J. Barnes, *A comparison of low-dose inhaled budesonide plus theophylline and high-dose inhaled budesonide for moderate asthma.* N Engl J Med, 1997. **337**(20): p. 1412-1418.
154. Cyr, M.C., M.F. Beauchesne, C. Lemiere, and L. Blais, *Effect of theophylline on the rate of moderate to severe exacerbations among patients with chronic obstructive pulmonary disease.* Br J Clin Pharmacol, 2008. **65**(1): p. 40-50.
155. Jalal, I., E. Zmaily, and N. Najib, *Dissolution kinetics of commercially available theophylline preparations controlled-release.* Int J Pharm, 1989. **52**: p. 63-70.
156. Antal, I., R. Zelkó, N. Röczey, J. Plachy, and I. Rácz, *Dissolution and diffuse reflectance characteristics of coated theophylline particles.* Int J Pharm, 1997. **155**(1): p. 83-89.
157. Zacchigna, M., G. Di Luca, F. Cateni, S. Zorzet, and V. Maurich, *Improvement of physicochemical and biopharmaceutical properties of theophylline by poly(ethylene glycol) conjugates.* Il Farmaco, 2003. **58**(12): p. 1307-1312.
158. Zacchigna, M., G. Di Luca, F. Cateni, V. Maurich, M. Ballico, G.M. Bonora, and S. Drioli, *New MultiPEG-conjugated theophylline derivatives: Synthesis and pharmacological evaluations.* Eur J Pharm Sci, 2007. **30**(3–4): p. 343-350.
159. Broseghini, C., R. Testi, G. Polese, R. Tosatto, and A. Rossi, *A comparison between inhaled salmeterol and theophylline in the short-term treatment of stable chronic obstructive pulmonary disease.* Pulm Pharmacol Ther, 2005. **18**(2): p. 103-8.
160. Ohta, K., Y. Fukuchi, L. Grouse, R. Mizutani, K.F. Rabe, S.I. Rennard, and N.-S. Zhong, *A prospective clinical study of theophylline safety in 3810 elderly with asthma or COPD.* Respir Med, 2004. **98**(10): p. 1016-1024.

161. BASF-Chemical-datasheet. *Theophylline micronized* Available from: www.pharma-ingredients.basf.com/.../en/basf_theophylline_micro1.pdf.
162. Lipworth, B.J., *Phosphodiesterase-4 inhibitors for asthma and chronic obstructive pulmonary disease.* Lancet, 2005. **365**(9454): p. 167-175.
163. Cazzola, M., G. Di Lorenzo, F. Di Perna, F. Calderaro, R. Testi, and S. Centanni, *Additive Effects of Salmeterol and Fluticasone or Theophylline in COPD.* Chest, 2000. **118**(6): p. 1576-1581.
164. Vignola, A.M., *PDE4 inhibitors in COPD—a more selective approach to treatment.* Respir Med, 2004. **98**(6): p. 495-503.
165. Fan Chung, K., *Phosphodiesterase inhibitors in airways disease.* Eur J Pharmacol, 2006. **533**(1-3): p. 110-7.
166. Boswell-Smith, V., M. Cazzola, and C.P. Page, *Are phosphodiesterase 4 inhibitors just more theophylline?* J Allergy Clin Immunol, 2006. **117**(6): p. 1237-43.
167. Makino, S., M. Adachi, K. Ohta, N. Kihara, S. Nakajima, S. Nishima, T. Fukuda, and T. Miyamoto, *A Prospective Survey on Safety of Sustained-Release Theophylline in Treatment of Asthma and COPD.* Allergol Int, 2006. **55**: p. 395-402.
168. Kirsten, D.K., R.F. Wegner, R.A. Jorres, and H. Magnussen, *Effects of Theophylline Withdrawal in Severe Chronic Obstructive Pulmonary Disease.* Chest, 1993. **104**(4): p. 1101-1107.
169. Rossi, A., P. Kristufek, B.E. Levine, M.H. Thomson, D. Till, J. Kottakis, and G.D. Cioppa, *Comparison of the Efficacy, Tolerability, and Safety of Formoterol Dry Powder and Oral, Slow-Release Theophylline in the Treatment of COPD.* Chest, 2002. **121**(4): p. 1058-1069.
170. Zhao, X., J.P. Liu, X. Zhang, and Y. Li, *Enhancement of transdermal delivery of theophylline using microemulsion vehicle.* Int J Pharm, 2006. **327**(1-2): p. 58-64.
171. Tsukagoshi, H., Y. Shimizu, S. Iwamae, T. Hisada, T. Ishizuka, K. Iizuka, K. Dobashi, and M. Mori, *Evidence of oxidative stress in asthma and COPD: potential inhibitory effect of theophylline.* Respir Med, 2000. **94**: p. 584-588.
172. Barnes, P.J., *Corticosteroid resistance in patients with asthma and chronic obstructive pulmonary disease.* J Allergy Clin Immunol, 2013. **131**(3): p. 636-45.
173. Dahl, R., B.B. Larsen, and P. Venge, *Effect of long-term treatment with inhaled budesonide or theophylline on lung function, airway reactivity and asthma symptoms.* Respir Med, 2002. **96**(6): p. 432-438.
174. Vale, A., *Theophylline.* Medicine, 2007. **35**(12): p. 657.
175. Kanehara, M., A. Yokoyama, Y. Tomoda, N. Shiota, H. Iwamoto, N. Ishikawa, Y. Taooka, Y. Haruta, N. Hattori, and N. Kohno, *Anti-inflammatory effects and clinical efficacy of theophylline and tulobuterol in mild-to-moderate chronic obstructive pulmonary disease.* Pulm Pharmacol Ther, 2008. **21**(6): p. 874-8.
176. Pinto Reis, C., R.J. Neufeld, A.J. Ribeiro, and F. Veiga, *Nanoencapsulation I. Methods for preparation of drug-loaded polymeric nanoparticles.* Nanomedicine, 2006. **2**(1): p. 8-21.
177. Govender, T., S. Stolnik, M.C. Garnett, L. Illum, and S.S. Davis, *PLGA nanoparticles prepared by nanoprecipitation: drug loading and release studies of a water soluble drug.* J Control Release, 1999. **57**: p. 171-185.
178. Wu, L., J. Zhang, and W. Watanabe, *Physical and chemical stability of drug nanoparticles.* Adv Drug Deliv Rev, 2011. **63**(6): p. 456-69.
179. Soppimath, K.S., T.M. Aminabhavi, A.R. Kulkarni, and W.E. Rudzinski, *Biodegradable polymeric nanoparticles as drug delivery devices.* J Control Release, 2001. **70**: p. 1-20.
180. Elzoghby, A.O., W.M. Samy, and N.A. Elgindy, *Albumin-based nanoparticles as potential controlled release drug delivery systems.* J Control Release, 2012. **157**(2): p. 168-82.
181. Yang, W., J.I. Peters, and R.O. Williams Iii, *Inhaled nanoparticles—A current review.* Int J Pharm, 2008. **356**(1–2): p. 239-247.

182. Sung, J.C., B.L. Pulliam, and D.A. Edwards, *Nanoparticles for drug delivery to the lungs.* Trends Biotechnol, 2007. **25**(12): p. 563-70.
183. Zhang, J., L. Wu, H.-K. Chan, and W. Watanabe, *Formation, characterization, and fate of inhaled drug nanoparticles.* Adv Drug Deliv Rev, 2011. **63**(6): p. 441-455.
184. Singh, R. and J.W. Lillard, Jr., *Nanoparticle-based targeted drug delivery.* Exp Mol Pathol, 2009. **86**(3): p. 215-23.
185. Panyam, J. and V. Labhasetwar, *Biodegradable nanoparticles for drug and gene delivery to cells and tissue.* Adv Drug Deliv Rev, 2003. **55**(3): p. 329-347.
186. d'Angelo, I., B. Casciaro, A. Miro, F. Quaglia, M.L. Mangoni, and F. Ungaro, *Overcoming barriers in Pseudomonas aeruginosa lung infections: Engineered nanoparticles for local delivery of a cationic antimicrobial peptide.* Colloids Surf B Biointerfaces, 2015. **135**: p. 717-725.
187. d'Angelo, I., C. Conte, M.I. La Rotonda, A. Miro, F. Quaglia, and F. Ungaro, *Improving the efficacy of inhaled drugs in cystic fibrosis: challenges and emerging drug delivery strategies.* Adv Drug Deliv Rev, 2014. **75**: p. 92-111.
188. Cohen-Sela, E., M. Chorny, N. Koroukhov, H.O. Danenberg, and G. Golomb, *A new double emulsion solvent diffusion technique for encapsulating hydrophilic molecules in PLGA nanoparticles.* J Control Release, 2009. **133**(2): p. 90-95.
189. Kumari, A., S.K. Yadav, and S.C. Yadav, *Biodegradable polymeric nanoparticles based drug delivery systems.* Colloids Surf B Biointerfaces, 2010. **75**(1): p. 1-18.
190. Dev, A., N.S. Binulal, A. Anitha, S.V. Nair, T. Furuike, H. Tamura, and R. Jayakumar, *Preparation of poly(lactic acid)/chitosan nanoparticles for anti-HIV drug delivery applications.* Carbohydr Polym, 2010. **80**(3): p. 833-838.
191. Date, A.A. and V.B. Patravale, *Current strategies for engineering drug nanoparticles.* Curr Opin Colloid Interface Sci, 2004. **9**(3-4): p. 222-235.
192. Misra, A., A.J. Hickey, C. Rossi, G. Borchard, H. Terada, K. Makino, P.B. Fourie, and P. Colombo, *Inhaled drug therapy for treatment of tuberculosis.* Tuberculosis, 2011. **91**(1): p. 71-81.
193. Song, X., Y. Zhao, S. Hou, F. Xu, R. Zhao, J. He, Z. Cai, Y. Li, and Q. Chen, *Dual agents loaded PLGA nanoparticles: systematic study of particle size and drug entrapment efficiency.* Eur J Pharm Biopharm, 2008. **69**(2): p. 445-53.
194. Song, X., Y. Zhao, W. Wu, Y. Bi, Z. Cai, Q. Chen, Y. Li, and S. Hou, *PLGA nanoparticles simultaneously loaded with vincristine sulfate and verapamil hydrochloride: systematic study of particle size and drug entrapment efficiency.* Int J Pharm, 2008. **350**(1-2): p. 320-9.
195. Song, X.R., Z. Cai, Y. Zheng, G. He, F.Y. Cui, D.Q. Gong, S.X. Hou, S.J. Xiong, X.J. Lei, and Y.Q. Wei, *Reversion of multidrug resistance by co-encapsulation of vincristine and verapamil in PLGA nanoparticles.* Eur J Pharm Sci, 2009. **37**(3-4): p. 300-5.
196. Wang, Y.C., Y.T. Wu, H.Y. Huang, H.I. Lin, L.W. Lo, S.F. Tzeng, and C.S. Yang, *Sustained intraspinal delivery of neurotrophic factor encapsulated in biodegradable nanoparticles following contusive spinal cord injury.* Biomaterials, 2008. **29**(34): p. 4546-53.
197. Puri, S., P. Kallinteri, S. Higgins, G.A. Hutcheon, and M.C. Garnett, *Drug incorporation and release of water soluble drugs from novel functionalized poly(glycerol adipate) nanoparticles.* J Control Release, 2008. **125**(1): p. 59-67.
198. Cheow, W.S. and K. Hadinoto, *Enhancing encapsulation efficiency of highly water-soluble antibiotic in poly(lactic-co-glycolic acid) nanoparticles: Modifications of standard nanoparticle preparation methods.* Colloids Surf A Physiochem Eng Asp, 2010. **370**(1-3): p. 79-86.
199. Ishihara, T., M. Takahashi, M. Higaki, and Y. Mizushima, *Efficient encapsulation of a water-soluble corticosteroid in biodegradable nanoparticles.* Int J Pharm, 2009. **365**(1-2): p. 200-5.

200. Ghosh, A., A.K. Mandal, S. Sarkar, S. Panda, and N. Das, *Nanoencapsulation of quercetin enhances its dietary efficacy in combating arsenic-induced oxidative damage in liver and brain of rats.* Life Sci, 2009. **84**(3-4): p. 75-80.
201. Beck-Broichsitter, M., J. Gauss, C. Schweiger, S. Roesler, T. Schmehl, M. Kampschulte, A.C. Langheinrich, and W. Seeger, *Micro-computed tomography imaging of composite nanoparticle distribution in the lung.* Int J Pharm, 2012. **439**(1-2): p. 230-3.
202. Menon, J.U., P. Ravikumar, A. Pise, D. Gyawali, C.C. Hsia, and K.T. Nguyen, *Polymeric nanoparticles for pulmonary protein and DNA delivery.* Acta Biomater, 2014. **10**(6): p. 2643-52.
203. Gasparini, G., R.G. Holdich, and S.R. Kosvintsev, *PLGA particle production for water-soluble drug encapsulation: degradation and release behaviour.* Colloids Surf B Biointerfaces, 2010. **75**(2): p. 557-64.
204. Gasparini, G., S.R. Kosvintsev, M.T. Stillwell, and R.G. Holdich, *Preparation and characterization of PLGA particles for subcutaneous controlled drug release by membrane emulsification.* Colloids Surf B Biointerfaces, 2008. **61**(2): p. 199-207.
205. Kwon, H.-Y., J.-Y. Lee, S.-W. Choi, Y. Jang, and J.-H. Kim, *Preparation of PLGA nanoparticles containing estrogen by emulsification-diffusion method.* Colloids Surf A Physiochem Eng Asp, 2001. **182**: p. 123-130.
206. Engwicht, A., U. Girreser, and B. Muller, *Critical properties of lactide-co-glycolide polymers for the use in microparticle preparation by the Aerosol Solvent Extraction System.* Int J Pharm, 1999. **185**: p. 61-72.
207. Musumeci, T., C.A. Ventura, I. Giannone, B. Ruozi, L. Montenegro, R. Pignatello, and G. Puglisi, *PLA/PLGA nanoparticles for sustained release of docetaxel.* Int J Pharm, 2006. **325**(1-2): p. 172-9.
208. Jensen, D., L. Jensen, K. S, B. L, C. D, N. HM, and F. C, *Design of an inhalable dry powder formulation of DOTAP-modified PLGA nanoparticles loaded with siRNA.* J Control Release, 2012. **157**(1): p. 141-148.
209. Faraji, A.H. and P. Wipf, *Nanoparticles in cellular drug delivery.* Bioorg Med Chem, 2009. **17**(8): p. 2950-62.
210. Ungaro, F., I. d'Angelo, C. Coletta, R. d'Emmanuele di Villa Bianca, R. Sorrentino, B. Perfetto, M.A. Tufano, A. Miro, M.I. La Rotonda, and F. Quaglia, *Dry powders based on PLGA nanoparticles for pulmonary delivery of antibiotics: modulation of encapsulation efficiency, release rate and lung deposition pattern by hydrophilic polymers.* J Control Release, 2012. **157**(1): p. 149-59.
211. Beck-Broichsitter, M., O.M. Merkel, and T. Kissel, *Controlled pulmonary drug and gene delivery using polymeric nano-carriers.* J Control Release, 2012. **161**(2): p. 214-24.
212. Yamamoto, H., Y. Kuno, S. Sugimoto, H. Takeuchi, and Y. Kawashima, *Surface-modified PLGA nanosphere with chitosan improved pulmonary delivery of calcitonin by mucoadhesion and opening of the intercellular tight junctions.* J Control Release, 2005. **102**(2): p. 373–381.
213. Irache, J.M., L. Bergougnoux, I. Ezpeleta, J. Gueguen, and A.-M. Orecchion, *Optimization and in vitro stability of legumin nanoparticles obtained by a coacervation method.* Int J Pharm, 1995. **126**: p. 103-109.
214. Irache, J.M., I. Esparza, C. Gamazo, M. Agueros, and S. Espuelas, *Nanomedicine: novel approaches in human and veterinary therapeutics.* Vet Parasitol, 2011. **180**(1-2): p. 47-71.
215. Liang, R., L. Dong, R. Deng, J. Wang, K. Wang, M. Sullivan, S. Liu, J. Wang, J. Zhu, and J. Tao, *Surfactant-free biodegradable polymeric nanoparticles generated from self-organized precipitation route: Cellular uptake and cytotoxicity.* Eur Polym J, 2014. **57**: p. 187-201.
216. Mu, L. and S.S. Feng, *A novel controlled release formulation for the anticancer drug paclitaxel (Taxol(R)): PLGA nanoparticles containing vitamin E TPGS.* J Control Release, 2003. **86**: p. 33-48.

217. Kim, D.H. and D.C. Martin, *Sustained release of dexamethasone from hydrophilic matrices using PLGA nanoparticles for neural drug delivery.* Biomaterials, 2006. **27**(15): p. 3031-7.
218. Mittal, G., D.K. Sahana, V. Bhardwaj, and M.N. Ravi Kumar, *Estradiol loaded PLGA nanoparticles for oral administration: effect of polymer molecular weight and copolymer composition on release behavior in vitro and in vivo.* J Control Release, 2007. **119**(1): p. 77-85.
219. Beck-Broichsitter, M., C. Schweiger, T. Schmehl, T. Gessler, W. Seeger, and T. Kissel, *Characterization of novel spray-dried polymeric particles for controlled pulmonary drug delivery.* J Control Release, 2012. **158**(2): p. 329-35.
220. Beck-Broichsitter, M., T. Schmehl, W. Seeger, and T. Gessler, *Evaluating the Controlled Release Properties of Inhaled Nanoparticles Using Isolated, Perfused, and Ventilated Lung Models.* J Nanomater, 2011. **2011**: p. 1-16.
221. Zhang, Q., Z. Shen, and T. Nagai, *Prolonged hypoglycemic effect of insulin-loaded polybutylcyanoacrylate nanoparticles after pulmonary administration to normal rats.* Int J Pharm, 2001. **218**: p. 75-80.
222. Seju, U., A. Kumar, and K.K. Sawant, *Development and evaluation of olanzapine-loaded PLGA nanoparticles for nose-to-brain delivery: in vitro and in vivo studies.* Acta Biomater, 2011. **7**(12): p. 4169-76.
223. Kompella, U.B., N. Bandi, and S.P. Ayalasomayajula, *Subconjunctival Nano- and Microparticles Sustain Retinal Delivery of Budesonide, a Corticosteroid Capable of Inhibiting VEGF Expression.* Investigative Opthalmology & Visual Science, 2003. **44**(3): p. 1192.
224. Rawat, A., E. Stippler, V.P. Shah, and D.J. Burgess, *Validation of USP apparatus 4 method for microsphere in vitro release testing using Risperdal Consta.* Int J Pharm, 2011. **420**(2): p. 198-205.
225. Kunda, N.K., I.M. Alfagih, S.R. Dennison, S. Somavarapu, Z. Merchant, G.A. Hutcheon, and I.Y. Saleem, *Dry powder pulmonary delivery of cationic PGA-co-PDL nanoparticles with surface adsorbed model protein.* Int J Pharm, 2015. **492**(1-2): p. 213-22.
226. Loira-Pastoriza, C., J. Todoroff, and R. Vanbever, *Delivery strategies for sustained drug release in the lungs.* Adv Drug Deliv Rev, 2014. **75**: p. 81-91.
227. Arnold, M.M., E.M. Gorman, L.J. Schieber, E.J. Munson, and C. Berkland, *NanoCipro encapsulation in monodisperse large porous PLGA microparticles.* J Control Release, 2007. **121**(1-2): p. 100-9.
228. Sinha, B., B. Mukherjee, and G. Pattnaik, *Poly-lactide-co-glycolide nanoparticles containing voriconazole for pulmonary delivery: in vitro and in vivo study.* Nanomedicine, 2013. **9**(1): p. 94-104.
229. Beija, M., R. Salvayre, N. Lauth-de Viguerie, and J.D. Marty, *Colloidal systems for drug delivery: from design to therapy.* Trends Biotechnol, 2012. **30**(9): p. 485-96.
230. Nolan, L.M., L. Tajber, B.F. McDonald, A.S. Barham, O.I. Corrigan, and A.M. Healy, *Excipient-free nanoporous microparticles of budesonide for pulmonary delivery.* Eur J Pharm Sci, 2009. **37**(5): p. 593-602.
231. El-Gendy, N., W. Pornputtapitak, and C. Berkland, *Nanoparticle agglomerates of fluticasone propionate in combination with albuterol sulfate as dry powder aerosols.* Eur J Pharm Sci, 2011. **44**(4): p. 522-33.
232. Matsuo, Y., T. Ishihara, J. Ishizaki, K. Miyamoto, M. Higaki, and N. Yamashita, *Effect of betamethasone phosphate loaded polymeric nanoparticles on a murine asthma model.* Cell Immunol, 2009. **260**(1): p. 33-8.
233. Salama, R., S. Hoe, H.-K. Chan, D. Traini, and P.M. Young, *Preparation and characterisation of controlled release co-spray dried drug-polymer microparticles for inhalation 1: influence of polymer concentration on physical and in vitro characteristics* Eur J Pharm Biopharm, 2008. **69**: p. 486-495.
234. El-Sherbiny, I.M. and H.D. Smyth, *Biodegradable nano-micro carrier systems for sustained pulmonary drug delivery: (I) self-assembled nanoparticles encapsulated*

in respirable/swellable semi-IPN microspheres. Int J Pharm, 2010. **395**(1-2): p. 132-41.
235. Al-Qadi, S., A. Grenha, and C. Remuñán-López, *Microspheres loaded with polysaccharide nanoparticles for pulmonary delivery: Preparation, structure and surface analysis.* Carbohydr Polym, 2011. **86**(1): p. 25-34.
236. Beck-Broichsitter, M., T. Schmehl, T. Gessler, W. Seeger, and T. Kissel, *Development of a biodegradable nanoparticle platform for sildenafil: formulation optimization by factorial design analysis combined with application of charge-modified branched polyesters.* J Control Release, 2012. **157**(3): p. 469-77.
237. Beck-Broichsitter, M., P. Kleimann, T. Gessler, W. Seeger, T. Kissel, and T. Schmehl, *Nebulization performance of biodegradable sildenafil-loaded nanoparticles using the Aeroneb Pro: formulation aspects and nanoparticle stability to nebulization.* Int J Pharm, 2012. **422**(1-2): p. 398-408.
238. Mezzena, M., S. Scalia, P.M. Young, and D. Traini, *Solid lipid budesonide microparticles for controlled release inhalation therapy.* AAPS J, 2009. **11**(4): p. 771-8.
239. Muller, R.H., C. Jacobs, and O. Kayser, *Nanosuspensions as particulate drug formulations in therapy Rationale for development and what we can expect for the future.* Adv Drug Deliv Rev, 2001. **47**: p. 3-19.
240. Roa, W.H., S. Azarmi, M.H. Al-Hallak, W.H. Finlay, A.M. Magliocco, and R. Lobenberg, *Inhalable nanoparticles, a non-invasive approach to treat lung cancer in a mouse model.* J Control Release, 2011. **150**(1): p. 49-55.
241. Leroux, J.-C., E. Allémann, F. De Jaeghere, E. Doelker, and R. Gurny, *Biodegradable nanoparticles — From sustained release formulations to improved site specific drug delivery.* J Control Release, 1996. **39**(2–3): p. 339-350.
242. Sahoo, S.K. and V. Labhasetwar, *Nanotech approaches to drug delivery and imaging.* Drug Discov Today, 2003. **8**(24): p. 1112-1120.
243. Hans, M.L. and A.M. Lowman, *Biodegradable nanoparticles for drug delivery and targeting.* Curr Opin Solid State Mater Sci, 2002. **6**(4): p. 319-327.
244. Budhian, A., S.J. Siegel, and K.I. Winey, *Haloperidol-loaded PLGA nanoparticles: systematic study of particle size and drug content.* Int J Pharm, 2007. **336**(2): p. 367-75.
245. Kreuter, J., *Nanoparticle-based dmg delivery systems.* J Control Release, 1991. **16**(1–2): p. 169-176.
246. Kreuter, J., *Physicochemical characterization of polyacrylic nanoparticles.* Int J Pharm, 1983. **14**(1): p. 43-58.
247. Lai, P., W. Daear, R. Lobenberg, and E.J. Prenner, *Overview of the preparation of organic polymeric nanoparticles for drug delivery based on gelatine, chitosan, poly(d,l-lactide-co-glycolic acid) and polyalkylcyanoacrylate.* Colloids Surf B Biointerfaces, 2014. **118**: p. 154-63.
248. Oppenheim, R.C., *Solid colloidal drug delivery systems: Nanoparticles.* Int J Pharm, 1981. **8**(3): p. 217-234.
249. Parveen, S., R. Misra, and S.K. Sahoo, *Nanoparticles: a boon to drug delivery, therapeutics, diagnostics and imaging.* Nanomedicine, 2012. **8**(2): p. 147-66.
250. Mora-Huertas, C.E., H. Fessi, and A. Elaissari, *Polymer-based nanocapsules for drug delivery.* Int J Pharm, 2010. **385**(1-2): p. 113-42.
251. Vrignaud, S., J.P. Benoit, and P. Saulnier, *Strategies for the nanoencapsulation of hydrophilic molecules in polymer-based nanoparticles.* Biomaterials, 2011. **32**(33): p. 8593-604.
252. Choi, J.-S., J. Cao, M. Naeem, J. Noh, N. Hasan, H.-K. Choi, and J.-W. Yoo, *Size-controlled biodegradable nanoparticles: Preparation and size-dependent cellular uptake and tumor cell growth inhibition.* Colloids Surf B Biointerfaces, 2014. **122**: p. 545-551.

253. Beck-Broichsitter, M., J. Gauss, C.B. Packhaeuser, K. Lahnstein, T. Schmehl, W. Seeger, T. Kissel, and T. Gessler, *Pulmonary drug delivery with aerosolizable nanoparticles in an ex vivo lung model.* Int J Pharm, 2009. **367**(1-2): p. 169-78.
254. Helle, A., S. Hirsjärvi, L. Peltonen, J. Hirvonen, and S.K. Wiedmer, *Quantitative determination of drug encapsulation in poly(lactic acid) nanoparticles by capillary electrophoresis.* J Chromatogr A, 2008. **1178**(1–2): p. 248-255.
255. Lee, J.-H., T.G. Park, and H.-K. Choi, *Effect of formulation and processing variables on the characteristics of microspheres for water-soluble drugs prepared by w:o:o double emulsion solvent diffusion method.* Int J Pharm, 2000. **196**: p. 75-83.
256. Labhasetwar, V.D. and A.K. Dorle, *Nanoparticles — a colloidal drug delivery system for primaquine and metronidazole.* J Control Release, 1990. **12**(2): p. 113-119.
257. Quintanar-Guerrero, D., E. Allémann, H. Fessi, and E. Doelker, *Preparation Techniques and Mechanisms of Formation of Biodegradable Nanoparticles from Preformed Polymers.* Drug Dev Ind Pharm, 1998. **24**(12): p. 1113-1128.
258. Dinarvand, R., N. Sepehri, S. Manoochehri, H. Rouhani, and F. Atyabi, *Polylactide-co-glycolide nanoparticles for controlled delivery of anticancer agents.* Int J Nanomedicine, 2011. **6**: p. 877-95.
259. Ito, F., H. Fujimori, H. Kawakami, K. Kanamura, and K. Makino, *Technique to encapsulate a low molecular weight hydrophilic drug in biodegradable polymer particles in a liquid–liquid system.* Colloids Surf A Physiochem Eng Asp, 2011. **384**(1-3): p. 368-373.
260. Jelvehgari, M., S. Dastmalch, and N. Derafshi, *Theophylline-Ethylcellulose Microparticles: Screening of the Process and Formulation Variables for Preparation of Sustained Release Particles.* Iran J Basic Med Sci, 2012. **15**(1): p. 608-622.
261. Bilati, U., E. Allemann, and E. Doelker, *Development of a nanoprecipitation method intended for the entrapment of hydrophilic drugs into nanoparticles.* Eur J Pharm Sci, 2005. **24**(1): p. 67-75.
262. Rao, J.P. and K.E. Geckeler, *Polymer nanoparticles: Preparation techniques and size-control parameters.* Prog Polym Sci, 2011. **36**(7): p. 887-913.
263. Simonoska, C.M., M. Glavas Dodov, and K. Goracinova, *Chitosan coated Ca-alginate microparticles loaded with budesonide for delivery to the inflamed colonic mucosa.* Eur J Pharm Biopharm, 2008. **68**(3): p. 565-78.
264. Mohammadpourdounighi, N., A. Behfar, A. Ezabadi, H. Zolfagharian, and M. Heydari, *Preparation of chitosan nanoparticles containing Naja naja oxiana snake venom.* Nanomed Nanotech Biol Med, 2010. **6**(1): p. 137-143.
265. Pillai, C.K.S., W. Paul, and C.P. Sharma, *Chitin and chitosan polymers: Chemistry, solubility and fiber formation.* Prog Polym Sci, 2009. **34**(7): p. 641-678.
266. Dash, M., F. Chiellini, R.M. Ottenbrite, and E. Chiellini, *Chitosan—A versatile semi-synthetic polymer in biomedical applications.* Prog Polym Sci, 2011. **36**(8): p. 981-1014.
267. Grenha, A., C.I. Grainger, L.A. Dailey, B. Seijo, G.P. Martin, C. Remunan-Lopez, and B. Forbes, *Chitosan nanoparticles are compatible with respiratory epithelial cells in vitro.* Eur J Pharm Sci, 2007. **31**(2): p. 73-84.
268. Sinha, V.R., A.K. Singla, S. Wadhawan, R. Kaushik, R. Kumria, K. Bansal, and S. Dhawan, *Chitosan microspheres as a potential carrier for drugs.* Int J Pharm, 2004. **274**(1–2): p. 1-33.
269. Wilson, B., M.K. Samanta, K. Santhi, K.P. Kumar, M. Ramasamy, and B. Suresh, *Chitosan nanoparticles as a new delivery system for the anti-Alzheimer drug tacrine.* Nanomedicine, 2010. **6**(1): p. 144-52.
270. Vrancken, M.N. and D.A. Claeys, *Process for encapsulating water and compounds in aqueous phase by evaporation*. 1970, Google Patents.

271. Tice, T.R. and R.M. Gilley, *Preparation of injectable controlled-release microcapsules by a solvent-evaporation process.* J Control Release, 1985. **2**: p. 343-352.
272. Vanderhoff, J.W., M.S. El-Aasser, and J. Ugelstad, *Polymer emulsification process*, Patent, U.S., Editor. 1979.
273. Gurny, R., N.A. Peppas, D.D. Harrington, and G.S. Banker, *Development of Biodegradable and Injectable Latices for Controlled Release of Potent Drugs.* Drug Dev Ind Pharm, 1981. **7**(1): p. 1-25.
274. Nguyen, C.A., Y.N. Konan-Kouakou, E. Allemann, E. Doelker, D. Quintanar-Guerrero, H. Fessi, and R. Gurny, *Preparation of surfactant-free nanoparticles of methacrylic acid copolymers used for film coating.* AAPS PharmSciTech, 2006. **7**(3): p. 63.
275. Moinard-Checot, D., Y. Chevalier, S. Briancon, L. Beney, and H. Fessi, *Mechanism of nanocapsules formation by the emulsion-diffusion process.* J Colloid Interface Sci, 2008. **317**(2): p. 458-68.
276. Wood, D.A., *Biodegradable drug delivery systems.* Int J Pharm, 1980. **7**.
277. Kitajima, M., T. Yarnaguchi, A. Kondo, and N. Muroya, *Encapsulation method*, Patent, U.S., Editor. 1972: Japan.
278. Morishita, M., Y. Inaba, M. Fukushima, Y. Hattori, S. Kobari, and T. Matsuda, *Process for encapsulation of medicaments* Patent, U.S., Editor. 1976: Japan.
279. Fukushima, M., Y. lnaba, S. Kobari, and M. Morishita, *Process for preparing microcapsules*, Patent, U.S., Editor. 1975: Japan.
280. Ogawa, Y., M. Yamamoto, H. Okada, T. Yashiki, and T. Shimamoto, *A new technique to efficiently entrap leuprolide acetate into microcapsules of polylactic acid or copoly(lactic/glycolic) acid.* Chem Pharm Bull (Tokyo), 1988. **36**(3): p. 1095-103.
281. Delie, F., M. Berton, E. Allemann, and R. Gurny, *Comparison of two methods of encapsulation of an oligonucleotide into poly(D,L-lactic acid) particles.* Int J Pharm, 2001. **214**: p. 25-30.
282. Okada, H., Y. Ogawa, and T. Yashiki, *Prolonged release microcapsule and its production*. 1987, Google Patents.
283. Wei, Q., W. Wei, B. Lai, L.Y. Wang, Y.X. Wang, Z.G. Su, and G.H. Ma, *Uniform-sized PLA nanoparticles: preparation by premix membrane emulsification.* Int J Pharm, 2008. **359**(1-2): p. 294-7.
284. Mishra, B., B.B. Patel, and S. Tiwari, *Colloidal nanocarriers: a review on formulation technology, types and applications toward targeted drug delivery.* Nanomedicine, 2010. **6**(1): p. 9-24.
285. Manchanda, R., A. Fernandez-Fernandez, A. Nagesetti, and A.J. McGoron, *Preparation and characterization of a polymeric (PLGA) nanoparticulate drug delivery system with simultaneous incorporation of chemotherapeutic and thermo-optical agents.* Colloids Surf B Biointerfaces, 2010. **75**(1): p. 260-7.
286. Jaiswal, J., S.K. Gupta, and J. Kreuter, *Preparation of biodegradable cyclosporine nanoparticles by high-pressure emulsification-solvent evaporation process.* J Control Release, 2004. **96**(1): p. 169-78.
287. Chan, J.M., L. Zhang, K.P. Yuet, G. Liao, J.W. Rhee, R. Langer, and O.C. Farokhzad, *PLGA-lecithin-PEG core-shell nanoparticles for controlled drug delivery.* Biomaterials, 2009. **30**(8): p. 1627-34.
288. Miladi, K., S. Sfar, H. Fessi, and A. Elaissari, *Encapsulation of alendronate sodium by nanoprecipitation and double emulsion: From preparation to in vitro studies.* Ind Crops Prod, 2015. **72**: p. 24-33.
289. Daniher, D.I. and J. Zhu, *Dry powder platform for pulmonary drug delivery.* Particuology, 2008. **6**(4): p. 225-238.
290. Sharma, K., S. Somavarapu, A. Colombani, N. Govind, and K.M. Taylor, *Crosslinked chitosan nanoparticle formulations for delivery from pressurized metered dose inhalers.* Eur J Pharm Biopharm, 2012. **81**(1): p. 74-81.

291. Krause, H.J., A. Schwarz, and P. Rohdewald, *Polylactic acid nanoparticles, a colloidal drug delivery system for lipophilic drugs.* Int J Pharm, 1985. **27**(2–3): p. 145-155.
292. Barichello, J.M., M. Morishita, K. Takayama, and T. Nagai, *Encapsulation of Hydrophilic and Lipophilic Drugs in PLGA Nanoparticles by the Nanoprecipitation Method.* Drug Dev Ind Pharm, 1999. **25**(4): p. 471-476.
293. Mainardes, R.M. and R.C. Evangelista, *PLGA nanoparticles containing praziquantel: effect of formulation variables on size distribution.* Int J Pharm, 2005. **290**(1-2): p. 137-44.
294. Zambaux, M.F., F. Bonneaux, R. Gref, P. Maincent, E. Dellacherie, M.J. Alonso, P. Labrude, and C. Vigneron, *Influence of experimental parameters on the characteristics of poly(lactic acid) nanoparticles prepared by a double emulsion method.* J Control Release, 1998. **50**(1–3): p. 31-40.
295. Li, G., D.-H. Lin, X.-X. Xie, L.-F. Qin, J.-T. Wang, and K. Liu, *Uptake and transport of furanodiene in Caco-2 cell monolayers: a comparison study between furanodiene and furanodiene loaded PLGA nanoparticles.* Chin J Nat Med, 2013. **11**(1): p. 49-55.
296. Palamoor, M. and M.M. Jablonski, *Comparative study on diffusion and evaporation emulsion methods used to load hydrophilic drugs in poly(ortho ester) nanoparticle emulsions.* Powder Technol, 2014. **253**: p. 53-62.
297. Nafee, N., M. Schneider, U.F. Schaefer, and C.M. Lehr, *Relevance of the colloidal stability of chitosan/PLGA nanoparticles on their cytotoxicity profile.* Int J Pharm, 2009. **381**(2): p. 130-9.
298. Niwa, T., H. Takeuchi, T. Hino, N. Kunou, and Y. Kawashima, *Preparations of biodegradable nanospheres of water-soluble and insoluble drugs with D,L-lactide/glycolide copolymer by a novel spontaneous emulsification solvent diffusion method, and the drug release behavior.* J Control Release, 1993. **25**: p. 89-98.
299. Kunda, N.K., I.M. Alfagih, E.N. Miyaji, D.B. Figueiredo, V.M. Goncalves, D.M. Ferreira, S.R. Dennison, S. Somavarapu, G.A. Hutcheon, and I.Y. Saleem, *Pulmonary dry powder vaccine of pneumococcal antigen loaded nanoparticles.* Int J Pharm, 2015. **495**(2): p. 903-12.
300. Radwan, M.A., *HPLC Assay of Theophylline and Zidovudine in rat Serum.* J Liq Chromatogr Relat, 1995. **18**(16): p. 3301-3309.
301. Radwan, M.A., I.Y. Zaghloul, and Z.H. Aly, *In vivo performance of parenteral theophylline-loaded polyisobutylcyanoacrylate nanoparticles in rats.* Eur J Pharm Sci, 1999. **8**(2): p. 95-98.
302. Lin, J.-K., C.-L. Lin, Y.-C. Liang, S.-Y. Lin-Shiau, and I.-M. Juan, *Survey of catechins, gallic acid, and methylxanthines in green, oolong, pu-erh, and black teas.* J Agric Food Chem, 1998. **46**(9): p. 3635-3642.
303. Sharma, V., A. Gulati, S.D. Ravindranath, and V. Kumar, *A simple and convenient method for analysis of tea biochemicals by reverse phase HPLC.* J Food Comp Anal, 2005. **18**(6): p. 583-594.
304. Zuo, Y., H. Chen, and Y. Deng, *Simultaneous determination of catechins, caffeine and gallic acids in green, Oolong, black and pu-erh teas using HPLC with a photodiode array detector.* Talanta, 2002. **57**(2): p. 307-316.
305. Bispo, M.S., M.C. Veloso, H.L. Pinheiro, R.F. De Oliveira, J.O. Reis, and J.B. De Andrade, *Simultaneous determination of caffeine, theobromine, and theophylline by high-performance liquid chromatography.* J Chromatogr Sci, 2002. **40**(1): p. 45-8.
306. Altun, M.L., *HPLC Method for the analysis of Paracetamol, Caffeine and Dipyrone.* Turk J Chem, 2006. **26**: p. 521-528.
307. Wang, H., K. Helliwell, and X. You, *Isocratic elution system for the determination of catechins, caffeine and gallic acid in green tea using HPLC.* Food Chem, 2000. **68**(1): p. 115-121.

308. Martin, T.M., N. Bandi, R. Shulz, C.B. Roberts, and U.B. Kompella, *Preparation of Budesonide and Budesonide-PLA Microparticles Using Supercritical Fluid Precipitation Technology.* AAPS PharmSciTech 2002. **3**(3).
309. Naikwade, S.R., A.N. Bajaj, P. Gurav, M.M. Gatne, and P. Singh Soni, *Development of budesonide microparticles using spray-drying technology for pulmonary administration: design, characterization, in vitro evaluation, and in vivo efficacy study.* AAPS PharmSciTech, 2009. **10**(3): p. 993-1012.
310. Tiwari, M.N., S. Agarwal, P. Bhatnagar, N.K. Singhal, S.K. Tiwari, P. Kumar, L.K.S. Chauhan, D.K. Patel, R.K. Chaturvedi, M.P. Singh, and K.C. Gupta, *Nicotine-encapsulated poly(lactic-co-glycolic) acid nanoparticles improve neuroprotective efficacy against MPTP-induced parkinsonism.* Free Radic Biol Med, 2013. **65**: p. 704-718.
311. Kumari, A., S.K. Yadav, Y.B. Pakade, V. Kumar, B. Singh, A. Chaudhary, and S.C. Yadav, *Nanoencapsulation and characterization of Albizia chinensis isolated antioxidant quercitrin on PLA nanoparticles.* Colloids Surf B Biointerfaces, 2011. **82**(1): p. 224-32.
312. Mora-Huertas, C.E., O. Garrigues, H. Fessi, and A. Elaissari, *Nanocapsules prepared via nanoprecipitation and emulsification–diffusion methods: Comparative study.* Eur J Pharm Biopharm, 2012. **80**(1): p. 235-239.
313. Silveira, N., M.M. Longuinho, S.G. Leitao, R.S. Silva, M.C. Lourenco, P.E. Silva, C. Pinto Mdo, L.G. Abracado, and P.V. Finotelli, *Synthesis and characterization of the antitubercular phenazine lapazine and development of PLGA and PCL nanoparticles for its entrapment.* Mater Sci Eng C Mater Biol Appl, 2016. **58**: p. 458-66.
314. Sharma, K., S. Somavarapu, A. Colombani, N. Govind, and K.M. Taylor, *Nebulised siRNA encapsulated crosslinked chitosan nanoparticles for pulmonary delivery.* Int J Pharm, 2013. **455**(1-2): p. 241-7.
315. Nabi-Meibodi, M., A. Vatanara, A.R. Najafabadi, M.R. Rouini, V. Ramezani, K. Gilani, S.M. Etemadzadeh, and K. Azadmanesh, *The effective encapsulation of a hydrophobic lipid-insoluble drug in solid lipid nanoparticles using a modified double emulsion solvent evaporation method.* Colloids Surf B Biointerfaces, 2013. **112**: p. 408-14.
316. Elsaid, N., S. Somavarapu, and T.L. Jackson, *Cholesterol-poly(ethylene) glycol nanocarriers for the transscleral delivery of sirolimus.* Exp Eye Res, 2014. **121**: p. 121-9.
317. Salama, R.O., D. Traini, H.K. Chan, and P.M. Young, *Preparation and characterisation of controlled release co-spray dried drug-polymer microparticles for inhalation 2: evaluation of in vitro release profiling methodologies for controlled release respiratory aerosols.* Eur J Pharm Biopharm, 2008. **70**(1): p. 145-52.
318. Redhead, H.M., S.S. Davis, and L. Illum, *Drug delivery in poly(lactide-co-glycolide) nanoparticles surface modified with poloxamer 407 and poloxamine 908: in vitro characterisation and in vivo evaluation.* Journal of Controlled Release, 2001. **70**: p. 353-363.
319. Wang, J.J., Z.W. Zeng, R.Z. Xiao, T. Xie, G.L. Zhou, X.R. Zhan, and S.L. Wang, *Recent advances of chitosan nanoparticles as drug carriers.* Int J Nanomedicine, 2011. **6**: p. 765-74.
320. Zhang, Z. and S.S. Feng, *The drug encapsulation efficiency, in vitro drug release, cellular uptake and cytotoxicity of paclitaxel-loaded poly(lactide)-tocopheryl polyethylene glycol succinate nanoparticles.* Biomaterials, 2006. **27**(21): p. 4025-33.
321. Panyam, J., M.M. Dali, S.K. Sahoo, W. Ma, S.S. Chakravarthi, G.L. Amidon, R.J. Levy, and V. Labhasetwar, *Polymer degradation and in vitro release of a model protein from poly(d,l-lactide-co-glycolide) nano- and microparticles.* J Control Release, 2003. **92**(1-2): p. 173-187.

322. Grama, C.N., D.D. Ankola, and M.N.V.R. Kumar, *Poly(lactide-co-glycolide) nanoparticles for peroral delivery of bioactives.* Curr Opin Colloid Interface Sci, 2011. **16**(3): p. 238-245.
323. Brown, C.K., H.D. Friedel, A.R. Barker, L.F. Buhse, S. Keitel, T.L. Cecil, J. Kraemer, J.M. Morris, C. Reppas, M.P. Stickelmeyer, C. Yomota, and V.P. Shah *FIP/AAPS Joint Workshop Report: Dissolution/In Vitro Release Testing of Novel/Special Dosage Forms.* Indian J Pharm Sci., 2011. **73**(3): p. 338-353.
324. Zolnik, B.S., J.L. Raton, and D.J. Burgess, *Application of USP Apparatus 4 and In Situ Fiber Optic Analysis to Microsphere Release Testing.* Dissolut Technol, 2005. **12**(2): p. 11-14.
325. Maghsoudi, A., S.A. Shojaosadati, and E. Vasheghani Farahani, *5-Fluorouracil-loaded BSA nanoparticles: formulation optimization and in vitro release study.* AAPS PharmSciTech, 2008. **9**(4): p. 1092-6.
326. Herrera, L.C., M.V.D. Tesoriero, and L.G. Hermida, *In Vitro Release Testing of PLGA Microspheres with Franz Diffusion Cells.* Dissolut Technol, 2012. **19**(2).
327. Nakamura, K., K. Yoshino, K. Yamashita, and H. Kasukawa, *Designing a novel in vitro drug-release-testing method for liposomes prepared by pH-gradient method.* Int J Pharm, 2012. **430**(1-2): p. 381-7.
328. Bhardwaj, U. and D.J. Burgess, *A novel USP apparatus 4 based release testing method for dispersed systems.* Int J Pharm, 2010. **388**(1-2): p. 287-94.
329. D'Souza, S., *A review of in vitro drug release test methods for nano-sized dosage forms.* Adv Pharmaceut, 2014: p. 1-12.
330. Kabir, M.A., D.R. Taft, C.K. Joseph, and R.A. Bellantone, *Measuring drug concentrations using pulsatile microdialysis: theory and method development in vitro.* Int J Pharm, 2005. **293**(1-2): p. 171-82.
331. Wischke, C. and S.P. Schwendeman, *Principles of encapsulating hydrophobic drugs in PLA/PLGA microparticles.* Int J Pharm, 2008. **364**(2): p. 298-327.
332. Riley, T., D. Christopher, J. Arp, A. Casazza, A. Colombani, A. Cooper, M. Dey, J. Maas, J. Mitchell, M. Reiners, N. Sigari, T. Tougas, and S. Lyapustina, *Challenges with developing in vitro dissolution tests for orally inhaled products (OIPs).* AAPS PharmSciTech, 2012. **13**(3): p. 978-89.
333. Williams, A.C., *Topical and transdermal drug delivery*, in *Aulton's Pharmaceutics-Dosage form design and manufacture*, Aulton, M.E. and K.M.G. Taylor, Editors. 2013, Churchill Livingstone- Elsevier UK.
334. May, S., B. Jensen, M. Wolkenhauer, M. Schneider, and C.M. Lehr, *Dissolution techniques for in vitro testing of dry powders for inhalation.* Pharmaceutical Research, 2012. **29**(8): p. 2157-2166.
335. Haghi, M., H.X. Ong, D. Traini, and P. Young, *Across the pulmonary epithelial barrier: Integration of physicochemical properties and human cell models to study pulmonary drug formulations.* Pharmacol Ther, 2014. **144**(3): p. 235-52.
336. Dhar, S., F.X. Gu, R. Langer, O.C. Farokhzad, and S.J. Lippard, *Targeted delivery of cisplatin to prostate cancer cells by aptamer functionalized Pt(IV) prodrug-PLGA-PEG nanoparticles.* Proc Natl Acad Sci U S A, 2008. **105**(45): p. 17356-61.
337. Salome, C., O. Godswill, and O. Ikechukwu, *Kinetics and Mechanisms of Drug Release from Swellable and Non Swellable Matrices: A Review.* Research Journal of Pharmaceutical, Biological and Chemical Sciences, 2013. **4**(2): p. 97-103.
338. Budhian, A., S.J. Siegel, and K.I. Winey, *Controlling the in vitro release profiles for a system of haloperidol-loaded PLGA nanoparticles.* Int J Pharm, 2008. **346**(1-2): p. 151-9.
339. Zolnik, B.S. and D.J. Burgess, *Effect of acidic pH on PLGA microsphere degradation and release.* J Control Release, 2007. **122**(3): p. 338-44.
340. Zolnik, B.S., P.E. Leary, and D.J. Burgess, *Elevated temperature accelerated release testing of PLGA microspheres.* J Control Release, 2006. **112**(3): p. 293-300.

341. Nazanin, P., S. Hasannia, A.S. Lotfi, and M. Ghanei, *Encapsulation of Alpha-1 antitrypsin in PLGA nanoparticles: In Vitro characterization as an effective aerosol formulation in pulmonary diseases.* J Nanobiotechnology, 2012. **10**(20).
342. Ji, J., S. Hao, D. Wu, R. Huang, and Y. Xu, *Preparation, characterization and in vitro release of chitosan nanoparticles loaded with gentamicin and salicylic acid.* Carbohydr Polym, 2011. **85**(4): p. 803-808.
343. Singhvi, G. and M. Singh *Review: In vitro drug release characterization models.* Int J Pharm Stu Res, 2011. **2**(1): p. 77-84.
344. Aulton, M.E., *Dissolution and solubility*, in *Aulton's Pharmaceutics- The design and manufacture of medicines*, Aulton, M.E. and K.M.G. Taylor, Editors. 2013, Churchill Livingstone- Elsevier: London.
345. York, P., *Design of dosage forms*, in *Aulton's Pharmaceutics- The design and manufacture of medicines*, Aulton, M.E. and K.M.G. Taylor, Editors. 2013, Churchill Livingstone- Elsevier: London. p. 7-19.
346. Ong, H.X., F. Benaouda, D. Traini, D. Cipolla, I. Gonda, M. Bebawy, B. Forbes, and P.M. Young, *In vitro and ex vivo methods predict the enhanced lung residence time of liposomal ciprofloxacin formulations for nebulisation.* Eur J Pharm Biopharm, 2014. **86**(1): p. 83-9.
347. Rawat, A. and D.J. Burgess, *USP apparatus 4 method for in vitro release testing of protein loaded microspheres.* Int J Pharm, 2011. **409**(1-2): p. 178-84.
348. Yas, A.A., Y.I. Khalil, and M.S. Mohamed, *Response Surface Methodology for Development and Optimization of Theophylline Pulmonary Delivery System.* Iraqi J Pharm Sci, 2013. **22**(1): p. 65-81.
349. Naikwade, S., *Preparation and In Vitro Evaluation of Budesonide Spray Dried Microparticles for Pulmonary Delivery.* Sci Pharm, 2009. **77**(2): p. 419-441.
350. Aucoin, H.R., A.N. Wilson, A.M. Wilson, K. Ishihara, and A.G. Guiseppi-Elie, *Release of Potassium Ion and Calcium Ion from Phosphorylcholine Group Bearing Hydrogels (Supplementary Information).* Polymers, 2013. **5**: p. S1-S4.
351. Pugh, W.J., *Kinetics*, in *Aulton's Pharmaceutics - The design and manufacture of medicines*, Aulton, M.E. and K.M.G. Taylor, Editors. 2013, Churchill Livingstone-Elsevier: London.
352. Maques, M.C., R. Loebenberg, and M. Almukainzi, *Simulated biological fluids with possible application in dissolution testing.* . Dissolution technologies. , 2011. **18**(3): p. 15-28.
353. Saxena, V., M. Sadoqi, and J. Shao, *Indocyanine green-loaded biodegradable nanoparticles: preparation, physicochemical characterization and in vitro release.* Int J Pharm, 2004. **278**(2): p. 293-301.
354. Avgoustakis, K., A. Beletsi, Z. Panagi, P. Klepetsanis, A.G. Karydas, and D.S. Ithakissios, *PLGA–mPEG nanoparticles of cisplatin: in vitro nanoparticle degradation, in vitro drug release and in vivo drug residence in blood properties.* J Control Release, 2002. **79**: p. 123-135.
355. Venter, J.P., D.G. Muller, J. du Plessis, and C. Goosen, *A comparative study of an in situ adapted diffusion cell and an in vitro Franz diffusion cell method for transdermal absorption of doxylamine.* Eur J Pharm Sci, 2001. **13**: p. 169-177.
356. Chattaraj, S.C., J. Swarbrick, and I. Kanfer, *A simple diffusion cell to monitor drug release from semi-solid dosage forms.* Int J Pharm, 1995. **120**: p. 119-124.
357. Park, J., P.M. Fong, J. Lu, K.S. Russell, C.J. Booth, W.M. Saltzman, and T.M. Fahmy, *PEGylated PLGA nanoparticles for the improved delivery of doxorubicin.* Nanomedicine, 2009. **5**(4): p. 410-8.
358. Gandhi, A., S. Jana, and K.K. Sen, *In-vitro release of acyclovir loaded Eudragit RLPO((R)) nanoparticles for sustained drug delivery.* Int J Biol Macromol, 2014. **67**: p. 478-82.
359. Yasir, M. and U.V.S. Sara, *Solid lipid nanoparticles for nose to brain delivery of haloperidol: in vitro drug release and pharmacokinetics evaluation.* Acta Pharm Sin B, 2014. **4**(6): p. 454-463.

360. Shah, K.B., P.G. Patel, A. Khairuzzaman, and R.A. Bellantone, *An improved method for the characterization of supersaturation and precipitation of poorly soluble drugs using pulsatile microdialysis (PMD).* Int J Pharm, 2014. **468**(1-2): p. 64-74.
361. Morais, J.M. and D.J. Burgess, *In vitro release testing methods for vitamin E nanoemulsions.* Int J Pharm, 2014. **475**(1-2): p. 393-400.
362. Engel, A., M. Ploger, D. Mulac, and K. Langer, *Asymmetric flow field-flow fractionation (AF4) for the quantification of nanoparticle release from tablets during dissolution testing.* Int J Pharm, 2014. **461**(1-2): p. 137-44.
363. Win, K.Y. and S.S. Feng, *Effects of particle size and surface coating on cellular uptake of polymeric nanoparticles for oral delivery of anticancer drugs.* Biomaterials, 2005. **26**(15): p. 2713-22.
364. Fonseca, C., S. Simoes, and R. Gaspar, *Paclitaxel-loaded PLGA nanoparticles: preparation, physicochemical characterization and in vitro anti-tumoral activity.* J Control Release, 2002. **83**: p. 273-286.
365. Wang, W., S. Chen, L. Zhang, X. Wu, J. Wang, J.F. Chen, and Y. Le, *Poly(lactic acid)/chitosan hybrid nanoparticles for controlled release of anticancer drug.* Mater Sci Eng C Mater Biol Appl, 2015. **46**: p. 514-20.
366. Grenha, A., C. Remunan-Lopez, E.L. Carvalho, and B. Seijo, *Microspheres containing lipid/chitosan nanoparticles complexes for pulmonary delivery of therapeutic proteins.* Eur J Pharm Biopharm, 2008. **69**(1): p. 83-93.
367. Heard, C.M., S. Johnson, G. Moss, and C.P. Thomas, *In vitro transdermal delivery of caffeine, theobromine, theophylline and catechin from extract of Guarana, Paullinia Cupana.* Int J Pharm, 2006. **317**(1): p. 26-31.
368. Cho, J.H., H.H. Baek, J.M. Lee, J.H. Kim, D.D. Kim, H.K. Cho, and I.W. Cheong, *Topical Delivery of Budesonide Emulsion Particles in the Presence of PEO-PCL-PEO Triblock Copolymers.* Macromol Res, 2009. **17**(12): p. 969-975.
369. Cortesi, R., L. Ravani, E. Menegatti, E. Esposito, and F. Ronconi, *Eudragit((R)) microparticles for the release of budesonide: a comparative study.* Indian J Pharm Sci, 2012. **74**(5): p. 415-21.
370. Salomon, J.J. and C. Ehrhardt, *Nanoparticles attenuate P-glycoprotein/MDR1 function in A549 human alveolar epithelial cells.* Eur J Pharm Biopharm, 2011. **77**(3): p. 392-7.
371. Foster, K.A., M.L. Avery, K.L. Audus, and M. Yazdanian, *Characterization of the Calu-3 cell line as a tool to screen pulmonary drug delivery.* Int J Pharm, 2000. **208**: p. 1-11.
372. Madlova, M., S.A. Jones, I. Zwerschke, Y. Ma, R.C. Hider, and B. Forbes, *Poly(vinyl alcohol) nanoparticle stability in biological media and uptake in respiratory epithelial cell layers in vitro.* Eur J Pharm Biopharm, 2009. **72**(2): p. 437-43.
373. Eidi, H., O. Joubert, G. Attik, R.E. Duval, M.C. Bottin, A. Hamouia, P. Maincent, and B.H. Rihn, *Cytotoxicity assessment of heparin nanoparticles in NR8383 macrophages.* Int J Pharm, 2010. **396**(1-2): p. 156-65.
374. Azarmi, S., W.H. Roa, and R. Lobenberg, *Targeted delivery of nanoparticles for the treatment of lung diseases.* Adv Drug Deliv Rev, 2008. **60**(8): p. 863-75.
375. Ciofani, G., S. Danti, D. D'Alessandro, S. Moscato, and A. Menciassi, *Assessing cytotoxicity of boron nitride nanotubes: Interference with the MTT assay.* Biochem Biophys Res Commun, 2010. **394**(2): p. 405-11.
376. Scherliess, R., *The MTT assay as tool to evaluate and compare excipient toxicity in vitro on respiratory epithelial cells.* Int J Pharm, 2011. **411**(1-2): p. 98-105.
377. Wang, S., H. Yu, and J.K. Wickliffe, *Limitation of the MTT and XTT assays for measuring cell viability due to superoxide formation induced by nano-scale TiO2.* Toxicol In Vitro, 2011. **25**(8): p. 2147-51.
378. Lobner, D., *Comparison of the LDH and MTT assays for quantifying cell death: validity for neuronal apoptosis?* J Neurosci Methods, 2000. **96**: p. 147-152.

379. Mendes, L.P., J.M. Delgado, A.D. Costa, M.S. Vieira, P.L. Benfica, E.M. Lima, and M.C. Valadares, *Biodegradable nanoparticles designed for drug delivery: The number of nanoparticles impacts on cytotoxicity.* Toxicol In Vitro, 2015. **29**(6): p. 1268-74.
380. Sharma, D., D. Maheshwari, G. Philip, R. Rana, S. Bhatia, M. Singh, R. Gabrani, S.K. Sharma, J. Ali, R.K. Sharma, and S. Dang, *Formulation and optimization of polymeric nanoparticles for intranasal delivery of lorazepam using Box-Behnken design: in vitro and in vivo evaluation.* Biomed Res Int, 2014. **2014**: p. 156010.
381. Vllasaliu, D., L. Casettari, R. Fowler, R. Exposito-Harris, M. Garnett, L. Illum, and S. Stolnik, *Absorption-promoting effects of chitosan in airway and intestinal cell lines: a comparative study.* Int J Pharm, 2012. **430**(1-2): p. 151-60.
382. Westmoreland, C., T. Walker, J. Matthews, and J. Murdock, *Preliminary investigations into the use of a human bronchial epithelial cell line (16HBE14o-) to screen for respiratory toxins in vitro.* Toxicol In vitro, 1999. **13**: p. 761-764.
383. Han, X., R. Gelein, N. Corson, P. Wade-Mercer, J. Jiang, P. Biswas, J.N. Finkelstein, A. Elder, and G. Oberdorster, *Validation of an LDH assay for assessing nanoparticle toxicity.* Toxicology, 2011. **287**(1-3): p. 99-104.
384. Fotakis, G. and J.A. Timbrell, *In vitro cytotoxicity assays: comparison of LDH, neutral red, MTT and protein assay in hepatoma cell lines following exposure to cadmium chloride.* Toxicol Lett, 2006. **160**(2): p. 171-7.
385. Basarkar, A., D. Devineni, R. Palaniappan, and J. Singh, *Preparation, characterization, cytotoxicity and transfection efficiency of poly(DL-lactide-co-glycolide) and poly(DL-lactic acid) cationic nanoparticles for controlled delivery of plasmid DNA.* Int J Pharm, 2007. **343**(1-2): p. 247-54.
386. Wang, J., C. Wang, X. Li, L. Kong, K. Gao, and R.Y. Liu, *The effects of anti-asthma drugs on the phagocytic clearance of apoptotic eosinophils by A549 cells.* Respir Med, 2009. **103**(11): p. 1693-9.
387. Gualtieri, M., L. Rigamonti, V. Galeotti, and M. Camatini, *Toxicity of tire debris extracts on human lung cell line A549.* Toxicol In Vitro, 2005. **19**(7): p. 1001-8.
388. Abraham, G., C. Kneuer, C. Ehrhardt, W. Honscha, and F.R. Ungemach, *Expression of functional beta2-adrenergic receptors in the lung epithelial cell lines 16HBE14o(-), Calu-3 and A549.* Biochim Biophys Acta, 2004. **1691**(2-3): p. 169-79.
389. Harcourt, J.L., H. Caidi, L.J. Anderson, and L.M. Haynes, *Evaluation of the Calu-3 cell line as a model of in vitro respiratory syncytial virus infection.* J Virol Methods, 2011. **174**(1-2): p. 144-9.
390. Paturi, D.K., D. Kwatra, H.K. Ananthula, D. Pal, and A.K. Mitra, *Identification and functional characterization of breast cancer resistance protein in human bronchial epithelial cells (Calu-3).* Int J Pharm, 2010. **384**(1-2): p. 32-8.
391. Babu, P.B., A. Chidekel, and T.H. Shaffer, *Protein composition of apical surface fluid from the human airway cell line Calu-3: effect of ion transport mediators.* Clin Chim Acta, 2004. **347**(1-2): p. 81-8.
392. Forbes, B. and C. Ehrhardt, *Human respiratory epithelial cell culture for drug delivery applications.* Eur J Pharm Biopharm, 2005. **60**(2): p. 193-205.
393. Forbes, B., A. Shah, G.P. Martin, and A.B. Lansley, *The human bronchial epithelial cell line 16HBE14o− as a model system of the airways for studying drug transport.* Int J Pharm, 2003. **257**(1-2): p. 161-167.
394. Ahsan, F., J.J. Arnold, T. Yang, E. Meezan, E.M. Schwiebert, and D.J. Pillion, *Effects of the permeability enhancers, tetradecylmaltoside and dimethyl-β-cyclodextrin, on insulin movement across human bronchial epithelial cells (16HBE14o−).* Eur J Pharm Sci, 2003. **20**(1): p. 27-34.
395. Kunda, N.K., I.M. Alfagih, E.N. Miyaji, D.B. Figueiredo, V.M. Gonçalves, D.M. Ferreira, S.R. Dennison, S. Somavarapu, G.A. Hutcheon, and I.Y. Saleem, *Pulmonary dry powder vaccine of pneumococcal antigen loaded nanoparticles.* Int J Pharm, 2015. **495**(2): p. 903-912.

396. Merchant, Z., K.M.G. Taylor, P. Stapleton, S.A. Razak, N. Kunda, I. Alfagih, K. Sheikh, I.Y. Saleem, and S. Somavarapu, *Engineering hydrophobically modified chitosan for enhancing the dispersion of respirable microparticles of levofloxacin.* Eur J Pharm Biopharm, 2014. **88**(3): p. 816-829.
397. Bhatt, H., B. Naik, and A. Dharamsi, *Solubility Enhancement of Budesonide and Statistical Optimization of Coating Variables for Targeted Drug Delivery.* J Pharm, 2014. **2014**: p. 13.
398. Jain, D.S., R.B. Athawale, A.N. Bajaj, S.S. Shrikhande, P.N. Goel, Y. Nikam, and R.P. Gude, *Unraveling the cytotoxic potential of Temozolomide loaded into PLGA nanoparticles.* DARU, 2014. **22**(18): p. 1-9.
399. Mura, S., H. Hillaireau, J. Nicolas, B. Le Droumaguet, C. Gueutin, S. Zanna, N. Tsapis, and E. Fattal, *Influence of surface charge on the potential toxicity of PLGA nanoparticles towards Calu-3 cells.* Int J Nanomedicine, 2011. **6**: p. 2591-2605.
400. Yoo, H.S., K.H. Lee , J.E. Oh , and T.G. Park, *In vitro and in vivo anti-tumor activities of nanoparticles based a on doxorubicin–PLGA conjugates.* J Control Release, 2000. **68**: p. 419-431.
401. Amjadi, I., M. Rabiee, and M.-S. Hosseini, *Anticancer Activity of Nanoparticles Based on PLGA and its Co-polymer: In-vitro Evaluation.* Iran J Pharm Res, 2013. **12**(4): p. 623-634.
402. Mathew, A., T. Fukuda, Y. Nagaoka, T. Hasumura, H. Morimoto, Y. Yoshida, T. Maekawa, K. Venugopal, and D.S. Kumar, *Curcumin loaded-PLGA nanoparticles conjugated with Tet-1 peptide for potential use in Alzheimer's disease.* PLoS One, 2012. **7**(3): p. e32616.
403. Jain, R.A., *The manufacturing techniques of various drug loaded biodegradable poly(lactide-co-glycolide) (PLGA) devices.* Biomaterials, 2000. **21**(23): p. 2475-2490.
404. Sharma, S., A. Parmar, S. Kori, and R. Sandhir, *PLGA-based nanoparticles: a new paradigm in biomedical applications.* Trend Anal Chem.
405. Engineer, C., J. Parikh, and A. Raval, *Effect of copolymer ratio on hydrolytic degradation of poly(lactide-co-glycolide) from drug eluting coronary stents.* Chem Eng Res Des, 2011. **89**(3): p. 328-334.
406. Brzoska, M., K. Langer, C. Coester, S. Loitsch, T.O. Wagner, and C. Mallinckrodt, *Incorporation of biodegradable nanoparticles into human airway epithelium cells-in vitro study of the suitability as a vehicle for drug or gene delivery in pulmonary diseases.* Biochem Biophys Res Commun, 2004. **318**(2): p. 562-70.
407. Uzun, N., T.D. Martins, G.M. Teixeira, N.L. Cunha, R.B. Oliveira, E.J. Nassar, and R.A. Dos Santos, *Poly(L-lactic acid) membranes: absence of genotoxic hazard and potential for drug delivery.* Toxicol Lett, 2015. **232**(2): p. 513-8.
408. Nguyen, J., R. Reul, T. Betz, E. Dayyoub, T. Schmehl, T. Gessler, U. Bakowsky, W. Seeger, and T. Kissel, *Nanocomposites of lung surfactant and biodegradable cationic nanoparticles improve transfection efficiency to lung cells.* J Control Release, 2009. **140**(1): p. 47-54.
409. Xiong, X.Y., X. Qin, Z.L. Li, Y.C. Gong, and Y.P. Li, *Synthesis, drug release and targeting behaviors of Novel Folated Pluronic F87/poly(lactic acid) block copolymer.* Eur Polym J, 2015. **68**: p. 233-242.
410. Yoon, I.S., J.H. Park, H.J. Kang, J.H. Choe, M.S. Goh, D.D. Kim, and H.J. Cho, *Poly(D,L-lactic acid)-glycerol-based nanoparticles for curcumin delivery.* Int J Pharm, 2015. **488**(1-2): p. 70-7.
411. Li, J., M. Kong, X.J. Cheng, Q.F. Dang, X. Zhou, Y.N. Wei, and X.G. Chen, *Preparation of biocompatible chitosan grafted poly(lactic acid) nanoparticles.* Int J Biol Macromol, 2012. **51**(3): p. 221-7.
412. Lu, W., Y. Zhang, Y.-Z. Tan, K.-L. Hu, X.-G. Jiang, and S.-K. Fu, *Cationic albumin-conjugated pegylated nanoparticles as novel drug carrier for brain delivery.* J Control Release, 2005. **107**(3): p. 428-448.

413. Zhu, B., M. Haghi, M. Goud, P.M. Young, and D. Traini, *The formulation of a pressurized metered dose inhaler containing theophylline for inhalation.* Eur J Pharm Sci, 2015. **76**: p. 68-72.
414. Yoncheva, K., M. Popova, A. Szegedi, J. Mihaly, B. Tzankov, N. Lambov, S. Konstantinov, V. Tzankova, F. Pessina, and M. Valoti, *Functionalized mesoporous silica nanoparticles for oral delivery of budesonide.* J Solid State Chem, 2014. **211**: p. 154-161.
415. Bandi, N. and U.B. Kompella, *Budesonide reduces vascular endothelial growth factor secretion and expression in airway Calu-1 and alveolar A549 epithelial cells.* European Journal of Pharmacology, 2001. **425**: p. 109-116.
416. Dombu, C.Y. and D. Betbeder, *Airway delivery of peptides and proteins using nanoparticles.* Biomaterials, 2013. **34**(2): p. 516-525.
417. Pohl, C., M.I. Hermanns, C. Uboldi, M. Bock, S. Fuchs, J. Dei-Anang, E. Mayer, K. Kehe, W. Kummer, and C.J. Kirkpatrick, *Barrier functions and paracellular integrity in human cell culture models of the proximal respiratory unit.* Eur J Pharm Biopharm, 2009. **72**(2): p. 339-349.
418. Ehrhardt, C., BKim, K-J, *In Vitro Models of the Tracheo-Bronchial Epithelium*, in *Drug Absorption Studies*. 2008, Springer US: America. p. 235-257.
419. Rotoli, B.M., O. Bussolati, M.G. Bianchi, A. Barilli, C. Balasubramanian, S. Bellucci, and E. Bergamaschi, *Non-functionalized multi-walled carbon nanotubes alter the paracellular permeability of human airway epithelial cells.* Toxicol Lett, 2008. **178**(2): p. 95-102.
420. dos Santos, M.A., C. Bosquillon, T. Russomano, A. Sundaresan, F. Falcão, C. Marriott, and B. Forbes, *Modelling the effects of microgravity on the permeability of air interface respiratory epithelial cell layers.* Adv Space Res, 2010. **46**(6): p. 712-718.
421. Ehrhardt, C., C. Kneuer, C. Bies, C.-M. Lehr, K.-J. Kim, and U. Bakowsky, *Salbutamol is actively absorbed across human bronchial epithelial cell layers.* Pulm Pharmacol Ther, 2005. **18**(3): p. 165-170.
422. Vllasaliu, D., R. Exposito-Harris, A. Heras, L. Casettari, M. Garnett, L. Illum, and S. Stolnik, *Tight junction modulation by chitosan nanoparticles: comparison with chitosan solution.* Int J Pharm, 2010. **400**(1-2): p. 183-93.
423. Hittinger, M., J. Juntke, S. Kletting, N. Schneider-Daum, C. de Souza Carvalho, and C.M. Lehr, *Preclinical safety and efficacy models for pulmonary drug delivery of antimicrobials with focus on in vitro models.* Adv Drug Deliv Rev, 2015. **85**: p. 44-56.
424. Hutter, V., C. Hilgendorf, A. Cooper, V. Zann, D.I. Pritchard, and C. Bosquillon, *Evaluation of layers of the rat airway epithelial cell line RL-65 for permeability screening of inhaled drug candidates.* Eur J Pharm Sci, 2012. **47**(2): p. 481-489.
425. Manford, F., A. Tronde, A.B. Jeppsson, N. Patel, F. Johansson, and B. Forbes, *Drug permeability in 16HBE14o- airway cell layers correlates with absorption from the isolated perfused rat lung.* Eur J Pharm Sci, 2005. **26**(5): p. 414-20.
426. Chana, J., B. Forbes, and S.A. Jones, *Triggered-release nanocapsules for drug delivery to the lungs.* Nanomedicine, 2015. **11**(1): p. 89-97.
427. Mukherjee, M., D.I. Pritchard, and C. Bosquillon, *Evaluation of air-interfaced Calu-3 cell layers for investigation of inhaled drug interactions with organic cation transporters in vitro.* Int J Pharm, 2012. **426**(1–2): p. 7-14.
428. Reus, A.A., W.J.M. Maas, H.T. Jansen, S. Constant, Y.C.M. Staal, J.J. van Triel, and C.F. Kuper, *Feasibility of a 3D human airway epithelial model to study respiratory absorption.* Toxicol in Vitro, 2014. **28**(2): p. 258-264.
429. Zhu, Y., A. Chidekel, and T.H. Shaffer, *Cultured Human Airway Epithelial Cells (Calu-3): A Model of Human Respiratory Function, Structure, and Inflammatory Responses.* Crit Care Res Pract, 2010. **2010**: p. 8.

430. Gamboa, J.M. and K.W. Leong, *In vitro and in vivo models for the study of oral delivery of nanoparticles.* Advanced Drug Delivery Reviews, 2013. **65**(6): p. 800-810.
431. Lansley, A.B., *Mucociliary clearance and drug delivery via the respiratory tract.* Adv Drug Deliv Rev, 1993. **11**: p. 299-327.
432. Rao, A., G.P. Martin, and A.B. Lansley, *Absorption characteristics of Salmeterol across Caco-2, 16HBE14o- and rat alveolar cells.* Eur J Pharm Sci, 1998. **6 (Supplement 1)**: p. S95.
433. Kidney, J.C. and D. Proud, *Neutrophil Transmigration across Human Airway Epithelial Monolayers.* Am J Respir Cell Mol Biol, 2000. **23**(3): p. 389-395.
434. Vila, A., A. Sanchez, M. Tobio, T.P. Calvo, and M.J. Alonso, *Design of biodegradable particles for protein delivery.* J Control Release, 2002. **78**(1-3): p. 15-24.
435. Jung, T., W. Kamm, A. Breitenbach, E. Kaiserling, J.X. Xiao, and T. Kissel, *Biodegradable nanoparticles for oral delivery of peptides: is there a role for polymers to affect mucosal uptake?* Eur J Pharm Biopharm, 2000. **50**(1): p. 147-160.
436. Fowler, R., D. Vllasaliu, F.H. Falcone, M. Garnett, B. Smith, H. Horsley, C. Alexander, and S. Stolnik, *Uptake and transport of B12-conjugated nanoparticles in airway epithelium.* J Control Release, 2013. **172**(1): p. 374-381.
437. Wilhelm, C., C. Billotey, J. Roger, J.N. Pons, J.C. Bacri, and F. Gazeau, *Intracellular uptake of anionic superparamagnetic nanoparticles as a function of their surface coating.* Biomaterials, 2003. **24**(6): p. 1001-1011.
438. Loh, J.W., G. Yeoh, M. Saunders, and L.Y. Lim, *Uptake and cytotoxicity of chitosan nanoparticles in human liver cells.* Toxicol Appl Pharmacol, 2010. **249**(2): p. 148-57.
439. Karanam, V., G. Marslin, B. Krishnamoorthy, V. Chellan, K. Siram, T. Natarajan, B. Bhaskar, and G. Franklin, *Poly (varepsilon-caprolactone) nanoparticles of carboplatin: Preparation, characterization and in vitro cytotoxicity evaluation in U-87 MG cell lines.* Colloids Surf B Biointerfaces, 2015. **130**: p. 48-52.
440. Egusquiaguirre, S.P., C. Manguan-Garcia, L. Pintado-Berninches, L. Iarriccio, D. Carbajo, F. Albericio, M. Royo, J.L. Pedraz, R.M. Hernandez, R. Perona, and M. Igartua, *Development of surface modified biodegradable polymeric nanoparticles to deliver GSE24.2 peptide to cells: a promising approach for the treatment of defective telomerase disorders.* Eur J Pharm Biopharm, 2015. **91**: p. 91-102.
441. Dekali, S., C. Gamez, T. Kortulewski, K. Blazy, P. Rat, and G. Lacroix, *Assessment of an in vitro model of pulmonary barrier to study the translocation of nanoparticles.* Toxicol Rep, 2014. **1**: p. 157-171.
442. Luo, L. and M.E. Lane, *Topical and transdermal delivery of caffeine.* International Journal of Pharmaceutics, 2015. **490**(1–2): p. 155-164.
443. McCall, A.L., W.R. Millington, and R.J. Wurtman, *Blood-brain barrier transport of caffeine: dose-related restriction of adenine transport.* Life Sci, 1982. **31**(24): p. 2709-15.
444. Franke, H., H.-J. Galla, and C.T. Beuckmann, *An improved low-permeability in vitro-model of the blood–brain barrier: transport studies on retinoids, sucrose, haloperidol, caffeine and mannitol.* Brain Res, 1999. **818**(1): p. 65-71.
445. Lexmuller, K., H. Gullstrand, B.O. Axelsson, P. Sjolin, S.H. Korn, D.S. Silberstein, and A. Miller-Larsson, *Differences in endogenous esterification and retention in the rat trachea between budesonide and ciclesonide active metabolite.* Drug Metab Dispos, 2007. **35**(10): p. 1788-96.
446. Wieslander, E., E.L. Delander, L. Jarkelid, E. Hjertberg, A. Tunek, and R. Brattsand, *Pharmacologic importance of the reversible fatty acid conjugation of budesonide studied in a rat cell line In vitro.* Am J Respir Cell Mol Biol, 1998. **19**(3): p. 477-84.

447. Miller-Larsson, A., H. Mattsson, E. Hjertberg, M. Dahlback, A. Tunek, and R. Brattsand, *Reversible fatty acid conjugation of budesonide. Novel mechanism for prolonged retention of topically applied steroid in airway tissue.* Drug Metab Dispos, 1998. **26**(7): p. 623-30.
448. Florea, B.I., M.L. Cassara, H.E. Junginger, and G. Borchard, *Drug transport and metabolism characteristics of the human airway epithelial cell line Calu-3.* J Control Release, 2003. **87**(1-3): p. 131-138.
449. Brattsand, R. and A. Miller-Larsson, *The role of intracellular esterification in budesonide once-daily dosing and airway selectivity.* Clin Ther, 2003. **25, Supplement 3**: p. C28-C41.
450. Stanaland, B.E., *Once-daily budesonide aqueous nasal spray for allergic rhinitis: A review.* Clin Ther, 2004. **26**(4): p. 473-492.
451. O'Connell, E.J., *Review of the unique properties of budesonide.* Clin Ther, 2003. **25 Suppl C**: p. C42-60.
452. Borchard, G., M.L. Cassara, P.E. Roemele, B.I. Florea, and H.E. Junginger, *Transport and local metabolism of budesonide and fluticasone propionate in a human bronchial epithelial cell line (Calu-3).* J Pharm Sci, 2002. **91**(6): p. 1561-7.
453. Eixarch, H., E. Haltner-Ukomadu, C. Beisswenger, and U. Bock, *Drug delivery to the lung: Permeability and Physicochemical characteristics of drugs as the basis for a Pulmonary Biopharmaceutical Classification System (pBCS).* J Epithel Biol Pharmacol, 2010. **3**: p. 1-14.
454. Ong, H.X., D. Traini, G. Ballerin, L. Morgan, L. Buddle, S. Scalia, and P.M. Young, *Combined inhaled salbutamol and mannitol therapy for mucus hyper-secretion in pulmonary diseases.* AAPS J, 2014. **16**(2): p. 269-80.
455. Hamishehkar, H., Y. Rahimpour, and Y. Javadzadeh, *The Role of Carrier in Dry Powder Inhaler*, in *Recent advances in novel drug carrier systems*. 2012.
456. Pilcer, G., F. Vanderbist, and K. Amighi, *Spray-dried carrier-free dry powder tobramycin formulations with improved dispersion properties.* J Pharm Sci, 2009. **98**(4): p. 1463-75.
457. Pilcer, G., N. Wauthoz, and K. Amighi, *Lactose characteristics and the generation of the aerosol.* Adv Drug Deliv Rev, 2012. **64**(3): p. 233-56.
458. Jaspart, S., P. Bertholet, G. Piel, J.M. Dogne, L. Delattre, and B. Evrard, *Solid lipid microparticles as a sustained release system for pulmonary drug delivery.* Eur J Pharm Biopharm, 2007. **65**(1): p. 47-56.
459. Demoly, P., P. Hagedoorn, A.H. de Boer, and H.W. Frijlink, *The clinical relevance of dry powder inhaler performance for drug delivery.* Respir Med, 2014. **108**(8): p. 1195-203.
460. Malcolmson, R.J. and J.K. Embleton, *Dry powder formulations for pulmonary delivery.* Research focus, 1998. **1**(9): p. 394-398.
461. Faulhammer, E., M. Fink, M. Llusa, S.M. Lawrence, S. Biserni, V. Calzolari, and J.G. Khinast, *Low-dose capsule filling of inhalation products: critical material attributes and process parameters.* Int J Pharm, 2014. **473**(1-2): p. 617-26.
462. Wu, L., X. Miao, Z. Shan, Y. Huang, L. Li, X. Pan, Q. Yao, G. Li, and C. Wu, *Studies on the spray dried lactose as carrier for dry powder inhalation.* Asian J Pharm Sci, 2014. **9**(6): p. 336-341.
463. Telko, M.J. and A. Hickey, *Dry powder inhaler formulation.* Respir Care, 2005. **50**(9): p. 1209-27.
464. Ashurst, I., A. Malton, D. Prime, and B. Sumby, *Latest advances in the development of dry powder inhalers.* Research focus, 2000. **3**(7).
465. Yang, M.Y., J.G. Chan, and H.K. Chan, *Pulmonary drug delivery by powder aerosols.* J Control Release, 2014. **193**: p. 228-40.
466. Young, P.M., D. Traini, M. Coates, and H.-K. Chan, *Recent advances in understanding the influence of composite-formulation properties on the performance of dry powder inhalers.* Physica B Condens Matter, 2007. **394**(2): p. 315-319.

467. Healy, A.M., M.I. Amaro, K.J. Paluch, and L. Tajber, *Dry powders for oral inhalation free of lactose carrier particles.* Adv Drug Deliv Rev, 2014. **75**: p. 32-52.
468. Islam, N. and E. Gladki, *Dry powder inhalers (DPIs)--a review of device reliability and innovation.* Int J Pharm, 2008. **360**(1-2): p. 1-11.
469. Islam, N. and M.J. Cleary, *Developing an efficient and reliable dry powder inhaler for pulmonary drug delivery--a review for multidisciplinary researchers.* Med Eng Phys, 2012. **34**(4): p. 409-27.
470. Kho, K. and K. Hadinoto, *Dry powder inhaler delivery of amorphous drug nanoparticles: effects of the lactose carrier particle shape and size.* Powder Technol, 2013. **233**: p. 303-311.
471. Kinnunen, H., G. Hebbink, H. Peters, D. Huck, L. Makein, and R. Price, *Extrinsic lactose fines improve dry powder inhaler formulation performance of a cohesive batch of budesonide via agglomerate formation and consequential co-deposition.* Int J Pharm, 2014. **478**(1): p. 53-59.
472. Young, P.M., S. Edge, D. Traini, M.D. Jones, R. Price, D. El-Sabawi, C. Urry, and C. Smith, *The influence of dose on the performance of dry powder inhalation systems.* Int J Pharm, 2005. **296**(1-2): p. 26-33.
473. Ooi, J., D. Traini, S. Hoe, W. Wong, and P.M. Young, *Does carrier size matter? A fundamental study of drug aerosolisation from carrier based dry powder inhalation systems.* Int J Pharm, 2011. **413**(1-2): p. 1-9.
474. Hoppentocht, M., P. Hagedoorn, H.W. Frijlink, and A.H. de Boer, *Technological and practical challenges of dry powder inhalers and formulations.* Adv Drug Deliv Rev, 2014. **75**: p. 18-31.
475. Traini, D., P.M. Young, M. Jones, S. Edge, and R. Price, *Comparative study of erythritol and lactose monohydrate as carriers for inhalation: atomic force microscopy and in vitro correlation.* Eur J Pharm Sci, 2006. **27**(2-3): p. 243-51.
476. Young, P.M., D. Roberts, H. Chiou, W. Rae, H.-K. Chan, and D. Traini, *Composite carriers improve the aerosolisation efficiency of drugs for respiratory delivery.* J Aerosol Sci, 2008. **39**(1): p. 82-93.
477. Coates, M.S., H.K. Chan, D.F. Fletcher, and J.A. Raper, *Influence of air flow on the performance of a dry powder inhaler using computational and experimental analyses.* Pharm Res, 2005. **22**(9): p. 1445-53.
478. Jones, M.D., P. Young, and D. Traini, *The use of inverse gas chromatography for the study of lactose and pharmaceutical materials used in dry powder inhalers.* Adv Drug Deliv Rev, 2012. **64**(3): p. 285-93.
479. Traini, D., S. Scalia, H. Adi, E. Marangoni, and P.M. Young, *Polymer coating of carrier excipients modify aerosol performance of adhered drugs used in dry powder inhalation therapy.* Int J Pharm, 2012. **438**(1-2): p. 150-9.
480. Hickey, A., Mansour HM, Telko MJ, Xu Z, Smyth HD, Mulder T, McLean R, Langridge J, and P. D, *Physical characterization of component particles included in dry powder inhalers: II: Dynamic characteristics* Journal of Pharmceutical sciences, 2007. **96**(5): p. 1302-1319.
481. Grasmeijer, F., H.W. Frijlink, and A.H. de Boer, *A proposed definition of the 'activity' of surface sites on lactose carriers for dry powder inhalation.* Eur J Pharm Sci, 2014. **56**: p. 102-4.
482. Jaffari, S., B. Forbes, E. Collins, D.J. Barlow, G.P. Martin, and D. Murnane, *Rapid characterisation of the inherent dispersibility of respirable powders using dry dispersion laser diffraction.* Int J Pharm, 2013. **447**(1-2): p. 124-31.
483. Behara, S.R., I. Larson, P. Kippax, D.A. Morton, and P. Stewart, *The kinetics of cohesive powder de-agglomeration from three inhaler devices.* Int J Pharm, 2011. **421**(1): p. 72-81.
484. Irngartinger, M., V. Camuglia, M. Damm, J. Goede, and H.W. Frijlink, *Pulmonary delivery of therapeutic peptides via dry powder inhalation: effects of micronisation and manufacturing.* Eur J Pharm Biopharm, 2004. **58**(1): p. 7-14.

485. Tulbah, A.S., H.X. Ong, P. Colombo, P.M. Young, and D. Traini, *Dry Powder formulation of Simvastatin.* Expert Opin Drug Deliv, 2015. **12**(6): p. 857-868.
486. Tulbah, A.S., H.X. Ong, P. Colombo, P.M. Young, and D. Traini, *Novel Simvastatin Inhalation formulation and characterization.* AAPS PharmSciTech, 2014. **15**(4): p. 956-962.
487. Behara, S.R.B., P. Kippax, I. Larson, D.A.V. Morton, and P. Stewart, *Kinetics of emitted mass—A study with three dry powder inhaler devices.* Chem Eng Sci, 2011. **66**(21): p. 5284-5292.
488. COPLEY-SCIENTIFIC, *Inhaler Brochure 2012*.
489. *European Pharmacopiea (Ph Eur 8th edition)*. Preparations for Inhalation 2015 [cited 2015; https://www.edqm.eu/].
490. Scalia, S., V. Trotta, D. Traini, P.M. Young, C. Sticozzi, F. Cervellati, and G. Valacchi, *Incorporation of quercetin in respirable lipid microparticles: effect on stability and cellular uptake on A549 pulmonary alveolar epithelial cells.* Colloids Surf B Biointerfaces, 2013. **112**: p. 322-9.
491. Young, P.M. and D. Traini, *Themed issue: Inhalation pharmaceutics--current technologies and approaches to respiratory drug delivery.* J Pharm Pharmacol, 2012. **64**(9): p. 1207-8.
492. Smith, I.J. and M. Parry-Billings, *The inhalers of the future? A review of dry powder devices on the market today.* Pulm Pharmacol Ther, 2003. **16**(2): p. 79-95.
493. Yakubu, S.I., K.H. Assi, and H. Chrystyn, *Aerodynamic dose emission characteristics of dry powder inhalers using an Andersen Cascade Impactor with a mixing inlet: the influence of flow and volume.* Int J Pharm, 2013. **455**(1-2): p. 213-8.
494. Wong, W., J. Crapper, H.K. Chan, D. Traini, and P.M. Young, *Pharmacopeial methodologies for determining aerodynamic mass distributions of ultra-high dose inhaler medicines.* J Pharm Biomed Anal, 2010. **51**(4): p. 853-7.
495. Grasmeijer, F. and A.H. de Boer, *The dispersion behaviour of dry powder inhalation formulations cannot be assessed at a single inhalation flow rate.* Int J Pharm, 2014. **465**(1-2): p. 165-8.
496. Chan, J.G., C.C. Duke, H.X. Ong, J.C. Chan, A.S. Tyne, H.K. Chan, W.J. Britton, P.M. Young, and D. Traini, *A novel inhalable form of rifapentine.* J Pharm Sci, 2014. **103**(5): p. 1411-21.
497. Haghi, M., D. Traini, D.S. Postma, M. Bebawy, and P.M. Young, *Fluticasone uptake across Calu-3 cells is mediated by salmeterol when deposited as a combination powder inhaler.* Respirology, 2013. **18**(8): p. 1197-201.
498. Scalia, S., M. Haghi, V. Losi, V. Trotta, P.M. Young, and D. Traini, *Quercetin solid lipid microparticles: a flavonoid for inhalation lung delivery.* Eur J Pharm Sci, 2013. **49**(2): p. 278-85.
499. Adi, H., P.M. Young, H.K. Chan, P. Stewart, H. Agus, and D. Traini, *Cospray dried antibiotics for dry powder lung delivery.* J Pharm Sci, 2008. **97**(8): p. 3356-66.
500. Adi, H., P.M. Young, H.K. Chan, H. Agus, and D. Traini, *Co-spray-dried mannitol-ciprofloxacin dry powder inhaler formulation for cystic fibrosis and chronic obstructive pulmonary disease.* Eur J Pharm Sci, 2010. **40**(3): p. 239-47.
501. de Boer, A.H., H.K. Chan, and R. Price, *A critical view on lactose-based drug formulation and device studies for dry powder inhalation: which are relevant and what interactions to expect?* Adv Drug Deliv Rev, 2012. **64**(3): p. 257-74.
502. Talasila, G.K.M., B.V.P. Mukkala, and S. Vattikuri, *Formulation and evaluation of CFC free inhalers for beclomethasone dipropionate.* Braz J Pharm Sci, 2013. **49**(2): p. 221-231.
503. Adi, S., H. Adi, P. Tang, D. Traini, H.K. Chan, and P.M. Young, *Micro-particle corrugation, adhesion and inhalation aerosol efficiency.* Eur J Pharm Sci, 2008. **35**(1-2): p. 12-8.

504. Hassoun, M., S. Ho, J. Muddle, F. Buttini, M. Parry, M. Hammond, and B. Forbes, *Formulating powder-device combinations for salmeterol xinafoate dry powder inhalers.* Int J Pharm, 2015. **490**(1-2): p. 360-7.
505. Muddle, J., D. Murnane, I. Parisini, M. Brown, C. Page, and B. Forbes, *Interaction of formulation and device factors determine the in vitro performance of salbutamol sulphate dry powders for inhalation* Journal of Pharmaceutical sciences, 2015.
506. Pandey, R., A. Sharma, A. Zahoor, S. Sharma, G. Khuller, and B. Prasad, *Poly (DL-lactide-co-glycolide) nanoparticles-based inhalable sustained drug delivery system for experimental tuberculosis.* J Antimicrob Chemo, 2003. **52**(6): p. 981-986.
507. Andrade-Lima, M., L.F. Pereira, and A.L. Fernandes, *Pharmaceutical equivalence of the combination formulation of budesonide and formoterol in a single capsule with a dry powder inhaler.* J Bras Pneumol, 2012. **6**(38): p. 748-756.
508. Andrade, F., D. Rafael, M. Videira, D. Ferreira, A. Sosnik, and B. Sarmento, *Nanotechnology and pulmonary delivery to overcome resistance in infectious diseases.* Adv Drug Deliv Rev, 2013. **65**(13-14): p. 1816-27.
509. *ICH Guidelines- Stability Testing of New Drug Substances and Products*. 2003.
510. Soares, S., P. Fonte, A. Costa, J. Andrade, V. Seabra, D. Ferreira, S. Reis, and B. Sarmento, *Effect of freeze-drying, cryoprotectants and storage conditions on the stability of secondary structure of insulin-loaded solid lipid nanoparticles.* Int J Pharm, 2013. **456**(2): p. 370-81.
511. Ranjan, A.P., A. Mukerjee, L. Helson, and J.K. Vishwanatha, *Scale up, optimization and stability analysis of Curcumin C3 complex-loaded nanoparticles for cancer therapy.* J Nanobiotechnology, 2012. **38**(10): p. 1-18.
512. Fang, C., N. Bhattarai, C. Sun, and M. Zhang, *Functionalized nanoparticles with long-term stability in biological media.* Small, 2009. **5**(14): p. 1637-41.
513. Dadparvar, M., S. Wagner, S. Wien, F. Worek, H. von Briesen, and J. Kreuter, *Freeze-drying of HI-6-loaded recombinant human serum albumin nanoparticles for improved storage stability.* Eur J Pharm Biopharm, 2014. **88**(2): p. 510-7.
514. Hafner, A., M. Durrigl, I. Pepic, and J. Filipovic-Grcic, *Short- and Long-Term Stability of Lyophilised Melatonin-Loaded Lecithin/Chitosan Nanoparticles.* Chem. Pharm. Bull, 2011. **59**(9): p. 1117-1123.
515. Abdelwahed, W., G. Degobert, S. Stainmesse, and H. Fessi, *Freeze-drying of nanoparticles: formulation, process and storage considerations.* Adv Drug Deliv Rev, 2006. **58**(15): p. 1688-713.
516. Holzer, M., V. Vogel, W. Mäntele, D. Schwartz, W. Haase, and K. Langer, *Physico-chemical characterisation of PLGA nanoparticles after freeze-drying and storage.* Eur J Pharm Biopharm, 2009. **72**(2): p. 428-437.
517. Sommerfield, P., U. Schroeder, and B. A. Sabel, *Long-term stability of PBCA nanoparticle suspensions suggests clinical usefulness.* Int J Pharm, 1997. **155**: p. 201-207.
518. Fonte, P., S. Soares, A. Costa, J.C. Andrade, V. Seabra, S. Reis, and B. Sarmento, *Effect of cryoprotectants on the porosity and stability of insulin-loaded PLGA nanoparticles after freeze-drying.* Biomatter, 2012. **2**(4): p. 329-39.
519. Blasi, P., A. Schoubben, G. Traina, G. Manfroni, L. Barberini, P.F. Alberti, C. Cirotto, and M. Ricci, *Lipid nanoparticles for brain targeting III. Long-term stability and in vivo toxicity.* Int J Pharm, 2013. **454**(1): p. 316-23.
520. Pooja, D., S. Panyaram, H. Kulhari, S.S. Rachamalla, and R. Sistla, *Xanthan gum stabilized gold nanoparticles: characterization, biocompatibility, stability and cytotoxicity.* Carbohydr Polym, 2014. **110**: p. 1-9.
521. Pinto, V.V., M.J. Ferreira, R. Silva, H.A. Santos, F. Silva, and C.M. Pereira, *Long time effect on the stability of silver nanoparticles in aqueous medium: Effect of the synthesis and storage conditions.* Colloids Surf A Physiochem Eng Asp, 2010. **364**(1-3): p. 19-25.

522. Sivera, M., L. Kvitek, J. Soukupova, A. Panacek, R. Prucek, R. Vecerova, and R. Zboril, *Silver nanoparticles modified by gelatin with extraordinary pH stability and long-term antibacterial activity.* PLoS One, 2014. **9**(8): p. e103675.
523. Kaialy, W., A. Alhalaweh, S.P. Velaga, and A. Nokhodchi, *Influence of lactose carrier particle size on the aerosol performance of budesonide from a dry powder inhaler.* Powder Technol, 2012. **227**: p. 74-85.
524. Hsu, P.-C., H.-L. Lin, S.-L. Wang, and S.-Y. Lin, *Solid-state thermal behavior and stability studies of theophylline–citric acid cocrystals prepared by neat cogrinding or thermal treatment.* J Solid State Chem, 2012. **192**: p. 238-245.
525. Otsuka, M. and M. Ishii, *Improvement of theophylline anhydrate stability at high humidity by surface-physicochemical modification.* Colloids Surf B Biointerfaces, 2010. **76**(1): p. 158-63.
526. Kulhari, H., D.P. Kulhari, M.K. Singh, and R. Sistla, *Colloidal stability and physicochemical characterization of bombesin conjugated biodegradable nanoparticles.* Colloids Surf A Physiochem Eng Asp, 2014. **443**: p. 459-466.
527. Shendge, R.S. and F.J. Sayyad, *Formulation development and evaluation of colonic drug delivery system of budesonide microspheres by using spray drying technique.* J Pharmacy Res, 2013. **6**(4): p. 456-461.
528. Lemoine, D., C. Francois, F. Kedzierewicz, V. Preat, M. Hoffman, and P. Maincent, *Stability study of nanoparticles of poly(e-caprolactone), poly(D,L-lactide) and poly(D,L-lactide-co-glycolide).* Biomaterials, 1996. **17**: p. 2191-2197.

CHAPTER 10 APPENDICIES

10.1 APPENDIX 1: SYNTHESIS AND CHARACTERIZATION OF THEOPHYLLINE AND BUDESONIDE NANOPARTICLES

10.1.1 ANALYTICAL METHOD DEVELOPMENT

System suitability testing is an integral part of implementing an analytical method for a test compound and the tests are based on the concept that the equipment, electronics, analytical operations and samples to be analysed constitute an integral system that can be evaluated as such. The system suitability of the assay is performed by injecting a known concentration of the test compound for example a 10 µg/ml sample for a total of 6 times and then calculating the following parameters. The parameters adopted for the test compound are based on ICH guidelines for the validation of analytical procedures, Q2 (R1). The targets to be achieved are shown in Table 10.1:

Table 10.1 System suitability targets based on ICH guidelines

Validation Parameter	Specification
Capacity factor (*k'*)	*k'* > 2
Precision/Injection Repeatability (%RSD)	%RSD < 2%
Tailing Factor (T)	T ≤ 2
Theoretical Plate Number (N)	N > 2000

CAPACITY FACTOR (*K'*)

This is a measure of where the peak of the drug substance is located with respect to the void volume, i.e. the elution time of the non-retained components.

$$k' = \frac{(t_R - t_0)}{t_0}$$

t_R is the retention time of the Test compound and t_0 is the elution time of the non-retained components or void volume. The Test compound peak must be well resolved from all other peaks in the chromatogram and it is recommended the value of κ' should be greater than two.

PRECISION/INJECTION REPEATABILITY

This is expressed as the %RSD and provides an assessment of the performance of the HPLC system including the plumbing, column and environmental conditions at the time the samples are analysed.

TAILING FACTOR (T)

This parameter must be calculated in order to achieve a high degree of accuracy in quantitation by reducing problems in determining where and when the peak of interest ends.

$$T = \frac{W_x}{2f}$$

W_x is the width of the peak determined at 5% from the baseline of the peak height and f is the distance between the peak maximum and the peak front at W_x. A T value less than or equal to 2 is recommended.

THEORETICAL PLATE NUMBER (N)

This parameter provides a measure of column efficiency.

$$N = 16 \times \left(t_R / t_W \right)^2$$

The theoretical plate number depends on the elution time and a value greater than 2000 should be achieved.

LINEARITY AND RANGE

The linearity of the assay is its ability (within a given range) to obtain test results that are directly proportional to the concentration of test compound in the sample. The range of the assay is the interval between the upper and lower concentration of the test compound in the samples for which it has been demonstrated that the assay has a suitable level of precision, accuracy and linearity. The linearity and range of the assay is determined based on the standard plots for the test compound.

ACCURACY

The accuracy (or trueness) of the assay expresses the agreement between the value that is accepted either as a conventional true value or an accepted reference value and the value determined. To determine the accuracy of the HPLC assay quality control (QC, accepted reference) samples are freshly prepared each time the standard concentration samples are analysed.

The accuracy of the standards (represented as %accuracy) is assessed by calculating the concentration (MC) of a freshly prepared QC sample using the relevant section of the standard curve and comparing it to the theoretical concentration (TC) according to the following equation:

$$\%\,\text{accuracy} = \left(\frac{MC}{TC} \right) x100$$

PRECISION

The precision of the assay expresses the closeness of agreement (degree of scatter) between a series of measurements obtained from multiple sampling of the same homogeneous sample under the same analytical conditions and is expressed as the %relative standard

deviation (%RSD). Six replicate injections of a known concentration for example a 10 µg/ml standard sample of the test compound is analysed on the same day and the %RSD of peak area was determined.

SENSITIVITY

The limit of detection (LOD) is the lowest amount of analyte that can be detected but not necessarily quantitated. The quantitation limit (LOQ) is the lowest amount of analyte in the sample that can be quantitatively determined with suitable precision and accuracy. The LOQ is a parameter of quantitative assays for low levels of compounds in sample matrices. The LOD and LOQ of the assay are identified from the standard curve using the equations below:

$$LOD = \left(\frac{STEYX}{Slope} \right) x3.3$$

$$LOQ = \left(\frac{STEYX}{Slope} \right) x10$$

STEYX: Returns the standard error of the predicted 'y'-value for each 'x' in a regression.

Table 10.2 System suitability results for HPLC methods developed (described in detail in Chapter 2, Table 2.2). The initial mobile phase used was Acetonitrile: 0.1%v/v formic acid (65:35), which was unsuitable due to theophylline peak eluting too close to the solvent front. System 3 was an additional HPLC system used for the analysis of data in the current study.

		System 1: Mobile phase: Acetonitrile: 0.1%v/v formic acid (65:35)		System 3: Mobile phase: Methanol: water (70:30)	
		Theophylline	Budesonide	Theophylline	Budesonide
System suitability factors	Specification	Results (mean ± SD, n=6)	Results (mean ± SD, n=6)	Results (mean ± SD, n=6)	Results (mean ± SD, n=6)
Capacity Factor (*k'*)	*k'* > 2	-0.15±0.00	1.82±0.00	0.41±0.013	5.44±0.031
Precision/Injection Repeatability (%RSD)	RSD < 2%	0.29%	1.08%	1.95%	0.88%
Tailing Factor (T)	T ≤ 2	0.02 ± 0.01	0.05 ± 0.01	0.00 ± 0.00	0.00 ± 0.00
Theoretical Plate Number (N)	N > 2000	131 ± 15	1070 ± 15	144 ± 33	455 ± 61
Linearity	$R^2 \geq 0.995$	0.9997	1	0.9975	0.9975
LOD	-	10ng/ml	4 ng/ml	1.42 ng/ml	1.53 ng/ml
LOQ	-	200ng/ml	20 ng/ml	4.29 ng/ml	4.64 ng/ml

Does not meet specification	Meets specification	Not applicable

10.1.2 AVERAGE PARTICLE SIZE, ZETA POTENTIAL ANALYSIS AND LOADING EFFICIENCY OF NANOPARTICLES SAMPLES FORMULATED USING VARIOUS THEOPHYLLINE, BUDESONIDE AND POLYMER RATIOS

Table 10.3 Quantities of theophylline and budesonide used in some nanoparticles formulations. These combinations of theophylline and/or budesonide were used to synthesize mono- or co-encapsulated nanoparticles using Methods 2 to 5. The quantity of polymer used is specified in Chapter 2, Table 2.1.

Sample	1	2	3	4	5	6	7	8	9	10	11
PLA (mg)	50 or 200 (specified in Table 2.1)										
Theophylline (mg)	5	10	50	5	10	50	5	10	50	X	X
Budesonide (mg)	X	X	X	1	5	1	5	1	5	1	5

Table 10.4 The average particle size and zeta potential of the nanoparticles synthesized using Methods 2-5 with various drug combinations specified in Table 10.3 (n=3).

Methods	2				3				4				5			
Sample	Average size± standard deviation (nm)	%RSD	Average zeta potential ±standard deviation (mV)	%RSD	Average size± standard deviation (nm)	%RSD	Average zeta potential ±standard deviation (mV)	%RSD	Average size± standard deviation (nm)	%RSD	Average zeta potential ±standard deviation (mV)	%RSD	Average size± standard deviation (nm)	%RSD	Average zeta potential ±standard deviation (mV)	%RSD
1	251.90±39.30	15.60	-11.57±6.18	53.40	403.98±97.84	24.22	-0.55±4.22	768.06	500.50±47.19	9.43	-12.12±5.02	41.45	263.50±21.62	8.21	-20.93±5.19	24.81
2	279.18±136.05	48.73	-9.96±7.01	70.31	242.05±68.04	28.11	-0.58±3.39	588.20	905.40±69.69	7.70	-8.47±4.09	48.29	353.50±66.41	18.79	-16.43±3.95	24.02
3	242.45±63.83	26.33	-11.00±7.90	71.85	479.37±208.33	43.46	-21.10±5.83	27.63	661.38±76.46	11.56	-18.75±4.32	23.06	247.69±12.94	5.22	-21.50±7.19	33.46
4	192.80±32.75	16.99	-8.19±5.37	65.55	287.95±70.61	24.52	-2.41±3.71	154.02	480.23±37.09	7.72	-17.60±4.12	23.42	327.57±29.21	8.92	-17.07±5.62	32.93
5	237.75±54.37	22.87	-1.30±5.84	449.23	322.30±83.29	25.84	-24.70±7.06	28.60	464.40±80.50	17.33	-12.97±7.21	55.60	322.70±28.43	8.81	-20.47±5.44	26.60
6	262.65±45.89	17.47	-4.30±2.43	56.51	251.25±81.41	32.40	-0.65±3.26	500.00	849.80±30.46	3.58	-6.77±5.71	84.30	280.57±23.68	8.44	-15.37±5.29	34.40
7	237.38±46.88	19.75	-6.45±6.00	93.06	264.93±58.65	22.14	-0.72±4.27	593.97	374.47±90.30	24.11	-16.41±5.65	34.42	380.77±33.17	8.71	-20.82±4.76	22.87
8	263.48±83.74	31.78	-10.78±6.58	61.02	229.83±54.61	23.76	-0.91±3.86	423.15	683.50±118.63	17.36	-19.95±5.76	28.86	239.09±21.42	8.96	-12.55±6.87	54.76
10	270.90±101.93	37.63	-8.71±3.94	45.25	214.93±60.78	28.28	-0.64±3.26	506.21	885.23±220.03	24.86	-17.47±5.15	29.48	272.04±28.37	10.43	-19.03±4.64	24.40
11	349.95±104.55	29.87	5.39±5.67	105.19	252.30±81.29	32.22	-0.63±3.22	511.10	399.35±66.35	16.62	-0.25±3.93	1552.04	352.50±43.35	12.30	-21.73±5.04	23.21

Table 10.5 The average loading efficiency of theophylline and budesonide in PLA nanoparticles synthesized using Methods 2-5 (Chapter 2,Table 2.1) using various drug and polymer combinations specified in Table 10.3 (n=3).

Method	2		3		4		5	
Sample	Theophylline loading ±SD (%)	Budesonide loading ±SD (%)	Theophylline loading ±SD (%)	Budesonide loading ±SD (%)	Theophylline loading ±SD (%)	Budesonide loading ±SD (%)	Theophylline loading ±SD (%)	Budesonide loading ±SD (%)
1	0.17±0.55	X	4.60±2.53	X	1.33±0.15	X	5.37±0.03	X
2	0.32±0.53	X	0.41±0.43	X	0.75±1.52	X	13.53±0.04	X
3	2.08±1.47	X	0.01±4.76	X	3.98±0.01	X	4.98±0.11	X
4	0.14±0.17	8.96±0.83	5.04±0.32	12.54±6.07	1.11±0.15	4.45±0.17	2.70±2.45	15.92±6.19
5	0.40±0.16	6.05±0.72	8.76±2.45	45.37±7.36	1.32±0.15	4.21±0.61	4.46±1.46	4.03±3.54
6	0.87±0.02	2.71±1.39	6.07±2.51	44.75±13.77	0.80±0.04	12.60±1.41	2.26±0.24	14.23±4.58
7	3.10±0.12	3.93±0.83	1.52±0.00	38.06±6.84	0.39±0.08	25.44±1.66	6.29±1.30	10.60±6.15
8	0.22±0.15	12.18±1.76	4.90±0.66	41.78±0.02	1.90±0.07	24.27±0.70	26.15±0.12	18.84±2.97
10	X	13.79±2.76	X	45.44±12.14	X	6.58±0.90	X	59.73±1.34
11	X	3.78±1.52	X	67.55±24.80	X	42.07±1.09	X	9.94±6.80

10.2 APPENDIX 2: THERMAL PROPERTIES DATA SHEET FROM MANUFACTURERS (PURAC BIOMATERIALS)

purac

Datasheet 06

Rev. No. 1 / September 2010

THERMAL PROPERTIES

Purac Biomaterials produces a wide range of resorbable polymers based on various monomers. This datasheet describes thermal properties of PURASORB polymers. The glass transition temperature (T_g) and melting temperature (T_m) are given in degrees Celsius. The data is derived from literature and own experiments and is provided as a general guideline.

Polymers for medical devices	T_g (°C)	T_m (°C)
PURASORB PL 18	60-65	185-195
PURASORB PL 24	60-65	185-195
PURASORB PL 32	60-65	185-195
PURASORB PL 38	60-65	185-195
PURASORB PL 49	60-65	185-195
PURASORB PL 65	60-65	185-195
PURASORB PD 24	60-65	180-190
PURASORB PDL 20	50-55	amorphous
PURASORB PLD 9655	60-65	155-165
PURASORB PLDL 7028	55-60	115-125
PURASORB PLDL 7038	55-60	115-125
PURASORB PLDL 7060	55-60	115-125
PURASORB PLDL 8038	55-60	125-135
PURASORB PLDL 8085	55-60	125-135
PURASORB PLG 1017	35-45	200-210
PURASORB PLG 8218	55-60	135-145
PURASORB PLG 8523	55-60	140-150
PURASORB PLG 8531	55-60	140-150
PURASORB PG 20	40-50	220-230
PURASORB PLC 7015	15-25	110-120
PURASORB PDLG 5010	45-50	Amorphous

Polymers for controlled release systems	T_g (°C)
PURASORB PDL 02	34-39
PURASORB PDL 02A	42-47
PURASORB PDL 04	42-47
PURASORB PDL 05	42-47
PURASORB PDLG 5002	32-37
PURASORB PDLG 5002A	40-45
PURASORB PDLG 5004	42-47
PURASORB PDLG 5004A	42-47
PURASORB PDLG 7502	35-40
PURASORB PDLG 7502A	40-45
PURASORB PDLG 7507	45-50

10.3 APPENDIX 3: CHAPTER 7: STABILITY TESTING OF THEOPHYLLINE AND BUDESONIDE PLA NANOPARTICLES

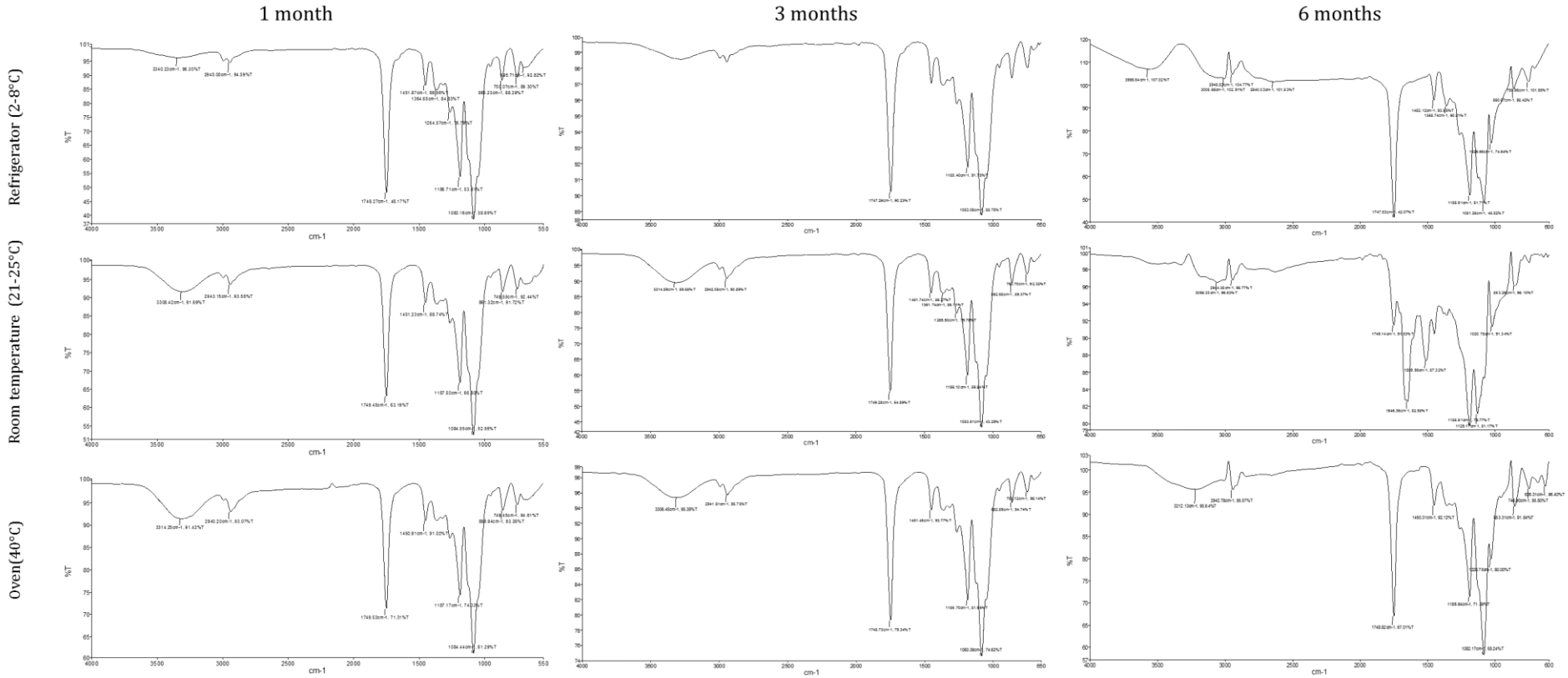

Figure 10.1FT-IR spectra of mono-encapsulated budesonide nanoparticles stored at 2-8°C, room temperature and 40°C at 1 month, 3 months and 6 months period to observe any changes in the surface characteristics of the nanoparticles

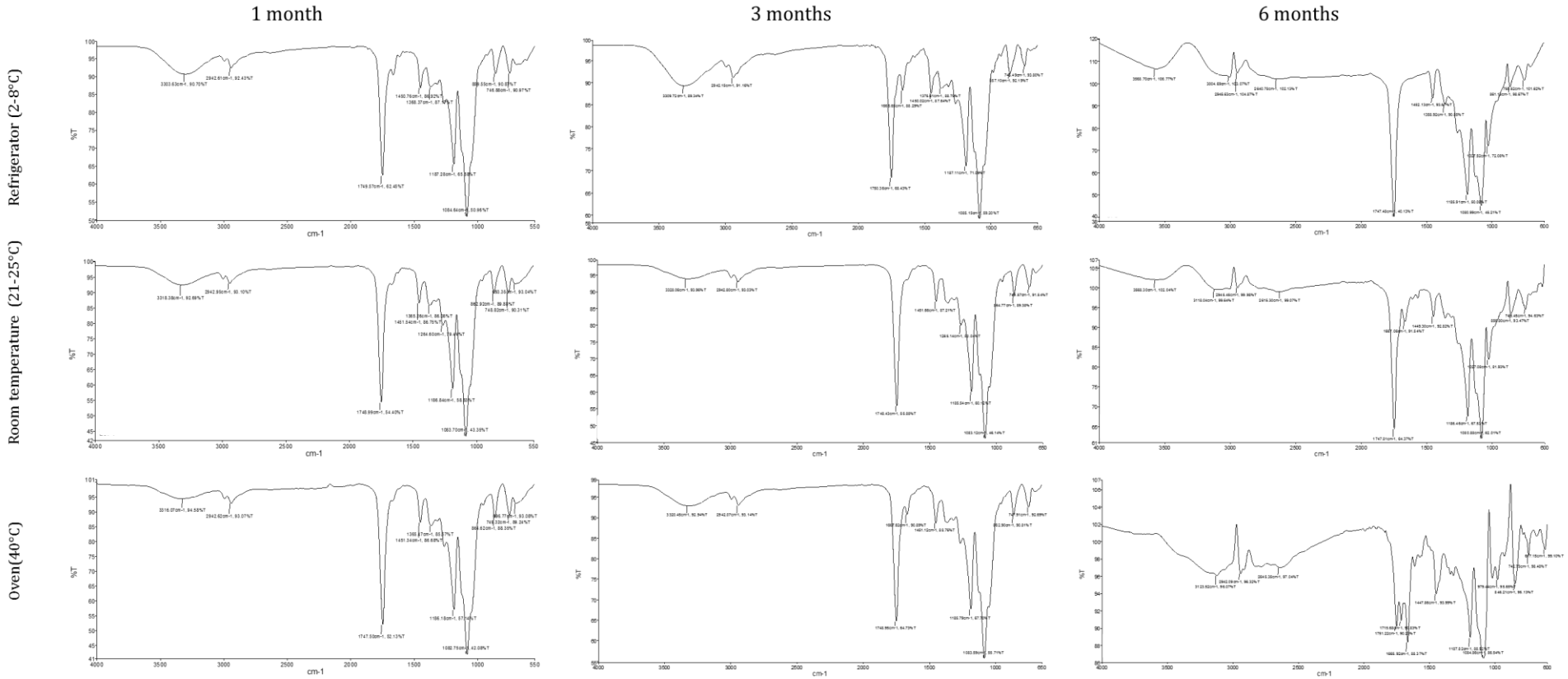

Figure 10.2FT-IR spectra of mono-encapsulated theophylline nanoparticles stored at 2-8°C, room temperature and 40°C at 1 month, 3 months and 6 months period to observe any changes in the surface characteristics of the nanoparticles